Time-Dependent Reliability Analysis of Flood Defences

By Foekje Buijs

Msc.

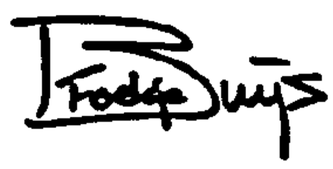

This is presented in part-fulfilment of the degree of Doctor of Philosophy in accordance with the regulations of Newcastle University

School of Civil Engineering and Geosciences
Faculty of Science, Agriculture and Engineering
Newcastle University
Cassie Building
Newcastle-upon-Tyne
NE1 7RU United Kingdom

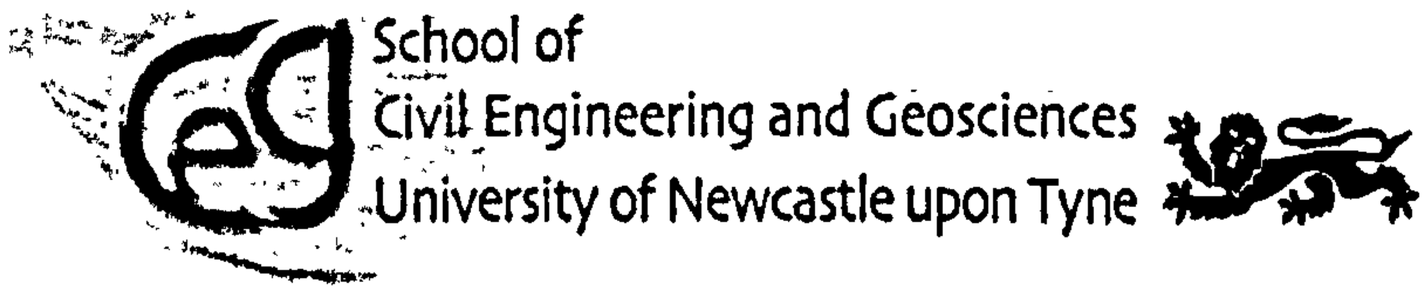

31-08-2007

Abstract

The aim of this thesis is to investigate how the time-dependent behaviour of flood defence properties can be appropriately characterised and incorporated in a reliability-based approach. Such an approach is required in a maintenance optimisation framework for flood defence management. The first objective shows that existing structural reliability methods are suitable for the analysis and incorporation of asset time-dependent processes in flood defence (system) reliability. Recent progress on quantitative maintenance optimisation frameworks for flood defence management is drawn together and complemented by theory from other engineering disciplines. The second objective develops three importance measure types to indicate the relevance of the time-dependent processes in the context of a rational maintenance optimisation approach. These importance measures support practical operational management as well as maintenance optimisation model design. The third objective develops a modelling methodology to describe asset time-dependent processes of flood defences by a statistical model. The first phase in the modelling methodology is problem formulation. The second conceptualisation phase is a five-step analysis of the asset time-dependent process. Firstly, existing field observations and scientific understanding are assembled. Secondly, the excitation, ancillary and affected features and uncertainty types of the asset time-dependent process are analysed. The third step describes the character of the process conditional on the excitation. The fourth step analyses the dependencies between different asset time-dependent processes. The fifth step formulates alternative statistical models for the asset time-dependent process. The last phase in the modelling methodology is parameter estimation, calibration and model corroboration. Historical observations on asset time-dependent processes are scarce and can either be used for further extension of this phase or Bayesian posterior updating. The fourth objective demonstrates the methods developed in this thesis in a (system) reliability model of the Dartford Creek to Swanscombe Marshes flood defence system along the Thames Estuary.

Acknowledgements

I would like to thank my academic supervisor Prof. Jim Hall, from Newcastle University, and industrial supervisor Paul Sayers, from HR Wallingford whose support has made the completion of this thesis possible. Many thanks go to my colleagues at HR Wallingford and Newcastle University, in particular Jonathan Simm, Ben Gouldby, Mike Wallis, Silvia Segura Domínguez, William Allsop and Mark Morris. Throughout the research my supervisors were also actively encouraging interactions with research or practitioners at HR Wallingford, the Environment Agency, Delft University of Technology, the Flood Risk Management Research Consortium and Floodsite. These interactions formed an important additional source of inspiration for this thesis. From these interactions I would like to highlight Alma Schellart from Sheffield University as a friend and colleague for proofreading and collaboration on a number of papers and secondly Nottingham University for a fruitful collaboration on visual inspection methods.

I would also like to highlight the contributions of Delft University of Technology, which is an important source of information in this area of research. The university staff, Pieter van Gelder, Han Vrijling, Ton Vrouwenvelder, Jan van Noortwijk and others, were easily accessible providing many illuminating discussions. I am grateful that I had the opportunity to spend a brief, but useful, period at this university at the end of my research project.

I would like to thank the Thames Estuary 2100 Project Team of the Environment Agency in the UK for providing the main financial support of my PhD research. I should also acknowledge them, and the staff at the Environment Agency in general, for supporting my research in various other ways. I would like to thank Owen Tarrant, David Kavanagh, Steve Newbold and Mervyn Bramley for keeping me posted on developments relevant to my research. In addition, I picked up a lot from the collaboration with the (board) team in the Performance and Reliability phase I project. Many thanks also go to Richard Francis who was generous with his extensive knowledge about the case study site, reaching back many years, and with providing me the information on the Dartford Creek to Swanscombe Marshes flood defence

system. Additional financial support was provided by the EPSRC funded Flood Risk Management Research Consortium in the UK.

Last, but not least, I would like to thank family and friends without whom the successful completion of this adventure would not have been possible.

Foekje Buijs

31-08-2007

Table of contents

1. Problem description

This thesis shows how the time-dependent behaviour of flood defences can be modelled and embedded in a reliability-based approach. A methodology is developed to capture time-dependent processes involved with flood defences by a statistical model. Measures to indicate the importance of those processes in a quantitative maintenance optimisation context are proposed. The appropriate reliability theory to incorporate the time-dependency in flood defence (system) reliability is brought forward. The methods are demonstrated on the Dartford Creek to Swanscombe Marshes flood defence system located along the Thames Estuary in the UK.

A general introduction of the thesis is given in section 1.1. The theoretical context of the thesis is formed by the rational flood defence management approach. Section 1.2 provides an overview of the development of rational flood defence management in the past decades. The current standing in risk-based design of flood defences and in the development towards a maintenance optimisation framework in flood defence management is discussed. Section 1.3 describes the aim and objectives of the thesis. Section 1.4 is an introduction into the Dartford Creek to Swanscombe Marshes flood defence system in the Thames Estuary. Section 1.5 is an outline of the thesis in the form of an overview of the individual chapters.

1.1. Introduction

Quantitative risk and reliability methods provide a rational basis to the design and operational management of flood defence systems. These methods incorporate the physics as well as uncertainties associated with hydraulic boundary conditions, i.e. high water levels or wave conditions, the failure processes leading to breach of the flood defence and the spatial distribution of economic damages in the floodplain.

The development of risk and reliability theory in flood defence management and more generally in the engineering industry has a long history. The emphasis was initially on the definition of the basics of structural reliability theory and finding computationally

feasible probabilistic calculation methods. Aspects in risk-based flood defence design that received attention early on were the statistical representation of hydraulic extremes and the understanding of the physical defence failure processes. The increasing computational capacity in the past decades enabled the incorporation of economic damages and of a reliability model of the defence failure processes in the risk analysis of flood defence systems. Currently, flood risk assessments for large scale flood defence systems are piloted and improved. The first initiatives have been taken towards a rational maintenance optimisation approach for flood defence management. However, a rational maintenance optimisation framework has not been fully specified yet for flood defence management. It is expected in this thesis that the most convenient model for the rational flood defence management decision-making framework is a mixture between a quantitative and qualitative optimisation framework. This approach merges the computational feasibility of a qualitative decision-making approach with quantitative objective prioritisation.

The current reliability-based design approach of flood defences does not systematically take time-dependent flood defence behaviour into account. Such an approach is required in the context of a maintenance optimisation framework for flood defence management. This thesis describes how the time-dependent behaviour of flood defences can be appropriately characterised with a reliability-based approach. A number of levels is covered from the individual time-dependent processes, the incorporation in flood defence (system) reliability to the influence of the time-dependency in an overarching maintenance optimisation model. More specifically, the thesis proposes a modelling methodology to describe time-dependent processes associated with flood defences by a statistical model. Measures are developed to indicate the importance of the time-dependent processes in the context of a rational maintenance optimisation approach. The time-dependent statistical models are incorporated in a flood defence (system) reliability model. The development of these methods are held in the perspective of the practical flood defence management environment.

The methods are applied to the Dartford Creek to Swanscombe Marshes flood defence system in the Thames Estuary. The safety level of the Thames Estuary flood defences is currently being reviewed. The next generation of the flood defence system is required to accommodate a sufficient safety level until the year 2100. Risk assessment methods are piloted to gain insight in the distribution of flood risk along the Thames

Estuary. The methods developed in this thesis are placed within the context of the practical flood defence management environment in the Thames Estuary and the UK.

1.2. Rational flood defence management

1.2.1. Brief historical overview of risk-based methods for flood defences

Quantitative risk and reliability based methods for flood defences have been developing continuously for decades, finding references in this research field as early as e.g. Van Dantzig (1956). This development reflects more generally the increasing interest in the engineering industry towards risk-based design.

Much effort was initially invested in the theoretical definition of the reliability of structural systems as well as finding computationally feasible probabilistic calculation methods, see for example Thoft-Christensen & Baker (1982), Vanmarcke (1983), Hasofer & Lind (1974), Hohenbichler & Rackwitz (1983), Hohenbichler & Rackwitz (1986) or Ditlevsen & Madsen (1996). Vrijling & Bruinsma (1980) employ a probabilistic model for the hydraulic design of the Eastern Scheldt barrier. A more general definition for probabilistic flood defence design is given in CUR 141 (1990) or e.g. Vrouwenvelder & Struik (1991). The introduction of probabilistic design in hydraulic engineering is also illustrated by Yen & Tung (1993), or Tung & Mays (1980). They cover a variety of topics from culvert design, probabilistic design of flood defences, probabilistic inspection modelling, analysis of water level and wave extremes to dam overtopping rates. Other examples are probabilistic dike slope stability analysis, Calle & Heijnen (1983), and the probabilistic design of dune flood defences described in Van de Graaff (1986). Hawkes et al. (2002) provides a modelling approach to the joint probability of waves and water levels in the UK, which is implemented in HR Wallingford (1998). The joint probability of waves and water levels is extended to estimate mean overtopping rates in Hawkes (1999).

The framework for flood risk assessment is currently defined as described by section 1.2.2 below. Structural reliability theory is discussed in more detail in chapter 2. The incorporation of the time-dependent flood defence behaviour in a reliability-based model is part of an overall life cycle costing optimisation context. The framework for

rational maintenance optimisation has not yet been defined for flood defence management. Section 1.2.3 provides background information about rational maintenance optimisation frameworks in the engineering industry. Chapter 3 describes practical flood defence management and theoretical details of maintenance optimisation.

1.2.2. Current standing risk-based design of flood defences

The fast increasing capacity of computers in recent years enabled the implementation of risk and reliability based methods for large scale systems of flood defences. Vrijling (2001) provides an outline for quantitative flood risk analysis. Vrouwenvelder et al. (1999, 2001a & 2001b), Van Gelder (1999), Voortman (2003) and Lassing et al. (2003) describe risk and reliability methods for flood defences developed in the Netherlands during the last decade. Several pilot applications have been carried out, for instance to four dike ring areas in TAW (2000) and a large number of dike ring areas in DWW (2006).

Sayers et al. (2002) and Hall et al. (2003) introduce tiered flood risk assessment methods in the UK. They build on Defra (2002), which characterises flood risk by means of the source-pathway-receptor-consequences framework shown in figure 1.1. The source component introduces the hydraulic loading on the flood defence structures in the form of a tide level and wave conditions or a river water level. The pathway to damage due to flooding is formed by failure processes leading up to breach of the flood defence structure. The consequences of flooding are economically

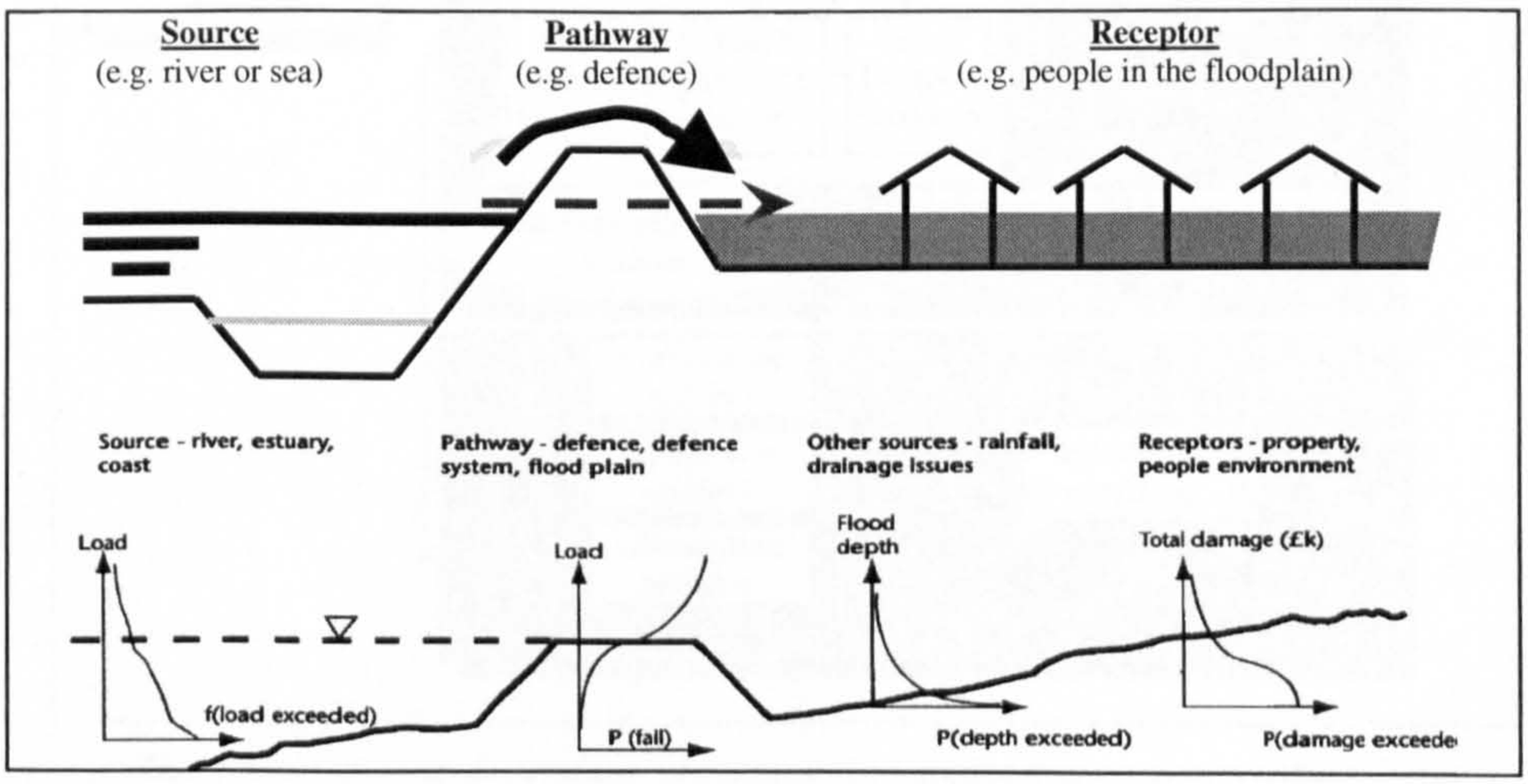

Figure 1.1 The source-pathway-receptor-consequences model for flood risk (Defra, 2002).

quantified damages to receptors such as people, residential or industrial properties. The improvement of the computational feasibility remains a continued subject of research interest due to the complexity of flood risk assessment models, see e.g. Dawson et al. (2005) and Dawson (2006).

The concept of fragility captures the structural response given different loading conditions (Casciati & Faravelli, 1991). HR Wallingford (2005) and Dawson & Hall (2002) specify fragility for flood risk assessment as the probability of flood defence breach (pathway), or a combination of breaches at different locations, given a range of hydraulic loading conditions (source), see bottom of figure 1.1 for an illustration. Fragility therefore expresses the probability of flood defence failure conditional on the source variables. Buijs et al. (2003) presents an application of the software developed in the Netherlands (Vrouwenvelder, 1999, 2001a & 2001b) to flood defence reliability analysis in the UK.

Figure 1.2 shows how time-dependent processes and operational activities affect the source-pathway-receptor-consequences model of flood risk. Several processes introduce time-dependency in flood risk such as relative sea level rise (source),

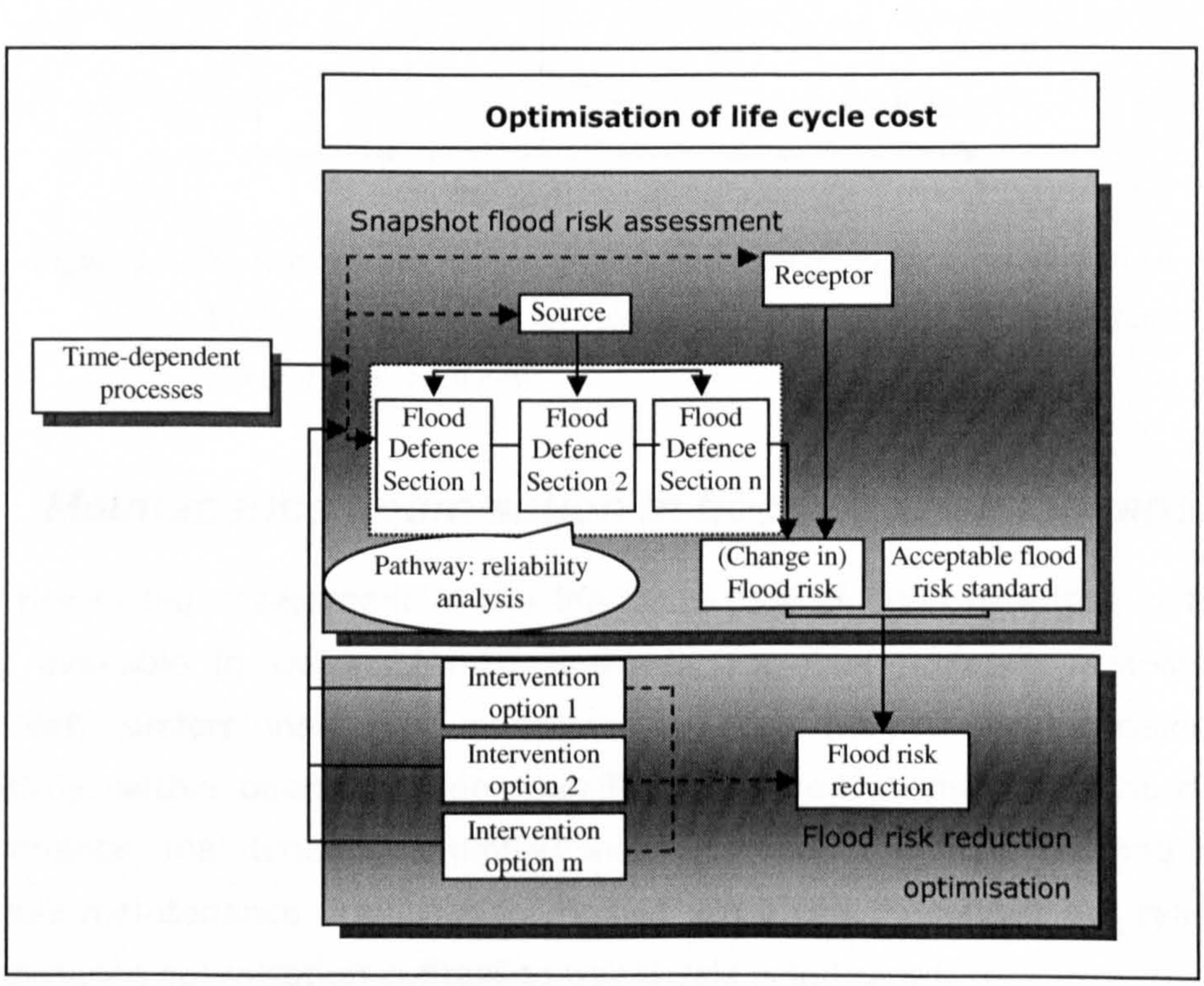

Figure 1.2 The place of time-dependent processes and maintenance intervention options in the source-pathway-receptor-consequences model of flood risk.

deterioration processes (pathway) or residential developments in the flood plain (receptor and consequences). This thesis describes how the time-dependent behaviour of the flood defences can be appropriately incorporated in a (system) reliability model.

If the actual occurring flood risk exceeds the acceptable risk standard at some location in the floodplain, the operational manager has a portfolio of intervention options to reduce the flood risk to an acceptable level. Design and operational decision-making aims to minimise the life-cycle cost of a system of flood defence structures, see figure 1.3 (according to Van Dantzig, 1956, and from Vrijling, 2003). Life-cycle costing requires an appropriate characterisation of the behaviour of flood risk in time, and hence of the hydraulic loading and fragility in time.

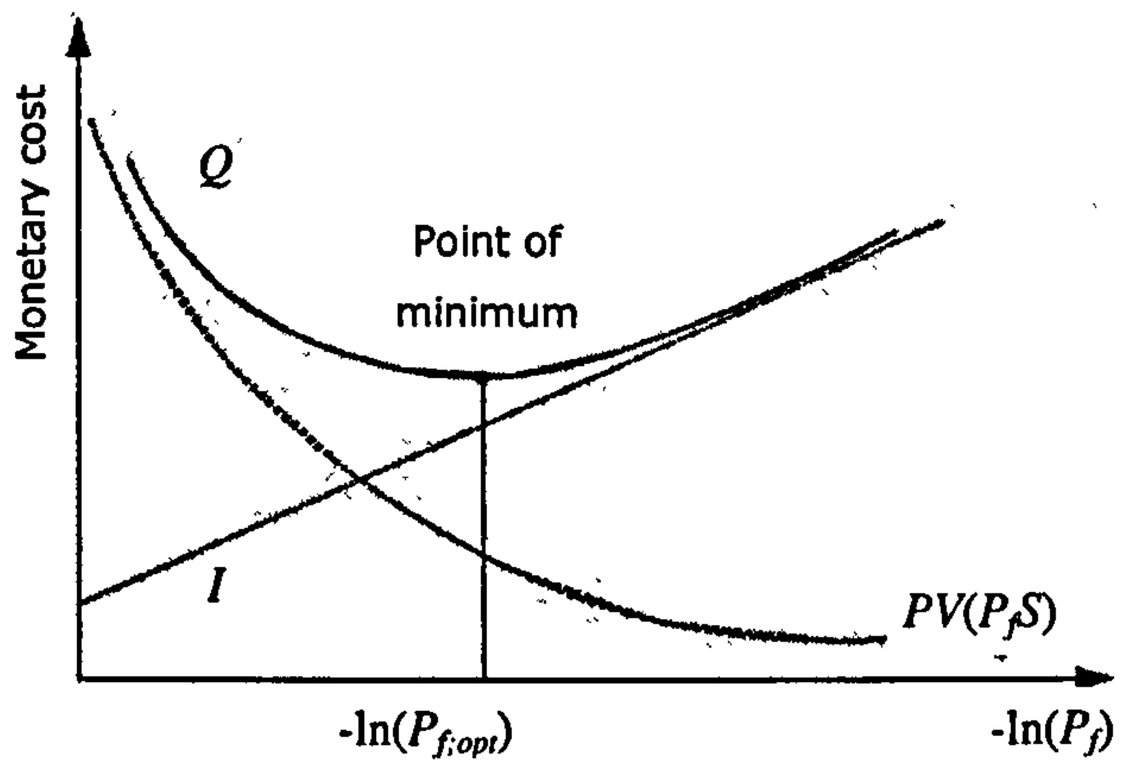

Figure 1.3 The economically optimal probability of failure P_f for a structure (from Vrijling, 2003). I is the investment in improvement, $PV(P_fS)$ the flood risk and Q the total cost.

1.2.3. Maintenance optimisation in flood defence management

A broad risk-based assessment of the life cycle cost of flood defences in the UK is currently available in Defra (2004). However, for flood defence systems a fully quantitatively underpinned risk or reliability-based maintenance decision-making framework is neither operational nor specifically defined. Below firstly the definitions of maintenance, maintenance optimisation models and the main building blocks in quantitative maintenance optimisation models are given. Secondly, the relevance of the maintenance optimisation context to this thesis is indicated.

Main definitions in a maintenance optimisation framework

Life cycle management for civil structures has been gaining more attention in practice in the course of the last ten to twenty years, e.g. in the Rock manual, CIRIA (2007) or port structures, PIANC (2007) and PIANC (1998). Vrijling (2003) defines maintenance in relation to flood defence systems as: all activities aimed at retaining an object's technical state or at reverting it back to this state, which is considered as a necessary condition for the object to carry out its function. Dekker (1996) and Petterson & Simola (2006) define maintenance in a more general context along the same lines as in Vrijling (2003). Dekker (1996) indicates a number of other issues besides its main aim that play a role in maintenance, such as: ensuring system function (availability, efficiency and product quality), ensuring system life (asset management), ensuring safety and ensuring human well-being.

Maintenance optimisation models underpin quantitative maintenance decision-making. Dekker (1996) defines maintenance optimisation models as those mathematical models whose aim it is to find the optimum balance between the costs and benefits of maintenance, subject to all kinds of constraints. Faber (2000) sets out a quantitative risk-based framework for inspection planning in the offshore industry.

According to Dekker (1996) maintenance optimisation models generally consist of four main building blocks. Pierskalla & Voelker (1976) bring forward a maintenance model consisting of similar components. Firstly, it contains a description of a technical system, its function and its importance. Secondly, it consists of a model of the deterioration of the system in time and possible consequences for the system. Thirdly, it requires a description of the available information about the system and the actions open to management. Finally, an objective function and an optimisation technique are included to assist in finding the best balance between maintenance costs and benefits.

Relevance maintenance optimisation to this thesis

As mentioned above, a quantitative rational maintenance optimisation framework has not yet been specified for flood defence management. The specification of such a framework requires an overview of current practice in flood defence management as well as knowledge about the types of rational decision-making approaches. There are three main types of rational maintenance decision-making frameworks: fully

quantitative, fully qualitative and mixtures of quantitative and qualitative decision-making approaches. A mixture approach combines the computational feasibility of a qualitative approach with quantitative objective prioritisation. This mixture approach is illustrated in 3.2.3 with an application to design dike monitoring programmes. It is expected that the mixture approach is the most convenient model for the rational flood defence management decision-making framework.

An impression of the maintenance optimisation context is relevant to this thesis for the following reasons. Firstly, it shows how the reliability-based approach for asset time-dependent processes contributes to an overarching rational maintenance optimisation model. Secondly, the choice to use a Markovian or Bayesian modelling approach for asset time-dependent processes is reviewed in the context of the overarching optimisation model. A Markovian or Bayesian approach determines how historical and future time series observations are incorporated. The choice therefore impinges on e.g. how monitoring events are modelled in the optimisation model and on which type of statistical time-dependency models are developed. Thirdly, the maintenance operations in flood defence management practice and the Bayesian decision-making framework form the context of the importance measures developed in chapter 4.

Chapter 3 provides an overview of current and developments in flood defence management practice and goes into the main types of rational maintenance optimisation frameworks.

1.3. Research aim and objectives

This section firstly defines what is meant by flood defence properties, deterioration or damage and makes a distinction between different time-dependent processes. Secondly, the aim of the research project is given followed by the objectives.

Flood defence properties, deterioration and time-dependency

Flood defence properties are all the characteristics included in the performance model of the flood defence structure. These characteristics consist of structural properties, such as geometry, soil properties and vegetation, as well as hydraulic boundary conditions, such as local water levels and wave conditions.

A time-dependent process affecting a flood defence property therefore refers to deterioration processes, sea level rise or climate change and processes that cause intermittently damage as well as improvement of the structure. This research project does not deal with all types of time-dependency. Before moving on to the aim of the research project, a definition is given of damage or deterioration. Then a distinction is made between asset time-dependent processes and system time-dependent processes.

Damage, deterioration and degradation are important notions in life cycle management. According to CIRIA (2007) damage is the result of an on-going deterioration or degradation process usually involving a decline in the state of structural properties. Deterioration or degradation is used to refer to the process causing the damage or to the damage itself. All three notions are therefore associated with a negative effect on the overall performance of the structure, and require a definition of what the structure entails. Damage, deterioration or degradation is thus only related to a specific class of time-dependent processes. CIRIA (1991) for instance defines damage as a certain change in the state of the structure, whereby the state of the structure is reflected by: the external boundaries or contours of the structure, typical cross sections of the structure and their configuration and finally the integrity of the constituent elements (e.g. rocks, crown wall).

Time-dependent processes take place at the flood defence system level and the flood defence asset level. *Flood defence system time-dependent processes* require simulation at the system level before they can be incorporated in the flood defence performance of individual assets. Climate change is an example of a time-dependent process at the system level affecting the local water levels and wave conditions. Morphological development of e.g. the river bathymetry, the coastline or the alignment of dunes is another example of a time-dependent process at the system level. A receding foreshore affects the local hydraulic boundary conditions and is able to cause slope or revetment instability. *Flood defence asset time-dependent processes* can be simulated for individual assets. Crest level settlements are an example of a time-dependent process at the flood defence asset level.

Both the flood defence system and asset time-dependent processes can be deterioration processes as long as they strictly have a negative effect on the structural performance.

Research aim

The research aim is to investigate how the time-dependent behaviour of flood defence properties can be appropriately characterised and incorporated in a reliability-based approach. As indicated above, the time-dependent behaviour of flood defence properties covers a variety of different time-dependent processes and needs to be specified for this research project. The investigation in this research project is restricted to flood defence asset time-dependent processes.

Main research objectives

The aim is achieved by the following research objectives:

1. Review existing time-dependent structural reliability methods, maintenance optimisation frameworks and statistical models for time-dependent processes in the engineering industry.
2. Develop a sensitivity analysis method to highlight relevant time-dependent processes and maintenance operations in the context of a rational maintenance framework.
3. Provide a systematic methodology to develop alternative statistical models for time-dependent processes at the flood defence individual asset level.
4. Incorporate the statistical models for time-dependent processes in the reliability analysis of the Dartford Creek to Swanscombe Marshes flood defence line.

1.4. The Dartford Creek to Swanscombe Marshes flood defence system

The first six chapters of the thesis present and develop the theory set out in the objectives above. The methods are then demonstrated in a reliability analysis of the Dartford Creek to Swanscombe Marshes flood defence system in chapter 7. This section is an introduction to this flood defence system and its setting formed by the Thames Estuary. See figure 1.4 for the location of the Dartford Creek to Swanscombe flood defence system in the Thames Estuary and for an indication of flood contours in the estuary.

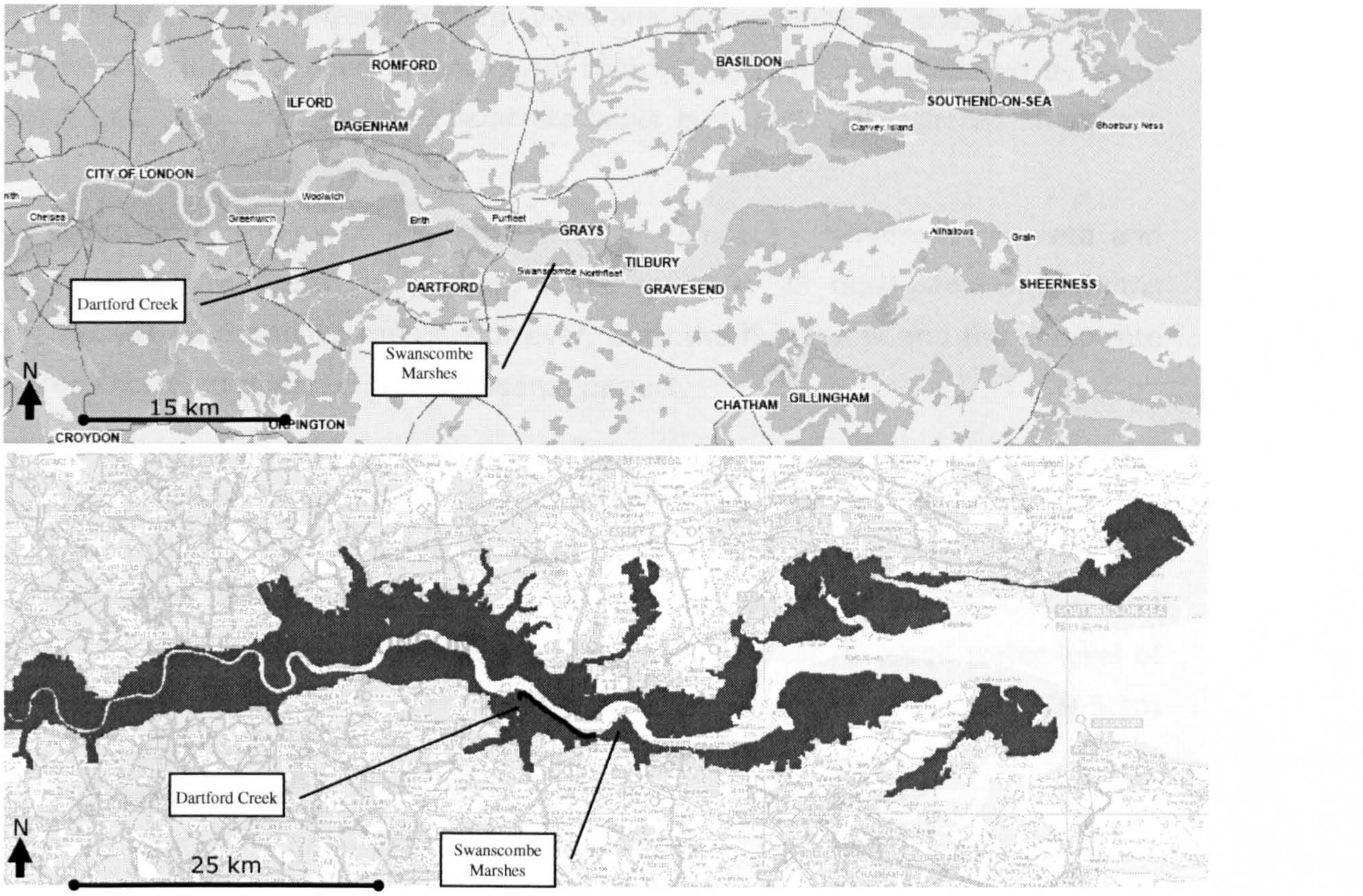

Figure 1. 4 The location of Dartford Creek and Swanscombe Marshes in the Thames Estuary (top). An indication of flood contours along the Thames Estuary and the location of the Dartford Creek to Swanscombe Marshes flood defence system (bottom).

In the late 1970s and early 1980s the flood defences along the Thames Estuary were subject to a major improvement scheme. After 30 years of service it will be approximately another 20 years before systematic refurbishment of the current flood defence system is required. The next generation of flood defences, ideally in place in 2030, will be designed to last beyond 2100. The Environment Agency launched the Thames Estuary 2100 project (TE2100 project) to initiate the design of these large scale refurbishment works. Part of the feasibility stage of the TE2100 project is to carry out flood risk assessments to identify the most flood prone areas. The results serve to compare the costs and risk reduction of different maintenance intervention or improvement options. To enable life-cycle costing, insight is required in the time-dependent reliability of the defences. This research project is conducted in that context.

The flood defence line between Dartford Creek and Swanscombe Marshes has a length of 10.6 km. Of the total flood defence line, approximately 63% is made up by earth embankments, 17% by reinforced concrete walls and 20% by anchored sheet pile walls.

The frontage also consists of a large variety of composite reinforced concrete and anchored sheet pile walls. In addition, there are over 25 floodgates with widths varying between 2.5 and 12 meter. However, both the floodgates and the composite structures are not considered in the research project.

Figure 1.5 presents the elevation of the defence line and the division into the main defence types. The elevation is compared between those recently surveyed and those indicated on as designed / constructed drawings of the improvements in the '70s and '80s. These crest levels relate to a floodplain elevation of between OD+0m and OD+2m. An indication of the tide levels is given by a highest recorded water level of about OD+4.9m downstream near Swanscombe Marshes and of about OD+5.1m

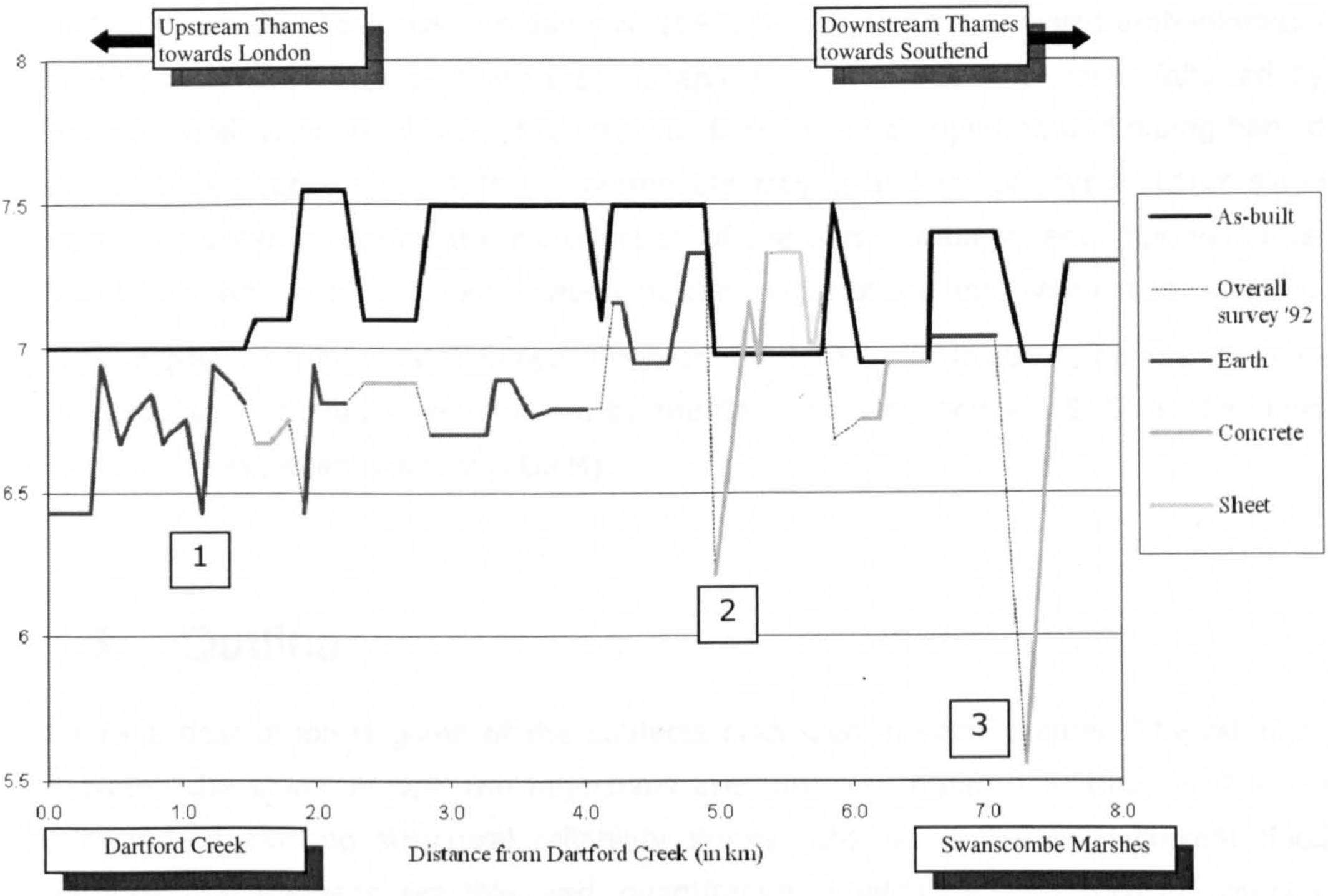

Figure 1.5 Elevation of the defence line between Dartford Creek to Gravesend: after '70s / '80s improvements (in continuous black) versus the recently surveyed defence line (light and dashed).

upstream near Erith.

Three details are brought to attention in figure 1.5. Area 1 consists of earth embankments. The variations in the crest level are attributed to compaction of the foundation underneath the earth embankments. The compaction is caused by the construction of an embankment behind the original flood defence embankment in the '70s and '80s. One explanation for the variations in compaction originates in differences in ground level. A relatively low ground level requires a thicker soil layer to achieve a design level of OD+7m and hence introduces more compaction load. Other explanations are variations in clay properties, the thickness of the alluvium layer or the presence of peat lenses. The troughs indicated by 2 and 3 in figure 1.5 are related to reinforced concrete walls. The thickness of the concrete wall crest is limited and not picked up by the survey. The actual measured level is the ground level just behind or in front of the reinforced concrete wall.

The '70s and '80s improvements to the Thames Estuary flood defences were triggered by the storm that took place in January 1953. During this storm earth embankments failed due to overtopping of the crest, seepage into fissures and cracks followed by slope instability. Another type of failure was brought on by uplifting and piping behind the earth embankments of the impermeable clayey and peaty layers. Later slope instability occurred during the construction of the earth embankment improvements. This failure was mainly caused by applying the weight of the improvement too quickly.

The inspection and maintenance intervention approach in the Thames Estuary corresponds with that recommended by the Environment Agency (1996) in the Flood Defence Management Manual (FDMM).

1.5. Outline

Below a description is given of the subjects discussed in each chapter. The relations between the chapters and the objectives are shown in figure 1.6. Chapter 2 is an overview of existing structural reliability theory. Chapter 3 describes current flood defence management practice and quantitative, qualitative and mixture rational maintenance optimisation frameworks. Chapter 4 develops the importance measures for asset time-dependent processes and maintenance operations in the context of the overarching maintenance optimisation context. These importance measures

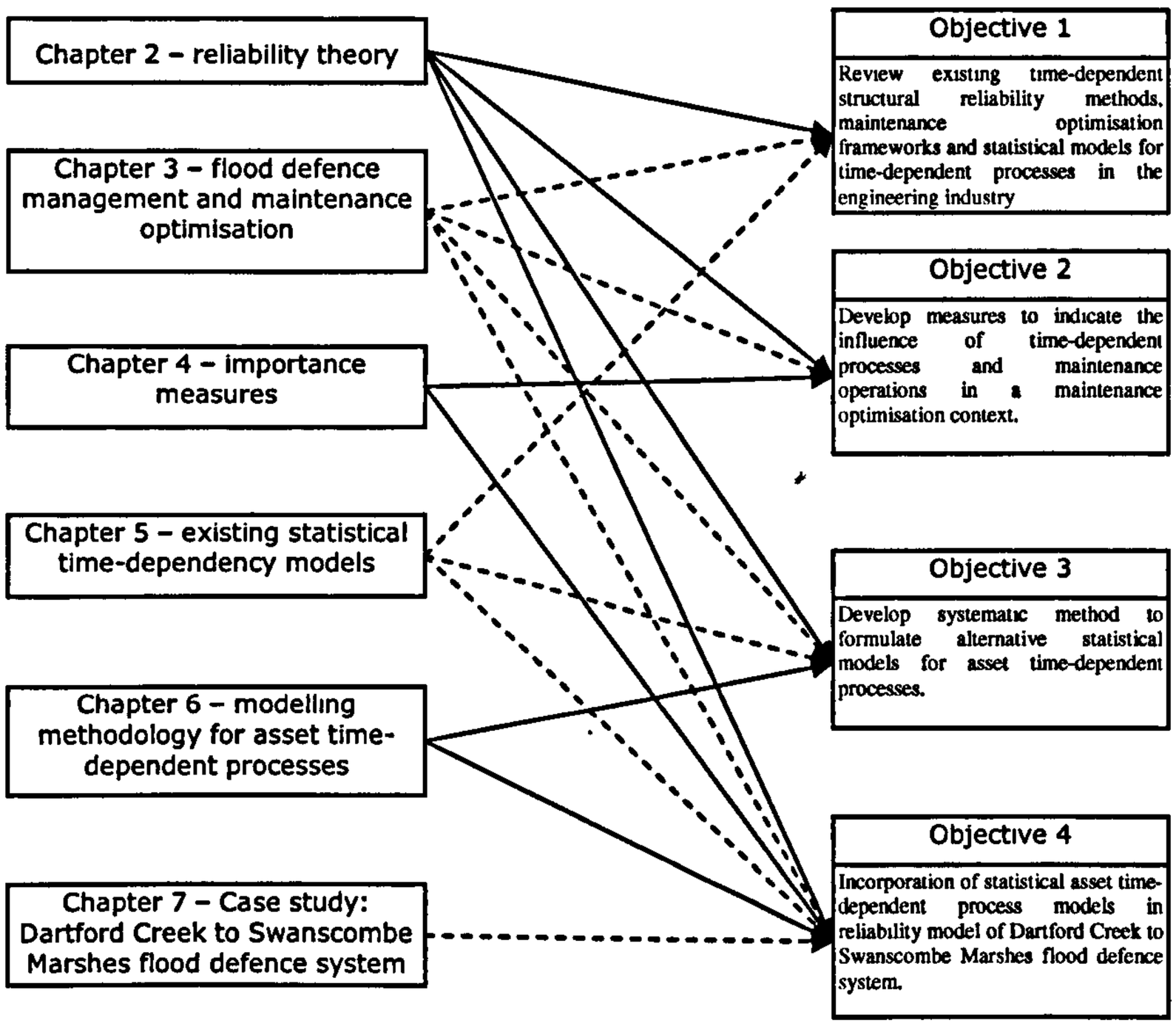

Figure 1.6 The relations between the chapters and the research objectives

correspond with objective 2 in this thesis. Chapter 5 gives additional theoretical background to existing statistical models for time-dependent processes. Chapter 6 sets out the modelling methodology for statistical models of asset time-dependent processes, corresponding with objective 3 in this thesis. Chapter 7 defines the time-dependent reliability model for the Dartford Creek to Swanscombe Marshes flood defence system.

Chapter 2 – Structural reliability methods

Chapter 2 presents theoretical background information about risk and reliability-based methods in the engineering industry. The types of uncertainty that are encountered in engineering problems are categorised. Fault trees, failure mechanisms and limit state equations form the basic model in a reliability analysis. The main probabilistic calculation methods in a quantitative reliability analysis for single as well as a system of flood defences are briefly discussed. The chapter shows how time-dependent processes are incorporated in a reliability analysis. The lifetime probability of failure

and hazard rate of a flood defence contribute to the rational maintenance decision-making framework.

Chapter 3 – Flood defence management and rational decision-making

A quantitative rational maintenance optimisation framework has not yet been specified for flood defence management. The specification of such a framework requires an overview of current practice in flood defence management as well as knowledge about the types of rational decision-making approaches. It is then possible to get an impression of how the research on asset time-dependent processes in this thesis contributes to a wider rational maintenance optimisation model.

Chapter 3 describes the flood defence management environment in practice. This overview provides an impression of the current maintenance prioritisation methods applied in practice and the maintenance operations open to management. This information is required in a rational maintenance decision-making framework such as described below. Current flood defence management and the development of current practice towards rational maintenance decision-making is discussed.

Chapter 3 then presents the theoretical background to rational maintenance decision-making frameworks applied in the engineering industry. Rational maintenance decision-making frameworks are quantitative, qualitative or a mixture of both. Fully quantitative maintenance decision-making frameworks are the foundation for whole life-cycle costing of a flood defence system. Generally, the main building blocks in a quantitative rational maintenance framework are: a functional system model, a risk and reliability system model, an operational management model and a calculation optimisation model. Existing theory in flood defence management relating to these building blocks is summarised and where possible complemented by theory from other branches in the engineering industry. Quantitative optimisation of the lifetime flood defence system performance is a complex problem and computationally very intensive. Qualitative maintenance decision-making frameworks for engineering systems set up a qualitative analysis of the failure mechanisms and their mutual relations. That analysis is used to structure operational activities. A disadvantage of qualitative maintenance decision-making is that prioritisation of activities is not quantitatively supported and therefore relatively subjective. It is expected that a mixture of a qualitative and quantitative approach is most suitable for flood defence

management. Such a mixture merges the computational feasibility of a qualitative approach with the objective prioritisation enabled by a quantitative approach.

Chapter 4 – Importance measures supporting risk-based flood defence management

Chapter 4 reviews and develops reliability-based and risk-based importance measures to support the management of flood defence systems without or in advance of a full life cycle optimisation. Firstly sensitivity measures are discussed indicating the sensitivity of the reliability analysis to different random variables, i.e. flood defence properties. This provides insight in the sensitivity of reliability to a change due to time-dependency or operational intervention. Secondly, importance measures to highlight the relevant time-dependent processes are developed, as a combination of increase in flood risk and costs of inspection and damage remediation. Knowledge about relevant time-dependent processes focuses research and monitoring efforts in advance of the life cycle optimization. It also enables the elimination of irrelevant time-dependent processes from the optimisation problem, increasing the computational feasibility. Thirdly, importance measures to indicate the impact of different operational activities on the flood risk reduction in relation to the cost of the activity are developed. These importance measures support an operational manager who has to achieve immediate flood risk reduction, but does not have the means or justification for a full life cycle optimization. In addition, they support the elimination of irrelevant operational activities in advance of the life cycle optimization.

Chapter 5 – Existing statistical models for time-dependent processes

Chapter 5 provides the theoretical background for statistical models for asset time-dependent processes. The definitions of stochastic processes and time series are presented. The statistical models for asset time-dependent processes is categorised according to three main compositions: a stochastic process for the overall time-dependent quantity, a hierarchical process or a parametric process. The suitability of existing statistical models for time-dependent processes is investigated in the context of flood defence asset time-dependency. Failure rate and time-dependent reliability index models are evaluated. Subsequently, the applicability of renewal models, continuous stochastic processes and hierarchical stochastic processes to represent

time-dependency is reviewed. Some dependency models are introduced to model correlated asset time-dependent processes.

Chapter 6 – Statistical models for asset time-dependent processes of flood defences

Chapter 6 develops the modelling process to establish statistical models for asset time-dependent processes of flood defences. The main steps in this modelling process are: problem formulation, conceptualisation, estimation and calibration and corroboration. The problem formulation outlines the task specification of the asset time-dependent process model itself and as part of the overarching maintenance framework. The conceptualisation issues a systematic methodology to develop alternative statistical models for the asset time-dependent process. This systematic methodology aims to achieve an appropriate quality of the internal properties of the statistical model. Estimation, calibration and corroboration aim to achieve an appropriate quality of the external properties of the statistical model. The methodology recommends in which cases point estimation, hypothesis testing, expert elicitation or Bayesian updating are relevant. It additionally explores how to evaluate the performance of the asset time-dependent process model in the context of the life cycle cost optimisation problem.

Chapter 7 – Case study: the Dartford Creek to Swanscombe Marshes flood defence system

The time-dependent reliability methods developed in the previous chapters are applied to the Dartford Creek to Swanscombe Marshes flood defence system in the Thames Estuary. Chapter 7 sets up the time-dependent reliability analysis of the Dartford Creek to Swanscombe Marshes flood defence system. The site description contains an evaluation of the information sources for geometry, soil conditions and hydraulic boundary conditions. The individual structure types are analysed in more detail. The historical failure processes are collected and the reliability analysis is set up consisting of fault trees, failure mechanisms and their limit state equations. The importance measures are calculated for the structure types on the case study site. Subsequently, the asset time-dependent processes of the structure type are analysed according to the modelling methodology outlined in chapter 5. Based on that analysis, time-dependent fragility and lifetime probability of failure is calculated. Finally, the

time-dependent system reliability model for the flood defence system is defined and the time-dependent system reliability results are produced.

Chapter 8 – Conclusions and recommendations

Chapter 8 starts with a brief overview of the main objectives mentioned in section 1.3 and figure 1.6. The conclusions are then presented according to the objectives. The conclusions with regard to objective 1 discuss the suitability and possible limitations of existing theory about reliability, quantitative rational maintenance optimisation and statistical models for time-dependent processes. The conclusions with regard to objective 2 consider the ability of the in chapter 4 developed importance measures to represent the sensitivity of reliability to random variables, compare the relevance of time-dependent processes and to provide a rational basis for comparison of operational activities such as monitoring and repair. The conclusions with regard to the modelling methodology for asset time-dependent processes contributed in chapter 6, objective 3, discuss the benefits of a structured conceptualisation approach. These conclusions also cover the implications of limited data availability for model calibration, corroboration and the incorporation of future observations. Finally, the possible advantages of a qualitative analysis of the asset time-dependent process for the choice of for example a state-or time-dependent maintenance approach are discussed. The conclusions with regard to objective 4 consider the results of the application of the time-dependent (system) reliability model to the Dartford Creek to Swanscombe Marshes flood defence system. The conclusions are subdivided into: the information availability; the application of the importance measures developed in chapter 4; the asset time-dependent process models developed according to the modelling methodology contributed in chapter 6; the time-dependent fragility / lifetime probability of failure results; the results of the time-dependent flood defence system reliability model. Section 8.3 provides the recommendations structured according to the 4 objectives in figure 1.6.

2. Structural reliability methods

This chapter provides background information about risk and reliability-based methods in the engineering industry. Statistical models for asset time-dependent processes, developed later in this thesis, are eventually embedded within the reliability analysis of flood defence systems. The reliability analysis forms part of an overarching rational maintenance framework for flood defence management, see chapter 3.

Section 2.1 introduces reliability-based design, failure mechanisms and system analysis. The reliability analysis in this thesis aims to capture the uncertainties related to flood defence structures. Section 2.2 provides a classification of uncertainties related to hydraulic structures. Section 2.3 discusses probabilistic calculation methods applied in reliability-based design. Section 2.5 introduces the most important concepts in time-dependent reliability. Existing reliability-based methods for flood defence design are described in section 2.6.

2.1. Reliability, failure mechanisms and system analysis

Engineering systems and its individual elements are built to fulfil one or more functions. Failure occurs in the event that a system or an individual element fails to fulfil one or more functions. Failure might therefore concern structural collapse as well as failure to provide a service for which the structure was designed. A failure mechanism is the process resulting in failure. The failure mechanism leads up to the limit state, a state in which failure is just occurring. The reliability is the probability that this limit state will not be exceeded during a specified reference period (Thoft-Christensen & Baker, 1982). A limit state equation quantifies the limit state and is generally represented by the following expression:

$$Z = R - S = g(X) \tag{2.1}$$

In which $Z \leq 0$ represents failure of the structure, R is the strength of the structure or element and S is the loading of the structure or element both expressed in the form of

process-based models. The probability of failure is calculated with the following probability integral, Thoft-Christensen & Baker (1982), CUR 190 (1997):

$$P_f = P(Z \leq 0) = \int_{-\infty}^{+\infty} F_R(x) f_S(x) dx \qquad (2.2)$$

In which P_f is the probability of failure, $F_R(x)$ is the cumulative probability distribution of the strength R, $f_S(x)$ is the probability density function of the loading S and x is the collection of basic random variables x_i, .., x_n. Each of these basic random variables is represented by a specific probabilistic distribution function type and associated parameters.

In an engineering system several different failure mechanisms interact involving a number of different individual elements. System analysis supports the calculation of a system reliability or risk. Examples of system analysis methods are (Moubray, 1997, CUR, 1997): fault tree analysis; Failure Mode, Effects and Criticality Analysis (FMECA); cause consequence charts. The most suitable system analysis method depends on the type of application. Reliability centred maintenance often uses FMECA to structure the analysis of the engineering system.

Probabilistic calculations of engineering system probability of failure usually benefit from a fault tree analysis. A fault tree lists the logical succession of all events that lead to one undesired top event. This event is placed in top of the tree. Fault trees are especially suitable for displaying cause-consequence chains that lead to an undesired top event, when one cause has two distinct consequences, e.g. yes or no, positive or negative, good or bad, failing or not failing. Only the negative consequences are listed in the fault tree.

2.2. Uncertainty classification

Many different kinds of uncertainty are involved with the design and construction of engineering structures. The classification of these uncertainty types enables the development of appropriate statistical models for the uncertainties in the engineering problem. Several sources suggest uncertainty classification in the engineering industry. A typical uncertainty classification is e.g. given by Ditlevsen & Madsen (1996) into physical uncertainty, statistical uncertainty and model uncertainty. Another example is provided by Paté-Cornell (1996) who suggests a main

classification into aleatory and epistemic uncertainties. Van Gelder (1999) further refines this classification in the context of risk-based design of flood defences. Figure 2.1 presents this uncertainty classification, in which inherent uncertainty is another term for aleatory uncertainty. Van Gelder (1999) and Vrijling & Van Gelder (2005) illustrate how such an uncertainty classification guides uncertainty reduction. In flood and coastal management in the UK Defra / Environment Agency (2002) recommends an uncertainty classification that builds amongst others on Van Gelder (1999). It refers to natural variability rather than inherent or aleatory uncertainty and adds decision uncertainty to the epistemic uncertainty branch.

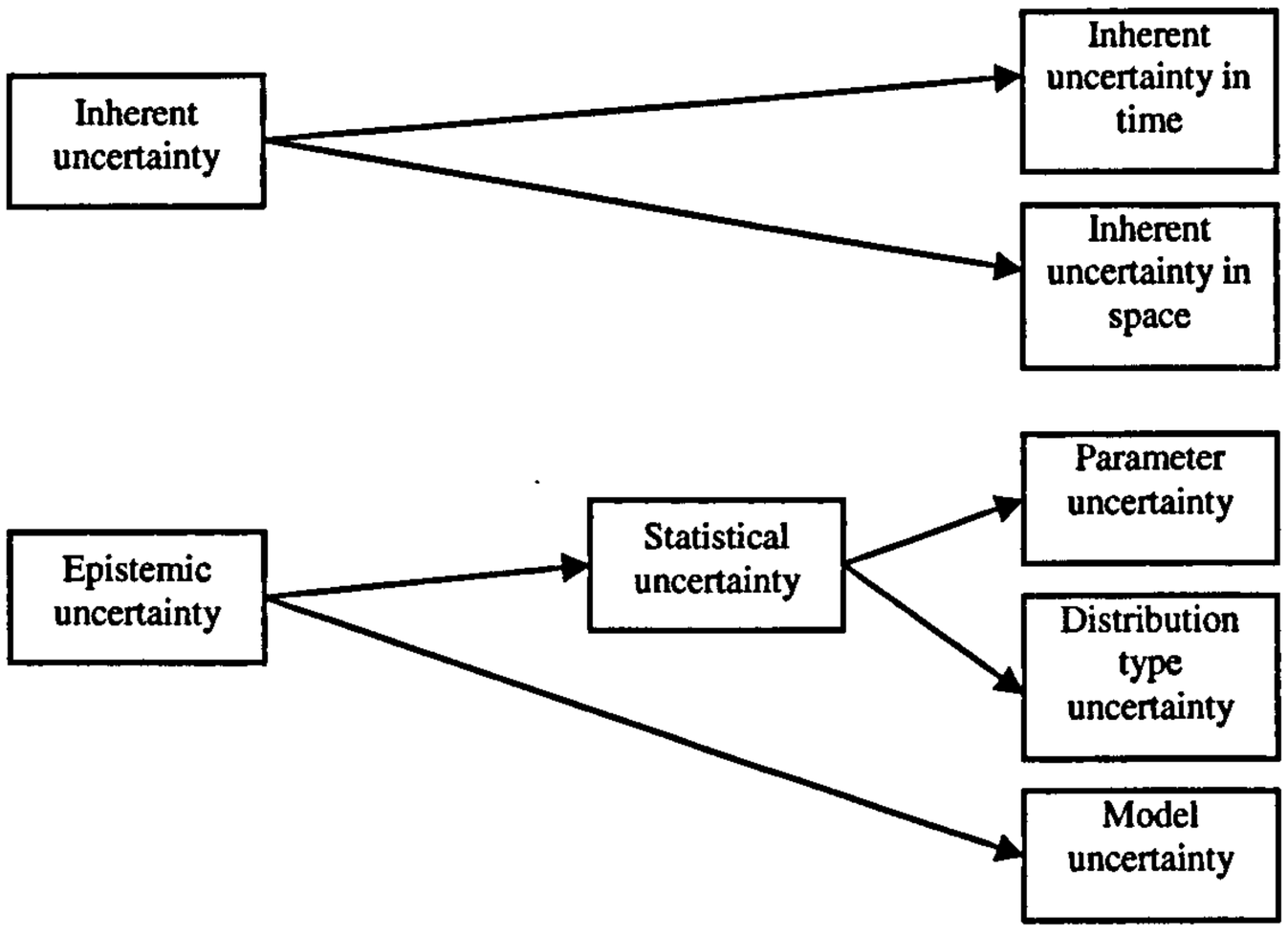

Figure 2.1 Uncertainty classification, from Vrijling & Van Gelder (2005)

Van Gelder (1999) provides a description of the different uncertainty types. Inherent uncertainty in time represents the uncertainty about the future realisation of a variable. Inherent uncertainty in space is the natural variation present in for instance soil properties. Statistical uncertainty is introduced when due to the restricted size of the dataset several different statistical distribution functions and parameter values may be equally credible. Statistical uncertainty of variations in time concerns the limited availability of time records to support the estimation of the probability of exceedance in the extreme tail. Statistical uncertainty of variations in space covers the limited ability to exactly measure the variations in space across all locations. Another type of spatial statistical uncertainty is the limited ability of statistical models to exactly represent the measurements, even if they are exactly known across all

locations. Model uncertainty refers to the extent of representation of physical reality provided by the process model predictions.

Inherent uncertainties in time and space are considered to be irreducible as they are naturally present, Vrijling & Van Gelder (2005). Consider the following idealised situation. It is assumed that the crest levels along the flood defence line are exactly known at each location. The (in this case exactly known) variations in crest levels along the flood defence line represent the inherent uncertainty in space. The flood risk assessment is carried out for a grid containing a limited number of flood defence sections. The inherent spatial variations of the flood defence properties between two flood defence sections within that grid are captured by a statistical distribution function and a correlation structure. The result would be equal if the uncertainties are taken into account by carrying out the flood risk assessment with an infinitely fine grid in which the crest level is deterministic at each location. The inherent spatial uncertainties are thus irreducible. Practically, the ability to carry out flood risk assessments with an infinitely fine grid is limited. Another practical limitation is the inability to measure flood defence properties at each location. As mentioned before, this limitation is considered to be statistical rather than inherent uncertainty of spatial variations, which is reducible epistemic uncertainty.

Epistemic uncertainties are caused by lack of knowledge and can generally be reduced by gathering data, research or expert elicitation.

2.3. Probabilistic calculation methods

Three levels of probabilistic calculation methods are distinguished. Level 3 methods approximate the integral in equation (2.2). For instance Riemann integration carries out step-by-step integration of (2.2), e.g. Lannoy (2004). Monte Carlo and directional sampling methods are described by Ditlevsen & Madsen (1996). Monte Carlo methods randomly sample from the (joint) probabilistic distribution functions of the basic random variables, Lannoy (2004), CUR 190 (1997). The joint probability distribution function $F_X(X)$ of the variables $X_1, \ldots, X_n$ in the limit state function can be written as:

$$F_X(X) = F_{X_1}(X_1) \cdot F_{X_2|X_1}(X_2|X_1) \cdots F_{X_n|X_1,X_2,\ldots,X_{n-1}}(X_n|X_1, X_2, \ldots, X_{n-1}) \qquad (2.3)$$

A cumulative distribution function F_X maps $X_1, \ldots, X_n$ onto the interval [0,1]. This mapping can be represented by a uniform distribution $U(0,1)$. The Monte Carlo

simulations sample m values from $U(0,1)$ and transform them with the inverse distribution F_X^{-1} to $X_1,\ldots, X_n$. For each sample the value of $g(X)$, equation (2.1) is calculated, and overall:

$$m_f = \sum_{j=1}^{m} I(g(X)) \tag{2.4}$$

In which $I(g(X))$ is the indicator function:

$$\begin{aligned} I(g(X)) &= 1 \qquad g(X) \le 0 \\ I(g(X)) &= 0 \qquad g(X) > 0 \end{aligned} \tag{2.5}$$

The number of times m_f that $Z \le 0$ is divided by the total number of simulations m to estimate the probability of failure P_f:

$$P_f \approx \frac{m_f}{m} \tag{2.6}$$

The standard deviation σ_ε of the probability of failure P_f in case of m simulations is given by:

$$\sigma_\varepsilon = \sqrt{\frac{1 - P_f}{m P_f}} \tag{2.7}$$

Level 2 methods iteratively approximate the probability of failure based on an

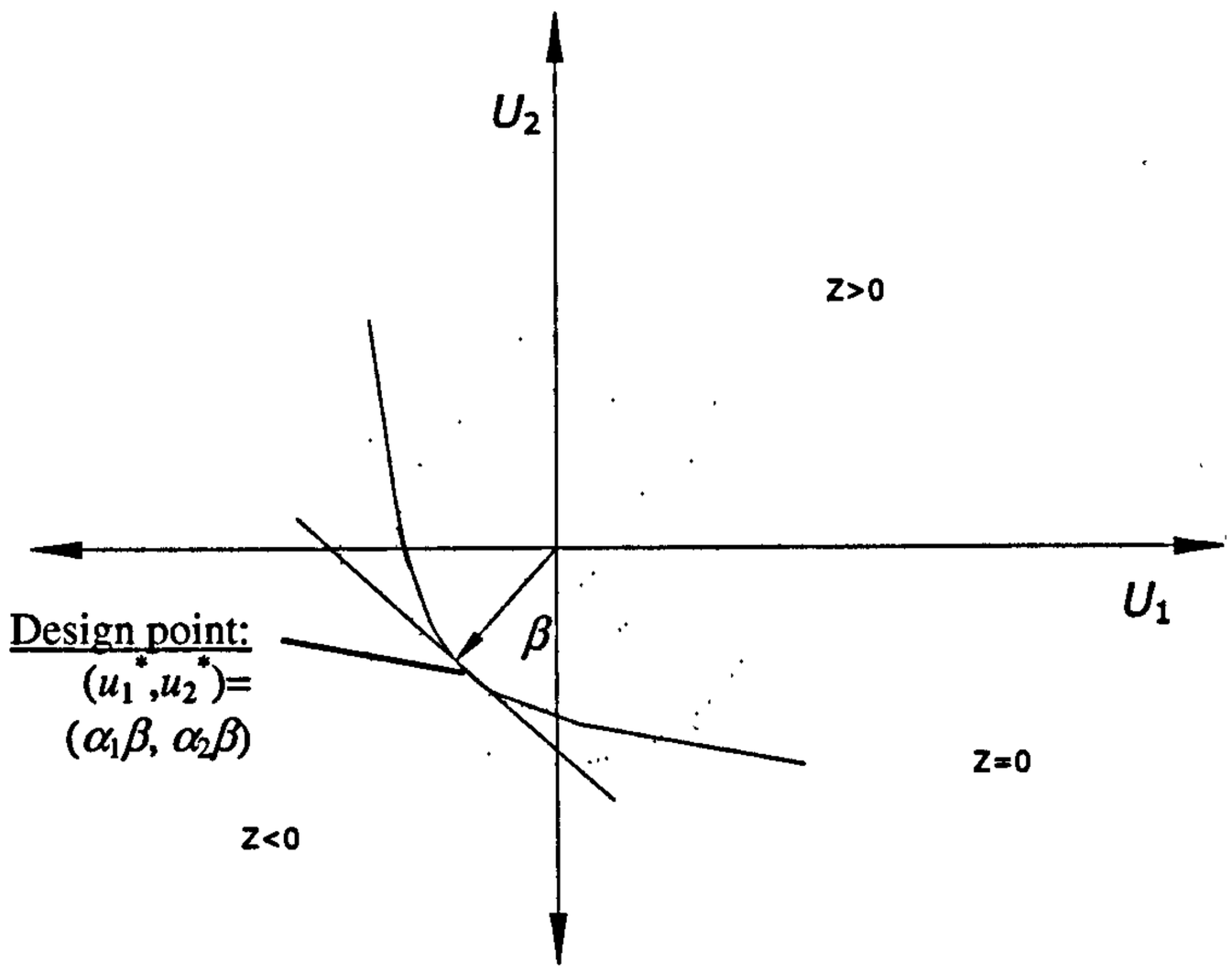

Figure 2.2 Linearization of Z as a function of standard normal variables U_1 and U_2. The reliability index β is the shortest distance between the origin and the limit state function.

idealization of the failure space and transformation of the basic random variables. See for details Thoft-Christensen & Baker (1982), Ditlevsen & Madsen (1996) or Melchers (1999). First Order Reliability Method, FORM, is an example of a level 2 method. FORM approximates the probability of failure by transformation of the limit state function to the standard normal space, followed by linearization and iteration to the design point, see figure 2.2. Hasofer & Lind (1974) show that the calculated probability of failure is invariant for the formulation of the limit state equation, if the limit state function is linearized in the design point. The design point is the realization of $X_1,..,\ X_n$ with the highest joint probability density in the normal space, usually found on the boundary between failure and non-failure $Z=g(X)=0$. The design point is characterized by the shortest distance between $Z=0$ and the origin in the standard normal space. This distance is indicated by β_{HL}, the reliability index, defined by:

$$\beta_{HL} = \frac{\mu_z}{\sigma_z} \tag{2.8}$$

in which μ_z is the mean value and σ_z is the standard deviation of the limit state function Z. The basic variables in equation (2.1) are transformed to standard normal variables $U_1,..,U_n$. Equation (2.1) then becomes a function g_u of standard normal variables $Z=g_u(U_1,..,\ U_n)$. Linearization of g_u in the design point with coordinates $(u_1^*,..,\ u_n^*)$ by means of a Taylor expansion leads to:

$$g_u(U_1,..,U_n) = g_u(\vec{u}^*) + \sum_{i=1}^{n} \frac{\partial g_u}{\partial U_i}(\vec{u}^*)(U_i - u_i^*) \tag{2.9}$$

$$g_u(u_1^*,..,u_n^*) = 0 \tag{2.10}$$

(2.10) is a requirement in the design point. Influence coefficients are defined by:

$$\alpha_i = -\frac{\frac{\partial g_u}{\partial U_i}(\vec{u}^*)}{\sqrt{\sum_{j=1}^{n}\left(\frac{\partial g_u}{\partial U_j}(\vec{u}^*)\right)^2}} \qquad i = 1,..,n \tag{2.11}$$

The coordinates of the design point $(u_1^*,..,\ u_n^*)$ equal $(\alpha_1\beta_{HL},..,\alpha_n\beta_{HL})$. The coordinates of the design point are unknown in advance and are found by iterative calculations of (2.10) and (2.11). Starting values are given to $\alpha_1,\ ..,\ \alpha_n$ and β_{HL}. The linearized limit state function in the standard normal space, $Z_{T;st}$, can also be written in a standardized form once $\alpha_1,\ ..,\ \alpha_n$ and β_{HL} have been established:

$$Z_{T;st} = \beta_{HL} - \alpha_1 u_1 + \cdots + \alpha_n u_n = \beta_{HL} - \alpha^T U \qquad (2.12)$$

(2.12) illustrates that the influence coefficients are in fact direction cosines. They indicate the contribution of the uncertainty of individual variables to the overall probability of failure. $(\alpha_i)^2$ is therefore the linear correlation coefficient, $\rho(Z,X_i)$, between the variable X_i and function Z in the design point, Hohenbichler & Rackwitz (1986). Transformation methods are available to deal with non-normally distributed variables and correlated basic random variables, Vrijling & Van Gelder (2000).

The probability of failure is approximated with:

$$P_f = P(Z \le 0) \approx P\left(\beta_{HL} - \alpha^T U \le 0\right) = \Phi(-\beta_{HL}) \qquad (2.13)$$

More sophisticated level 2 methods exist such as the Second Order Reliability Method, SORM. First a FORM approximation of the design point is carried out to find a design point. SORM refines the reliability index by fitting a second order curvature to the design point rather than a Taylor expansion, see Breitung (1984) or Ditlevsen & Madsen (1996).

Level 1 methods embed the uncertainty with regard to structural properties in reliability estimates by means of safety factors. For example strength properties are adjusted to represent a value which is exceeded in 95% of the cases, whilst loading properties are adjusted to represent a value which is exceeded in 5% of the cases.

2.4. Time-dependent reliability analysis

Structural reliability is a relative measure depending on the specified reference period over which it is calculated, see section 2.1.2. As will be seen in section 2.2, the reliability or probability of failure during a lifetime interval of a structure is required to carry out quantitative life-cycle costing. The hazard rate is closely related to the probability distribution function of structural lifetime. These two notions are therefore firstly introduced below. Secondly, the correlation between two limit state functions in time is presented and its implications for lifetime probability and hazard rate. Finally, the two main approaches to derive interval reliability are brought forward: time-integrated and time-dependent reliability.

2.4.1. Lifetime probability and hazard rate

The lifetime probability distribution function $F_L(t)$ is (with reference to: Melchers, 1999, CUR 190, 1997, Vrouwenvelder, 2005):

$$F_L(t) = P(L \le t) = P_L(t) \tag{2.14}$$

in which L is the lifetime and t is the specified period of interest, $P_L(t)$ is therefore the probability of structural failure in this period. The lifetime probability density function is given by $f_L(t)$:

$$f_L(t) = \frac{dF_L(t)}{dt} \tag{2.15}$$

The probability of failure in a specified period dt during the lifetime is:

$$P(t < L < t + dt) = F_L(t + dt) - F_L(t) = f_L(t)dt \tag{2.16}$$

This can also be formulated as:

$$f_L(t)dt = P((\textit{failure for } \tau \in (t, t + dt)) \cap (\textit{no failure for } \tau \in (0, t))) \tag{2.17}$$

The hazard rate, $r(t)$, is the probability that failure occurs in a specified period given that no failure occurred in the preceding period, and is formulated as follows:

$$\begin{aligned} r(t)dt &= P\left((\textit{failure for } \tau \in (t, t + dt)) \,\middle|\, (\textit{no failure for } \tau \in (0, t))\right) \\ &= \frac{f_L(t)dt}{(\textit{no failure for } \tau \in (0, t))} = \frac{f_L(t)dt}{1 - F_L(t)} \end{aligned} \tag{2.18}$$

The relationship between the hazard rate on the one hand and the lifetime probability distribution and density on the other hand is:

$$f_L(t)dt = r(t)dt(1 - F_L(t)) \tag{2.19}$$

$$r(t) = \frac{f_L(t)}{1 - F_L(t)} \tag{2.20}$$

The lifetime probability distribution is found by solving the differential equation below.

$$\frac{dF_L(t)}{dt} = (1 - F_L(t))r(t) \tag{2.21}$$

$$F_L(t) = 1 - \exp\left\{-\int_0^t r(\tau)d\tau\right\} \tag{2.22}$$

In mechanical engineering practice the hazard rate is often associated to the notion of the bathtub curve. The hazard rate decreases in the early stages of the object's

lifetime, due to infant mortality. Infant mortality is followed by a relatively constant hazard rate, finally overtaken by an increasing hazard rate due to aging. Moubray (1997) speaks of a 'bathtub curve' fallacy based on age-reliability patterns for non-structural aircraft equipment. According to this research only 4% of the equipment displayed age-reliability behaviour in the form of a bathtub curve. Most of the equipment, 82%, had infant mortality followed by a slowly increasing hazard rate, or a generally constant failure rate. In terms of maintenance the interesting effect is that replacement or repair as-good-as-new of such components does not change the time to failure. On the contrary, the new component might show infant mortality and therefore increase the probability of failure.

2.4.2. Time-integrated and time-dependent reliability

One or more variables can introduce time-dependency in the reliability analysis, in both the strength and the loading models. For instance in (2.23) below $X_{i;t}$ introduces time-dependency in $Z(t)$:

$$Z(t) = g(X_1, \ldots, X_{i;t}, \ldots, X_n) \tag{2.23}$$

Time-integrated reliability analysis captures the time-dependency of $X_{i;t}$ by means of one statistical distribution function for a period of interest $[0,T]$. Subsequently, the probability of failure during that period is calculated. The reference period can be any convenient duration, e.g. one year or ten years. Such statistical distribution functions are for example the annual maximum water levels, the distribution function of the significant wave height during a storm or other extreme value distributions of loading variables.

Time-dependent reliability analysis describes $X_{i;t}$ by means of a time-dependent process based model or a stochastic process and calculates the reliability per unit time (with reference to: Melchers, 1999, CUR 190, 1997, Vrouwenvelder, 2005). With

$$F_L(T) = P(L \le T) = 1 - P[Z(X(t), t) > 0] \qquad \forall t \in [0,T] \tag{2.24}$$

Equation (2.24) can generally not be solved analytically, Engelund et al. (1995b). $F_L(T)$ in equation (2.24), or the probability of failure in specified time interval $[0,T]$ of interest can be approximated with the outcrossing approach. The outcrossing approach then approximates the lifetime probability $F_L(T)$ with a Poisson distribution based on the assumption of independent outcrossings, Engelund et al. (1995b):

$$F_L(T) \approx 1 - \exp\left\{- E\left[N^+(T)\right]\right\} \tag{2.25}$$

in which $E[N^+(T)]$ is the mean number of crossings of $X(t)$ into the failure domain during $[0,T]$. In the stationary case $E[N^+(T)] = \nu^+T$, where ν^+ is the outcrossing intensity. In this paper the lifetime period of interest $[0,T]$ is subdivided into N time intervals Δt. The mean number of crossings in a time interval is approximated by $P_f(\Delta t_i)$, the time-dependent probability of failure during a period Δt_i, and relates to (2.17). The numerical implementation to calculate $P_f(\Delta t_i)$ is described in appendix E.

2.4.3. Autocorrelation between reliability at two moments in time

Investigation into the autocorrelation between the reliability at two moments in time indicates whether this correlation can be attributed to loading uncertainty or strength uncertainty. Vrijling & Van Gelder (1998) derive the following expression for the correlation between the reliability at $t=i$ and that at $t=j$, $\rho(Z_i, Z_j)$:

$$\rho(Z_i, Z_j) = \frac{\rho_{R_i,R_j}\sigma_{R_i}\sigma_{R_j} + \rho_{S_i,S_j}\sigma_{S_j}\sigma_{S_i}}{\sigma_{Z_i}\sigma_{Z_j}} \tag{2.26}$$

In which ρ_{R_i,R_j} is the correlation between the strength R at $t=i$ and $t=j$, σ_{R_i} is the standard deviation of the strength at $t=i$, σ_{R_j} is the standard deviation of the strength at $t=j$, ρ_{S_i,S_j} is the correlation between the loading S at $t=i$ and at $t=j$, σ_{S_i} is the standard deviation of the loading at $t=i$ and σ_{S_j} is the standard deviation of the loading at $t=j$.

(2.26) corresponds with the autocorrelation coefficient in space between two segments of dike ring given by CUR 141 (1990), characterised by Z_i and Z_j. Equation (2.26) can therefore be considered from both a spatial and a temporal autocorrelation point of view. From a temporal point of view (2.26) strength variables are assumed to be fully correlated in two consecutive time steps i and j. Additionally, loading variables are assumed to be uncorrelated if the loading is formed by the hydraulic climate.

These two assumptions lead to $\rho_{R_i,R_j} \approx 1$ and $\rho_{S_i,S_j} \approx 0$, leaving together with (2.26) the following expression, see Vrijling & Van Gelder (1998):

$$\rho(Z_i, Z_j) = \frac{\sigma_R^2}{\sigma_R^2 + \sigma_S^2} \tag{2.27}$$

Therefore if $\sigma_S >> \sigma_R$ then $\rho(Z_i, Z_j) \rightarrow 0$, which implies that consecutive time steps can assumed to be independent, then (2.26) approximates α_R^2. The coefficient of influence or direction cosine α_R is defined according to (2.11). So, if the coefficients of influence of the strength variables are negligible compared to those of the loading variables, then the correlation between the reliability at two consecutive time steps is practically zero. Zero correlation between the reliability at two consecutive time steps implies independent probabilities of failure at $t=i$ and at $t=j$. This situation allows a simplification of the lifetime probability integral:

$$F_L(N) = 1 - (1 - p)^N \approx 1 - \exp(-Np) \qquad (2.28)$$

in which $F_L(N)$ is the probability that the lifetime L is smaller than N years and p is the probability of failure during a unit time, e.g. a year.

Flood defences with a high uncertainty related to loading, σ_S, relative to that related to strength, σ_R, are characterised by a low correlation coefficient (Vrijling & Van Gelder, 1998). A low correlation coefficient implies a relatively constant hazard rate and independent annual probabilities of failure. Conversely, a low uncertainty related to loading relative to that related to strength leads to a nearly fully correlated reliability in time. A high correlation coefficient implies that the annual probability of failure equals the lifetime probability of failure and that the hazard rate decreases to a constant probability or even zero. This behaviour relates to the concept of proven strength. Proven strength implies that once a flood defence has been able to withstand a representation of typical storms, it can be expected to do so in future. Proven strength relates to the constant hazard rate to which the 'infant mortality' part of the bathtub curve stabilises.

2.5. Reliability-based flood defence design

The benefits of probabilistic methods for flood defences were recognised early (Van Dantzig, 1956 and the Delta commission, 1960). The Delta commission (1960) made recommendations about the required safety levels in the dike ring areas in the Netherlands and set out how to achieve and maintain them. It was recognised at the time that probabilistic methods provided a rational approach, but were not computationally feasible. In the course of the last decades the computational capacity of computers developed sufficiently to enable flood defence system reliability models.

Probabilistic reliability analysis approaches for flood defences were formulated, e.g. CUR 141 (1990), Vrijling (2001), Van Gelder (1999), Vrouwenvelder et al. (2001a & 2001b), Vrouwenvelder (1999) and piloted, e.g. DWW (2006) and TAW (2000). Following and extending these developments are the probabilistic reliability analyses for flood defences in Kortenhaus & Oumeraci (2002) and Buijs et al. (2006). The improvement of the computational feasibility remains a continued subject of research interest due to the complexity of flood risk assessment models, see e.g. Dawson et al. (2005) and Dawson (2006)

Reliability-based methods for flood defences embedded in software developed in the Netherlands (Vrouwenvelder (1999, 2001a & 2001b) is summarised below. The following main parts are discussed: modelling approaches of the flood defence system, failure mechanisms statistical models and probabilistic methods.

Modelling approaches for flood defence systems

The first step in the modelling approach is a definition of the flood defence system and its main structure types. The definition of the system is related to the boundaries of the floodplain protected by the flood defence line. The historical failure processes of the main structure types are established. Secondly, the failure mechanisms and their mutual relations are analysed per structure type and organised in a fault tree. Limit state equations are formulated for the failure mechanisms. The fault tree captures the logical relations between the failure mechanisms. Thirdly, the flood defence line is discretised into flood defence sections. Each section is represented by one cross section and its corresponding characteristics. The extracted information from the flood defence system serves as a basis for the probabilistic calculations. This model is developed in specific for the Dartford Creek to Swanscombe Marshes flood defence system in chapter 7. Another illustration of the process to capture a real flood defence system in a reliability analysis can be found in Buijs et al. (2003) (after CUR, 1990).

Failure mechanisms

Vrouwenvelder et al. (2001a) recasts existing failure mechanism models into limit state equations. These failure mechanism models correspond to or are similar to the mainly deterministic safety assessment of flood defences in practice, see TAW (1985), TAW (1989), TAW (1995), TAW (1997), TAW (1999). These process models provide a fairly detailed representation of the main failure mechanisms of dikes. In the mean

time they are computationally feasible within a system reliability model which is applied in large scale safety evaluations. Floodsite (2007) and Kortenhaus & Oumeraci (2002) represent failure mechanisms by process models and limit state functions with a similar degree of complexity. Floodsite (2007) is a comprehensive source covering a variety of structure types subject to different types of hydraulic loading conditions.

Process models of varying complexity are available for flood defence failure mechanisms, e.g. Finite Element Methods or even one equation models, and are applicable within a reliability analysis. The required detail of the reliability analysis, and hence the detail of the failure mechanism representation, depends on the decision-making context, see Defra / Environment Agency (2002) and table 2.3.

Statistical models

In a reliability analysis of a flood defence system statistical models are relevant regarding: the individual random variables in the limit state equations, the spatial random field involved with material properties and the statistical model of the hydraulic boundary conditions.

Vrouwenvelder et al. (2001b) applies the following spatial autocorrelation function to soil properties (figure 2.3):

$$\rho(\Delta x) = \rho_x + (1 - \rho_x)\exp\left\{-\frac{\Delta x^2}{d_x^2}\right\} \tag{2.29}$$

In which ρ_x is a constant correlation and d_x is the correlation distance. A similar function can be found in Baecher & Christian (2003). The correlation distance can

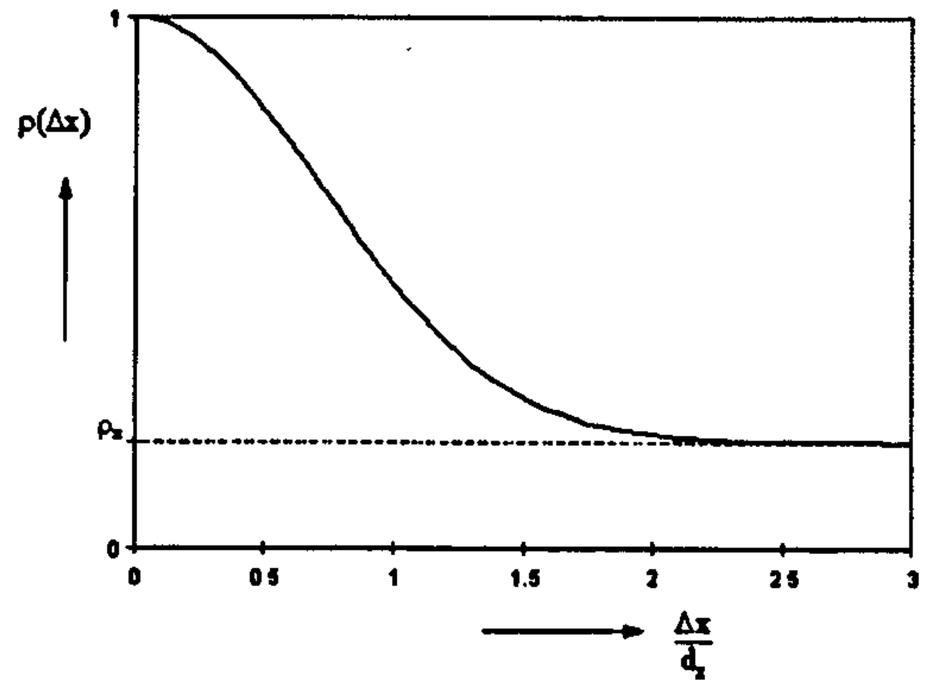

Figure 2.3 Left: shape of the correlation function, Vrouwenvelder et al., 2001.

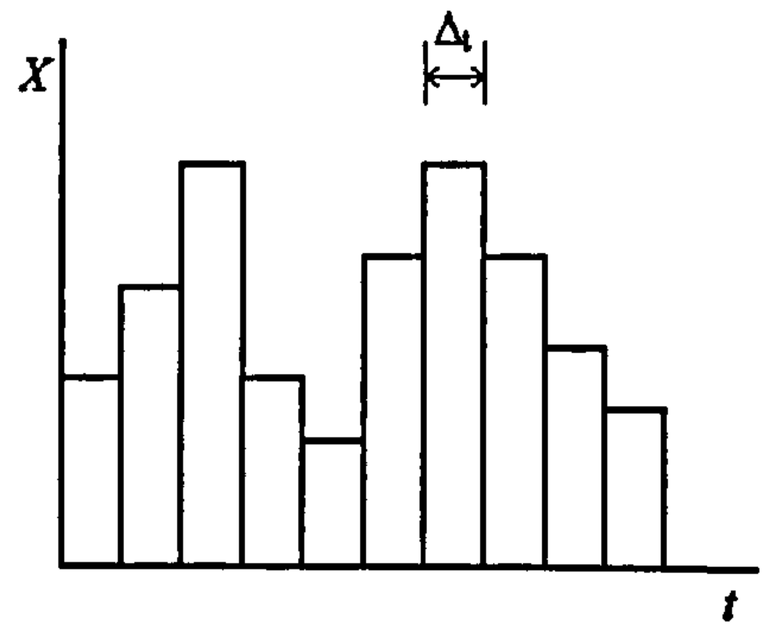

Figure 2.4 Representation of the Borges Castanheta model, Vrouwenvelder et al., 2001.

either be considered in the vertical or horizontal direction. The autocorrelation of a soil property between two closely located points along the flood defence line is practically one. The autocorrelation of a soil property between two points with a distance of more than two times the correlation distance goes to a constant value, ρ_x, or zero.

Coastal flood defence systems are loaded by correlated sea water levels, i.e. astronomical tide plus wind set up and additional surge due to low barometric pressures, and wave conditions. Examples of statistical models for sea water levels and wind speeds during storms are Join-Sea, Hawkes et al. (2002) and HR Wallingford (1998), or Diermanse et al. (2001).

Fluvial flood defence systems are loaded by high water events brought on by high river discharges. In Vrouwenvelder (1999, 2001a & 2001b) the return periods of peak discharge values are modelled with a logarithmic function. The peak discharge values are related to the period during which a discharge exceeding a defined discharge threshold persists, see Diermanse et al. (2001) for a description of the statistical model. The high water events are represented by means of the Borges Castanheta renewal model, i.e. the high water events are independent and have a constant discharge value during a time interval, see figure 2.4.

The water level and wave conditions at tidal rivers or estuaries are determined by river discharges as well as correlated sea water levels and wind speeds. Models such as Isis, TUFlow or Sobek serve to predict estuarial and tidal river local water levels. Mani Raj Dahal et al. (2005) set up a response database that contains the local water level predictions in an estuary as a function of different combinations of discharges, local water levels and wind speeds. The advantage is that during the probabilistic calculations the local water level corresponding to a combination of a river discharge, sea water level and wind speed can be looked up in the database. That saves time in running a full numerical model for each FORM iteration or Monte Carlo simulation. Vrouwenvelder et al. (2001) apply a similar approach and the same procedure is adopted in Buijs et al. (2006).

Probabilistic calculation methods

The probabilistic calculation methods to approximate the probability of failure for one failure mechanism are discussed in section 2.1.3. FORM, SORM, Monte Carlo

simulation, Latin hypercube and directional sampling are often applied in this context. The overall probability of failure of a flood defence section consists of an assembly of failure mechanisms connected with e.g. logical AND-gates or OR-gates. The overall probability of failure can be approximated by means of Monte Carlo or Hohenbichler (1983). Vrouwenvelder (1999) employs a procedure based on Hohenbichler & Rackwitz (1983) to combine multiple correlated failure mechanisms of flood defences. Vrouwenvelder (1999) also deals with flood defence system reliability. The material or soil properties in the flood defence line and the foundation thereof form a random field. In other words, material properties, geometry, vegetation, hydraulic boundary conditions or other characteristics that make up flood defence reliability can have dependent statistical properties along the flood defence line. Because of these dependencies, it is possible that failure occurs simultaneously over certain defence stretches and breach locations tend to be spatially related. Vrouwenvelder (1999) considers the flood defence system as consisting of n elements. An element can for instance be: a flood defence (cross) section, a tide, a wind direction, a stretch, a failure mode. Each element is represented by one limit state function. Two elements of the system are chosen and are combined to form one equivalent representative element. In other words two limit state functions are combined to one. The total amount of elements in the system is then reduced from n to n-1. Repeating this procedure over and over again will eventually reduce the amount of elements in the system to one. In other words, the system is "wrapped up". The procedure to find one equivalent representative limit state function is based on the method according to Hohenbichler & Rackwitz (1983). This procedure calculates $P(Z_1<0 \text{ AND } Z_2<0)$ taking the mutual correlation between element 1 and element 2 into account. If this probability is known, then $P(Z_1<0 \text{ OR } Z_2<0)$ follows.

2.6. Review

This chapter provides background information about risk and reliability-based methods in the engineering industry. The uncertainty classification in reliability-based flood defence design is a suitable framework for the analysis of uncertainties associated with asset time-dependent processes. The definitions in structural reliability are given and probabilistic calculation methods are explained. The most important concepts in

time-dependent reliability are introduced. In the last section existing reliability-based methods for flood defence design are discussed.

Statistical models for deterioration processes are eventually embedded within the reliability analysis of flood defence systems. The time-dependent reliability approach is followed in this thesis rather than the time-integrated reliability approach to derive lifetime probability of failure in chapter 7. The reliability analysis forms part of an overarching rational maintenance framework for flood defence management. Current practice in flood defence management and rational maintenance decision-making frameworks are the subject of chapter 3.

3. Flood defence management and rational maintenance decision-making

A quantitative rational maintenance optimisation framework has not yet been defined specifically for flood defence management. The specification of such a framework requires an overview of current practice in flood defence management as well as of knowledge about the types of rational decision-making approaches. This overview provides insight in the type of maintenance optimisation framework that is expected to be suitable for rational flood defence management.

Such an impression is necessary for this thesis firstly to understand how the reliability-based approach for asset time-dependent processes contributes to an overarching rational maintenance optimisation model. Secondly, the choice to use a Markovian or Bayesian modelling approach for asset time-dependent processes is reviewed in the context of the overarching optimisation model. A Markovian or Bayesian approach determines how historical and future time series observations are incorporated. The choice therefore impinges e.g. on how monitoring events are modelled in the optimisation model and on which type of statistical time-dependency models are developed. Thirdly, the maintenance operations in flood defence management practice and the Bayesian decision-making framework form the context of the importance measures developed in chapter 4.

Section 3.1 describes the flood defence management environment in practice. Flood defence management in the Thames Estuary, introduced in 3.1.1, is the main context in this thesis. Section 3.1.2 and 3.1.3 discuss current flood defence management and developments of current practice towards rational management methods. Rational maintenance decision-making methods are outlined in 3.2. These methods can be fully quantitative, as in 3.2.1, or fully qualitative, as in 3.2.2. The rationalisation of practical

management problems often results in the adoption of a mixture of qualitative and quantitative maintenance decision-making methods.

3.1. Flood defence management in practice

3.1.1. Introduction

The flood defence management environment in the UK, more specifically in the Thames Estuary, serves as the context for this thesis. The tidal levels in the Thames Estuary show an upward trend over the centuries, see figure 3.1. Extrapolation of that trend to the present day would entail a water level of around OD+6m. However, this trend is not taken into account in the study and is not picked up by the applied distribution of hydraulic boundary conditions. The flooding in 1953 was the trigger for a major flood defence improvement scheme carried out in the 1970s and 1980s. As part of this improvement scheme new earth embankments were designed, concrete walls added to raise existing embankments, floodgates put into place to provide flood protection and access to the docks, private frontages raised and existing sheet pile walls refurbished. The safety level of the Thames Estuary flood defence system is currently being reviewed. The flood defence system is required to accommodate a

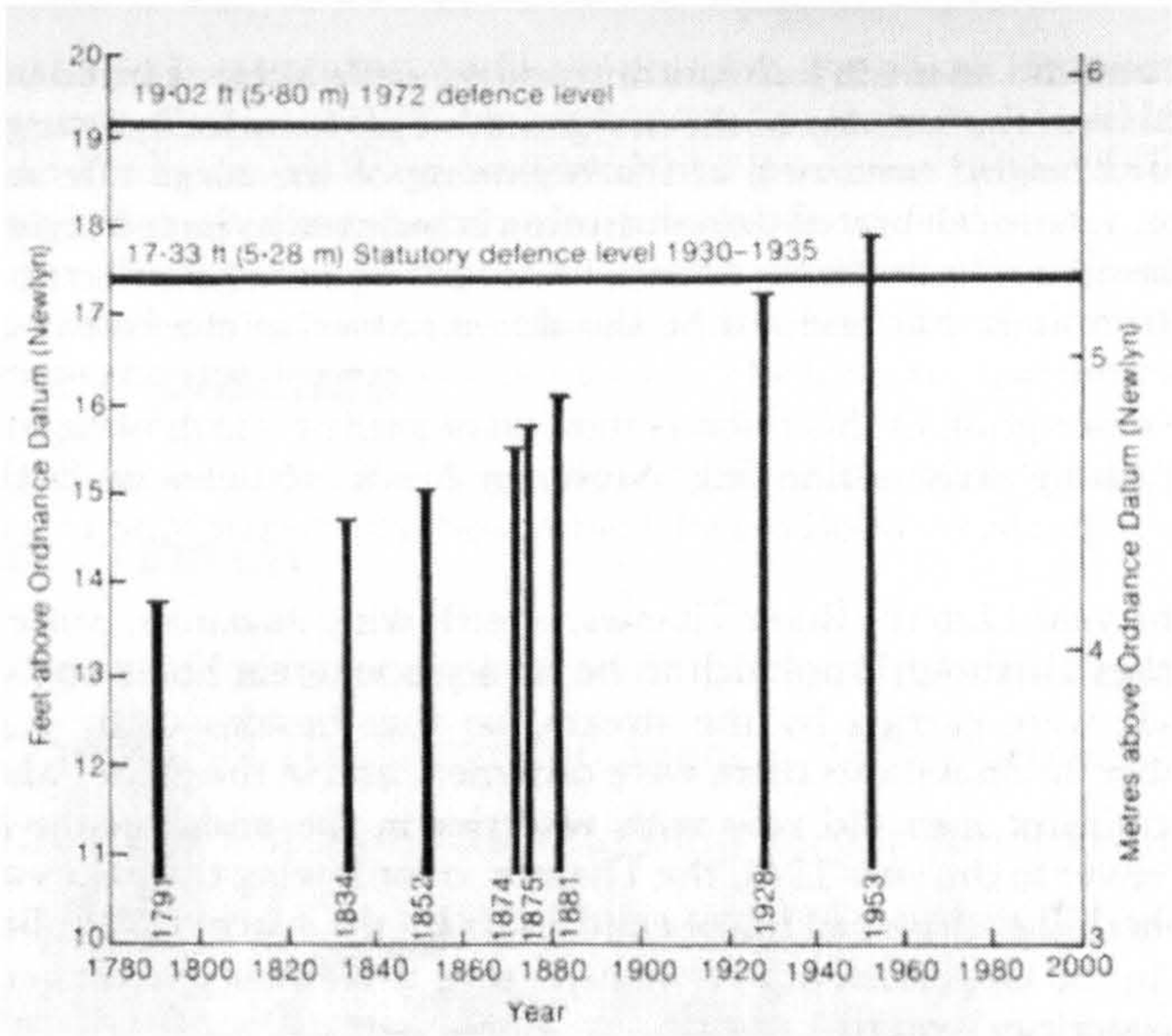

Figure 3.1 High water levels at the London Bridge in the Thames Estuary, from Gilbert & Horner (1984).

sufficient safety level until the year 2100. Risk assessment methods have been piloted to gain insight in the distribution of flood risk along the Thames Estuary. At locations where the safety level is deemed to be too low, flood defences will be replaced or refurbished to meet the required standard.

The inspection and maintenance intervention approach in the Thames Estuary corresponds with that recommended by the Environment Agency (1996) in the Flood Defence Management Manual (FDMM). Several flooding events in the 1990s and 2000s spurned further development of flood defence management in the UK. Examples of research and development in this area are Defra (2002), HR Wallingford (2004a), Simm et al. (2005).

Throughout history, the Netherlands has paid especially much attention to flood defence management and is particularly far advanced in this field. The next sections will therefore introduce the context in the Netherlands in more detail, in addition to the flood defence management context in the UK.

Flooding is receiving much attention worldwide due to damaging flooding events and climate change. Other examples of more advanced flood defence management systems than the Netherlands and the UK can be found in Germany and the USA. The differences in legislation in countries is a factor defining the flood defence management approach besides the physical aspects of the flood defence infrastructure, such as flood defence structure, hydraulic loading and type of floodplain. The next sections will highlight general aspects of flood defence management in other countries in addition to the approaches in the UK and the Netherlands.

3.1.2. Current practice

Current practice in the UK

Currently two types of guidance play an important role in flood and coastal defence management. The FDMM (Environment Agency, 1996) provides guidance on routine asset management, whilst projects requiring larger funding budgets are appraised according to the Flood and Coastal Defence Project Appraisal Guidance (FCDPAG).

The general aim for flood and coastal management in England and Wales is defined by FCDPAG 1 (MAFF, 2001). The more specific aim for performance evaluation of

flood and coastal defences is given by FCDPAG 6, Defra / Environment Agency (2003): "Performance evaluation involves collecting evidence about how a given flood or coastal management process is performing when compared with its objectives... The main purpose of flood and coastal defence is to reduce risk to a level compatible with the land use and the cost of mitigation works at an acceptable benefit to cost ratio..."

FCDPAG 6 (Defra / Environment Agency, 2003), recommends the following seven sequential components in performance evaluation.

1. The policy starting point or problem identification sets off the performance evaluation.
2. The objective setting spans in addition to flood protection a number of additional areas of interest, such as: environment (habitat and environmental effects of construction or maintenance), health and safety of construction and assets, amenity, public and sociological aspects and finally knowledge and innovation whereby reduction in uncertainty due to data acquisition or R&D is achieved.
3. Condition assessment aims to capture information about the state of the flood defence structure.
4. Performance assessment is the assessment of performance and failure probability of critical defences and overall system under current and projected conditions.
5. The need for management intervention is investigated, leading to a decision for management intervention or do-nothing. This decision-making is based on the consideration of the resulting risk reduction and the improvement in risk or reliability due to management intervention. Several priority and management options including 'whole life' strategies for managing aging assets are tested.
6. The preferred management intervention option is identified based on re-examining risk reduction, and assessing the costs and benefits.
7. The implementation of the management intervention option (or do-nothing). Subsequently, the flood defence performance must be regularly monitored and reviewed by iterating the previous six steps.

In contrast to the objective setting for flood defence performance evaluation in FCDPAG 6, the FDMM (Environment Agency, 1996), is not transparent in its objective setting specific to flood defence management. Therefore, the condition indicators

(condition grading) and performance indicators (Standards of Service) do not clearly reflect performance targets. Additionally (perhaps partly consequently), the prioritisation procedure is generally perceived to be confusing (see Defra / Environment Agency, 2004a).

As mentioned above, condition assessment acquires information about the state of a flood defence structure. Defra / Environment Agency (2004a) breaks inspection activities in current practice down into two main categories: routine inspection and specific inspection.

Routine inspections are directed at the external properties of flood defence structures. They refer according to Defra / Environment Agency (2004a) either to routine visual inspection or to quantitative activities in the form of remote sensing or monitoring. In the first place, routine visual inspection is the visual condition assessment of flood and coastal defences, which is mainly driven according to the FDMM. The procedure breaks the flood or coastal defence down into structural elements. It then requires an asset inspector to assign an assessment of condition to each flood or coastal defence element on a scale from 1 to 5, corresponding with: very good (1), good (2), fair (3), poor (4) and very poor (5). The asset inspectors are supported in their assessment by their experience and standard photographic guidelines accompanying the FDMM (Environment Agency, 1996). Practically this system leads to problems with subjectivity, consistency and comparability. Secondly, quantitative activities in the form of remote sensing or monitoring cover for instance specific issues such as: non-intrusive measurements, simple intrusive techniques, or strategic issues like topography levelling, bathymetry and seabed sediments.

Specific inspections are directed at the internal properties of the flood defence. They refer according to Defra / Environment Agency (2004a) either to non-destructive (geo-physical) testing or to intrusive testing. In the first case, non-destructive (geo-physical) testing investigates the internal state of the flood defence from the surface of the defence. For instance by use of: electromagnetic cover meter (monitoring steel reinforcement in concrete), ultrasonic pulse velocity (for cracking and honeycombing in concrete structures), geo-radar (subsurface stratification, voids or differences in material in earth embankments). Secondly, intrusive testing investigates the internal state of the flood defence by taking samples from the defence. Examples according to material: concrete – dynamic response techniques for structural integrity, internal fracture to test the strength; metals – liquid dye penetrant for surface defects; soils –

window sampling, core cutter method for the density of soil, vane test for the in-situ shear strength of soils.

As mentioned above, performance assessment and management prioritisation is currently not underpinned by a transparent process of objective setting, definition of performance standards and comparison with performance indicators. At an asset level, Defra / Environment Agency (2004a) summarises two types of maintenance from the FDMM, Environment Agency (1996): periodic maintenance and routine maintenance.

Periodic maintenance consists typically of structural and embankment repairs. This type of maintenance is prioritised on the basis of condition grading, e.g. grade 5 assets are maintained in preference to grade 3.

Routine maintenance represents the majority of the maintenance activities and consists typically of dredging, weed cutting, grass cutting. For prioritisation, the FDMM, Environment Agency (1996), suggests the use of the Standard of Service rating (SoS rating). This rating is awarded to a flood defence stretch based on the properties that are at risk of flooding due to the state of the flood defence and the land use in the floodplain. A SoS rating of 1 is well below target whereas 6 is well above target. The FDMM, Environment Agency (1996), does not provide guidance on how to incorporate quantitative measurements into the condition grading or Standards of Service rating.

Some regions in England and Wales establish simple risk-based inspection frequencies, such as displayed in table 3.1.

Table 3.1 Risk-based frequency of flood defence asset inspections (from Environment Agency work instruction)

		Asset re-inspection frequency in months		
Impact of failure within the reach	High	12	6	6
	Medium	36	12	6
	Low	36	36	12
		Low	Medium	High
		Likelihood of failure within the reach		

Current practice in the Netherlands

In the Netherlands, according to Ministerie van Verkeer en Waterstaat (2004), the Law on flood defence prescribes a five yearly safety assessment for flood defences.

The strength of the flood defence must thereby be sufficient to withstand a design water level with a frequency of exceedance that is specified in the law (figure 3.2). The frequency of exceedance differs across the regions in the Netherlands.

Ministerie van Verkeer en Waterstaat (2004) points out that the perspective on safety safety assessments depends on the context in which it is carried out. The flood defence designer starts from scratch and optimises the costs of construction and maintenance given all the functions the flood defence is designed to fulfil during its lifetime. The flood defence manager determines the management policy to keep the defence in a good condition minimising the costs and assuring a sufficient fulfilment of its functions. The five yearly safety assessments are thereby solely focussed on the function of water retention.

The safety assessment of a flood defence consists of a comparison of the strength of the defence against the loading introduced by the design water level. The strength of

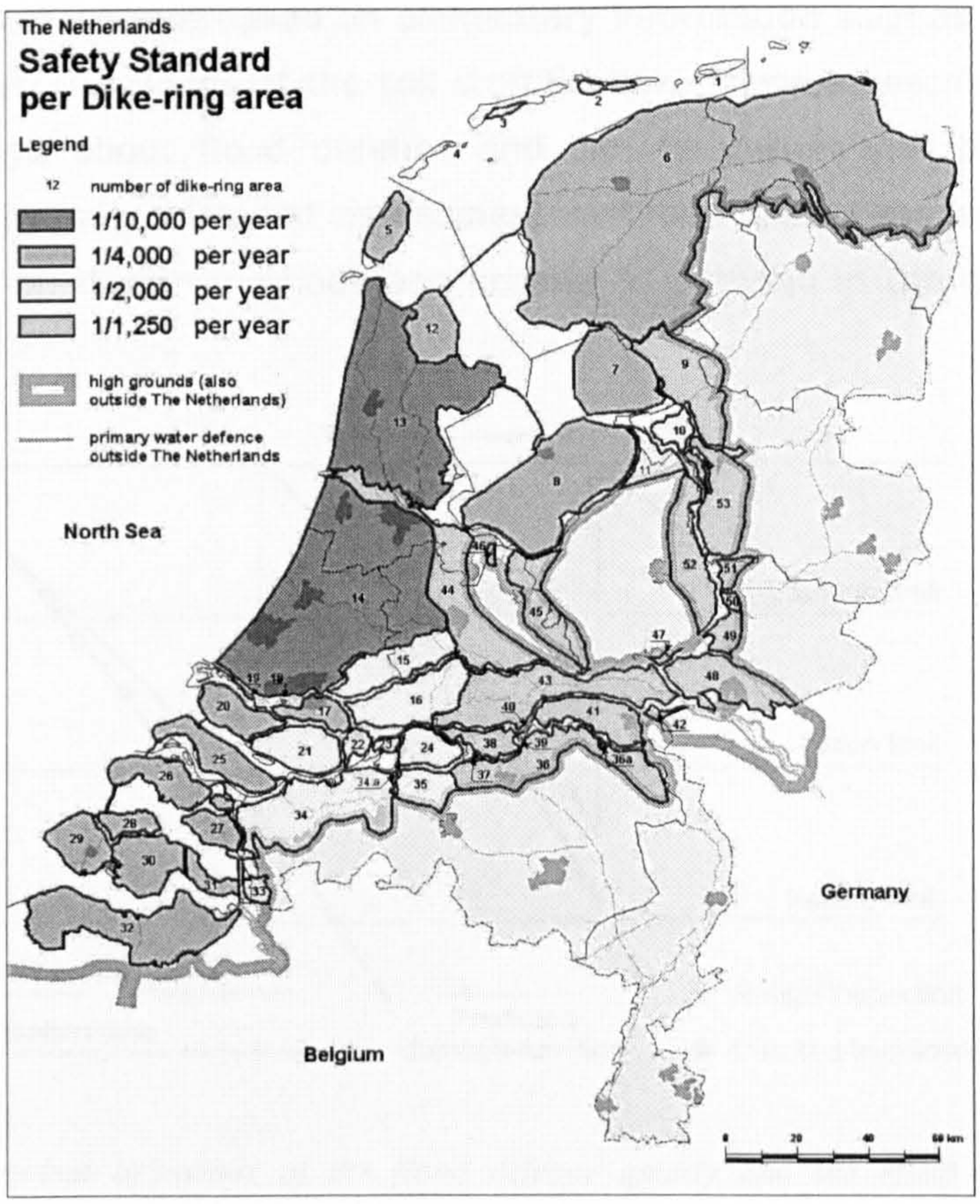

Figure 3.2 Frequency of exceedance for design water levels across the ring dike areas in the Netherlands.

the defence is represented by a number of failure mechanisms, which are individually tested. It is the responsibility of the local flood defence manager to carry out these safety assessments. The assessment results in a score: good, insufficient, sufficient or no judgement (in case of e.g. insufficient information). The score 'good' is awarded to flood defences that have their original design quality. The score 'insufficient' is awarded to a flood defence with insufficient strength that directly needs to be improved. The score 'sufficient' represent a broader range of flood defences. This score does not require immediate improvement, but close flood defence manager involvement is advised in this judgement. 'No judgement' is awarded in case of insufficient data on the defence characteristics and hydraulic boundary conditions or if there is no assessment method available.

There are three levels of safety assessment leading up to the aforementioned scores. Each level increases in detail and required expertise (Ministerie van Verkeer en Waterstaat, 2004). Firstly, simple or geometrical assessment methods assess the dimensions of the flood defence based on elementary information such as the defence geometry or indicative knowledge of the soil stratification. These assessments require elementary knowledge about flood defence and can be carried out by the flood defence manager. Secondly, detailed assessment methods assess the safety of the flood defence based on design methods and criteria as outlined in the guidelines or

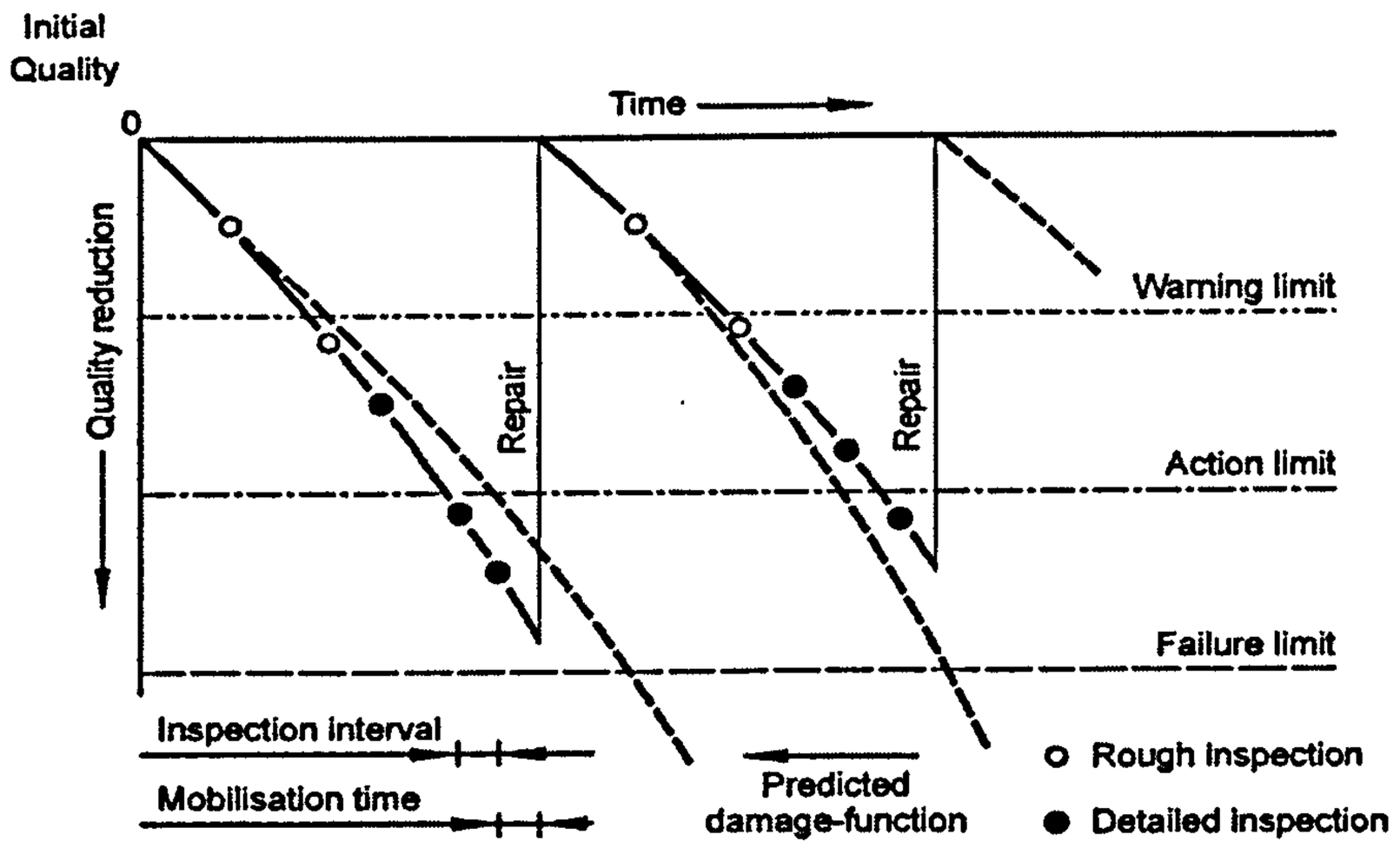

Figure 3.3 The time-dependent behaviour of the flood defence quality and the effect of repair and inspection hereupon.

technical reports according to the Technical Advisory Committee on flood defence (TAW). These assessments require knowledge regarding failure mechanisms and design methods. They require more technical expertise from flood defence managers or flood defence experts. Thirdly, advanced assessment methods are used when the generally accepted methods such as the TAW guidelines or technical reports are insufficient. The assessment can then be tailored to the specific flood defence building on the state-of-the-art knowledge from experts.

The actual assessed and the required safety provided by the flood defence system are documented and in the care of the flood defence manager. The actions that the flood defence manager can take to bring the flood defence up to its required standards are: variable maintenance, improvement works, restoration measures or regular maintenance. In the first case, variable maintenance restores the original state by conservation, renovation or replacement. The flood defence manager can decide to carry out this type of maintenance, following a safety assessment. For this action no approval at a provincial level is required. Secondly, improvement works are activities that put the safety bar higher than the required standards specified in the documentation of the flood defence manager. In that case provincial approval is required to carry out the works. Thirdly, restoration measures restore other functions than flood defence to their desired standards. In the fourth case, regular maintenance carries out the maintenance at regular time intervals, e.g. on a yearly basis.

Figure 3.3 illustrates the effect of repair and inspection on the time-dependent behaviour of the flood defence quality.

Current practice in the USA

In the USA the US Army Corps of Engineers (USACE) is responsible for the management of civil works, including flood defence structures. According to ERDC (2000) the responsibility of the USACE is to evaluate, maintain, repair, and rehabilitate these (hydraulic) structures. The primary objective of Repair, Evaluation, Maintenance, and Rehabilitation (REMR) Management Systems is to help managers obtain the best facility condition for a given budget level, ERDC (1996a).

A central role in condition assessment and prioritisation of operational management is the condition index (CI), a numerical indicator of facility condition and function level, ERDC (1996b). Table 3.2 relates the condition index to a linguistic condition

description and an appropriate level of management action. The combination of the condition indices of different components within a structure is underpinned by partly physical, partly expert judgement based arguments. ERDC (1996b) points out that the condition index should be derived from measurements or observations which can be directly related to the physical condition and performance (function) of the facility. It must also be aimed to carry out monitoring in such a way that repeatable measurements or observations are achieved. It must be possible to make them consistent over time and they must be acceptable to those who manage the facility. A number of technical reports and notes are tailored to a hydraulic structure or material and define the condition measurements / observations required for an algorithm to derive the condition index.

Table 3.2 Zoning of the condition index, condition description and recommended actions, from ERDC (1996b)

Zone	Condition Index	Condition Description	Recommended Action
1	85 to 100	Excellent: No noticeable defects. Some aging or wear may be visible.	Immediate action is not required.
	70 to 84	Good: Only minor deterioration or defects are evident.	
2	55 to 69	Fair: Some deterioration or defects are evident, but function is not significantly affected.	Economic analysis of repair alternatives is recommended to determine appropriate action.
	40 to 54	Marginal: Moderate deterioration. Function is still adequate.	
3	25 to 39	Poor: Serious deterioration in at least some portions of the structure. Function is inadequate.	Detailed evaluation is required to determine the need for repair, rehabilitation, or reconstruction. Safety evaluation is recommended.
	10 to 24	Very Poor: Extensive deterioration. Barely functional.	
	0 to 9	Failed: No longer functions. General failure or complete failure of a major structural component.	

Decision support tools building on the condition index enable the comparison of the conditions between structures, the possibility to perform life-cycle costing and the systematic organisation of data. However, ERDC (2001) points out that two thirds of the Corps Districts utilise the condition index in some way, of which only one third fully apply the developed procedures. The Districts' main criticism of the condition indexing procedures is that it requires too much time, money and personnel to carry out. Although the condition index is seen as a useful tool, it is not believed that they need the condition index for the prioritisation of management works. Guidance on condition index inspection frequencies is currently lacking.

Besides the inspections in connection to the condition index the following types of increasingly detailed inspections are available, ERDC (2001): operational inspection,

annual inspection, periodic inspections, fracture critical members inspection and engineering inspection. Firstly, operational inspection aims to detect obvious indications of local failures or changes in project performance during the operation of a facility. Annual inspection identifies and prioritises maintenance needs for the budget cycle, described in a short summary report. These inspections may result in an engineering inspection related to particular concerns. Periodic inspections occur on a 5-yearly periodic cycle and include visits by representatives of all applicable engineering disciplines. Usually, the site visits include little investigation beyond an informal visual inspection. An important result is the Periodic Inspection Report that provides a descriptive and pictorial review of the project's condition. Along with the memories of senior personnel, it serves as the primary record of historical condition. Fracture critical members inspection is the 5-yearly inspection for fatigue cracks of fracture critical hydraulic steel structures. Finally, engineering inspection can occur as a result of concerns of project personnel and can be performed to determine if repairs are needed.

ERDC (2001) evaluates the status of the condition indexing system since its conception in the REMR programme. One benefit of the condition index is that it provides a standard language for the quantification of condition. Another benefit is that the condition index assists the operational manager to investigate known concerns and to identify specific problems that otherwise stay unknown. The condition index additionally encourages the creation of a condition history and the documentation of prioritisation of decision-making. Even though the condition index is criticised for requiring too many resources, it has a potential as data source for even more data hungry quantitative risk assessments and provides a replacement for these time intensive, expensive assessments.

Current practice in other countries

Current practice in other countries is summarised in Environment Agency (2004b) based on COMRISK. In Germany the State Water Act classifies the flood defences into two categories: "state dikes" or "other dikes". The "state dikes" protect the interest of the public wealth and fall under the responsibility of the state. These flood defences are required to protect the lowland against all storm surges and the standards associated with this level of protection are strictly defined. The "other dikes" fall under the responsibility of the local dike boards, also protect the interest of the public

wealth and are required to protect against storm surges in a less strict sense. The standards associated with the level of protection of "other dikes" are more flexible and set by the local dike boards. According to the State Water Act the flood and coastal defences must be inspected at least once a year and once in 10 to 15 years detailed safety assessments should be carried out.

In Belgium currently the focus is purely on the flood and coastal defences itself rather than as a system of defences protecting against loss of life and economic consequences. The main aims are to make the flood defences broader, stronger and wider and to fix the coastline. The safety of the flood defences are assessed according to the frequency of exceedance method as employed in The Netherlands. The coastline is monitored by yearly topographic surveys.

In Denmark the Performance of Flood Risk Management is embedded in a contractual framework between the Ministry of Transport (MT) and the Danish Coastal Authority (DCA), the latter falls under the responsibility of the MT. The framework addresses other issues besides those directly involved with flood defence performance such as e.g. the representation of the public interest in harbour facilities and coastal protection and more practically, for example providing information services for the public. The main guidelines with respect to maintaining the performance of flood and coastal defences are very focussed on finding the optimal technical solution to protect the value of the assets at stake whilst reducing interventions in the natural environment. Inspections are required to be carried out two times per year. Assessments of the dike profiles, extreme water levels and wave conditions are performed every five years. Coastal retreat and changes in dune width are monitored once per year and also five yearly evaluations of the hydraulic climate are made. For coastal defence a Share Agreement must be made every 4 years containing its performance targets and every two years the progress must be reported in an interim report.

3.1.3. Ongoing developments

Ongoing developments in the UK

The latest developments in the UK in flood and coastal management show an inclination to adopt risk and reliability-based methods. Defra / Environment Agency (2002) reviews and recommends suitable risk, performance and uncertainty methods

in flood and coastal defence. Sayers et al. (2002) recommend a tiered risk-based decision-making methodology, which is further developed by HR Wallingford (2004a). This tiered hierarchy aims to accommodate the differences in objective settings ranging from strategic to scheme levels, see table 3.3.

Table 3.3 Tiered hierarchy in objective setting and data supply, from Sayers et al. (2002).

Level	Decisions to inform	Data sources	Methodologies
High	National assessment of economic risk, risk to life or environmental risk Prioritisation of expenditure	Defence type Condition grades Standard of Service Indicative flood plain maps Socio-economic data Land use mapping	Generic probabilities of defence failure based on condition assessment and crest freeboard Assumed dependency between defence sections Empirical methods to determine likely flood extent
Intermediate	*Above plus:* Flood defence strategy planning Regulation of development Prioritisation of maintenance Planning of flood warning	*Above plus:* Defence crest level and other dimensions where available Joint probability load distributions Flood plain topography Detailed socio-economic data	Probabilities of defence failure from reliability analysis Systems reliability analysis using joint loading conditions Modelling of limited number of inundation scenarios
Detailed	*Above plus:* Scheme appraisal and optimisation	*Above plus:* All parameters required describing defence strength Synthetic time series of loading conditions	Simulation based reliability analysis of system Simulation modelling of inundation

The methodology builds on the Source-Pathway-Receptor-Consequences model (SPRC model) brought forward by Defra / Environment Agency (2002). A national flood risk assessment according to this methodology was carried out in 2002, Environment Agency (2002), as well as in the years 2004-2006. Further application is currently postponed until more refinement of the underlying methodology is achieved. The pathway in the SPRC model is represented by the concept of fragility, which provides the probability of flood defence failure given different loading conditions. HR Wallingford (2005) recommends probabilistic structural reliability methods to underpin the concept of fragility. Reviews of failure processes, available process-based models and indicators for flood defence structures in the UK are available in for example Environment Agency (2004a), HR Wallingford (2004b & 2004c), Floodsite (2007).

Defra / Environment Agency (2004a, 2004b & 2004c) report the findings of a scoping study for a performance-based asset management system (PAMS) for flood and

coastal management. This system aims to underpin operational decision-making with performance-based prioritisation. An operational framework centrally coordinates the links between condition assessment, performance assessment and management prioritisation. The next stage is to improve current asset management practice and flood risk appraisal by means of a number of Measured Steps Forward, Simm et al. (2006). The aim of these steps is to initiate a gradual change in flood defence management practice.

Ongoing developments in the Netherlands

A project initiated by the Dutch Directorate-General for Public Works and Water Management titled FLORIS, Flood Risks and Safety in the Netherlands, piloted numerical flood risk methods on a large number of ring dike areas in the Netherlands (DWW, 2006).

One of the main objectives was to determine the probabilities of flooding of the ring dike areas. The improvement on current practice is that the uncertainties in all the strength and (hydraulic) loading characteristics of the flood defence structure are taken into account. The results indicate the areas in the ring dike areas with the highest probabilities of flooding. These areas can be targeted in inspection, maintenance and improvement activities. Once an area with a high probability of flooding is targeted, the most relevant flood defence properties can be identified by analysing their uncertainty contribution.

A second main objective was to make a probabilistic assessment of hydraulic structures, taking into account: human error in gate closure procedures, historical information on the hydraulic structure, identification of information gaps.

A third main objective was to economically quantify the consequences of flooding by prediction of flood extent and depth etc. The consequences are only determined for a limited number of dike failures and storm loadings. This approximation is made based on the assumption that the flat nature of the floodplain results in near complete inundation regardless of the location of a breach. At present it is also assumed that a breach failure implies a full depth wide breach.

The fourth objective was to investigate methods to cope with the uncertainties associated with the results. These methods aim to provide e.g.: insight in the nature

and scope of uncertainties, ways to influence the uncertainties, ways to use the uncertainty results to inform safety improvement measures.

The results for the dike ring areas in the Netherlands for which a flood risk assessment was completed are published in DWW (2006). Debate is ongoing about the flood risk levels and the magnitude of the probabilities of inundation found in the assessment.

Ongoing developments in the USA

ERDC (2001) recognises that risk analysis allows the use of a logical framework to make estimates using time-dependent, distributed probabilities. The condition index is merely a condition-based measure of performance based on observations / measurements at a specific point in time. Reliability is based on both observable and non-observable conditions. The condition index therefore partially relates to reliability, but has a complimentary role in terms of summarising visual inspection information.

Ongoing developments in other countries

Probabilistic approaches of failure of sea dikes in Germany are discussed in Prodeich by Kortenhaus & Oumeraci (2002). Kortenhaus bases his approach on the development of reliability analysis for flood defences in the Netherlands. It contains a very comprehensive discussion of limit state functions in connection to earth embankments (sea dikes).

In most other countries the existence and increasing feasibility of risk-based methods for flood defences is recognised by participation in EU funded projects such as Floodsite. However, implementation of risk-based methods for flood defences is not yet achieved at a significant scale.

3.2. Rational maintenance decision-making

A quantitative rational maintenance optimisation framework has not yet been specified for flood defence management. The specification of such a framework requires an overview of current practice in flood defence management as well as knowledge about the types of rational decision-making approaches. An overview of current practice in flood defence management is given in the previous section. The following sections

introduce three types of rational maintenance decision-making frameworks: fully quantitative, fully qualitative and mixtures of quantitative and qualitative decision-making approaches.

The quantitative maintenance optimisation framework is a convenient overall structure for flood defence management. Four main building blocks in a quantitative framework are: functional system model, risk and reliability system model, operational management model and the calculation optimisation model (table 3.4). This approach is illustrated with a framework which has been developed for risk-based inspection planning in the offshore industry (Faber, 2000). This illustration shows where a time-dependent reliability contribution is required and in which form. In the context of the quantitative maintenance optimisation framework the choice for a Markovian or Bayesian modelling approach for statistical time-dependent process models is reviewed. The Markovian or Bayesian approach determines how historical and future time series observations are incorporated in the optimisation model. The choice therefore impinges e.g. on how monitoring events are modelled in the optimisation model and on which type of statistical time-dependency models are developed. The Markovian or Bayesian approach is an example of an assumption that affects the overall structure of the maintenance optimisation model. A mixture between a quantitative and qualitative maintenance decision-making approach combines the computational feasibility of a qualitative approach with quantitative objective prioritisation. This mixture approach is demonstrated with an application to design dike monitoring programmes. It is expected that the mixture approach is the most convenient model for the rational flood defence management decision-making framework.

Section 3.2.1 describes existing approaches and complements the building blocks of a quantitative maintenance optimisation model for flood defence systems. Sections 3.2.2 and 3.2.3 are illustrations of a qualitative and a mixture of a qualitative and quantitative rational maintenance decision-making framework. These are alternatives if the fully quantitative approach is not feasible due to the constraints in time and resources.

3.2.1. Quantitative maintenance decision-making

Maintenance optimisation models underpin quantitative maintenance decision-making. Dekker (1996) defines maintenance optimisation models as those mathematical

models whose aim it is to find the optimum balance between the costs and benefits of maintenance, subject to all kinds of constraints.

Table 3.4 The four main building blocks and an overview of the development in rational flood defence management.

Building blocks	Development in flood defence management
1. Functional system model	System function: flood protection, ground retention Bayesian decision-making framework
2. Risk and reliability system model	Rational flood risk assessment, section 1.2.2 Evaluation of Bayesian or Markovian approach to time-dependent processes
3. Operational management model	Management operations, section 3.1.2 Operational management after Vrijling (2003) or Defra / Environment Agency (2004c)
4. Calculation optimisation model	Mathematical formulation of the decision-making model and calculations. Not specified for flood defence management. Example: Faber (2000) risk-based inspection planning offshore industry. Shows place of system probability of failure in a time interval in the maintenance optimisation context.

Such optimisation models generally consist of four main building blocks (table 3.4), Dekker (1996). Pierskalla & Voelker (1976) describe similar components. The first building block is the functional system model and contains a description of a technical system, its function and its importance. The second building block is the risk and reliability system model. It consists of a model of the deterioration of the system in time and possible consequences for the system. The third building block is the operational management model and describes the available information about the system and the actions open to management. The fourth building block is the calculation optimisation model. This model includes an objective function and an optimisation technique to assist in finding the best balance between maintenance costs and benefits.

These four building blocks are shown in table 3.4 with an overview of the available information with respect to flood defence management. They are discussed more extensively below.

1st building block: functional system model

This building block relates to the technical system and the decision problem definition. The technical system is formed by the system of flood defences whose primary function is to provide flood protection, and secondary functions can consist of e.g. ground retention, or a mooring and loading dock facility.

The most well-known probabilistic decision-making model is the Bayesian decision problem in e.g. Raiffa & Schlaifer (1961), Benjamin & Cornell (1970):

1. Set of possible terminal acts: $A = \{a_1, a_2, ..., a_n\}$
2. Set of possible "states of the world": $S = \{s_1, s_2, ..., s_n\}$, whereby s' is the unknown true state.
3. Set of possible experiments: $E = \{e_0, e_1, e_2, ..., e_n\}$ in which e_0 indicates the possibility that the decision maker chooses not to experiment.
4. Set of potential outcomes of all experiments in E: $Z = \{z_1, z_2, ..., z_n\}$, whereby z' is the as-yet-unobserved outcome.
5. Utility function: u. This function is associated with a choice of experiment e and its outcome z. The subsequent choice for an action a combined with a particular state s will result in a consequence to which the decision-maker assigns the value $u(e, z, a, s)$.
6. Probability measure: P. It is assumed that the decision-maker can give an internally consistent set of probability assessments to events involving the 'unknown true state', related to S, and the 'as-yet-unobserved-outcome', related to Z.

Bernardo & Smith (2003) suggest a similar structure for sequential decision-making problems in case of design of experiments. The Bayesian decision problem is visualised by means of a decision tree, whereby square nodes represent a decision moment and a decision branch is followed by a possible range of outcomes, indicated by a circular node. Figure 3.4 shows an example of a sequential decision-making problem in case of design of experiments. The notation of *a, s, e, z* correspond with

those in the decision-making model described above. The upper branch is a situation whereby an experiment *e* delivers an outcome z_i, which forms the basis for an action *a* leading to state s_i. The lower branch is a situation whereby an action *a* is directly taken without an initial experiment, e_0, and leads to state s_i. In the flood defence management context, inspections are a form of experiments and repairs or replacements are a form of actions.

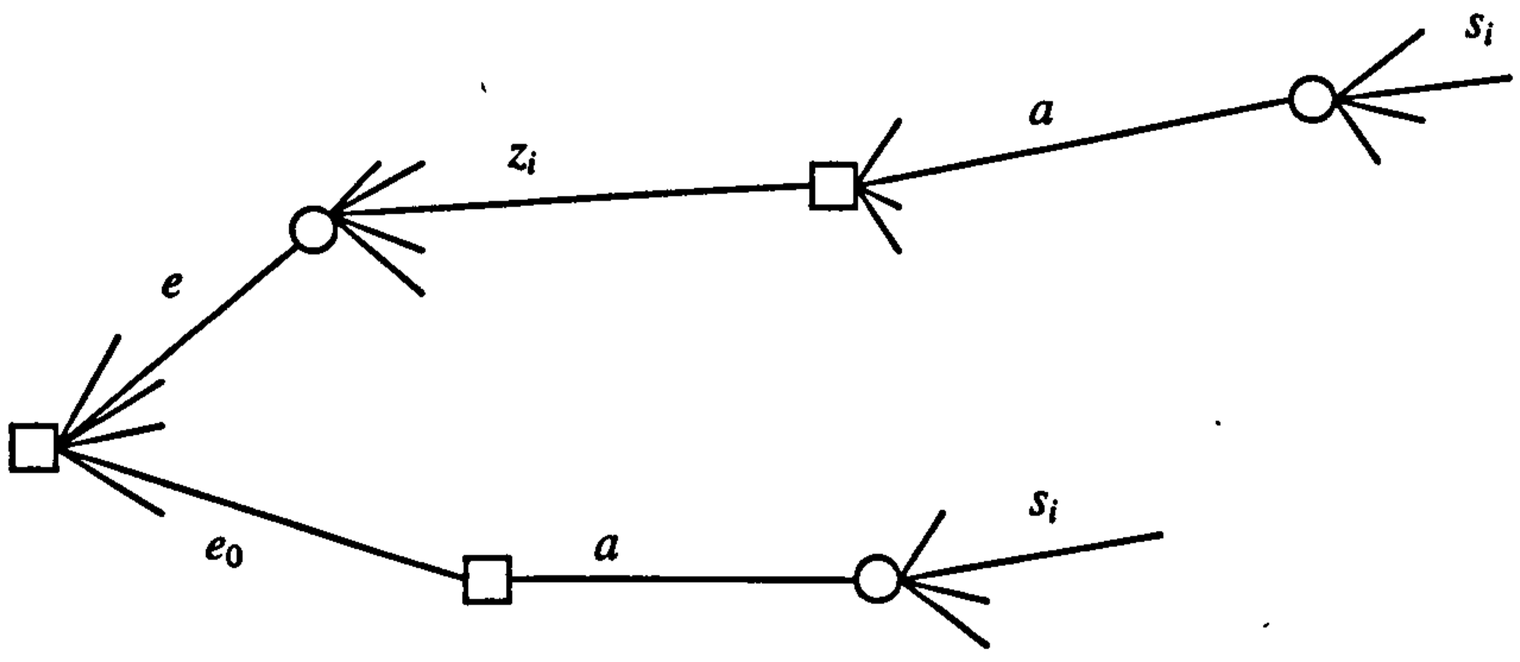

Figure 3.4 Example of sequential decision-making tree in case of design of experiments, following Bernardo & Smith (2003).

2nd building block: risk and reliability system model

This building block consists of a model of the deterioration of the system in time and possible consequences for the system. An overview of risk-based flood defence design is given in section 1.2.2. The place of time-dependent system reliability and consequences modelling in the existing rational flood risk assessment approach is shown in figure 1.2. The aim of this is thesis to investigate how the time-dependent behaviour of flood defences can be appropriately incorporated in a (system) reliability model.

Eventually the time-dependent system reliability model is intended to fit into the decision-making framework presented in figure 3.4. Inspections are in that context a form of experiments and repairs or replacements are a form of actions. The construction of a feasible maintenance optimisation framework according to figure 3.4 requires modelling assumptions and simplifications. Such assumptions can have a large impact on the formulation of the optimisation framework. It is for example possible to include the information from all inspections in the distribution function of a

flood defence property by posterior analysis, referred to as the Bayesian approach. It is also possible to incorporate the last inspection only and discard the rest of the historical observations about the flood defence property, referred to as Markovian decision processes. The difference between these two approaches is therefore how historical or future time series observations are processed in the decision-making. This choice has two implications for decision-making framework. Firstly, it determines the type of statistical models for the asset time-dependent processes. It is noted that the Bayesian maintenance optimisation framework also allows the incorporation of Markovian asset time-dependent process models. Secondly, it determines how the information from monitoring (experiments) is taken into account in the maintenance optimisation model. Below firstly some more details are given on both the Bayesian and the Markovian approach. Secondly, the two approaches are evaluated.

The Bayesian approach allows the assignment of subjective beliefs to flood defence properties and their time-dependent processes, in the form of distribution functions, as well as the incorporation of observations therein. Bayesian updating derives a posterior distribution function, *f''*, for a variable based on the subjectively estimated prior distribution function *f'* and observations z^*. Bayes' Theorem, e.g. Pratt et al. (1995), is defined as follows:

$$f''\left(s\middle|z^*\right)=\frac{P\left(z'=z^*\middle|s'=s\right)f'(s)}{\int_{-\infty}^{+\infty}P\left(z'=z^*\middle|s'=t\right)f'(t)dt} \qquad (3.1)$$

In which *s*, *z'*, z^*, *s'* are defined as in the Bayesian decision-making framework presented above and in figure 3.4. Bayesian updating therefore internalizes the observations into the prior judgment to find a revised distribution function, the posterior. The Bayesian approach thus allows the full incorporation of knowledge about historical time series in the optimization model. The structure provided by the Bayesian approach enables: the evaluation of different decision-making scenarios and their probabilities, the representation of continuous time-dependent processes and the internalization of observations therein.

Markovian decision processes are based on the Markovian property, with reference to e.g. Grimmet & Stirzaker (2001) or Ross (2003). The Markovian property entails that:

$$P_{ij}=\Pr\left\{X_{n+1}=j\middle|X_0=i_0,\ldots,X_{n-1}=i-1,X_n=i\right\}=\Pr\left\{X_{n+1}=j\middle|X_n=i\right\} \qquad (3.2)$$

which implies that the future state of the system only depends on its current state and not on its past states. The transition probabilities between all possible condition state pairs define the Markov chain X_n. The transition probabilities for one step are laid down in a one-step transition matrix:

$$\begin{bmatrix} P_{11} & P_{12} & \cdots & P_{1N} \\ P_{21} & P_{22} & \cdots & P_{2N} \\ \vdots & \vdots & \ddots & \vdots \\ P_{N1} & P_{N2} & \cdots & P_{NN} \end{bmatrix} \tag{3.3}$$

In the decision-making context (Frangopol et al., 2004), a finite set of actions A and Costs (i,a) are defined, which are incurred when the process is in state i and action $a \in A$ is taken. When the process is currently in state i and an action a is taken, the process moves into state j with probability

$$P_{ij}(a) = \Pr\{X_{n+1} = j | X_n = I, a_n = a\} \tag{3.4}$$

The definition of Markov decision processes involves the definition of stationary distributions or mean time to failure for the transition of one state into the other. The inspection, repair or improvement actions are related to specific states of the flood defence property. Two other applications of the Markovian property are mentioned in the context of statistical models for asset time-dependent processes. Firstly, it is possible to model discrete state processes. Secondly, stochastic processes such as Poisson processes or gamma processes are based on the loss of memory property. Advantages and disadvantages of the Bayesian and Markov decision processes are considered below.

Firstly, where Markov decision processes only process the current or contemporary state of the system the Bayesian approach incorporates the full historical time series. The Bayesian approach therefore contains more information about the actual time-dependent process. Secondly, modelling time-dependent processes which display dependency on their historical behaviour, with Markov processes is hard to justify. A third disadvantage is related to using the Markovian decision process for the overall maintenance optimisation framework. Castanier et al. (2003) demonstrate how continuous statistical models of degradation processes can be discretised to fit into a Markov decision-making framework. They consider elementary deterioration increments occurring between two successive maintenance times. A similar approach is adopted by Hontelez et al. (1996). The derivation of stationary distributions or

mean time to failure is based on the assumption that the continuous distribution functions of deterioration are not updated according to new observations.

A disadvantage of the Bayesian approach is that Bayesian updating of prior distribution functions with observations can become computationally very intensive. Especially complex systems require updating procedures for several flood defence sections and failure mechanisms simultaneously. In the mean time, the gain in information in the form of the posterior might not make very much difference in the reliability. It can then be desirable to partly discard historical information and apply a Markovian process model (section 1.2 Vanmarcke, 1983).

In this thesis the Bayesian approach for a maintenance optimisation framework is preferred over Markovian decision processes. The Bayesian approach enables modelling historical dependencies and the incorporation of historical and future time series observations. Markovian models for asset time-dependent processes are also applicable in the Bayesian approach. For example for discrete processes or when the loss of memory property is applicable, e.g. Poisson processes or gamma processes. The assumption of the Markov property for the whole overarching maintenance optimisation framework would per definition not allow for the incorporation of all the historical observations.

3rd building block: operational management model

This building block describes the available information about the system and the actions open to management. Maintenance operations in the flood defence industry are presented in section 3.2.1, based on Defra/Environment Agency (2004a), Ministerie van Verkeer en Waterstaat (2004) and ERDC (2001). In e.g. Castanier et al. (2003) the main maintenance operations are defined in a more general context. In all cited cases, the main categorisation of maintenance operations is: inspection, repair, replacement or improvement. Inspection of an object is tiered from superficial frequent visual inspections carried out by low-expertise staff to low frequent specific measurements carried out by high-expertise staff. Repair of an object can lead to an as good as new condition, or partial recovery in case of imperfect maintenance. Replacement involves the removal of an object and replacement by a new one.

Vrijling (2003) discusses several types of triggers that prompt a maintenance operation, derived from maintenance approaches in mechanical engineering. A flow

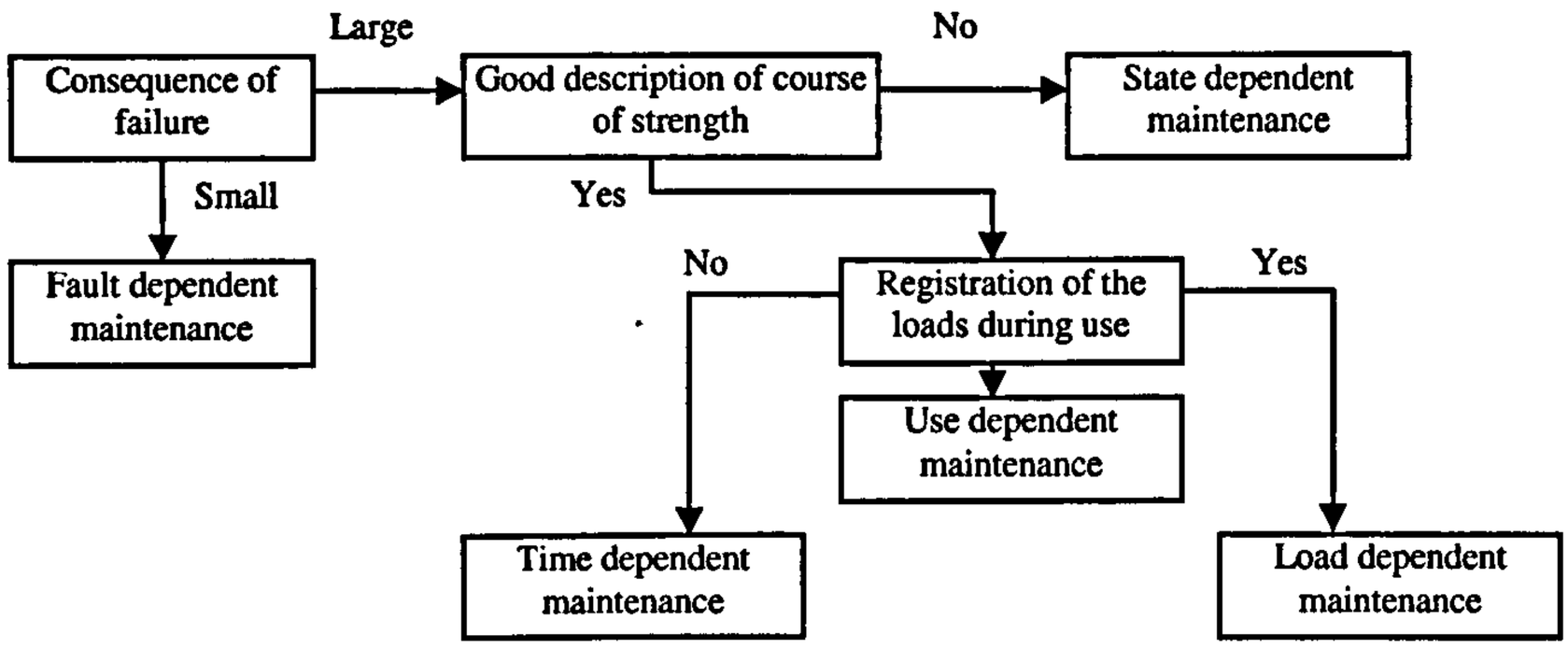

Figure 3.5 Selection of maintenance strategy in mechanical engineering, from Vrijling (2003)

chart is illustrated in figure 3.5. The two main strands are curative maintenance and preventive maintenance. *Curative or fault-dependent maintenance* repairs or replaces an object when it can no longer fulfil its function. Such a maintenance strategy is sometimes also referred to as Run-To-Failure. It requires the definition of a failure norm and the complete lifetime of the object is used. *Preventive maintenance* aims to intervene before the object fails to fulfil its function and is either use-dependent or condition-dependent. With use-dependent maintenance the trigger of a maintenance operation depends on the number of usage units. The total lifetime of the object is therefore not fully utilised. The types of triggers can be further broken down into load-dependent and time-dependent maintenance. Load-dependent maintenance registers the fluctuations in the loading of the hydraulic structure. Intervention takes place after a certain loading norm is exceeded, e.g. a cumulative load or an extreme loading condition. Time-dependent maintenance discretizes the lifetime of an object into constant time intervals between two subsequent maintenance operations. Condition-dependent or state-dependent maintenance carries out inspections at an optimal frequency to establish the condition. The decision whether or not to repair depends on the observations. Intervention norms can be related to each of the maintenance operations, e.g. a condition threshold triggering an increased inspection frequency or a repair activity. The lifetime of the object is usually better exploited than with a use-dependent maintenance approach.

The selection of an operational strategy can be made based on an approach such as shown in figure 3.5. According to Vrijling (2003) the choice between condition- or time-dependent maintenance in hydraulic engineering does not only depend on whether a good description of the strength in time is available. Time-dependent

maintenance is often chosen when inspection is not possible or expensive relative to the repair actions. Condition-dependent maintenance is applied when the prognosis of the strength in time is not possible or if the inspection is cheap.

Alternatively, Defra / Environment Agency (2004c) suggests a number of operational flood defence management options. These options organise the maintenance operations in section 3.2.1 in a performance-based context. The management options do not categorise the operations as being fault-dependent, time-dependent, load-dependent or condition-dependent.

4th building block: definition of the optimisation problem

The fourth building block includes an objective function and an optimisation technique to assist in finding the best balance between maintenance costs and benefits. The formulation of this optimisation technique is a function of the risk assessment model and the maintenance operations. The choice for a fully Bayesian or Markovian decision-making framework influences the formulation of the optimisation problem. The reader is referred to Castanier et al. (2003) for an illustration of a Markovian decision process for degradation and maintenance. In this thesis, the fully Bayesian approach is preferred over the Markovian decision processes as it allows the incorporation of historical dependencies and historical information in the optimisation model.

An illustration of such a maintenance optimisation model in the offshore industry is described below. Faber (2000) formulates a theoretical framework for Risk-Based Inspection (RBI) planning, see figure 3.6, after Raiffa & Schlaifer (1961) and Benjamin & Cornell (1970). This framework is based on the Bayesian decision-making

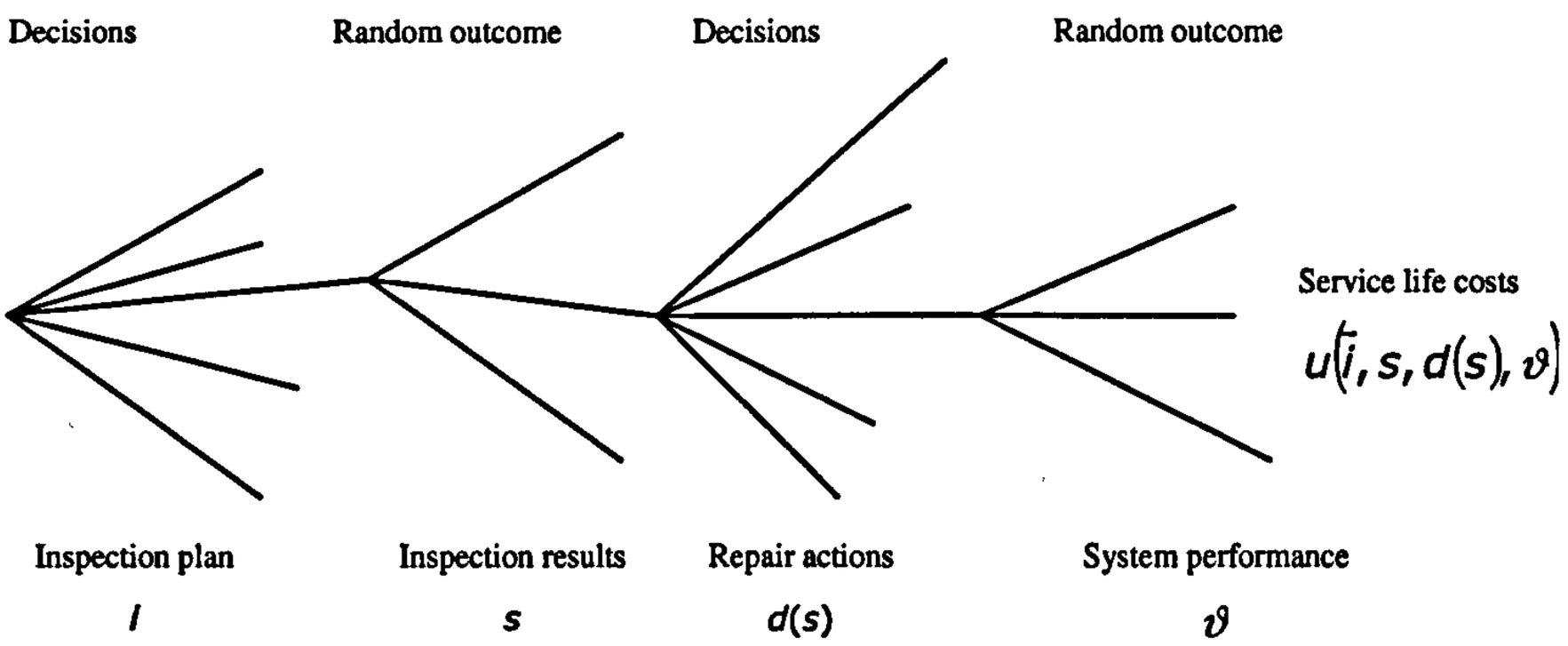

Figure 3.6 Bayesian decision-making context from Faber (2000)

model introduced above, compare figure 3.4 and figure 3.6. The example shows how a risk and reliability system model and an operational plan come together in the mathematical formulation of a maintenance optimisation problem. The example indicates the role of time-dependent system reliability and the required form of the time-dependent reliability calculation results.

Table 3.5 presents the main components of the inspection plan in the theoretical framework proposed by Faber (2000). The theoretical framework means to answer the questions: Where to inspect? What to inspect? How to inspect? When to inspect? RBI planning is a condition based approach whereby risk is considered for the structure or installation as a whole, targeting high risk elements. It is an approach that quantifies the effect on risk of different inspection options. The inspections encapsulate inspection effort, inspection quality and costs. The inspection option associated with the smallest risk is chosen.

Table 3.5 Components of the inspection plan in the theoretical framework proposed by Faber (2000)

Expression	Description
$\mathbf{i} = (\mathbf{\Delta t}, \mathbf{l}, \mathbf{r})^T$	Inspection plan, consisting of:
$\mathbf{\Delta t} = (\Delta t_1, \ldots, \Delta t_N)^T$	The intervals between the times of N inspections $\mathbf{t} = (t_1, \ldots, t_N)^T$
$\mathbf{l} = (\mathbf{l}(t_1), \ldots, \mathbf{l}(t_N))^T$	The locations to inspect at the inspection times with $\mathbf{l}(t_1) = (l_1, \ldots, l_{M(t_l)})^T$
$\mathbf{r} = (r_1, \ldots, r_N)^T$	The reliability (quality) of the planned inspections
$\mathbf{S} = (S(t_1), \ldots, S(t_N))^T$	Random vector of the uncertain inspection results, whereby the individual components refer to the results obtained from the inspections at the different locations $\mathbf{l}(t_i)$
$M(t_l)$	The total number of inspection locations at time t_l
$d(\mathbf{s})$	Decision rule defining the repair action to take depending on the inspection result
ϑ	Is the realisation of the uncertainties ϑ influencing the state of the system

Figure 3.7 shows a number of possible sequences of events. The life cycle optimisation problem is expressed as follows:

$$\min_{\mathbf{i},d}\left(C_I(\mathbf{i}, \mathbf{S}, d(s), \vartheta, M(t_l)) + C_R(\mathbf{i}, \mathbf{S}, d(s), \vartheta, M(t_l)) + C_F(\mathbf{i}, \mathbf{S}, d(s), \vartheta, M(t_l))\right)$$
$$s.t. \qquad \beta(T) \geq \beta_{\min} \tag{3.5}$$

in which C_I are the expected inspection costs, C_R the expected repair costs, C_F the expected failure costs and the generalised safety index β, which is defined as:

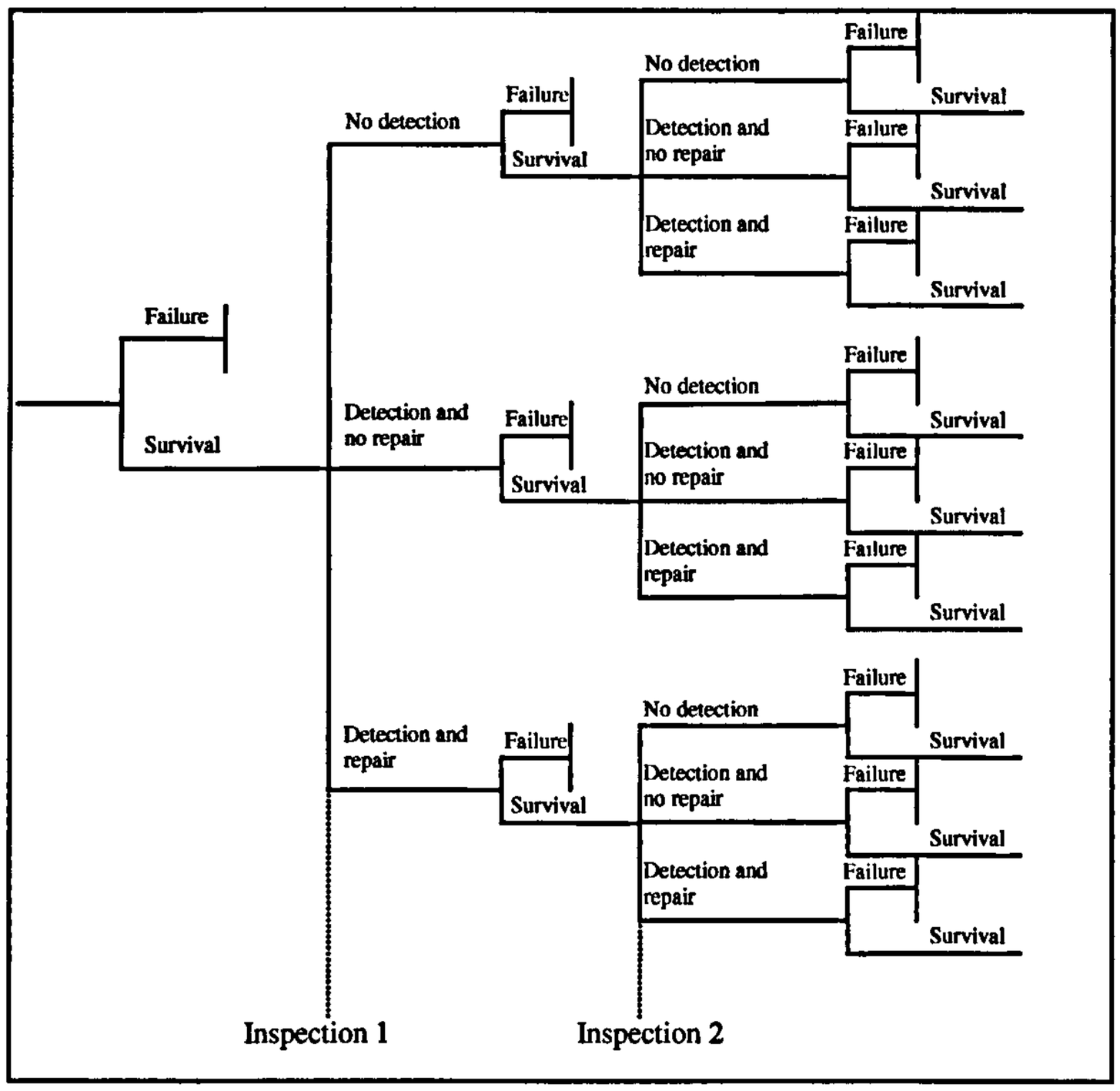

Figure 3.7 Analysis of possible sequences of events supporting risk-based maintenance from Faber (2000).

$$\beta(T) = -\Phi^{-1}(P_F(T)) \tag{3.6}$$

In which $P_F(T)$ is the probability of system failure in a specified reference period T such as one year, the service life or another interval of interest. The probability of failure in periods longer than one year can be calculated with expression (2.26).

The definitions of C_I, C_R and C_F are given by equations (3.7) to (3.9):

$$C_I = \sum_{i=1}^{N} M(t_i) C_I(r_i)(1 - P_F(t_i)) \frac{1}{(1+\gamma)^{t_i}} \tag{3.7}$$

In (3.7) it is assumed that at each location and time inspections with the same quality are made, $C_I(r_i)$ is the inspection cost of inspection I with inspection reliability r_i, N is the number of inspections, γ is the discount factor and $P_F(t_i)$ stands for the probability of system failure between 0 and t_i.

$$C_R = \sum_{i=1}^{N} \sum_{j=1}^{M(t_i)} C_{R,I,J} P_{R,I,J} (1 - P_F(t_i)) \frac{1}{(1+\gamma)^{t_i}} \tag{3.8}$$

in which $C_{R,I,J}$ are the costs of repair and $P_{R,I,J}$ is the probability of repair (combination between the probability that the structure has deteriorated to a certain level and the success of the repair) at time t_I and at location j.

$$C_F \cong \sum_{I=1}^{N+1} \sum_{j=1}^{M(t_I)} C_F(t_I)\{(1 - P_{R,I,J})(P_F(t_I) - P_F(t_{I-1})) + P_{R,I,J}(P_{F,R}(t_I) - P_F(t_{I-1}))\}\frac{1}{(1+\gamma)^{t_I}} \qquad (3.9)$$

in which $C_F(t_I)$ are the costs of system failure at time t_I and $P_{F,R}$ is the probability of system failure after a repair has taken place.

The equations above illustrate how a maintenance strategy can be quantified. In addition to the costs above, the cost of replacement and the cost and probability involved with an increased inspection frequency are desirable to include in the framework. This thesis contributes to this type of optimisation problem by providing the $P_F(t_I)$, i.e. the probability of system failure between 0 and t_I.

3.2.2. Qualitative maintenance decision-making

A disadvantage of quantitative maintenance optimisation models is that they are often very information dependent and computationally intensive. Reliability Centred Maintenance is a qualitative maintenance decision-making framework. Moubray (1997) describes four features central to Reliability Centred Maintenance (RCM) planning. Firstly, the primary objective of RCM is to preserve system functions. Secondly, the specific failure modes that can lead to loss of function or functional failure are identified. Thirdly, prioritisation is based on the function need, by prioritising the importance of the failure modes. Fourthly, only applicable and effective Preventive Maintenance (PM) tasks are selected. Applicable means that the task accomplishes one of three main reasons to carry out PM, i.e. prevent or mitigate failure, detect onset of a failure, or discover a hidden failure. Effective means that there is willingness to spend resources to carry out the task.

In order to achieve those four features, RCM planning consists of the main steps listed below, compiled from Moubray (1997), Smith (1993) and Duthie et al. (1997):

1. *System selection and information collection*.
2. *System boundary definition*.
3. *System description and functional block diagram*. Five items of information are further developed in this step: i) system description; ii) functional block diagram

– a top level representation of the system's major functions in the form of functional subsystems; iii) IN / OUT interfaces – documentation of the variety of elements that cross the system boundary; iv) system work breakdown structure – a compilation of the equipment (component) lists for each of the functional subsystems in the functional block diagram; v) equipment history – with respect to prior usage and operational experience.

4. *System functions and functional failures.*
5. *Failure modes and effects analysis (FMEA).* This step firstly constructs the component-function matrix – leading to insight in which system equipments could play a role in the creation of a functional failure. Secondly, the FMEA is carried out, which amounts to a definition of the specific component failure modes and causes that can defeat the functions at a local, system or plant level. Thirdly, the general redundancy rule is applied. I.e., if available redundancy essentially eliminates any effect at the system level, the failure mode is dropped from further consideration and is placed on the Run-To-Failure list. Fourthly, a check of redundancy, alarm and protection logic is made. I.e. whether alarm and protection equipment form an exception at the preceding rule.
6. *Logic tree analysis.* The consequences of each failure mode are investigated by answering three questions: Is the failure mode hidden or revealed? Does the failure mode cause a safety problem? Does the failure mode result in plant outage?
7. *Task Selection.* The appropriate maintenance task is then selected by answering four further questions: Is the age-reliability relationship for this failure known? Are there any applicable time-dependent tasks? Are there any applicable condition-dependent tasks? Are there any applicable failure-finding tasks?
8. *Task comparison* (i.e. compare recommended tasks with previous regime)
9. *Sanity check* (i.e. check that it all makes sense).

A disadvantage of the qualitative reliability centred maintenance approach is the subjective prioritisation often related to qualitative approaches. The following section therefore presents an approach that combines the computationally feasible qualitative decision-making with quantitative objective prioritisation.

3.2.3. Mixture of quantitative and qualitative decision-making

Delft Cluster (2001) applies a mixture of quantitative and qualitative decision-making approaches in a procedure to design monitoring strategies for dikes. This approach compares to the quantitative maintenance optimisation model based on the Bayesian decision-making model (figures 3.4 and 3.6) and the steps in reliability centred maintenance in the previous section.

According to Delft Cluster (2001), the first question that should be answered as part of a rational monitoring philosophy is: why carry out monitoring? The answer relates to the need to have knowledge about the reliability of function fulfilment of a structure. This need for knowledge can be interpreted within different contexts: an operational decision-making context; an inferential scientific context for validation, calibration, enhancement of models and hypothesis testing; finally a legislation context: e.g. license arrangements or fulfilment of the law.

Delft Cluster (2001) describes a four-element procedure to design rational dike monitoring strategies. *The first element* relates to step one to three in the RCM planning approach: the project boundaries and relevant environmental conditions are defined. This consists for example of an overview of (functional) requirements, physical shape of the structure, loading characteristics, available design models and simplifications during the design process, construction details, geotechnical soil properties or stratification of the foundation. *The second element* of the monitoring design procedure mixes step four of RCM planning with quantitative reliability analysis. This element aims to establish the dominant failure mechanisms. A quantitative reliability analysis of the structure under consideration is carried out, or failure rate information derived from the FMEA (Failure Mode Effect Analysis) that was set up during the design phase. The dominant failure mechanism(s) and the relevant or sufficiently sensitive indicators are derived from the reliability analysis. *The third element* consists of a consideration of which questions must be answered by the monitoring strategy and so establishing the objectives of the monitoring strategy. This step is relevant as the monitoring instruments each serve to answer a specific question, otherwise the instrument is redundant. These questions can usually be derived from the dominant failure mechanisms from the reliability analysis. The monitoring strategy does not need to remain restricted to the dominant failure mechanisms but can also include other failure mechanisms before they become

relevant. *The fourth element* of the procedure is to decide on the rational monitoring strategy, i.e. a formulation of the decision problem and repeated observations. Delft Cluster (2001) suggests asking the following questions to support the development of the monitoring strategy: Monitor what? Monitor where? Monitor when? Monitor to which degree?

Bayesian decision theory (see section 3.2.1) is suggested as a rational way to structure this decision problem and allow rational quantified risk analysis, similar to Faber (2000). Figure 3.8 provides a simplified illustration of such a decision problem, see also figure 3.4 and figure 3.6. Such a decision tree enables a rational risk analysis. Delft Cluster (2001) then formulates the theoretical structure of the decision problem in terms of a practical approach. One aspect of this practical approach concerns the desired precision of the monitoring strategy to appropriately inform the questions. A second aspect concerns the extent to which the monitoring strategy returns the desired information, shown in figure 3.9. The return of desired information is firstly related to the precision and reliability of the observations of observation variables *y*. It is secondly related to the sensitivity of the (uncertainty in the) variables *x* for the observation variables *y*. The return of desired information is thirdly related to the sensitivity of the (uncertainty in the) performance for the variables *x*. The desired precision of the measurements has implications for the implementation of the

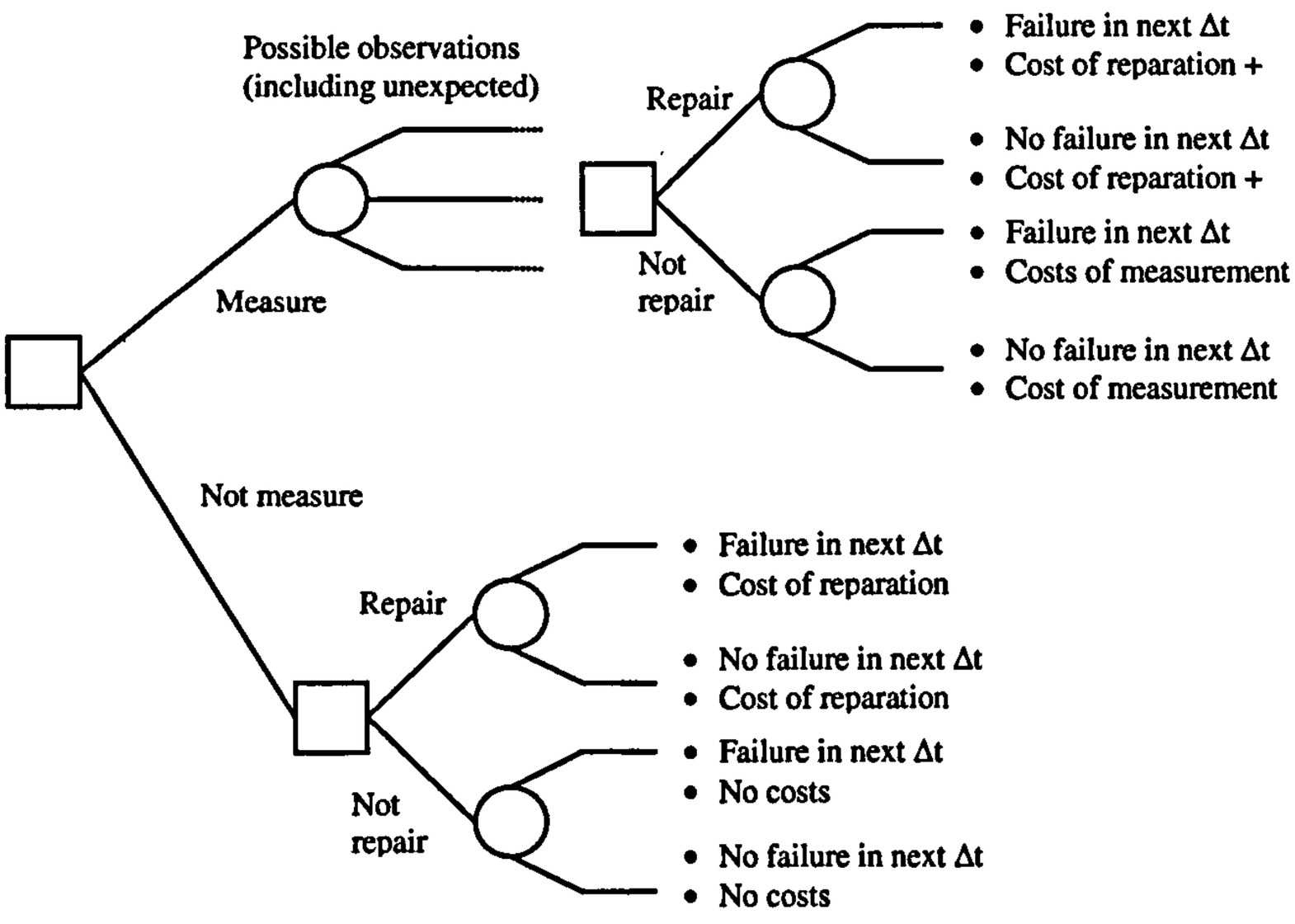

Figure 3.8 Simplified illustration of a monitoring and repair decision problem in a Bayesian context.

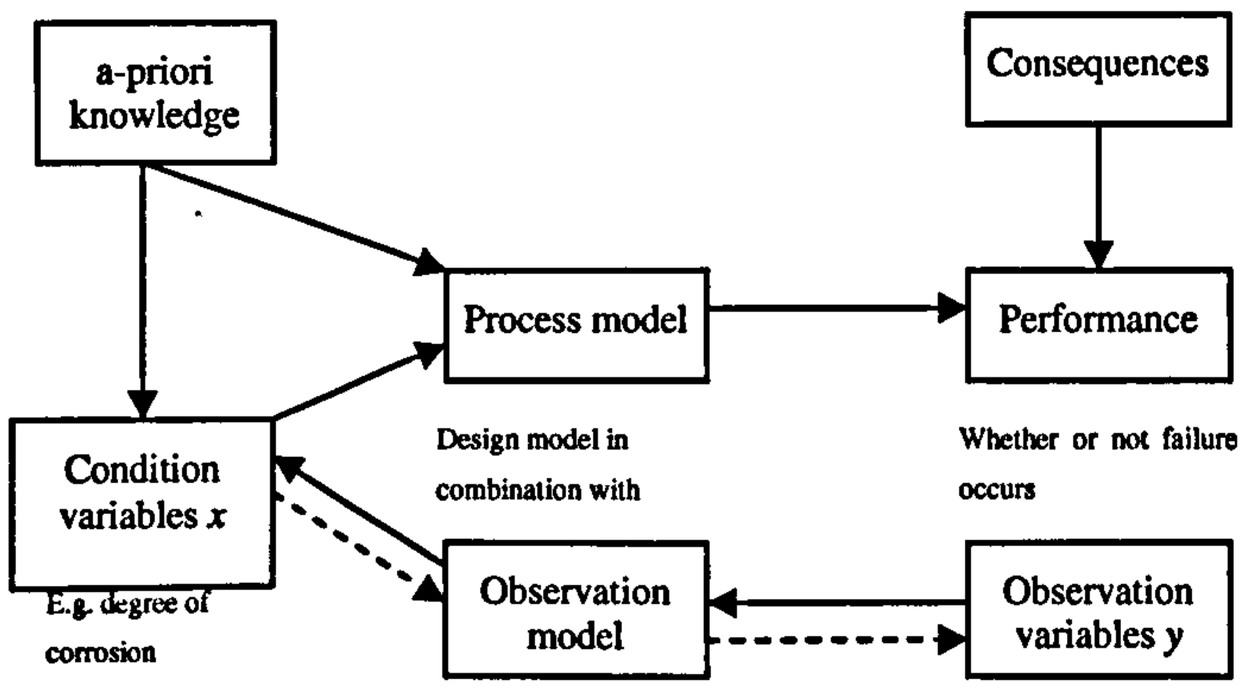

Figure 3.9 The information flow associated with the evaluation of the performance of a structure (Delft Cluster, 2001)

monitoring strategy and how it is carried out, in terms of e.g.: the design and incorporation of the measuring system; the diagnostic facilities (– does the measurement equipment function as desired?); the monitoring protocol (– who, what, how?).

A monitoring strategy consists of many repeated measurements and hence decision moments. Representing all possible decision sequences results in a very complex decision tree. Delft Cluster (2001) points out that systematic straightforward calculation of all possible decision sequences is next to impossible. Instead, it is recommended to incorporate simplified assumptions and estimations in the decision tree, e.g. based on RCM planning or supported by figure 3.4. These simplifications must be introduced in collaboration with the decision-maker and in dialogue with the domain specialists. The functional requirements and the available possibilities should be respected.

3.3. Review

The specification of a maintenance optimisation framework requires an overview of current practice in flood defence management as well as knowledge about the types of rational decision-making approaches. The maintenance optimisation context is relevant to this thesis for the following reasons. Firstly, it shows the perspective of time-dependent reliability in the overarching optimisation framework. Secondly, the choice of a Markovian or Bayesian modelling approach for time-dependency must be

made in the maintenance optimisation context. Thirdly, the importance measures for asset time-dependent processes and maintenance operations are developed in the context of the overarching maintenance optimisation model. Current flood defence management practice is also relevant to the importance measures. The main characteristics of the overarching rational maintenance optimisation framework for flood defence management are derived based on this chapter. These main characteristics and the relevance of the maintenance optimisation context for this thesis are discussed below.

The four building blocks in a quantitative maintenance framework discussed in section 3.2.1 divide the optimisation problem into useful model components, i.e.: the functional system model, the risk and reliability system model, the operational management model, the calculation optimisation model. Table 3.4 provides an overview of the building blocks that are currently specified for flood defence management. The Bayesian decision-making framework in figure 3.4 is a suitable theoretical structure. It allows the definition of the time-dependent risk and reliability system model and the monitoring and repair operations in the operational model in a 'common currency'. The Bayesian decision-making framework has been successfully employed in for example risk-based inspection planning in the offshore industry, compare figure 3.4 and 3.6. This illustration shows where and in which form the time-dependent reliability contribution is required. For statistical time-dependent process models, the Bayesian approach based on posterior analysis is preferred over the Markovian approach based on discarding the historical time series observations. This choice has two implications for the maintenance framework. Firstly, it determines the type of statistical models for the asset time-dependent processes. It is noted that the Bayesian maintenance optimisation framework also allows the incorporation of Markovian asset time-dependent process models. Secondly, it determines how the information from monitoring (experiments) is taken into account in the maintenance optimisation model. A mixture of a qualitative and quantitative decision-making framework combines the advantage of a rational computationally feasible qualitative approach with that of a quantitative objective prioritisation. Section 3.2.3 illustrates how such a mixture decision-making approach supports the design of dike monitoring programmes. It is expected that the mixture approach is the most convenient model for the rational flood defence management decision-making framework.

The maintenance operations in flood defence management practice and the Bayesian decision-making framework form the context of the importance measures developed in the following chapter 4.

3. Flood defence management and rational decision-making

4. Risk-based importance measures for flood defence management

This chapter develops a method to highlight relevant time-dependent processes and maintenance operations in the context of a rational maintenance framework. This corresponds with objective 2 in chapter 1 and in figure 1.6. This method is developed by reviewing and developing reliability-based and risk-based importance measures to support the management of flood defence systems. An overarching rational maintenance framework for hydraulic structures has been set out in the previous chapter. The importance measures in this chapter are intended to support the management of flood defences without or in advance of a full life cycle optimisation. Section 4.1 provides a more detailed description of the role of importance measures in flood defence management. It outlines the objectives that the importance measures are meant to fulfil. Section 4.2 reviews the existing risk and reliability-based importance measures for flood defence management. Section 4.3 develops the reliability and risk-based importance measures for flood defence management. A summary of this chapter is given in Buijs et al. (2007).

4.1. Role of importance measures and sub-objectives

Section 4.1.1 describes the research and operational context which the importance measures aim to support. Section 4.1.2 formulates the sub-objectives of the importance measures

4.1.1. The importance measures in context

Rational flood defence management is supported by life cycle optimisation. The optimisation of life cycle costs is a complex problem, as introduced by section 1.2.2, 1.2.3, figure 1.2 and 1.3 and section 3.2.1. It involves on one hand estimation of flood

risk in time and space and valuation of its acceptable level. On the other hand it consists of operational activities with a cost, flood risk reduction, time and space dimension. The building blocks of a quantitative framework for life cycle cost optimisation are described in section 3.2.1. Due to the complexity of the optimisation problem the production of a monetary cost – performance curve such as figure 1.3 is not straightforward. Simplifying assumptions are often required to enable quantitative maintenance planning, see e.g. Sørensen and Faber (2001).

The use and interpretation of the life cycle optimisation model, and therefore of the importance measures developed in this chapter, depends on the application context. The following application contexts are considered: the research context and the operational context. *The research context* is an inferential scientific context aiming to increase the quality of the life cycle optimisation model and its building blocks. The quality is increased by the validation, calibration, enhancement of models and hypothesis testing (Delft Cluster, 2001). The aim of maintenance within *the operational context* is according to Vrijling (2003): all activities aimed at retaining an object's technical state or at reverting it back to this state, which is considered as a necessary condition for the object to carry out its function. Performance-based asset management in the UK, Simm et al. (2006), is focussed on achieving efficient flood risk reduction. Figure 1.2 shows that the aim according to Vrijling (2003) and Simm et al. (2006) are related. The necessary condition for the objects to carry out their function follows from the optimisation of flood risk reduction. Several maintenance intervention options are considered.

4.1.2. Sub-objectives of the importance measures

Objective 2 described in chapter 1 is: to develop a method to highlight relevant time-dependent processes and maintenance operations in the context of a rational maintenance framework. To achieve this objective, chapter 4 reviews and develops risk and reliability-based importance measures to support the management of flood defence systems without or in advance of full life cycle optimisation. This main objective can be broken down into three sub-objectives.

Sub-objective 2.1 is to indicate the influence of individual random variables, i.e. flood defence properties, on the reliability analysis. This provides insight in the sensitivity of reliability to a change in a flood defence property due to time-dependency or an operational activity. All flood defence properties are taken into account, even if it is

clear that the property is not time-dependent or part of common operational activities. Section 4.3.2 develops importance measures for sub-objective 2.1.

Sub-objective 2.2 is to highlight relevant time-dependent processes. This knowledge enables targeting monitoring activities or eliminating irrelevant processes from the life cycle optimisation model. The monitoring intends to improve the scientific understanding of time-dependency, populate and update the optimisation model or to identify trigger condition levels for more detailed inspection or repair. The intention is to use these importance measures without or in advance of a full life cycle optimisation. Section 4.3.3 develops importance measures for sub-objective 2.2.

Sub-objective 2.3 is to indicate the impact on flood risk reduction of different operational activities in relation to the cost of the activity. The main types of operational activities are according to section 3.1.2: inspection, repair, replacement or improvement. These importance measures support an operational manager who has to achieve immediate flood risk reduction, but does not have the means or justification for a full life cycle optimization. In addition, they support the elimination of irrelevant operational activities in advance of the life cycle optimization. Section 4.3.4. develops importance measures for sub-objective 2.3.

It is noted that inspection or monitoring is mentioned both in sub-objective 2.2, highlight time-dependent processes, and in sub-objective 2.3, indicate the flood risk impact of operational activities. To make the distinction between monitoring in both sub-objectives, they are held against the Bayesian decision-making framework for expected opportunity loss or value of information. This distinction is explained in section 4.3.1. The following section reviews existing risk and reliability based importance measures in the engineering industry.

4.2. Existing risk and reliability-based importance measures

4.2.1. Introduction

Sensitivity and uncertainty analysis are relevant to sub-objective 2.1 mentioned in section 4.1. The main aim of sensitivity analysis is to study how the variation in the output of the model can be qualitatively or quantitatively apportioned to different

sources of variation, and how the given model depends on the information fed into it, Saltelli et al. (2000). Local sensitivity analysis considers deterministic basic variables and process model predictions. Global sensitivity analysis takes the probabilistic distribution of the basic random variables and the process model prediction into account. Unlike local sensitivity analysis, it therefore captures the range of the variables as well as non-linear process model behaviour.

Publications such as Janssen et al. (1990), Saltelli & Scot (1997), Saltelli et al. (1999) and Saltelli et al. (2000) provide an overview of existing measures in sensitivity and uncertainty analysis. Following Saltelli et al. (2000), Homma & Saltelli (1996) and Janssen et al. (1990) the next sensitivity analysis techniques are identified: screening, differential analysis, response surface methods, Monte Carlo based regression analysis and correlation coefficients, variance decomposition according to Sobol' or Fourier Amplitude Sensitivity Test (FAST), FORM and SORM as introduced in section 3.1.3.

Screening can be used as a local sensitivity analysis method, involving the one-by-one variation of parameters and recording the variation in the model prediction. The method only considers deterministic basic variables and model prediction rather than random variables. Differential analysis only investigates the process model sensitivity for deterministic basic variables and is therefore a local sensitivity analysis technique as well. The response surface method fits an approximation to the relevant deterministic prediction space of the original process-model. The simplified approximation of the response can then be used as a basis for different sensitivity analysis methods. Monte Carlo based regression analysis linearises the model predictions across the probabilistic range of the basic random variables. Even though it is a global sensitivity analysis method taking random rather than deterministic variables into account, however, it does not pick up on non-linear process model behaviour. Variance decomposition methods indicate the uncertainty contribution of individual variables as well as combinations of joint variables. Variance decomposition of complex system models is often hard (Jarzemba & Sagar, 2000). Direction cosines from FORM and SORM therefore tend to be preferred over variance decomposition in structural reliability. FORM and SORM are relatively fast methods amalgamating the uncertainty contribution as well as the sensitivity of the process model. Direction cosines and partial derivative based importance measures as part of global sensitivity analyses are further considered for review and development in 4.2.2 and 4.2.3.

Risk and reliability-based importance measures are used to support the design and operational planning of structural systems in the nuclear and engineering industry. These measures are usually part of safety assessments, design or maintenance of engineering systems rather than the analysis of the underlying process models. This type of importance measure serves sub-objective 2.2 and sub-objective 2.3 mentioned in section 4.1.

Importance measures as an integral part of the overall life cycle costing model are not considered in detail in this chapter. An example is Dekker (1995) who mentions priority criteria in form of penalty functions, or the influence of postponing maintenance activities on a particular component on the average lifetime cost. Another example is Worm & Van Harten (1996) who discuss a road maintenance optimisation model.

In section 4.2.2 direction cosines are discussed and their potential to indicate where most uncertainty reduction can be achieved. In section 4.2.3 existing partial derivative based concepts are reviewed as part of global sensitivity analyses. Finally, section 4.2.4 discusses risk-based importance measures applied in the engineering industry.

4.2.2. Direction cosines

Section 3.1.3 describes the origin of the direction cosines in the FORM method. They are also referred to as coefficients of influence. The direction cosine is defined by (2.11). The linearised limit state function in the standard normal space expressed by (2.12) demonstrates that the coefficients are in fact direction cosines of the reliability index. Hohenbichler & Rackwitz (1986) show that $(\alpha_i)^2$ is the linear correlation coefficient, $\rho_{Z;X_i}$, between the variable X_i and function Z in the design point. The direction cosine therefore indicates the uncertainty contribution of individual random variables to the overall probability of failure.

Figure 2.1 shows which uncertainty types such an uncertainty contribution might represent. Vrijling & Van Gelder (2005) and Van Gelder (1999) show how knowledge about uncertainty contributions of flood defence properties enables judgement about uncertainty reduction in the probability of failure. The main activities to reduce uncertainty are: data gathering, research and elicitation by means of expert knowledge. It is possible to compose uncertainty reduction policies of a combination of those activities. Quantitatively such policies are most effective when they are directed

at the flood defence properties with the highest uncertainty contribution, i.e. the highest α_i. The effectiveness of these policies is also determined by the type of uncertainty they are meant to reduce, see table 4.1 and explanation below. Inherent uncertainty in time and space are for instance irreducible, even though they often contribute highly. Other uncertainty types are usually only partially reducible.

Table 4.1, from Vrijling & Van Gelder (2005), summarises four uncertainty reduction policy options whose uncertainties are integrated in the probability of failure, indicated by *Pf*, and which are reduced, indicated by -. Uncertainty contributions to the probability of failure *Pf* are represented by the direction cosine α_i. The direction cosine indicates which random variables contribute highly, but does not distinguish between the contribution of different uncertainty types. Option 1 entails no reduction of uncertainty. Option 2 represents the reduction of statistical uncertainty in space and model uncertainty by taking measurements and doing research. Option 3 considers the situation whereby all epistemic uncertainties are reduced. Option 4 is a policy that manages to reduce all uncertainties except inherent uncertainty in time.

Table 4.1 Four different uncertainty reduction options, from Vrijling & Van Gelder (2005).

	Option 1	Option 2	Option 3	Option 4
Inherent uncertainty (in time)	*Pf*	*Pf*	*Pf*	*Pf*
Inherent uncertainty (in space)	*Pf*	*Pf*	*Pf*	-
Statistical uncertainty (of variations in time)	*Pf*	*Pf*	-	-
Statistical uncertainty (of variations in space)	*Pf*	-	-	-
Model uncertainty	*Pf*	-	-	-

4.2.3. Partial derivative based concepts

Borgonovo & Apostolakis (2001) recommend Differential Importance Measures (DIM) in the context of the Probabilistic Safety Assessment (PSA) in the nuclear industry. The total variation of a function due to a differential variation of its parameters x_1, .., x_n is expressed as:

$$dR = \frac{\partial R}{\partial x_1} dx_1 + \frac{\partial R}{\partial x_2} dx_2 + \ldots + \frac{\partial R}{\partial x_n} dx_n \qquad (4.1)$$

in which R is a risk or reliability metric such as Core Damage Frequency (CDF), written as a function $R=g(x_1, .., x_n)$ of generic parameters $x_1,\ldots,x_n$, such as the frequency of

an initiating event, the failure rate of a component, etc. It is also possible to choose a mean value or standard deviation as a parameter. Borognovo & Apostolakis (2001) suggest that the variations of dx_1, ..., dx_n can either entail values of equal magnitude or of an equal percentage. An approach based on Cauchy's convergence criterion is proposed to achieve changes in the parameters that represent a differential change. The DIM is subsequently defined as the proportion between a change due to one variable and the total change in the risk or reliability metric:

$$DIM(x_i) \equiv \frac{dR_{x_i}}{dR} = \frac{\frac{\partial R}{\partial x_i} dx_i}{\sum_j \frac{\partial R}{\partial x_i} dx_j} \tag{4.2}$$

Another possibility is that time-dependent processes or operational activities affect several flood defence properties simultaneously. The change in reliability due to a change in two random variables simultaneously is e.g. given by Hong & Lie (1993) in the form of:

$$I_G(i, j) = \partial^2 R(G) / \partial p_i \partial p_j \tag{4.3}$$

In which $I_G(i,j)$ is the joint importance of components with indices i and j, $R(G)$ is the reliability of system G, p_i and p_j are the probabilities of failure of components i and j. This joint importance measure indicates the change in reliability due to correlated deterioration processes affecting p_i and p_j. Armstrong (1995) shows that this measure is generally applicable, i.e. also to two correlated components.

Another illustration of joint importance is given by Cho et al. (1989) in the nuclear industry. They consider probabilistic importance measures of a system or function that is a naturally defined cluster of components or subsystems:

$$\frac{\partial h_{CD}}{\partial h_{sub}} \tag{4.4}$$

In which they look at the change in core damage frequency, defined in this case as h_{CD}, due to a change in reliability of a subsystem h_{sub}. The neutralisation of such a subsystem is another way to establish the influence of a cluster of components or subsystems, Eisenberg & Sagar (2000). Barlow & Proschan (1975) consider the relative component importance, essentially the conditional probability that system failure is caused by (i.e. coincides with) the failure of a given component.

4.2.4. Risk-based importance measures

Cost-benefit analysis is a well-known concept in engineering economics, e.g. Newnan et al. (2000). In this context, Veseley (1999) discusses the principles of resource-effectiveness and regulatory-effectiveness for risk-informed applications. The relative Burden-to-risk-Importance-Ratios (BIRs) are defined as a first basic cost-benefit principle:

$$BIR = \frac{\text{Relative Burden}}{\text{Relative Importance}} = \frac{\text{Cost}}{\text{Benefit}} \qquad (4.5)$$

here the relative burden represents the resources spent on the activity or requirement. The relative importance can be established with risk importance measures such as shown in table 4.2. The second basic cost-benefit principle is BIR=1, which is a formal objective in standard cost-benefit analyses or resource and optimization problems. Undertaking an activity is therefore justified if the cost (relative burden) of the activity is less than the benefit (relative risk importance) achieved with that activity. Vesely (1999) mentions that in conventional cost-benefit analyses often activities are cut with a small risk importance. Cutting the cost of those activities then results in only a small increase in system risk. Instead, Veseley encourages the redistribution of activities to achieve optimal system risk and therefore proposes the BIR terminology rather than the cost-benefit terminology.

Table 4.2 Risk importance measures and their definitions.

Name risk importance measure	Definition risk importance measure
Risk Reduction	$R(\text{base}) - R(x_i=0)$
Fusell- Veseley	$\{R(\text{base})-R(x_i=0)\}/R(\text{base})$
Risk Reduction Worth	$R(\text{base})/R(x_i=0)$
Criticality importance	$x_i(\text{base})\{R(x_i=1)-R(x_i=0)\}/R(\text{base})$
Risk achievement	$R(x_i=1)-R(\text{base})$
Risk Achievement Worth	$R(x_i=1)/R(\text{base})$
Partial Derivative	$\{R(x_i+\partial x_i)-R(x_i)\}/\partial x_i$
Birnbaum importance	$R(x_i=1)-R(x_i=0)$

Table 4.2 summarises risk importance measures that are well-known in binary system reliability in the nuclear industry, see e.g. Van der Borst & Schoonakker (2001), and in the dam industry, see Hartford & Baecher (2004). $R(\text{base})$ in table 4.2 is the base system risk scenario. $R(x_i=0)$ is the scenario whereby the risk R is fully optimized for

parameter x_i. Parameter x_i is for example a dam section. $R(x_i=1)$ refers to the scenario whereby parameter x_i is fully failed. x_i(base) represents the parameter value for x_i in the base case. ∂x_i is the differential change in the parameter x_i.

4.3. Development of risk-based importance measures for flood defence management

The rational maintenance optimisation context is addressed in section 4.3.1. It is noted that the scope of this research project is focused on asset time-dependent processes rather than maintenance optimisation. The importance measures in this chapter are therefore meant as a possible starting point for more detailed importance measures. Section 4.3.2 subsequently discusses and develops importance measures to indicate the influence of variables, i.e. flood defence properties, on the reliability. Section 4.3.3 develops importance measures to highlight relevant asset time-dependent processes. Section 4.3.4 develops importance measures to indicate the flood risk impact of operational activities.

4.3.1. Rational maintenance optimisation context

In the end, the importance measures developed in section 4.3 are meant to support the population of a rational maintenance optimisation model, see e.g. figure 4.1 after figure 3.8 (Delft Cluster, 2001). Especially the value of monitoring is difficult to capture without having a fully populated life cycle cost model available. Below, firstly a discussion is given of different types of monitoring and the limitations of the importance measures in this thesis to capture the value of monitoring activities. Secondly, an example is given to illustrate the Bayesian decision-making problem and to relate the importance measures developed later in this section to that problem.

Different types of monitoring activities

Inspection or monitoring activities have many different benefits. Monitoring can be for example directed at the development of the state of the structure or components in time. An aim of such monitoring is the identification of trigger levels for repair or improvement, the representation of the flood defence properties in the time-dependent reliability model or the increase of scientific understanding. It is also

possible to carry out monitoring to specifically discover the occurrence of an ongoing failure mechanism. Monitoring directed at the state of the structural components often overlaps with monitoring failure mechanisms. Figure 4.1 illustrates the decision-making problem for monitoring condition levels and monitoring failure mechanisms, after figure 3.8 (Delft Cluster, 2001). Finally, it is possible to use monitoring for the reduction of statistical uncertainty in flood defence properties by e.g. increasing the measurement quality or the grid of the measurements.

Monitoring condition levels refers to monitoring of the state levels in time and the discovery of ongoing failure mechanisms. Monitoring condition levels is an ongoing monitoring process in time. It has a direct as well as an indirect effect on life cycle

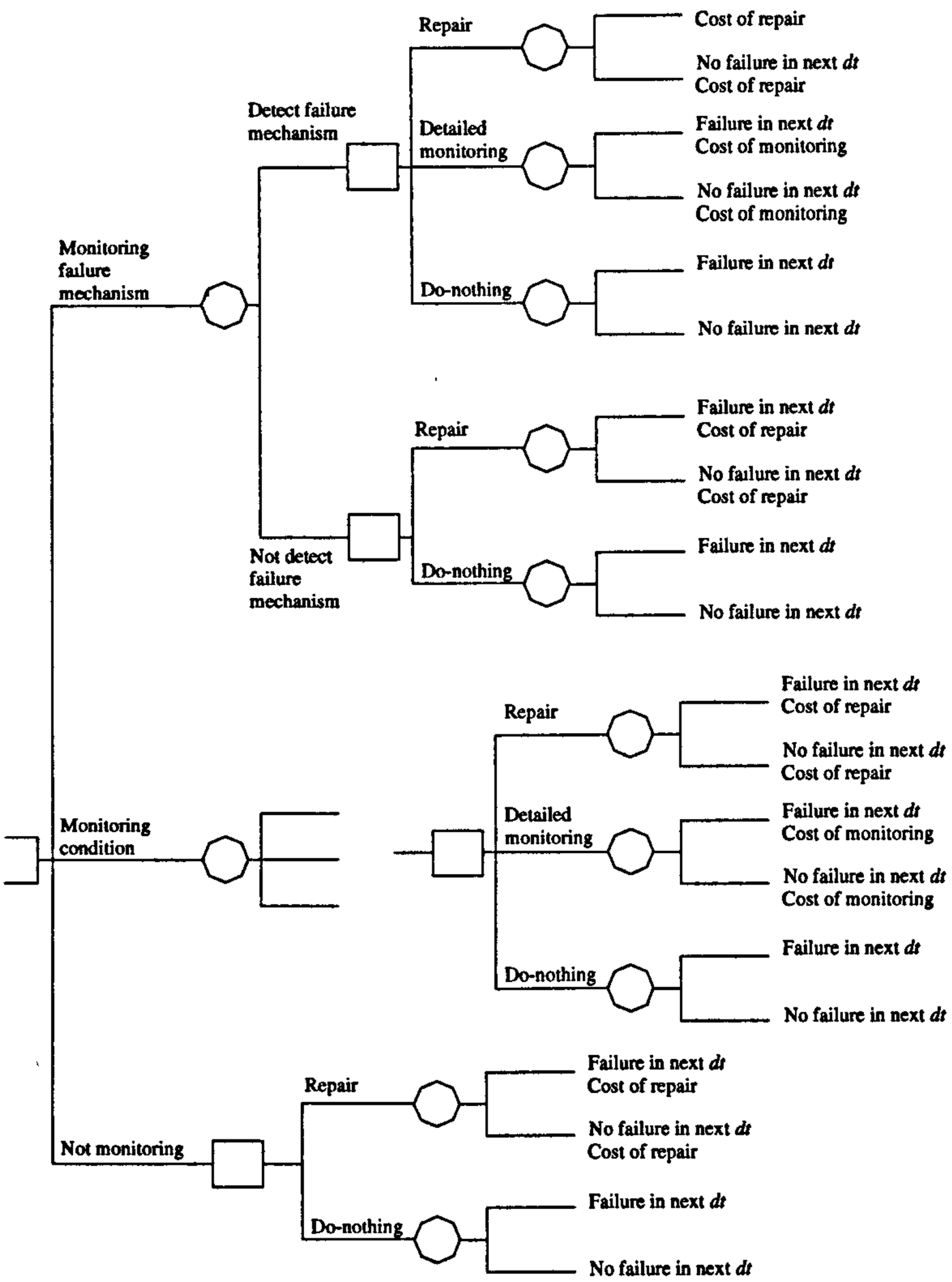

Figure 4.1 Bayesian decision problem for monitoring condition level, after Delft Cluster (2001).

costing. It allows a condition-dependent timing of maintenance activities rather than fixed time intervals. It identifies failure processes that could culminate in failure. Finally, depending on the type of monitoring it increases the quantitative knowledge about the flood defences. The value of monitoring condition levels is therefore its reduction in cost in the overall life cycle of the flood defence. This can only be determined as part of the overall life cycle costing optimisation model.

However, the possibility to establish the sensitivity to monitoring condition levels is subject to several restrictions such as the following. Firstly, an indication of relevant time-dependent processes is required in order to rationally populate and set up a comprehensive life cycle costing model. Even once such an optimisation model exists, it is not always feasible to support each decision moment with this model. A second complication is that the repair or improvement measures depend on the state of the component that is measured and the level to which it needs to be improved. Thirdly, the decision-making problem is ongoing and not bounded as shown in figure 4.1. For example, detailed monitoring can be followed by repair or even more monitoring. In the light of these restrictions importance measures in section 4.3.3 are a first indication of relevant time-dependent processes. Relevant time-dependent processes are an indication of how to target monitoring condition levels.

The second type of monitoring is referred to with statistical uncertainty reduction monitoring. This type of monitoring is worthwhile considering if a number of flood defence properties significantly contribute reducible uncertainties to the probability of failure. The value of this type of monitoring is determined by a combination of the change in flood risk and the cost of the monitoring activity. It is compared to repair or improvement if an operational manager finds that the flood risk in a floodplain needs to be reduced on a short term in section 4.3.4.

In sub-objective 2.2 monitoring consists of the identification of trigger condition levels for more detailed inspection or repair. Another application of this type of monitoring is the registration of condition levels to increase the scientific understanding about the process, e.g. in the research context. This type of monitoring is referred to as monitoring condition levels. Importance measures in section 4.3.3 support targeting this type of monitoring. In sub-objective 2.3, monitoring considers the immediate impact on flood risk reduction by reducing uncertainty through data collection. This type of monitoring is referred to as statistical uncertainty reduction monitoring.

Illustration of a Bayesian decision-making problem

An example below illustrates the Bayesian decision-making problem as well as the relation to the importance measures that are further developed in the next few sections. The decision problem describes a flood defence section in a floodplain that is characterised by a crest level h_c. The three situations that are considered are given in figure 4.2. Table 4.3 summarises the main information with regard to the decision problem.

Table 4.3 Characteristics of Bayesian decision making problem example

Variables in Bayesian decision problem example	*Description*
h_c	Crest level of one flood defence section
C_I	Cost of inspection
C_{tot}	Total costs to minimise
x	Change in crest level either due to settlements or repair / improvement
$B(x)=a+bx$	Construction costs as a function of the change in crest level, standalone construction costs a and raise dependent costs b
$R(h_c+x)=R_0 \cdot \exp(-s(h_c+x))$	Flood risk as a function of the initial risk R_0, the crest level h_c and the change in crest level x
h_T	The crest level which triggers repair / improvement
$h_{c;I}$	The crest level to which the repair / improvement activity extends

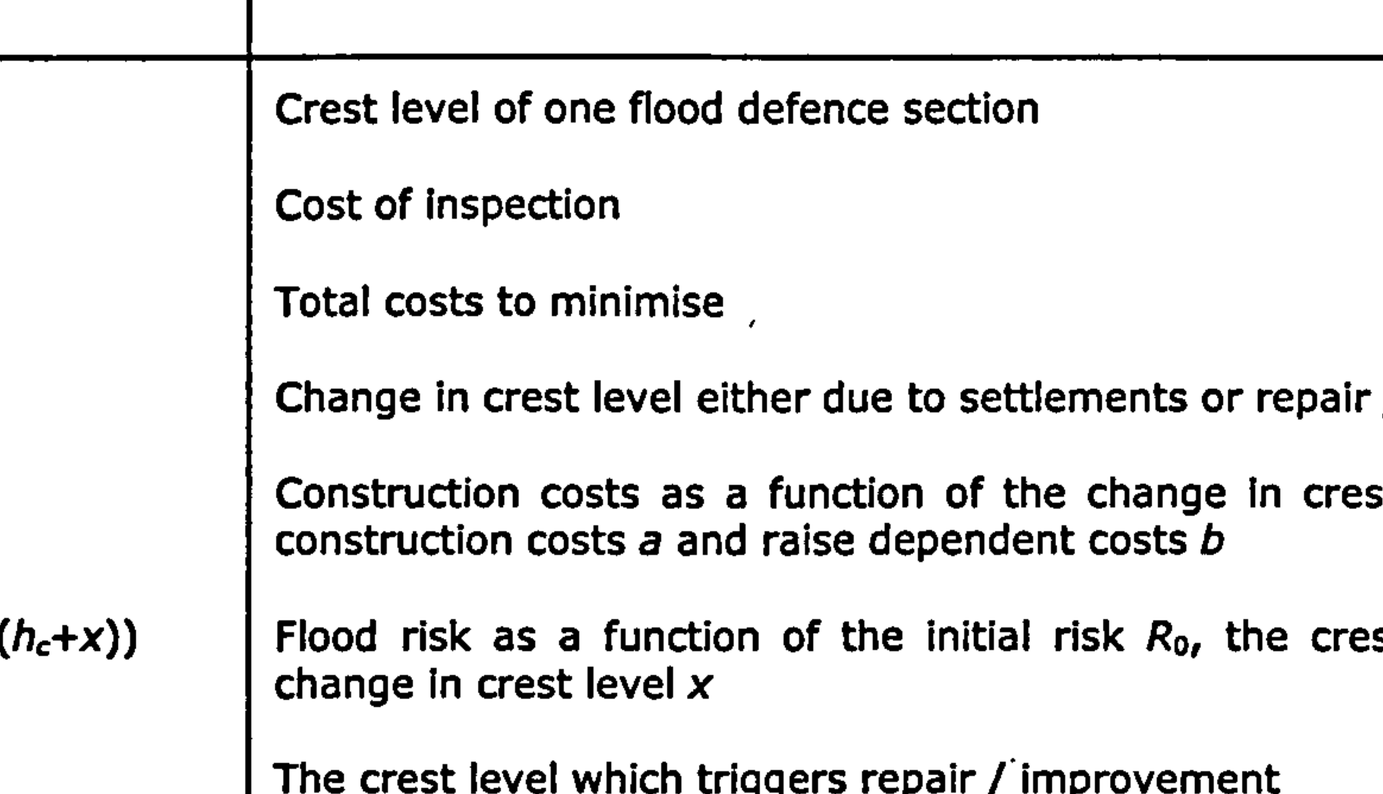

Figure 4.2 Example of a simplified Bayesian decision problem.

The costs in the three situations are derived following the definitions given in equations (3.5), (3.7), (3.8) and (3.9). Situation 1 is the do-nothing scenario. The total cost is derived by integrating the flood risk related to crest level h_c over the probability density function $f(h_c)$:

$$C_{tot} = \int_{h_c=0}^{\infty} f(h_c) \cdot \{R_0 \exp[-s(h_c)]\} dh_c \qquad (4.6)$$

Situation 2 consists of a repair or improvement activity without first carrying out an inspection. The crest level is then raised from h_c to $h_{c;I}$ without first acquiring information by an inspection. The flood risk reduces with an increasing improved crest level $h_{c;I}$ while the construction costs increase. The optimum investment can be found similar to figure 1.3.

$$C_{tot} = \int_{h_c=0}^{\infty} f(h_c) \cdot \{B(h_{c;I} - h_c) + R_0 \exp[-s(h_{c;I})]\} dh_c \qquad (4.7)$$

Situation 3 consists of an inspection activity which leads to increased information on the crest level. The increased information then informs a decision to repair or to do nothing. If the crest level is lower than a level h_T then a repair / improvement activity is triggered which raises the crest from h_c to a level $h_{c;I}$. If the crest level h_c is above the trigger level h_T, nothing is done. The total cost in situation 3 is a function of the inspection cost C_I, the construction cost $B(h_{c;I}-h_c)$ and the flood risk $R(x)$ in the repair case and in the do-nothing case (figure 4.2):

$$C_{tot} = C_I + \int_{h_c=0}^{h_T} f(h_c) \cdot \{B(h_{c;I} - h_c) + R_0 \exp[-sh_{c;I}]\} dh_c + \int_{h_c=h_T}^{\infty} f(h_c) \cdot \{R_0 \exp(-sh_c)\} dh_c \qquad (4.8)$$

The addition of the inspection event makes the total cost a combination of repair (4.7)in the first part of the equation and do-nothing (4.6) in the second part of the equation. If the crest level is in a very good state, the second part of the equation dominates: mainly inspection costs are made instead of high construction costs and the flood risk is low as the crest level is large. If the crest level is in a bad state, the first part of the equation dominates: mainly construction costs are made and the improvement $h_{c;I}$ reduces the flood risk. Equation (4.8) can also be optimised similar to figure 1.3.

If the crest level is in a good state it is possible that do-nothing is more beneficial than inspect and repair. If in advance is known that the crest level is in a very bad state,

then directly the decision to repair can be made. If the crest level is in a moderate state it is beneficial to first inspect and then decide to repair or not.

As explained in section 3.2.1, the equations (4.6), (4.7) and (4.8) can be expanded with a numerical representation of flood risk, multiple time-dependent processes, inspection, repair options and flood defence sections. The most relevant time-dependent processes can be established as part of a Bayesian decision-making problem as shown in figure 4.1, but then covering a lifetime of a flood defence system. In this decision-making context, and with a fully populated life cycle cost model available it is possible to develop detailed importance measures for time-dependent processes and operational activities. Such a fully populated life cycle cost model is not available, the aim of the sub-objectives 2.1 to 2.3 is to limit the effort involved with realising such a decision-making problem.

The sensitivity of the reliability to random variables indicates how much a flood risk function such as $R(h_c+x)$ in table 4.3 changes as a result of a change in crest level h_c. The cost-benefit approach to time-dependent processes is developed in section 4.3.3. The previous example does not relate to a time-dependent process. However, a time-dependent process can be expressed cost benefit wise as follows:

$$BIR_{time} = \frac{Cost\ of\ remediation}{Change\ in\ flood\ risk} = \frac{B(h_c - h_{c;d})}{R_0\{\exp(-sh_c) - \exp(-sh_{c;d})\}} \tag{4.9}$$

with $B(h_c-h_{c;d})$ and $R_0\exp(-s{\cdot}h_c)$ following table 4.3. Whereby the change in flood risk is a result of a deteriorated crest level $h_{c;d}$ and the cost of remediation is the cost involved with bringing the crest level back to its initial level. If the crest level was for example originally at the optimum point in figure 1.3, the cost of remediation indicates how much has to be invested to bring the crest level back to the optimum point after deterioration. The comparison of the BIR_{time} for different deterioration processes indicates how steep the development away from the optimum point is.

The importance of repair or improvement measures is indicated similar to (4.9):

$$BIR_{imp} = \frac{Cost\ of\ improvement}{Change\ in\ flood\ risk} = \frac{B(h_{c;I} - h_c)}{R_0\{\exp(-sh_{c;I}) - \exp(-sh_c)\}} \tag{4.10}$$

The cost of improvement is compared to the change in flood risk. If the initial crest level is on the left from the optimum in figure 1.3, the comparison of the BIR_{imp} for different improvement measures shows how steep the curve in figure 1.3 is towards the optimum point.

The BIR, or conventional cost benefit ratio, has a number of limitations compared to the Bayesian decision-making approach. One example is that it does not take the possibility into account that the improvement is beyond the optimum point. A second example is that depending on the cost function and the flood risk model, it is possible that an improvement leading to the optimum point cost-benefit wise scores less favourable than an improvement that only leads to a small improvement. A third example is that the benefits of inspection cannot be captured with such a cost benefit ratio, as it implies the shift in emphasis on the first or second part in equation (4.8). A last example is that the do-nothing option with a cost benefit approach or BIR leads to the insignificant indicator of 0/0.

4.3.2. Indicate the influence of variables on the reliability

A indication of the influence of variables on the reliability is a starting point to gain insight in the sensitivity of decision-making problems such as in figure 4.1. In relation to sub-objective 2.1 – indicate the influence of individual random variables on the reliability – direction cosines capture the uncertainty contribution of random variables to the probability of failure. They represent the influence of the random variables at a point in time. However, low uncertainty contributing properties are also able to introduce a significant improvement or decline in the reliability due to the sensitivity of the model for that variable. Time-dependent processes and operational activities change the uncertainty of random variables as well as their mean values and thus the probability of failure. Direction cosines do not fully pick up on this type of sensitivity. Complementary insight in the sensitivity of the reliability and risk to changing mean values and standard deviations of random variables is therefore beneficial.

The following sensitivity measure is suggested in Buijs et al. (2005) to capture the sensitivity to a mean value or standard deviation:

$$PD_{X_I} = \varepsilon\tau_{XI}\int_{Z\leq 0}\cdots\int\frac{\partial Z}{\partial X_I}\cdot f_X(X)dX = \varepsilon\tau_{XI}E\left(\frac{\partial Z^-}{\partial X_I}\right) \quad (4.9)$$

In which PD_{XI} is the sensitivity to a change in mean value or standard deviation, τ_{XI} is the standard deviation or mean value, ε is a small change which is given to each of the variables, e.g. 1% of the mean value or standard deviation τ_{XI}, f_X is the joint probability density function of $(X_1,.., X_n)$. The integral represents the expected value E of the partial derivative in the failure space Z^-, or $Z\leq 0$, illustrated by the right hand

part of (4.9). Figure 4.3 illustrates a change in the limit state equation Z due to time-dependency t=0 and t=1. The hatched area marks the change in density in the failure space $Z \leq 0$. The sensitivity measure in (4.9) evaluates the average change of the limit state equation Z at t=0 in the failure space due to a change in a variable X_i. It therefore considers the sensitivity of the function Z itself, rather than the probability of failure. In the latter case, the variation associated with the random variables would still play dominant role.

The PD_{Xi} are demonstrated alongside direction cosines in a reliability analysis of earth embankments in table 7.2, section 7.3.3, reinforced concrete walls in table 7.12, section 7.4.3, and anchored sheet pile walls in table 7.18, section 7.5.3.

4.3.3. Highlight time-dependent processes

In relation to sub-objective 2.2 – highlight relevant time-dependent processes – a risk-based importance measure is most suitable. A risk-based measure allows taking into account the increase in flood risk and the costs of both inspection and damage remediation. It therefore indicates how the different time-dependent processes impact on an optimisation curve such as figure 1.3. As mentioned before, time-dependent processes need to be represented and populated before the first life cycle optimisation can be carried out. Once such an optimisation model exists it is due to its complexity probably not feasible to produce results for each decision-making situation. Restrictions in capturing the full decision-making problem, information availability and

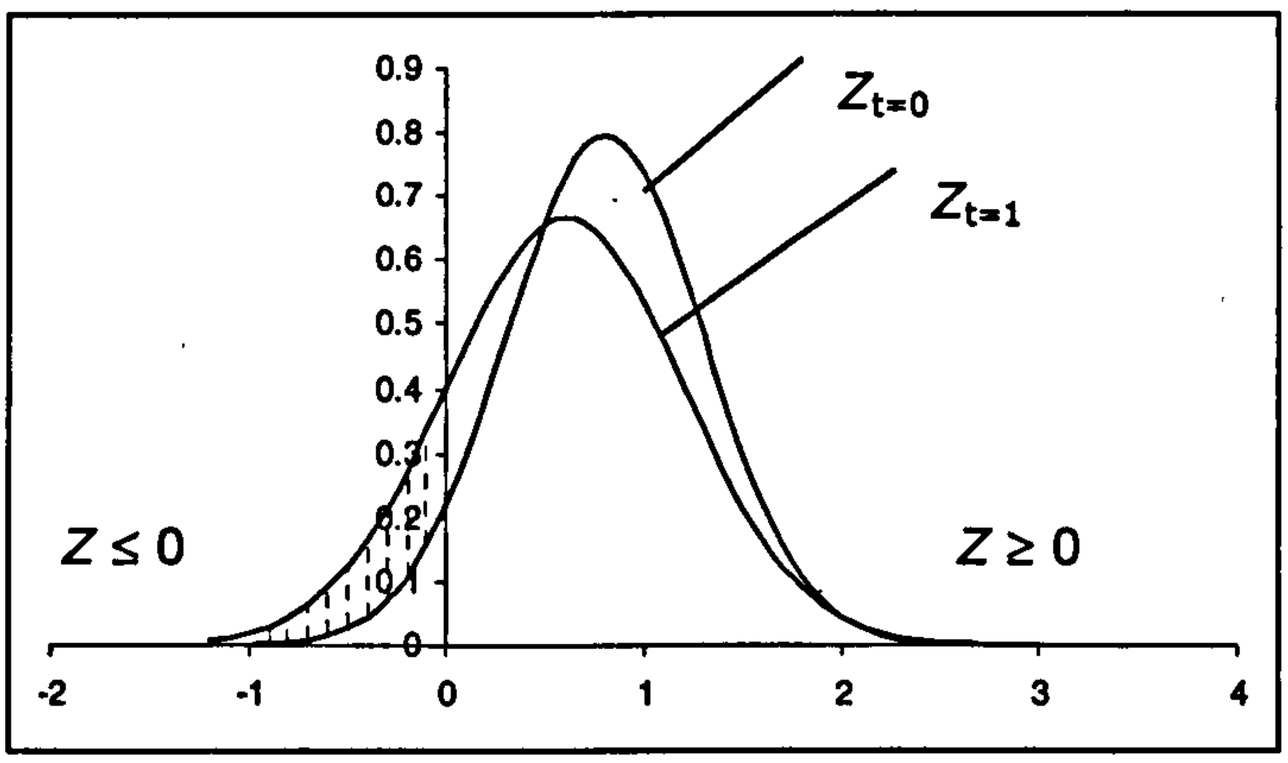

Figure 4.3 Change in shape of the density of limit state equation Z at t=0 and Z at t=1. The vertically hatched area is the increase in density in the failure space Z≤0.

knowledge about condition level standards limit the current level of detail of importance measures for time-dependent processes. The importance measures introduced below are a first indication to target monitoring to relevant time-dependent processes to identify repair or detailed inspection trigger condition levels. As discussed in section 4.3.1 a more refined representation of the relevance of time-dependency requires a life cycle optimisation model, which does not exist at this stage. Monitoring refers in this context to monitoring condition levels mentioned in section 4.1.2.

Relevant deterioration processes are therefore highlighted by a combination of the increase in flood risk and the cost of both inspection and damage remediation. The latter relates to the burden to risk importance ratio as defined in equation (4.5). Risk Achievement in table 4.2, or $R(x_i=1)$-R(base), comes closest to the risk importance associated with deterioration processes. $R(x_i=1)$ is the risk when the component x_i is fully failed. Instead of a fully failed component the increase in flood risk due to deterioration of a variable is taken. The change in flood risk is therefore caused by a change in probability of failure of a defence section ΔP_f:

$$\Delta P_f = \int_{Z(X_1,..X_i-\Delta_i,..X_n)\leq 0} f_{X,\Delta_i}(X,\Delta_i)dXd\Delta_i - \int_{Z(X)\leq 0} f_X(X)dX \qquad (4.10)$$

In which Δ_i is a deterioration increment with probability density function $f_{\Delta;i}(\Delta_i)$ and affects random variable X_i, $f_{X,\Delta i}$ is the joint density function of the vector of random variables X and the increment Δ_i, Z is the limit state equation whereby $Z\leq 0$ represents failure of the defence structure. The burden in the BIR is defined as the cost of the operational activities that have to be undertaken to remediate the deterioration increment and bring the flood risk back to its original level R(base).

A demonstration of importance measures highlighting asset time-dependent processes is given for earth embankments in section 7.3.3, reinforced concrete walls in section 7.4.3 and anchored sheet pile walls in section 7.5.3.

4.3.4. Indicate the flood risk reduction impact of operational activities

Decision-making problems such as in figure 4.1 consist of many different types of operational activities. The importance measures presented in this section allow an initial insight of the influence of standalone operational activities on a life cycle cost model. Reasons to make the scope of the importance measures not too specific to a

decision-making problem are mentioned in the following. It is not always possible to predict in advance which operational activity will be chosen at a specific moment in time. Moreover, time-dependent processes need to be represented and populated before the first life cycle optimisation can be carried out. Once such an optimisation model exists it is due to its complexity probably not feasible to produce results for each decision-making situation. Finally, restrictions in capturing the full decision-making problem, information availability and knowledge about condition level standards limit the current level of detail of importance measures for time-dependent processes.

In relation to sub-objective 2.3 – indicate the impact on flood risk reduction of different operational activities – a risk-based importance measure is most suitable. It takes the impact on flood risk reduction into account as well as the costs of the operational activities. It therefore indicates how the alternative operational activities impact on an optimisation curve such as figure 2.3. In the situation that immediate flood risk reduction needs to be achieved, the importance measure allows an evaluation of the alternative operational activities.

Definition importance measure for monitoring

Monitoring or inspection can be used to reduce the uncertainty of flood defence properties and therefore the flood risk in the floodplain. This type of monitoring is defined in section 4.3.1 as statistical uncertainty reduction monitoring. Section 4.2.2 shows that an effective uncertainty reduction policy is directed at high uncertainty contributing variables whose uncertainties are reducible. In addition, the amount of uncertainty reduction is determined by the performance of the monitoring strategy. Below firstly the BIR for monitoring is defined in general. Secondly the main inspection methods in the flood defence industry in the UK are described. These inspection methods have many different benefits in the context of monitoring condition levels as well as statistical uncertainty reduction monitoring. This section only considers the value of these inspections to statistical uncertainty reduction. These inspection methods are evaluated according to the following two aspects, see 3.2.3 based on Delft Cluster (2001). One aspect is the accuracy of the measurements of the observation variables **y**. Another aspect is the relationship between the (uncertainty in the) random variables x in the flood defence reliability model to the observations **y**.

This section introduces an importance measure to compare monitoring as an alternative activity to repair or improvement to achieve immediate flood risk reduction. Statistical uncertainty reduction monitoring relates to the discussion on reducible uncertainties in section 2.1. Measurements might lead to the adjustment of the mean value or standard deviation of a measured flood defence property. Such an adjustment can be in the form of an increase or decrease in mean value or standard deviation. For example, the crest level might turn out to be 0.1 meter higher or lower than anticipated. In addition, an increase in the measurement grid would provide a more precise representation of the variations in the crest level. The measured variability in the field can either be higher or lower than initially anticipated. However, in this context it is assumed that measurements only lead to a reduction of the standard deviation. The improved knowledge in the form of an increase or decrease of the mean value can result in an increase as well as a decrease in the flood risk level. Revision of the flood risk leading to an increase in flood risk level requires a larger operational response to bring the flood risk down to an acceptable level than initially anticipated. Knowledge about this necessity for more risk control is counted as a benefit.

The extent of the adjustment in mean value and standard deviation due to monitoring is unknown in advance and additionally depends on the measurement quality. $f(\theta_{Xl})$ is the probability density function of the adjustment in the parameter θ_{Xl} (e.g. mean value or standard deviation) of random variable X_l due to a measurement. For each realization of θ_{Xl} the contribution to the absolute change in flood risk ΔFR is calculated:

$$\Delta FR = \int_{\theta_{X_l}} \left| \left(FR \middle| \theta_{X_l} \right) - (FR) \right| d\theta_{X_l} \tag{4.11}$$

in which FR is the initial flood risk level in the floodplain. This expression only considers the relevance of monitoring in the context of statistical uncertainty reduction. The contribution of monitoring to identifying condition levels and failure mechanisms is not taken into account. In the BIR, the risk importance measure that is chosen corresponds with the Risk Reduction measure $R(\text{base})$-$R(x_i=0)$. Instead of taking $R(x_i=0)$, the risk whereby component x_i is fully optimized, the absolute change in flood risk due to monitoring of a flood defence section is taken. The distribution functions of simultaneous adjustments in mean value and standard deviation for one

random variable due to monitoring are assumed to be independent. The burden in the BIR corresponds with the costs of the monitoring activity.

Defra (2004), and section 2.2.1, distinguishes three types of inspection activities in the flood defence industry in the UK: visual inspection, routine inspection and specific inspection. The benefit of these inspections is only considered in the light of uncertainty reduction.

Visual inspection returns qualitative information about the flood defence properties. There is seldom a direct relationship between the observations and random variables in the reliability model. The impact of visual inspection as a means to achieve immediate flood risk reduction is therefore limited, Dawson & Hall (2002). It is, however, a cheap method to roughly identify condition levels that require further monitoring or a repair activity. Visual inspection therefore has a role in monitoring relevant time-dependent processes. It therefore has an indirect rather than a direct role in flood risk control.

Routine inspection involves quantitative monitoring of mainly external flood defence properties, e.g. collecting geometrical information. The accuracy of the inspection method is assumed to be good, i.e. the measurement error is assumed to be negligible. It is furthermore assumed that the observed variables are directly related to the random variables featuring in the reliability model. Routine inspection as a means to reduce flood risk is considered as distinct from monitoring time-dependent changes in geometrical properties.

Specific inspection entails the detailed inspection of external as well as internal flood defence properties, for example geometry as well as soil density information. The accuracy of the inspection method is good, i.e. the measurement error is assumed to be negligible. It is assumed that the observed variables are directly related to the random variables featuring in the reliability model. Specific inspection as a means to reduce flood risk is considered as distinct from monitoring time-dependent changes in flood defence properties, such as section 4.3.3.

Importance measure for repair and improvement

Below firstly the importance measure for repair or improvement is defined. Secondly, the main repair activities in the UK are mentioned. The importance measures consider repair and improvement as standalone activities in the life cycle cost problem. They

therefore provide an initial insight in the sensitivity of life cycle costing to different contributors in the model.

Repair activities either fully or partially recover flood defence properties to their original condition level. Improvements bring flood defence properties beyond their original condition level. In both cases the risk importance in the BIR corresponds with the Risk Reduction measure in table 3, $R(\text{base})$-$R(x_i=0)$, whereby $R(x_i=0)$ represents the flood risk in case of a repaired or improved flood defence section. The change in flood risk is caused by a change in probability of failure, analogous to equation (4.10):

$$\Delta P_f = \int_{Z(X)\leq 0} f_X(X)dX - \int_{Z(X_1,..,X_i+\Delta_i,..,X_n)\leq 0} f_{X,\Delta_i}(X,\Delta_i)dXd\Delta_i \qquad (4.11)$$

In which Δ_i is the repair or improvement increment with probability density function $f_{\Delta;i}(\Delta_i)$ affecting random variable X_i. The burden in the BIR is defined as the cost of the repair or improvement activity.

Defra (2004), and section 2.2.1, describes routine maintenance and periodic maintenance in the flood defence industry in the UK. Routine maintenance consists of activities such as grass cutting or dredging. Periodic maintenance involves more comprehensive structural repairs.

A demonstration of importance measures indicating the impact on flood risk of monitoring, repair and improvement activities is given for earth embankments in section 7.3.3, reinforced concrete walls in section 7.4.3 and anchored sheet pile walls in section 7.5.3.

Comparability of importance measures for monitoring with repair / improvement

The importance measures for statistical uncertainty reduction monitoring, repair and improvement all relate the change in flood risk due to the activity to the cost of the activity. The importance measures therefore make the impact of the operational activities on the flood risk comparable. It may seem counter-intuitive that monitoring leads to an improvement in the flood risk level without actually doing something to the flood defence system, like a physical improvement measure does.

Before commenting further on this issue, it is pointed out that in this context the uncertainties must be reducible by an increase in knowledge. An example of reducible uncertainty is more precise information on the crest levels. As pointed out in section

2.1 and 4.2.2 not all uncertainty types are reducible by measurements, e.g. natural variations in the water level. These uncertainties can be recognised by means of the direction cosines. Analysis of the high direction cosines leads to insight about the uncertainty types and their reducibility.

The incorporation of epistemic uncertainty, i.e. lack of knowledge, increases the probability of failure and hence the flood risk level. This effect is comparable to using higher safety factors in a deterministic design approach in case there is limited confidence about the values of the design variables. Such an adjustment leads to a more conservative and more expensive design reflecting the lack of confidence. Carrying out monitoring leads to a more precise description of the flood defence system and therefore increases the confidence in the flood risk levels. If the flood risk level turns out to be lower under increased knowledge, it might not be necessary to carry out a more expensive repair / improvement. If the flood risk level turns out to be higher under increased knowledge, a repair / improvement might be better justified.

In other words, the importance measures compare the value of increased confidence in the flood risk level by monitoring with the value of a physical repair or improvement. Monitoring therefore removes the lack of knowledge from the flood risk level. It is finally noted that the effect of statistical uncertainty reduction monitoring diminishes with an increasing number of monitoring activities. The measurements decrease the lack of knowledge and hence the reducible uncertainty.

4.4. Review

This chapter supports objective 2 described in chapter 1: to develop a sensitivity analysis method to highlight relevant asset time-dependent processes and maintenance operations in the context of a rational maintenance framework. This main objective can be broken down into three sub-objectives. Sub-objective 2.1 is to indicate the influence of individual random variables, i.e. flood defence properties, on the reliability analysis. Sub-objective 2.2 is to highlight relevant asset time-dependent processes. Sub-objective 2.3 is to indicate the impact on flood risk reduction of different operational activities in relation to the cost of the activity. Table 4.4 provides

an overview of the sub-objectives, the corresponding importance measures and where they are demonstrated in the case study in chapter 7.

Table 4.4 Overview of PhD objective 2 developed in chapter 4. Below the sub-objectives, the corresponding importance measures and the demonstration of the measures in chapter 7.

PhD objective 2:

Develop a method to highlight relevant asset time-dependent processes and maintenance operations in the context of a rational maintenance framework

Sub-objective	Importance measure	Demonstration in chapter 7
2.1 Indicate the influence of individual random variables	Direction cosines Partial derivative based concept	Earth embankments: Table 7.2 Reinforced concrete walls: Table 7.12 Anchored sheet pile walls: Table 7.18
2.2 Highlight relevant asset time-dependent processes	Cost-benefit ratio	Earth embankments: Table 7.3 Anchored sheet pile walls: Table 7.19
2.3 Indicate the impact on flood risk of operational activities	Cost-benefit ratio	Earth embankments: Table 7.4 Reinforced concrete walls: Table 7.13 Anchored sheet pile walls: Table 7.20

The first step is to review existing risk and reliability-based importance measures in the engineering industry. An overview of sensitivity analysis methods is given. The direction cosines and the reducibility of uncertainty types in flood risk management is discussed. Partial derivative based concepts are explored to capture the influence on the reliability of variables with a relatively low uncertainty contribution. Cost benefit ratio approaches in the engineering industry are reviewed. The Burden to risk Importance Ratio (BIR) provides a useful perspective. It stimulates the redistribution of operational activities to balance the cost benefit ratio rather than resorting to cutting low cost activities.

Based on this review importance measure to support risk-based flood defence management in advance or without full life cycle optimisation are developed and proposed. Before developing the importance measures, a distinction is made between monitoring condition levels, related to sub-objective 2.2, and statistical uncertainty reduction monitoring, related to sub-objective 2.3. This distinction is made in the

context of value of information theory. It is appropriate to reflect the value of monitoring condition levels in the overarching life cycle costing problem as it is an ongoing monitoring process in time. In the absence of a life cycle costing model this type of monitoring activity can best be targeted at the relevant time-dependent processes, highlighted under sub-objective 2.2. Statistical uncertainty reduction monitoring has an immediate impact on the flood risk. It is possible to compare this type of monitoring together with repair and improvement activities.

The influence of random variables on the reliability, sub-objective 2.1, is indicated by direction cosines and a partial derivative based concept (table 4.4). The latter complements the information from the direction cosines. Such information indicates which random variables might introduce time-dependency or a significant change in reliability due to operational activities. It needs to be placed in a cost benefit context to provide a basis for rational comparison of the impact of asset time-dependent processes or of operational activities. The cost benefit ratio, or BIR, is used to highlight relevant asset time-dependent processes, sub-objective 2.2. The increase in flood risk due to the asset time-dependent process is balanced with the cost of a remediation activity to bring the flood risk back to its original level. The cost benefit ratio is used to indicate the impact on the flood risk of operational activities, sub-objective 2.3. The change in flood risk due to the monitoring, repair or improvement activity is balanced with the cost of the operational activity. In this approach the value of the increased confidence in the flood risk level due to statistical uncertainty reduction monitoring is compared to the value of a physical repair or improvement activity. There are two benefits that are not quantified in this thesis. The first benefit is that routine inspection activities often increase the knowledge about the whole flood defence system in the same inspection activity. This thesis only considers individual flood defence sections. The second benefit is that specific inspection detects ongoing failure processes in addition to increasing the level of knowledge.

The importance measures supporting flood risk management are demonstrated for earth embankments in section 7.3.3, reinforced concrete walls in section 7.4.3 and anchored sheet pile walls in section 7.5.3 as part of the Dartford Creek to Swanscombe Marshes flood defence system. An overview is provided in table 4.4.

The importance measures highlight the relevant asset time-dependent processes in the flood defence system. The next step is to characterise these asset time-dependent processes with an appropriate statistical model. Chapter 5 reviews existing statistical

models for time-dependent processes in the engineering industry. Chapter 6 develops a modelling methodology for alternative statistical models of the asset time-dependent processes.

5. Existing statistical models for time-dependent processes

The importance measures developed in the previous chapter serve to highlight the relevant asset time-dependent processes as formulated in objective 2. Objective 3 is to develop a modelling methodology for statistical models of these asset time-dependent processes. This chapter reviews existing statistical models for time-dependent processes. Section 5.1 provides general definitions for stochastic processes and time series. It also discusses statistical properties that are relevant to the context of data analysis. Section 5.2 deals with time-dependent statistical models for overarching concepts such as failure rate, time-dependent reliability index or parametric processes. Sections 5.3 and 5.4 describe the properties of stochastic processes suitable to model time-dependent processes. Time-dependent processes can be related in a variety of different ways, e.g. correlation or displaying process model dependency. The nature of those relationships is discussed in chapter 5. Section 5.5 presents statistical models that are appropriate for correlated time-dependent processes.

5.1. Basic definitions related to stochastic processes and time series

5.1.1. Stochastic processes and time series

This section firstly goes into the definition of stochastic processes and their most important statistical properties. Secondly, the three main compositions of time-dependent processes are defined. Thirdly, the definition of time series is given.

Stochastic processes: definition and main statistical properties

A stochastic process described in popular terms is, Ross (2003): "a family of random variables that describes the evolution through time of some (physical) process." Ross' formal definition of a stochastic process $\{X(t),\ t \in T\}$ is a collection of random variables, for which for each $t \in T$, $X(t)$ is a random variable. The index t often represents time and therefore $X(t)$ is referred to as the state of the process at time t. The set T is the index set of the process. When T is countable the stochastic process is said to be a discrete-time process. If T is an interval of the real line, the stochastic process is said to be a continuous-time process. Finally, the state space of a stochastic process is defined as the set of all possible values that the random variable $X(t)$ can assume.

Melchers (1999) defines a number of basic properties associated with a stochastic process. In these properties, the outcome $x(t)$ of $X(t)$ is governed by the probability density function $f_X(x,t)$ as a function of time t. The development of the expectation in time is given by $\mu_x(t)$:

$$\mu_X(t) = \int_{-\infty}^{\infty} x f_X(x,t)dx \tag{5.1}$$

The autocorrelation function, $R_{xx}(t_1, t_2)$, plays an importance role in spectral analysis in section 5.1.2 and is defined by:

$$R_{XX}(t_1,t_2) = E[X(t_1)X(t_2)] = \int_{-\infty}^{\infty}\int_{-\infty}^{\infty} x_1 x_2 f_{XX}(x_1 x_2; t_1 t_2)dx_1 dx_2 \tag{5.2}$$

In which f_{XX} is the joint probability density function, x_i is the stochastic process at time $t=i$. The covariance function $C_{xx}(t_1, t_2)$ is defined as:

$$C_{XX}(t_1,t_2) = E\{[X(t_1)-\mu_X(t_1)][X(t_2)-\mu_X(t_2)]\} = R_{XX}(t_1,t_2) - \mu_X(t_1)\mu_X(t_2) \tag{5.3}$$

The autocovariance function becomes for $t_1 = t_2 = t$,

$$\sigma_X^2(t) = C_{XX}(t,t) = R_{XX}(t,t) - \mu_X^2(t) \tag{5.4}$$

Which is the variance function $\sigma^2_x(t)$.

Below the three main compositions of time-dependent processes are further explained according to figure 5.1.

Three main compositions of time-dependent processes

Figure 5.1 shows how a time-dependent process fits into a limit state function. It also presents the main ways to build up a time-dependent process with stochastic processes. Three types of process compositions are distinguished in figure 5.1 that are all a stochastic process according to the definition above. The types are: a parametric process, a stochastic process and a hierarchical process.

Limit state equation:

$Z = g(t)$

$g(t) = g(X_1, .., X_i(t), .., X_n, t)$

Time-dependent process $X_i(t)$ is a stochastic process, three main compositions:

1) $X_i(t)$	→ the overall time-dependent quantity is modelled with *a stochastic process*.
2) $X_i(t) = f(d_1, .., d_i(t), .., d_n)$	→ $X_i(t)$ is *a hierarchical process*, a function of random variables d_1 to d_n, among which $d_i(t)$ is a stochastic process.
3) $X_i(t) = f(d_1, .., d_n, t)$	→ $X_i(t)$ is *a parametric process*, I.e. a function of random variables d_1 to d_n and a deterministic time variable t.

Figure 5.1 Time-dependent processes in a limit state equation, and three main types of asset time-dependent process compositions.

In order to avoid confusion an explanation of the process-based model in this context is given. A process-based model refers to any kind of deterministic physical process representation irrespective of whether it is a function of time or not. A process-based model can either be used as a basis for a parametric process or for a hierarchical process.

A *parametric process* refers in figure 5.1 to a function $f(\mathbf{d},t)$ of random variables $\mathbf{d}$ and a deterministic time t. One realisation of the random variables $\mathbf{d}$ at t=0 fully fixes one deterministic sample path, see figure 5.2. A parametric process often corresponds with an existing deterministic process model for a time-dependent process, whereby the variables are considered random. If those random variables exhibit e.g. purely inherent uncertainty in space, such an approach is justified. However, there is often an aspect of the time-dependent process that exhibits inherent uncertainty in time. A *stochastic process* in figure 5.1 then refers to a random quantity $X_i(t)$ whose future predictions are not fixed by the preceding sample path. Figure 5.2 illustrates the

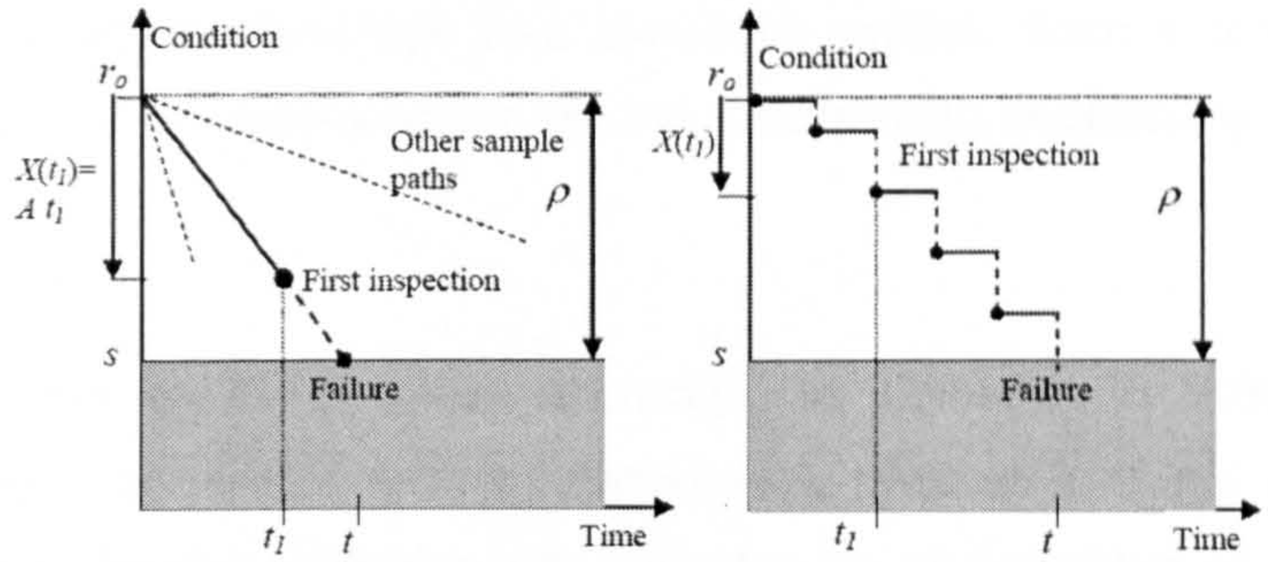

Figure 5.2 Sample paths in case of a parametric process (left) compared to the sample paths in case of a stochastic process approach (right), from Pandey & Van Noortwijk (2004)

difference between a parametric process and a stochastic process. Finally, a *hierarchical process* in figure 5.1 is a combination of a parametric process and stochastic processes. As mentioned above, all three types of processes are stochastic. Nevertheless, from this point on the distinction between a parametric process, a stochastic process and hierarchical process is made according to figure 5.1.

In some cases the time-dependent quantity is modelled with an aggregate stochastic process $X_i(t)$, even though a qualitative analysis suggests a hierarchical process. There are a number of reasons to resort to such a solution. Firstly, an overall stochastic process attempts to represent the inherent uncertainty in time which is an advantage over a simplification with a parametric process. A second reason can be that due to lack of scientific understanding it is not possible to find a satisfactory hierarchical process formulation. A stochastic process model allows in that case a rough estimate of the time-dependent process. A third reason is limited data availability to populate a process-based model. In some situations there is some field information about the development of the overall time-dependent quantity of interest, but not about random variables d_1 to d_n. A last reason mentioned here is the representation of asset time-dependency in broad risk assessments as introduced in section 3.1.2, figure 3.3. Broad risk assessments require a computationally feasible stochastic process representation given the constraints of such an assessment. Broad risk assessments are carried out under constraints of limited financial and time resources and limited information availability. Still, the time-dependent behaviour needs to be represented as closely as possible. An overall stochastic process approach can offer a suitable solution in that context. Such a solution is computationally

feasible within the available time due to a simplified model. Such a solution provides rough time-dependency estimates under limited information availability.

Time series

The definition of time series is taken according to Grimmet & Stirzaker (2001). Therein the realisation or sample path of a stochastic process X at $\omega \in \Omega$ (the sample space) is represented by the collection $\{X_t(\omega) : t \in T\}$ of members of state space S. Sequences of observations $\{x_n : 0 \leq n \leq N\}$, referred to as time series, are often suitably modelled by stochastic processes. The challenge is to bring the underlying structure in such observation sequences to light, and capture that structure with an appropriate stochastic process model.

5.1.2. Stationary processes, ergodicity and spectral analysis

Stationarity, ergodicity and spectral analysis are important notions in time series analysis. Below, firstly the definitions of stationary processes and ergodicity are given. They underpin assumptions allowing the straightforward derivation of statistical properties from time series with a limited sample size. Secondly, an explanation of spectral analysis is given. It presents the relationship between the statistical properties of theoretical stochastic process models and of the time series samples they are meant to represent.

Stationarity

A stochastic process can either be strictly stationary or weakly stationary. Reference for definitions is made to e.g. Melchers (1999) or Ross (2003). A stochastic process is said to be strictly stationary if its statistical properties do not change in time, i.e. all the moments are independent of time. The stochastic process is weakly stationary or covariance stationary if only the mean $\mu_X(t)$ and the autocorrelation $R_{XX}(t_1,t_2)$ are independent of time.

Ergodicity

Melchers (1999) asserts that a process is weakly ergodic if the mean and correlation function can be defined by the time average over a single realisation of the process. The process is called strictly ergodic if the equality holds for all moments of a strictly

stationary process. The ergodicity property only holds for stationary processes. The property is of considerable practical value in estimating statistical parameters from one or a few sufficiently long records of the process. The obtained accuracy depends on the duration T of available records. Often stationarity and ergodicity are assumed to hold in the analysis of stochastic process records unless (and until) there is evidence to the contrary, Melchers (1999).

Ergodicity in the mean is defined as:

$$\mu_X = \lim_{T\to\infty}\left[\frac{1}{T}\int_0^T x(t)dt\right] \tag{5.5}$$

In which μ_x is the mean of the stochastic process $X(t)$ and T is the duration of the available time series record. Ergodicity in the correlation is defined by:

$$R_{XX}(\tau) = \lim_{T\to\infty}\left[\frac{1}{T}\int_0^T x(t+\tau)x(t)dt\right] \tag{5.6}$$

In which τ is a time interval $[t,t+\tau]$.

Spectral analysis

Background to spectral analysis and its relations to time series analysis is e.g. provided in Percival & Walden (1993). A time series X_t can be written as a sum of harmonic components:

$$X_t = \mu + \sum_{j=1}^{N/2}\left[A_j\cos(2\pi f_j t) + B_j\sin(2\pi f_j t)\right] \qquad j = 1,2,\ldots,N \tag{5.7}$$

In which μ is the trend, A_j the amplitude of the sine elements, B_j the amplitude of the cosine elements, t is time, N is the length of the time series sample. The Fourier standard frequency f_j is defined as:

$$f_j = \frac{j}{N}$$

For a stationary process the following holds:

$$E(A_j) = E(B_j) = 0$$

$$E(A_j^2) = E(B_j^2) = \sigma_j^2$$

$$E(X_t) = \mu$$

$$E(X_t - \mu)^2 = \sum_{j=1}^{N/2} \sigma_j^2$$

The autocorrelation function ρ_k between $t=0$ and $t=k$ can therefore be expressed as:

$$\rho_k = \frac{\sum_{j=1}^{N/2} \left(\sigma_j^2 \cos(2\pi f k)\right)}{\sum_{j=1}^{N/2} \sigma_j^2} \qquad (5.8)$$

$$\sigma^2 = \sum_{j=1}^{N/2} S_j \qquad (5.9)$$

S_j is the spectrum, or the spectral density function, whereby the area over a frequency width equals the contribution of the variance of those frequencies to the total variance of the time series. Spectral analysis considers the time series, a set of observations, as a sample from the underlying infinitely continuing random process. The spectrum is thereby representative of the observations, not of the underlying random process.

The spectral distribution function $F(\omega)$ is defined as the contribution to the variance of the series which is accounted for by frequencies in the range $(0, \omega)$.

The spectral density function is:

$$f(\omega) = F(\omega) / d\omega = S(\omega) \qquad (5.10)$$

The relationships between the spectrum and the autocovariance $\gamma(k)$ and autocorrelation $\rho(k)$ are given below.

$$\gamma(k) = \int_0^{\infty} \cos(\omega k) dF(\omega) \qquad (5.11)$$

$$dF(\omega) = S(\omega) d\omega$$

The spectral density as a function of the autocovariance function is defined as:

$$f(\omega) = \frac{1}{\pi}\left[\gamma(0) + 2\sum_{k=1}^{\infty} \gamma(k)\cos(\omega k)\right] \qquad (5.12)$$

The normalized spectrum is defined as a function of the autocorrelation function:

$$f^*(\omega) = f(\omega) / \sigma_X^2 = \frac{1}{\pi}\left[1 + 2\sum_{k=1}^{\infty} \rho(k)\cos(\omega k)\right] \qquad (5.13)$$

The sample autocorrelation can then be used to estimate the spectral density of the time series.

Grimmet & Stirzaker (2003) relate the autocorrelation and the characteristic function of a statistical distribution. The definition of the characteristic function of a statistical distribution is as follows:

$$\phi(t) = E\left(e^{itX}\right) = \int e^{itX} dF(x) = E\{\cos(tX)\} + E\{i \sin(tX)\} \tag{5.14}$$

The autocorrelation function $\rho(t)$ of a weakly stationary process X with strictly positive variance is the characteristic function of some distribution function F whenever $\rho(t)$ is continuous at t=0:

$$\rho(t) = \int_{-\infty}^{\infty} e^{it\lambda} dF(\lambda) \tag{5.15}$$

If the autocorrelation function $\rho(t)$ satisfies (5.15) then $F(\lambda)$ is the spectral distribution function. Derivation of the characteristic function of a stochastic process enables the determination of the autocorrelation function. Comparison of the theoretical autocorrelation function to the sample autocorrelation allows an evaluation of the quality of the representation of the underlying structure in the time series by the stochastic process model.

5.2. Failure rate, time-dependent reliability index and reliability analysis

This section discusses time-dependent statistical models for overarching concepts such as the failure rate or the time-dependent reliability index. Such models treat the failure rate or reliability index as a time-dependent random variable. A reliability-based approach consists of time-dependent limit state equations and a probabilistic model. The time-dependent reliability index and / or the failure rate are then simulated by means of that model. The time-dependent limit state equations are of the form introduced in figure 5.1.

Failure rate models originate from the mechanical and electrical engineering disciplines. In these fields usually two states are considered: the functioning state and the failed state. The expressions which are used in failure rate models are the failure

rate function and the lifetime distribution. Failure rates are in this approach derived from data collection about the failure of components. Such an approach corresponds with the classical or frequentistic view of probability based on the limiting relative frequency in repeated identical trials, Pratt et al. (1995). This frequentistic approach is often feasible within the mechanical or electrical disciplines. The lifetime of components is relatively short and it is possible to test a large number of identical components. A more comprehensive description of the expressions below is given in section 2.1.4.

$$r(t) = \frac{f(t)}{1 - F(t)} = \frac{f(t)}{\overline{F}(t)}, \qquad t > 0 \tag{5.16}$$

$$\overline{F}(t) = \exp\left\{ - \int_0^t r(\tau) d\tau \right\} \tag{5.17}$$

In which $f(t)$ is the density function of the lifetime, $F(t)$ is the cumulative distribution function, $r(t)$ is the hazard function (also referred to as the conditional failure rate) and $\overline{F}(t)$ is the complement of the cumulative distribution function $F(t)$.

Frangopol (2004) presents an approach for the time-dependent reliability index. This concept defines the reliability profile as a variation of the reliability index with time. E.g. the bilinear reliability profile given below:

$$\beta(t) = \begin{cases} \beta_0 & for \;\; 0 \le t \le t_I \\ \beta_0 - \alpha_1 (t - t_I) & for \;\; t > t_I \end{cases} \tag{5.18}$$

Or for a non-linear relationship:

$$\beta(t) = \begin{cases} \beta_0 & for \;\; 0 \le t \le t_I \\ \beta_0 - \alpha_2 (t - t_I) + \alpha_3 (t - t_I)^2 & for \;\; t > t_I \end{cases} \tag{5.19}$$

In which $\beta(t)$ is the time-dependent reliability index, β_0, α_1, α_2, etc., are coefficients in the equations. These coefficients are usually estimated by means of expert elicitation. Maintenance activities are triggered when a target reliability level is reached. The reliability profile of the total system is hereby obtained by statistically combining the reliability profiles of the individual components. Other applications incorporate a time-dependent condition index in the reliability profile.

A frequentistic statistical approach for the probability of failure, failure rate or time-dependent reliability of a flood defence structure is not practical. Long-term data of

flood defence failures and the site specific circumstances are not plentiful to underpin such an approach. Another possibility is to estimate failure rate, time-dependent reliability index, risk and reliability indicators with expert elicitation (Cooke, 1991 and Cooke & Goossen, 2004). However, relationships for the time-dependent reliability index, such as (5.18) or (5.19), do not appreciate the physical process driving the time-dependency.

A reliability-based approach based on parametric processes is chosen as overarching approach. This probabilistic model builds on the (time-dependent) physical behaviour and quantitative knowledge of the flood defence system. In addition, it enables the probabilistic derivation of the lifetime probability of failure and failure rate. The latter two reliability concepts are required in maintenance optimisation problems (section 3.2.1).

5.3. Renewal models

5.3.1. Rectangular wave renewal and pulse processes

Vrouwenvelder (2005) and Karadeniz & Vrouwenvelder (2003) describe a variety of statistical time-dependent models. In the rectangular wave renewal and pulse process category, a number of aspects may vary amongst those statistical models. One aspect is for instance whether the time intervals are random or deterministic. Another aspect is whether the values in subsequent intervals are dependent or independent. Whether the process is stationary or non-stationary is a third aspect that may be considered differently.

A well-known example of a rectangular wave renewal process is the Ferry Borges Castanheta process, shown in figure 5.3. This process represents the simplest case of wave renewal processes. It is constructed of deterministic and equal time intervals Δt. The values of the process in the various intervals are independent. The value in each interval is characterised by the same statistical distribution function $F_x(X)$.

A well-known example of a pulse process is the Poisson process, see figure 5.3, Vrouwenvelder (2005). This process is characterised by short pulses at random time intervals making it a type of rectangular wave process. The probability to have a pulse in short interval Δt is usually indicated as $\lambda \Delta t$. The time between pulses is equal to $1/\lambda$.

A Poisson process is a renewal process with exponentially distributed arrival times with rate λ, Ross (2003):

$$f(x) = \lambda \exp\{-\lambda x\} \tag{5.20}$$

Amounts to a Poisson process, with for N_t:

$$P\{N_t = m\} = \frac{(\lambda t)^m \exp\{-\lambda t\}}{m!} \qquad (m = 0,1,\ldots,) \tag{5.21}$$

A wave renewal process is suitable to model properties that display for instance seasonal effects, such as pore pressure distributions. Poisson processes make a finite number of jumps in finite intervals. Poisson processes are therefore suitable to model damage due to sporadic shocks, Frangopol et al. (2004).

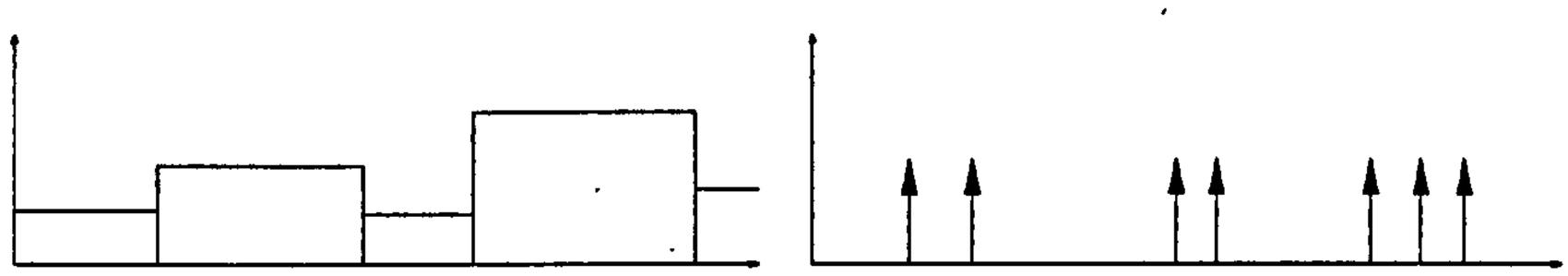

Figure 5.3 Examples of a wave renewal process (left) and a Poisson pulse process (right)

5.3.2. Gamma processes

In Van Noortwijk et al. (1997) a generalised gamma process model is recommended to represent deterioration processes such as erosion and the occurrence of scour holes. The gamma process as a model for degradation first appears in Abdel-Hameed (1975). One way of explaining the appropriateness of the gamma process to model deterioration corresponds with the cumulative renewal process indicated in (5.28) below after Cox (1962). Another explanation is given in more detail below.

According to Van Noortwijk et al. (1997), two assumptions underlie the gamma process model. The first is that the deterioration increments are non-negative and exchangeable. The second is that the amounts of deterioration are l_1-isotropic, see Van Noortwijk et al. (1995). The latter property entails that the decision-maker is indifferent in the way in which the average rate of deterioration is achieved; all combinations of deterioration increments leading to the same average receive the same belief. The mathematical consequence is that the vector of deterioration increments is invariant under all n! permutations of the increments:

$$(\delta_1(\tau),\ldots,\delta_n(\tau)) = (\delta_{\pi(1)}(\tau),\ldots,\delta_{\pi(n)}(\tau))$$

Where δ_i is the i^{th} deterioration increment, τ is the length of the time interval and the subscript π stands for permutation. A consequence of the l_1-isotropic property includes that the sequence of deterioration increments exhibits the 'lack of memory' property. The probability distribution functions of future increments are then independent of the distribution function of those in the past.

Based on the assumptions described above, the joint probability density function for an infinite sequence of deterioration increments given the average rate of deterioration θ turns out to be:

$$p(\delta_1,\ldots,\delta_n) = \int_0^\infty \prod_{i=1}^{n} p(\delta_i)\,dP(\theta)$$
$$\theta = \lim_{N\to\infty} \frac{1}{n}\sum_{i=1}^{n} \delta_i \qquad (5.22)$$

Which shows that the deterioration increments are conditionally independent given the average rate of deterioration. $dP(\theta)$ represents the uncertainty in θ which are not addressed in this case study. The model corresponds with the De Finetti general representation theorem, see Bernardo & Smith (2000).

The temporal variability of the deterioration has been modelled as a so-called gamma process, according to van Noortwijk et al. (1997). A gamma process is a non-decreasing cumulative stochastic process for which the increments are statistically independent, gamma-distributed random quantities with identical scale parameter. The mathematical definition of the gamma process is given as follows. Recall that a random quantity X has a gamma distribution with shape parameter $v > 0$ and scale parameter $u > 0$ if its probability density function is given by:

$$\mathrm{Ga}(x \mid v,u) = \frac{u^v}{\Gamma(v)} x^{v-1} \exp\{-ux\} I_{(0,\infty)}(x), \quad x > 0, \qquad (5.23)$$

$$\Gamma(a) = \int_{t=0}^{\infty} t^{a-1} e^{-t} dt \qquad (5.24)$$

In which $I_{(0,\infty)}=1$ for $x\in(0,\infty)$ and $I_{(0,\infty)}=0$ for $x\notin(0,\infty)$. The latter is the gamma function for $a > 0$. It is assumed that the probability density function of the cumulative deterioration $X(t)$ can be written as:

$$p_{X(t)} = Ga(x|a,b) = Ga\left(x\left|\left[\mu^2 t\right]/\sigma^2, \mu/\sigma^2\right.\right)$$
$$E(X(t)) = \mu t \qquad (5.25)$$
$$Var(X(t)) = \sigma^2 t$$

In which μ is the expected deterioration per unit time and σ^2 is the variance of the deterioration per unit time. A consequence of the application of the model based on the mathematical foundation above is that the development of the deterioration in time is a linear model. Estimates of μ and σ can be made in the following ways: expert elicitation; in-situ data about the deterioration process; physical process-based models of the deterioration process. In some situations a combination of the three might be desired.

Gamma processes are suitable to model gradual deterioration in time. The process makes an infinite number of jumps in finite intervals. In addition, the gamma process model only takes on non-negative values, which makes spontaneous improvement of the structure impossible. Another advantage of the gamma process model is that in the absence of proper models to describe the deterioration in time, expert elicitation can be used to estimate the average rate of deterioration.

Speijker et al. (2000) and Van Noortwijk and Klatter (1999) are examples in which a non-linear physical process-based deterioration model is applied to the expectation of the gamma process. Speijker et al. (2000) applies a non-linear crest level settlement model in the context of a gamma process. Van Noortwijk and Klatter (1999) introduce a non-linear scour hole erosion model in combination with the gamma process approach.

It is noted however that the mathematical derivation of the gamma process model is based on the exchangeability of the increment vectors. The exchangeability of the deterioration increments leads to the De Finetti representation theorem (Bernardo and Smith, 2000). If the deterioration behaves non-linear in time, the increments are not exchangeable. Thus in the non-linear case there is no explicit justification to apply the gamma process model. However, it is a flexible stochastic process model among the other alternative stochastic process models in non-linear applications.

5.3.3. Compound renewal processes

Examples of compound renewal processes are: superposed renewal processes, alternating renewal processes, cumulative renewal processes. Some general characteristics of these processes are discussed below.

Superposed renewal processes are illustrated in figure 5.4. The crosses represent realisations of the individual processes 1, 2 and 3 on the top three time bars. Superposed the three processes are represented by the realisations, indicated by crosses, on the pooled output time bar. The pooled number of renewals in $(0,t)$ $N_{t(p)}$ is defined in Cox (1962) as:

$$N_{t(p)} = N_t^{(1)} + N_t^{(2)} + \ldots + N_t^{(p)} \tag{5.26}$$

In which $N_t^{(i)}$ is the i^{th} contributing renewal process; these are independently normally distributed with mean t/μ and variance $\sigma^2 t/\mu^3$ for large t. Thus, $N_{t(p)}$ is asymptotically normal with mean pt/μ and variance $p\sigma^2 t/\mu^3$. Furthermore to the time to the r^{th} renewal the following applies:

$$prob(S_{r(p)} > t) = prob(N_{t(p)} < r) \tag{5.27}$$

and therefore $S_{r(p)}$ is asymptotically normal with mean $\mu r/p$ and variance $\sigma^2 r/p^2$.

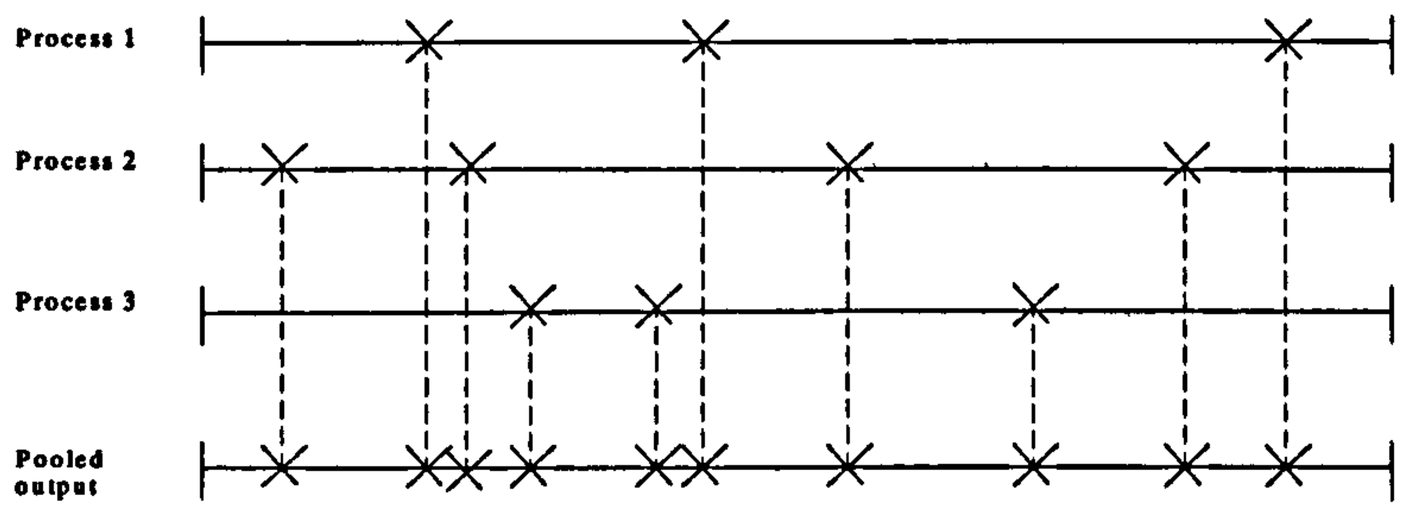

Figure 5.4 Illustration of superposed renewal processes, after Cox (1962)

Ross (2003) categorises *alternating renewal processes* as an example of regenerative processes. A regenerative process is a stochastic process which has the property that time points exist on which the process probabilistically restarts itself. Cox (1962) suggests that one generalisation is to have k types of components following one another in cyclic order. Another is to have k types of components and a matrix of p_{ij} transition probabilities specifying the probability that a type i component is replaced by a type j component. Such processes are also referred to as semi-Markov processes.

Cox (1962) describes *cumulative processes* whereby a second variable W_i is associated with the failure of the i^{th} component, X_i. W_i and X_i can hereby be dependent. If W_i are assumed to be independent and identically distributed and independent of X_i then the random variable Z_t can be written as:

$$Z_t = \sum_{i=1}^{N_t} W_i \qquad (N_t = 1,2,\ldots), \qquad (5.28)$$
$$= 0 \qquad (N_t = 0)$$

One of the examples in Cox (1962) is a component subject to wear due to a series of blows administered with a hammer. The blows occur in a renewal process (e.g. a Poisson process) and W_t is the amount of wear produced by the i^{th} blow. Z_t then represents the total wear of the component at time t.

Similar to compound Poisson processes, general compound renewal processes have a finite number of jumps in finite time intervals. They are therefore suitable to model sporadic shock damages.

5.4. Gaussian processes and Brownian Motion

5.4.1. Gaussian processes

Ross (2003) defines a Gaussian process as follows. A stochastic process $\{X(t), t\geq 0\}$ is called a Gaussian, or a normal, process if $X(t_1),\ldots, X(t_n)$ has a multivariate normal distribution for all $t_1, \ldots, t_n$. According to Vrouwenvelder (2005), having single Gaussian distribution functions is a sufficient condition to achieve that. Furthermore, a Gaussian process is fully described if the mean and variance for each point in time is known. Secondly, the covariance for all combinations of two points in time has to be defined. Knowledge about the autocovariance function $R_{xx}(\tau)$ and the mean μ_x is sufficient to define a Gaussian stationary process.

A parametric time-dependent function, i.e. a function of random variables and a deterministic time, can also be a Gaussian stochastic process as long as it fulfils the conditions defined above. Time-dependent processes modelled by a Gaussian process can assume negative as well as positive increments. A strictly increasing deterioration process would not be appropriately captured by such a model. However, there are

deterioration processes that are known to develop according to positive as well as negative increments. For instance morphological changes involve accretion as well as erosion. Erosion of rock armour revetments can also lead to a temporary increase in strength, if the rocks are forced into a stronger position.

5.4.2. Brownian motion

Ross (2003) shows how the Brownian motion can be related back to the symmetrical random walk. The latter is a Markov process that during each unit of time Δt can take a step Δx to the left or to the right with equal probability. Taking $\Delta t \rightarrow 0$ and $\Delta x \rightarrow 0$ leads to the Brownian motion, a continuous stochastic process. It originates from a model for the behaviour of a particle which is fully immersed in liquid or gas, developed by an English botanist Robert Brown. It has been widely applied since to all sorts of continuous stochastic processes such as price levels at stock market and quantum mechanics, Ross (2003).

The theoretical definition of a Brownian motion, also referred to as a Wiener process, can be found in references such as Ross (2003) or Grimmet & Stirzaker (2003). Below a definition is given of the Wiener process and the most common variations on the Brownian motion, i.e. the standard Brownian motion and the Brownian motion with drift. Subsequently, a number of other frequently occurring variations are mentioned to provide a flavour of the type of problems that can be modelled with a Brownian motion. Such Brownian motion processes are: the geometric Brownian motion, Brownian bridge, Brownian motion with a reflecting barrier, Brownian motion with an absorbing barrier, integrated Brownian motion.

A *Wiener process* W = $\{W(t): t \geq 0\}$, starting from $W(0) = w$, say, is a real-valued Gaussian process such that:

(a) W has independent increments

(b) $W(s+t) - W(s)$ is distributed as $N(0,\sigma^2 t)$ for all $s, t \geq 0$ where σ^2 is a positive constant

(c) the sample paths of W are continuous

The autocovariance function is given by:

$$c(s,t) = E([W(s) - W(0)][W(t) - W(s)])$$
$$= E\left([W(s) - W(0)]^2 + [W(s) - W(0)][W(t) - W(s)]\right) \quad (5.29)$$
$$= \sigma^2 s + 0$$

For σ=1, the process is called a *standard Brownian motion*.

A stochastic process $\{X(t), t \geq 0\}$ is a *Brownian motion with drift* with coefficient μ and variance parameter σ^2 when:

(i) $X(0) = 0$

(ii) $\{X(t), t \geq 0\}$ has stationary and independent increments

(iii) $X(t)$ is normally distributed with mean μt and variance $t\,\sigma^2$

Equivalently, the standard Brownian motion can be used to define the Brownian motion with drift:

$$X(t) = \sigma B(t) + \mu t \quad (5.30)$$

In which again μ is the drift coefficient and σ^2 the variance parameter.

A *geometric Brownian motion* process, $X(t)$, is defined as a function of $\{Y(t), t \geq o\}$ which is a Brownian motion process with drift:

$$X(t) = \exp(Y(t)) \quad (5.31)$$

A *Brownian bridge* excludes all zero values from the diffusion process. A *Brownian motion with a reflecting barrier* is a diffusion process only taking on positive values. Such a time-dependent process does not take on negative values. Grimmet & Stirzaker (2003) define a Wiener process with reflecting barrier as: $W^r(t) = |w+W(t)|$. The density function of the random variable $W^r(t)$ then becomes:

$$f^r(t,y) = f(t,y-w) + f(t,y+w), \qquad y > 0 \quad (5.32)$$

In which $f(t,y)$ is the $N(0,t)$ density function. The density is hereby mirrored in the horizontal axis. A *Brownian motion with an absorbing barrier* is a diffusion process only taking on positive values and stopping after first hitting zero. *Integrated Brownian motion* is a process $Z(t)$ whereby the rate of change is a Brownian motion $X(t)$, i.e.

$$\frac{d}{dt} Z(t) = X(t)$$
$$Z(t) = Z(0) + \int_0^t X(s)ds \quad (5.33)$$

For example a Brownian motion is applied to model the rate of change of a time series. Depending on the persistence of a negative rate of change, it is possible that the actual time series becomes negative.

The following comment is made in 5.4.1 with regard to the Gaussian stochastic processes and also applies to the Brownian motion. Some time-dependent (deterioration) processes strictly increase in time. A Wiener process would then not be an appropriate representation as it leads to negative as well as positive increments.

5.5. Correlated time-dependent processes

Time-dependent processes can be related in a variety of different ways, e.g. correlation or displaying process model dependency. The nature of those relationships is discussed in chapter 5. This section describes three main types of statistical models that are appropriate for correlated time-dependent processes. These main types are: arbitrary multivariate distribution functions, transformation to the normal space and a copula dependency structure.

Arbitrary multivariate distribution functions

Dependent deterioration processes are each represented by a marginal distribution function. The challenge is to find an appropriate multivariate distribution function that captures the dependency as well as the marginal statistical distribution functions. Details about multivariate distribution functions can be found in Kotz et al. (2000).

Buijs et al. (2005a) provides an example of a multivariate distribution function, whereby two singular deterioration processes with a common deterioration excitation are represented. The singular deterioration processes are each modelled with a gamma process marginal statistical model. This allows an expert elicitation-based approach to estimate average deterioration rates. The double-gamma distribution function is then applied to represent the dependencies between the two singular gamma processes.

Transformation to multivariate normal space

It is possible to model multivariate dependency by transforming the marginal variables to the normal space and applying a multivariate normal distribution function, Kotz et al. (2000).

This method provides an outcome if there is no multivariate distribution function that both appropriately represents the dependency and the marginal distributions. Additionally, the multivariate normal distribution function is numerically easy to handle. On the other hand, the dependency structure in the normal space is not necessarily the appropriate representation of the dependency.

Copula dependency structure

Another method to capture dependencies between dependent deterioration processes is the application of copulas between the statistical marginal models. Copulas are a recently emerging method to model statistical dependencies between random variables. One of the main advantages is that the multivariate distribution function can be derived whilst keeping the marginal distributions in tact. Diermanse & Van der Klis (2005) apply copulas to model the statistical dependency between the discharge of the IJssel river and that formed by other tributaries to the IJssel lake. Diermanse & Van der Klis (2005) provide the basics of the copula approach for K random variables, with marginal distribution functions $F_1,\ldots,F_K$:

$$F(x_1,\ldots,x_K) = P(X_1 \le x_1,\ldots,X_K \le x_K)$$

A function C: $[0,1]^K \rightarrow [0,1]$ is then a copula function of F if:

$$C(F_1(x_1),\ldots,F_K(x_K)) = F(x_1,\ldots,x_K) \qquad (5.34)$$

The multivariate distribution function F has one unique copula function if all marginal distribution functions are continuous. An algorithm to generate data with a specific copula structure corresponding to Archimedean copulas (one type of copula family) is:

$$C(u_1,\ldots,u_K) = P(U_1 \le u_1,\ldots,U_K \le u_K) \qquad (5.35)$$

$$C_l(u_l|u_1,\ldots,u_{l-1}) = P(U_l \le u_l|U_1 = u_1,\ldots,U_{l-1} = u_{l-1}) \qquad (5.36)$$

In which C is the copula function, U_1, ..., U_K are standard uniformly distributed random variables and whereby the conditional distribution function can be derived as follows:

$$C_l = \frac{\partial^{l-1} C_l(u_1,\ldots,u_l)}{\partial u_1 \ldots \partial u_{l-1}} \Bigg/ \frac{\partial^{l-1} C_{l-1}(u_1,\ldots,u_{l-1})}{\partial u_1 \ldots \partial u_{l-1}} \qquad (5.37)$$

The generic algorithm is as follows:

1) Generate a sample u_1 from the standard uniform distribution function

2) Generate a sample u_2 from the distribution function $C_2(u_2|u_1)$

3) Generate a sample u_3 from the distribution function $C_3(u_3|u_1, u_2)$

⋮

K) Generate a sample u_K from distribution function $C_K(u_K|\ u_1, u_2, \ldots, u_{K-1})$

Cherubini et al. (2004) shows how a copula function relates to the original marginal distributions and the bivariate distribution function:

$$\begin{aligned} C(F_1(x), F_2(y)) &= \Pr(U_1 \le F_1(x), U_2 \le F_2(y)) \\ &= \Pr\left(F_1^{-1}(U_1) \le x, F_2^{-1}(U_2) \le y\right) \\ &= \Pr(X \le x, Y \le y) \\ &= F(x, y) \end{aligned} \tag{5.38}$$

Cherubini et al. (2004) refers to several families of copula functions for bivariate or multivariate dependency: the multivariate Gaussian copula (which generates the standard joint normal distribution function), the multivariate Student's t copula, the multivariate dispersion copula and Archimedean copulas. Examples of the latter dependency structure are: Gumbel n-copula, Clayton n-copula and Frank n-copula. Archimedean copulas use the random generator as described above in equations (5.35) to (5.37). By randomly sampling from the standard uniform distribution function, the copula function can be calculated. The corresponding marginal variables can be found by transformation of the random draws. A limitation of the Archimedean copulas is that there are only one or two parameters that can be used to define the dependence structure.

This method provides an outcome if there is no multivariate distribution function that both appropriately represents the dependency and the marginal distributions. It also provides alternative dependency structures to the multivariate normal distribution function. The original marginal distribution functions remain thereby in tact.

5.6. Review

Three main compositions of time-dependent processes in reliability analysis are brought forward, i.e.: stochastic process, hierarchical process and parametric process. All three types of compositions are a stochastic process strictly according to the definition of a stochastic process. A parametric process is a function of random

variables and a deterministic time variable. A parametric process is usually derived from a process-based model. A hierarchical process consists of random variables and one or more stochastic processes introducing inherent uncertainty in time. A stochastic process represents the inherent uncertainty in time associated with one time-dependent quantity. A stochastic process for an overall asset time-dependent quantity is in some cases favoured over a more detailed hierarchical process model. Lack of scientific understanding or the unavailability of field information are for example reasons to choose for such an approximation. It is also possible that due to financial and time constraints in some situations a detailed approach is not feasible.

It is possible to estimate the time-dependency in overarching reliability concepts such as the failure rate or the time-dependent reliability index by expert elicitation. However, a reliability-based approach to time-dependency is preferred over these methods. The main advantage of a reliability-based approach to time-dependency is the possibility to take the physics of the time-dependent process into account.

Existing statistical models for time-dependent processes are reviewed in two main categories, i.e. the renewal models and continuous stochastic processes. The following renewal models for stochastic processes are discussed: wave renewal and pulse processes, gamma processes, compound renewal processes. Rectangular wave renewal processes are suitable to model e.g. seasonal variations. The year is for example divided into four intervals each representing a season. The value of the random variable is characterised by a distribution function each time interval. A Poisson process is an example of a pulse process and is suitable to model deterioration in the form of shock damages. Gamma processes model deterioration processes as strictly increasing cumulative damage processes, making an infinite number of jumps in finite intervals. The gamma process model is based on the estimation of an average rate of deterioration and its standard deviation. Compound renewal processes are for example superposed or cumulative Poisson processes. The compound renewal processes are also suitable to model shock damages. The following continuous stochastic processes are discussed: Gaussian processes and Brownian motion. Gaussian processes are a general umbrella for stochastic processes whose joint distribution function for all t_1 ,..., t_n is multivariate normal. Brownian motion is a stochastic process with independent $N(0,\sigma^2 t)$ distributed increments and continuous sample paths. There are a number of variations based on the Brownian motion. The Brownian motion with drift is a variation relevant to the case study in chapter 7. It is a

stochastic process $X(t)$ which is normally distributed with mean μt and standard deviation $\sigma^2 t$.

A brief review is described of multivariate distributions that might be suitable to model correlated time-dependent processes. The main challenge is usually to find a multivariate distribution which captures the correlation as well as the marginal distributions of the singular time-dependent processes. Three main model approaches are discussed: finding the appropriate multivariate distribution, transformation to the multivariate normal space and using copulas. An example of a situation for which it is possible to find an appropriate bivariate distribution function is the double-gamma distribution. It is a suitable bivariate structure to represent the correlation between two singular gamma processes. Transformation to multivariate normal space is further explored in this thesis in chapter 7. The copula approach is used for example to couple dependent financial time series. An advantage of the copula function is that it is possible to have arbitrary marginal distribution functions.

Objective 3 is to develop a modelling methodology for statistical models of the asset time-dependent processes of flood defences. This chapter reviews existing statistical models for time-dependent processes which can be applied in the modelling methodology. In chapter 6 the modelling methodology for alternative statistical models of asset time-dependent processes of flood defences is outlined.

6. Statistical models for flood defence asset time-dependency

The previous chapters developed importance measures to highlight relevant time-dependent processes and reviewed existing statistical models for time-dependent processes. In this chapter the modelling methodology for alternative statistical models of asset time-dependent processes of flood defences is outlined. This corresponds with objective 3 in section 1.3 and in figure 1.6. Section 6.1 introduces a methodology to systematically analyse asset time-dependent processes and formulate statistical models. Sections 6.2 to 6.4 describe the phases in the proposed modelling process for asset time-dependent processes in more detail. Section 6.2 goes into the problem formulation. Section 6.3 provides a systematic methodology to develop alternative statistical models, capturing the conceptual structure of the asset time-dependent process. Section 6.4 deals with the quantitative aspects of the statistical model for the asset time-dependent process, i.e. estimation, calibration and corroboration.

6.1. Modelling methodology for asset time-dependent processes

This section firstly goes into the steps generally taken in a modelling process of natural systems according to e.g. Scot et al. (2000). Quality aspects relating to this modelling process are also discussed, Beck & Jining Chen (2000), Oreskes et al. (1994) and Konikow & Bredehoeft (1992). Subsequently, the modelling methodology for asset time-dependent processes is outlined.

6.1.1. General modelling process of environmental systems

Konikow & Bredehoeft (1992) define the terms model, conceptual model and mathematical model. A model is defined as a representation of a real system or process. A conceptual model is a hypothesis of how a system or process operates, whereby the idea can be quantitatively expressed in the form of a mathematical model. Mathematical models are abstractions that replace objects, forces and events by expressions that contain mathematical variables, parameters and constants.

Below firstly the main steps in the modelling process of environmental systems are discussed. Secondly, some comments on the qualitative and quantitative evaluation of the model quality are made.

Steps in modelling methodology of environmental systems

Scot et al. (2000) describe the main steps in the modelling process of environmental systems. These steps are often iterative: problem formulation, conceptualisation, estimation and calibration, corroboration and analysis. The first step is *problem formulation* and impacts on the whole modelling process. The objectives of the model are defined and the key statements and variables that in the end need to be corroborated are formulated. The second step, *conceptualisation*, is a process of comparing the performance of different conceptual structures according to the scientific evidence. It results in the selection of appropriate and the elimination of inappropriate alternative conceptual structures. Once suitable conceptual structures have been selected the modelling process continues with the third step: *model estimation, parameter estimation and calibration*. The fourth step is *corroboration*, amounting to an overall assessment and testing of the process. In the context of modelling often the terms verification and validation are used. Oreskes et al. (1994) defines verification as the establishment of truth and validation as the establishment of legitimacy. In Konikow & Bredehoeft (1992) it is stated that both validation and verification imply the authentication of both the truth and accuracy of the model. However, according to Popper (1959) statements can only be falsified not verified. Therefore physical models can only be improved through invalidation, but cannot be proven valid. Konikow & Bredehoeft (1992) point out that the definitions of validation or verification invoke unfounded confidence in a process that in the end is inherently subjective. Oreskes et al. (1994) therefore introduces the term corroboration. A piece

of evidence is said to corroborate a model when it does not contradict it. They argue that the use of models should thus be limited to: corroboration of theories, falsification of other models and answering 'what if' questions by means of a sensitivity analysis. Corroboration of a model can serve in two main contexts. In the explicative context the model attempts to improve the scientific understanding of physical behaviour. In the predictive context the model provides future predictions. Finally, the *analysis* step revisits the initial problem formulation and objectives. It is in this step important to be aware of the general limitations of predictive power.

Qualitative and quantitative aspects of the model quality

The quality of the model can be assessed on two different levels. The first level is that of the internal properties of the model, i.e. the qualitative representation of the physical processes. This consists of a process of peer review whereby the acceptability is assessed of the primary theoretical material and constituent hypotheses of which the model is composed. It is therefore subjective and depends on the extent of scientific understanding of the physical system under analysis. The second level is that of the external properties, i.e. the quality of the quantitative predictions. Beck & Jining Chen (2000) point out that quantitative assessment is not so straightforward and objective as it seems. Historical observations over a long period of time are often not available to support such a quantitative assessment. Moreover, even a physical process model with abundant historical data embedded within it does not guarantee an appropriate extrapolation many decades in the future. Beck & Jining Chen (2000) suggest assessing the quality of a model in the capacity of a tool that has been designed against a task specification. Ideally, the performance of the model against a task specification is then expressed in terms of a quantifiable measure. According to Beck & Jining Chen (2000) a policy forecast can in this respect be just as 'objective' as a scientific prediction. Important quantifiable measures for the quality of the conceptual process models are in this context delivered by for instance sensitivity and uncertainty analysis.

6.1.2. Overview modelling methodology for asset time-dependent processes

Objective 3 in section 1.3 and in figure 1.6 is: to provide a systematic methodology to develop statistical models for time-dependent processes at the flood defence individual

asset level. Below an overview is given of the steps in the modelling methodology for asset time-dependent processes. Secondly, some aspects about the quality evaluation of the asset time-dependent statistical model are discussed.

Modelling methodology for asset time-dependent processes

As main structure in the systematic methodology the main phases in the modelling process of environmental systems as introduced in the previous section are adopted. The main phases in model development are: problem formulation, conceptualisation, estimation and calibration, corroboration and analysis.

Section 6.2 deals with the problem formulation in the modelling methodology of statistical models for asset time-dependent processes. The problem formulation defines the expectation about the performance of the asset time-dependent process statistical model, on the level of the process and of the overarching maintenance framework. This task specification forms the basis of the quality evaluation, consisting of a qualitative and quantitative quality evaluation. Section 6.3 develops the conceptualisation of the modelling methodology of asset time-dependent processes. This conceptualisation firstly starts with a review of existing scientific understanding and the availability of field information. The second step is to identify the flood defence properties that are involved with the asset time-dependent process in some way: the excitation, ancillary and affected features. This provides insight in the features driving the time-dependency (excitation), the features that contribute in another way (ancillary) and the features that are subject to the time-dependency (affected). A more detailed definition is given in section 6.3.1. The third step is to describe the character of the asset time-dependent process conditional on the excitation, discussed in section 6.3.2. The fourth step, given in 6.3.3, is to analyse the dependencies among different asset time-dependent processes. Some examples of the type of dependencies are given. The correlation is one alternative structure to represent these dependencies. Finally, the alternative statistical models are formulated in section 6.3.4. Section 6.4 deals with aspects about the estimation, calibration and corroboration of the asset time-dependent process statistical model. This section also goes into the quality evaluation of the developed models. An introduction about the quality evaluation is given below. The modelling methodology is demonstrated in chapter 7 on the Dartford Creek to Swanscombe Marshes flood defence system.

Quality evaluation of the asset time-dependent statistical models

The assessment of the quality of model predictions is discussed above mainly in the context of hydrological problems. The same deliberations with respect to quality assessment are applicable to (long term) flood risk assessment and life cycle optimisation models. However, the data availability in long term flood risk assessment is more limited than in hydrological models. This limitation introduces an additional strain on the quality assessment of the models.

During the modelling process the quality of the asset time-dependent process model is considered by its internal and external properties. The absence or scarcity of historical observations usually restricts the ability to make a quantified assessment of the external properties of the model. What is more, embedding many historical observations in the model does not guarantee an appropriate extrapolation of model predictions over many decades in the future. The best way to safeguard the quality of the predictions of the asset time-dependent processes is therefore by taking systematic care of the internal properties of the model whilst incorporating as much quantitative information as possible.

Figure 6.1 provides an outline of the issues that require attention to ensure the quality of the asset time-dependent process model. The quality of the internal properties is underpinned by a combination of a clear problem formulation and a systematic statistical model development methodology, corresponding with the conceptualisation phase (sections 6.2 and 6.3, figure 6.1). The quality of the external properties is considered from the perspective of the individual process and its influence on overarching performance criteria such as life cycle cost, risk and reliability. The evaluation of the external model properties corresponds with the estimation, calibration and corroboration phases (section 6.4, figure 6.1).

6.2. Problem formulation

The objective is to develop statistical models to characterise the asset time-dependent process. The problem formulation is part of the internal properties of the model, see figure 6.1. The problem formulation contains a definition of the flood defence properties that are mainly affected by the asset time-dependent process(es).

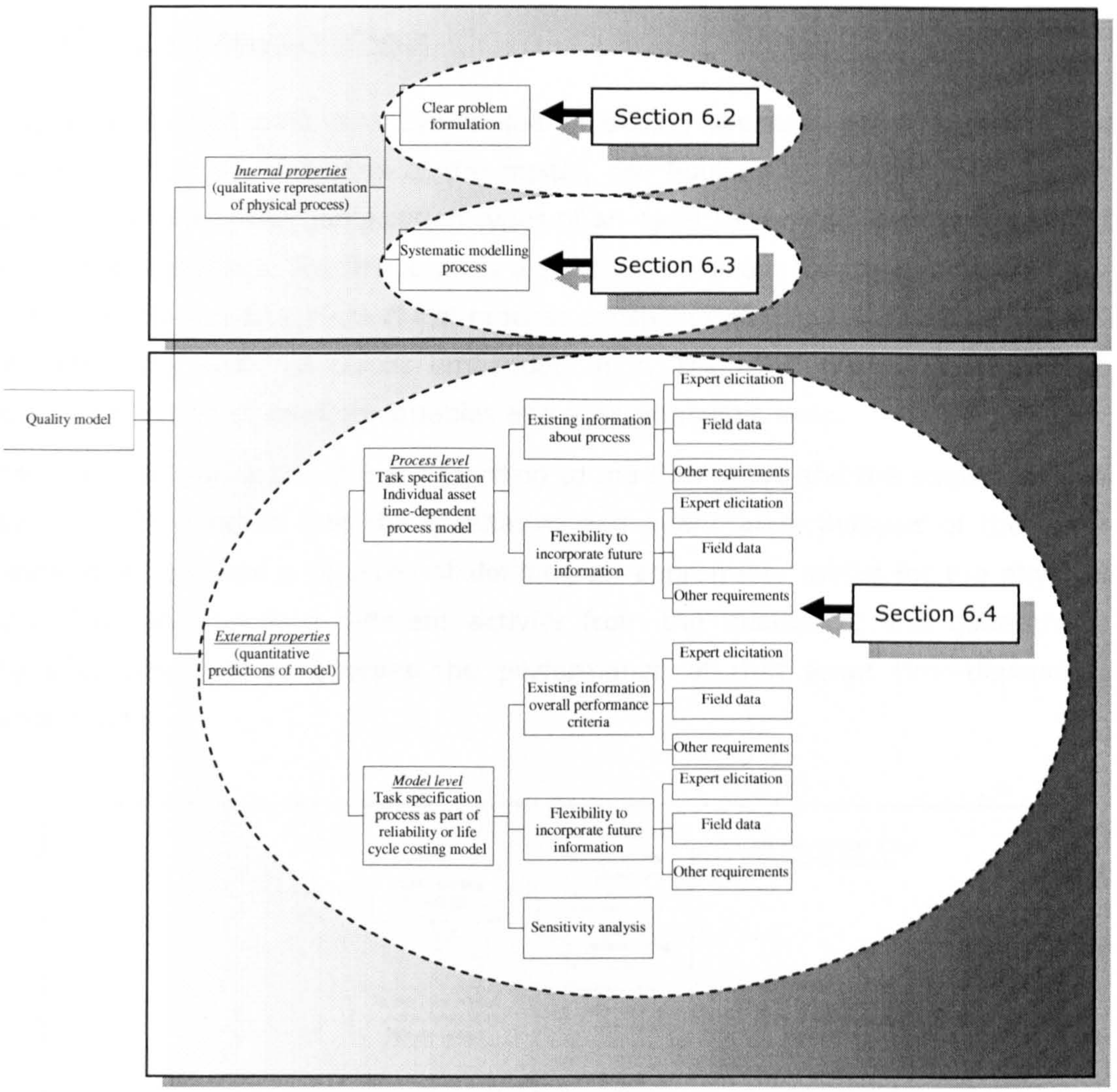

Figure 6.1 Components in the quality assessment of an asset time-dependent process statistical model.

The problem formulation also provides a task specification of the asset time-dependent process model. The quality of the quantitative asset time-dependent process model predictions (external model properties) are tested against this task specification. Figure 6.1 indicates that the quantitative predictions of the model can be considered on two levels: the process level and the model level. At the process level, the model is meant to represent the time-dependent flood defence properties corresponding with experience and field measurements at an individual process level. At the model level, the time-dependent processes are meant to be represented in such a way that the results of the overarching maintenance framework make sense.

6.3. Conceptualisation

The conceptualisation defines a systematic modelling process, which supports the quality of the internal properties of the model, see figure 6.1. Section 5.1.1, figure 5.1, shows the three main composition types of an asset time-dependent process $X_i(t)$ in a limit state equation. The first type is a stochastic process for the overall quantity $X_i(t)$. The second type is a hierarchical process consisting of random variables and has one or more stochastic processes embedded in it. The third type is a parametric process as a function of random variables and a deterministic time.

The conceptualisation is structured according to the flow chart and the steps provided in figure 6.2. It is noted that the qualitative and quantitative analysis of the asset time-dependent process is directed at defining an appropriate model for the physical process. That analysis is a different activity from the qualitative and quantitative quality evaluation which assesses the performance of that asset time-dependent statistical model.

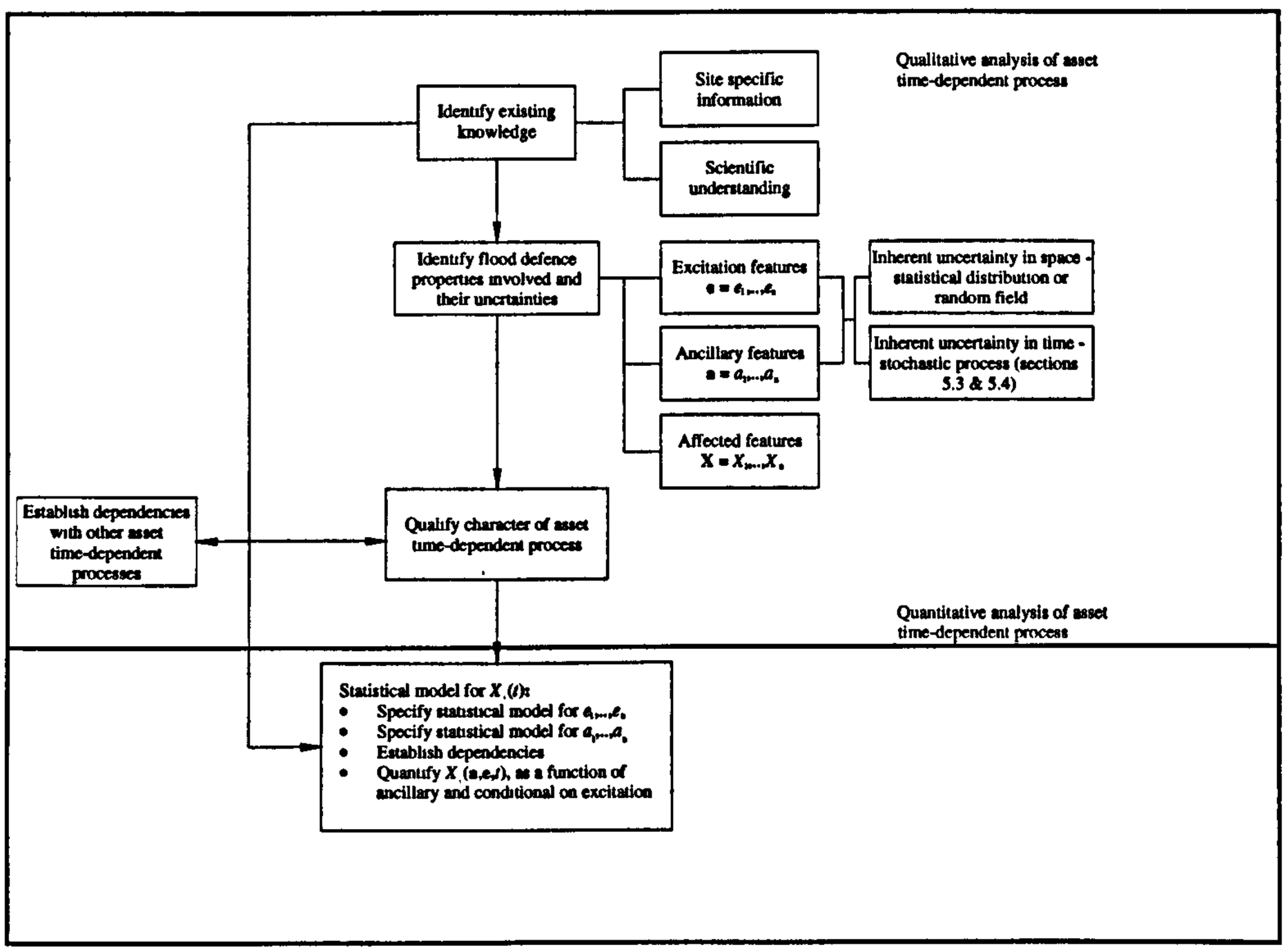

Figure 6.2 Qualitative and quantitative evaluation of an asset time-dependent process and the sequence of steps to take in the modelling process.

The qualitative analysis identifies the flood defence properties (excitation / ancillary / affected features) that are involved with the asset time-dependent process. The wave climate of a sequence of storms is an example of excitation in revetment damage. The size of revetment blocks, the rock density or the slope are for example ancillary features determining the amount of damage achieved by the wave climate. The revetment weight or size are examples of damaged or otherwise time-dependent affected features in the limit state functions of failure mechanisms. It also provides a qualitative description of the behaviour of the asset time-dependent process and analyses the dependencies with other asset time-dependent processes. The quantitative analysis sets up the alternative statistical models for the asset time-dependent processes. These models are then further specified in the calibration, estimation and corroboration phases, see section 6.4. This specification builds on the quality evaluation of external model properties according to figure 6.1.

A number of the steps in the flow chart in figure 6.2 are discussed in more detail below, i.e.: the identification of the flood defence properties (section 6.3.1), the character of the asset time-dependent process (section 6.3.2), the dependencies between the asset time-dependent processes (section 6.3.3) and the formulation of the statistical models (section 6.3.4).

The advantage of a systematic modelling process as presented in figure 6.2 is that the quantitative results can be assessed against the internal properties of the model and form a qualitative model quality evaluation (figure 6.1). Such an assessment compares whether the quantitative model predictions properly reflect the influence of the excitation / ancillary features, the uncertainties that they introduce and the character of the asset time-dependent process.

6.3.1. Excitation, ancillary and affected features

The *excitation features* are the flood defence properties that initiate and drive the asset time-dependent process (water level and wave conditions are also considered to be flood defence properties, see section 1.3). Without those features no asset time-dependency takes place. The wave climate during storms for example could entail a recurrent loading force on the revetment damaging the stones. Another example is the static loading after crest level raising on an earth embankment which causes settlements. Table 6.1 tabulates a number of excitation features, their time-dependent

behaviour and the types of uncertainties that they introduce in asset time-dependent processes.

Table 6.1 Examples of excitation features, the characteristics of the time-dependent behaviour and the types of uncertainties that they introduce in asset time-dependent processes.

Excitation feature	*Characteristics time-dependent behaviour*	*Uncertainty types*
Wave climate: significant wave height and wave period	Recurrent / storm sequence	Inherent uncertainty in time / space
River current velocity	Reversing tides / recurrent high water events	Inherent uncertainty in time / space
Pore pressure distribution in flood defence structure or foundation	Rainfall and drought cycles / seasons / event sequence / accumulation	Inherent uncertainty in time / space
Water head difference between river or sea and floodplain	Tides / recurrent / storm sequence / rainfall events / rainfall sequence	Inherent uncertainty in time / space
Third party loading, e.g. traffic (vehicle weight, tyre acceleration, profile)	Recurrent / event sequence	Inherent uncertainty in time / space
Third party loading, e.g. animal burrowing	Three-dimensional random walk / entrance shifting with river water levels	Inherent uncertainty in time / space
Superimposed loading	Constant in time	Inherent uncertainty in space
Atmospheric CO_2 concentration and moisture around the reinforced concrete wall in relation to carbonation	Seasonal / climate	Inherent uncertainty in time / space
The presence of oxygen and moisture in or around the steel flood defence structure components, in relation to corrosion	Seasonal / climate	Inherent uncertainty in time / space
Bacterial attack (in anaerobic environment)	Circumstances stimulating the multiplication or demise of bacteria	Inherent uncertainty in time / space
Third party activity, dredging	Recurrent / system effects	Inherent uncertainty in time / space
Third party activity, naval activity causing currents and waves	Recurrent / sequence / fluctuations naval activity	Inherent uncertainty in time / space

The asset time-dependent process is a function of the *ancillary features* in addition to the excitation features. The ancillary features are the flood defence properties that

transform the excitation features into the asset time-dependent process. The damage of the revetment caused by wave impact is also a function of e.g. the slope, shape and weight of the revetment. The settlement due to embankment crest level raising is e.g. a function of the soil stratification and the soil properties.

The *affected features* are the flood defence properties that are subject to the asset time-dependent process, indicated in section 5.1.1, figure 5.1, with $X_i(t)$. In case of revetment damage affected features may be the revetment density or grading in different limit state functions. The affected features appear in one or more failure mechanisms and thus influence the fragility. Chapter 7 provides a more detailed description of excitation, ancillary and affected features for: earth embankment compaction (Table 7.5), trafficking damaging the crest level (Table 7.7), seepage length reduction (Table 7.9), carbonation and corrosion of reinforced concrete walls (Table 7.15), sheet pile corrosion (Table 7.22), sheet pile anchor corrosion (Table 7.24) and sheet pile toe accretion / erosion (Table 7.26).

This step in the modelling process provides an overview of the flood defence properties that are part of the asset time-dependent process of interest, categorised according to excitation, ancillary or affected features. The analysis of the excitation and ancillary features should also include a classification of the uncertainties that they introduce and their time-dependent behaviour.

6.3.2. Character of the asset time-dependent process

The character of the asset time-dependent process depends on how the variability in time is introduced and transformed. It therefore builds on the uncertainty and time-dependent behaviour analysis of the excitation and ancillary features. The three main compositions of an asset time-dependent process $X_i(t)$ in a limit state equation are shown in section 5.1.1, figure 5.1. As shown in figure 6.2, the character of the asset time-dependent process is qualified as a function of the ancillary features and conditional on the excitation. A number of aspects about the character of the asset time-dependent process that require attention in the modelling process are listed in table 6.2. It is noted that this table does not present an exhaustive list.

Firstly, it should be determined whether it is preferable to model the asset time-dependent process with a stochastic process or a parametric process, i.e. a function of a deterministic time *t*. The difference between the two is discussed in section 5.1.1.

Secondly, it is important to establish whether the asset time-dependent process displays dependency on the history of its own evolvement. For example the sequence of storm events loading a revetment determines the evolvement of damage. Another example is the compaction of an earth embankment which is influenced by previous loading pressures. Thirdly, the process can be intermittent, continuous, cyclical in time or a combination of those. If the time-dependent process is driven by recurrent events or shock damages then the character of that process is intermittent. Continuous processes gradually evolve in time and take place continuously. The continuous process can display fluctuations or can be smooth. Cyclical processes are for instance caused by seasonality. Fourthly, the process is either strictly deterioration or might involve improvement. Finally, the physical behaviour of the cyclical process, continuous process or the increments in an intermittent process might be e.g. linear, exponential, polynomial or logarithmic.

Table 6.2 Examples of aspects about the character of an asset time-dependent process

Parametric process			Stochastic process	
History-dependent			Not history-dependent	
Continuous	Intermittent		Cyclical	
Strictly deterioration			Positive as well as negative increments	
Linear	Exponential	Polynomial	Logarithmic	Other

6.3.3. Dependencies between asset time-dependent processes

Table 6.3 provides examples of dependencies among asset time-dependent processes and suggestions of approaches to model these dependencies. The dependencies are not necessarily captured by a correlation structure as follows from the examples below.

Asset time-dependent processes caused by the same excitation are for example damage to the revetment and toe erosion. Asset time-dependent processes based on similar ancillary features are for instance settlements and fissuring, i.e. these processes share similar soil properties. Asset time-dependent processes that affect the same flood defence properties are settlements and decrease in crest level by e.g. cattle trampling. Asset time-dependent processes that affect the same failure mechanisms are for instance settlements and fissuring, both affecting overtopping and

slope instability. One asset time-dependent process forming the excitation of another asset time-dependent process is for example chloride ingress in concrete setting off reinforcement corrosion. An asset time-dependent process affecting the ancillary features of another is for example vermin infestation in the revetment, which causes a different development of revetment damage due to wave impact. Multiple interacting asset time-dependent processes are for example seepage, fissuring, animal burrowing and internal erosion.

Table 6.3 Examples of the types of dependencies among asset time-dependent processes and suggestions of modelling approaches

Type of dependency between the asset time-dependent processes	Possible modelling approaches
Same excitation	Process-based model containing the same excitation feature. A correlation model capturing the mutual dependency.
Same ancillary features	Process-based model containing the same excitation feature. A correlation model capturing the mutual dependency.
Affect the same flood defence properties	Process-based model containing the same excitation feature. A correlation model capturing the mutual dependency.
Affect the same failure mechanisms	Both processes appear in the limit state equation
One process (partly) forming the excitation of another	One process appears in the process-based model of the other. A threshold value for one process marks the start for the other. A correlation model capturing the mutual dependency.
One process affecting the ancillary features of another	One process appears in the process-based model of the other. A correlation model capturing the mutual dependency.
Multiple interacting processes	Fault tree analysis to set up a reliability analysis incorporating the processes. Complemented by one of the approaches above.

6.3.4. The development of alternative statistical models

In the demonstration of the modelling methodology for asset time-dependent process statistical models in the case study in chapter 7, three alternative statistical models are considered.

The first one is a conventional engineering approach based on a parametric process. An existing process-based model or, in the absence of such a model, a random deterioration rate as a function of deterministic time serves this purpose. The second alternative statistical model is a gamma process model. This model is a stochastic process approach allowing expert elicitation on the average rate of the time-dependent process. This model provides a strictly increasing time-dependent

stochastic process and is therefore deterioration. The gamma process either takes the behaviour according to an existing process model into account or replaces it by the average deterioration rate. The parametric process or gamma process approaches are based on different kinds of assumptions than the more detailed hierarchical process model as described below. In some cases the parametric or gamma process models may be preferable over the hierarchical process, examples of reasons are in brief: lack of scientific understanding, limited data availability or e.g. a broad risk assessment application context. Section 5.1.1 contains a more detailed discussion on the reasons to apply an aggregate stochastic process model rather than a more detailed approach as given below.

The third alternative statistical model is developed according to the modelling process above, and outlined in figure 6.2. The excitation and ancillary features introduce inherent uncertainties in space and / or time. If these features introduce time variability, then a statistical model is selected to represent that variability from sections 5.3 and 5.4. Table 6.4 shows examples of suitable stochastic processes for different types of time variability. These stochastic process models are suitable for both excitation or ancillary features introducing time variability. The character of the overall process is then quantified as a function of ancillary features conditional on the excitation of the asset time-dependent process. Subsequently, the statistical models for the ancillary features are incorporated in the model. In some cases the relationship between the excitation and the overall time-dependent quantity is indirect. The statistical model of the excitation then serves as a guideline to make an appropriate selection for the statistical model of the overall quantity, i.e. composition 1, stochastic process, rather than 3, parametric process, in figure 5.1.

The next step is to represent the dependencies among asset time-dependent processes. This step is straightforward if process-based models are available for both processes. The common excitation and ancillary features then appear in both process models. Dependency models in the form of threshold values and fault tree analysis provide a structured approach as well. Complications arise in the absence of process-based models as the dependencies need to be captured by a correlation model such as presented in section 5.5. The challenge is twofold. Firstly, an appropriate selection for the marginal distributions of the individual stochastic processes needs to be made. Secondly, a correlation model needs to be found that appropriately captures the

dependency as well as the marginal distributions. An example is the model developed in Buijs et al. (2005a).

Table 6.4 Examples of suitable stochastic process models for different types of time-dependent behaviour.

Stochastic process	*Type of time-dependent behaviour*	*Details in*	*Illustration*
Rectangular wave process (e.g. Borges Castanheta)	Seasonality in hydraulic loading variables such as: high river discharges / floodplain water levels / pore pressures	Section 5.3.1	Section 7.3.4, 7.3.5, 7.4.4, 7.5.4
Pulse / Poisson process	Arrival of storm events / arrival of trafficking events / arrival of pit corrosion	Section 5.3.1	Section 7.3.5, 7.3.6, 7.5.5
Gamma process	Strictly increasing excitation features, ancillary features or overall quantity $X_i(t)$	Section 5.3.2	Section 7.3.4, 7.3.5, 7.3.6, 7.4.4, 7.5.4, 7.5.5, 7.5.6
Compound renewal process (e.g. superposed, alternating, cumulative)	Arrival of trafficking events causing cumulative damages	Section 5.3.3	Section 7.3.5
Gaussian / Brownian	Continuous process	Section 5.4	Section 7.3.4, 7.3.5, 7.5.6

The estimation, calibration and corroboration of the statistical models is discussed in the following section 6.4 and form the quantitative quality evaluation.

This section, 6.3, and the previous sections 6.2 and 6.1, formulate a systematic modelling methodology to develop statistical models for asset time-dependent processes. The quality of the internal properties is underpinned by a combination of a clear problem formulation and a systematic statistical model development methodology, corresponding with the conceptualisation phase (figure 6.1 and 6.2). The advantage of such a systematic modelling process is that the quantitative model predictions can be assessed against the internal model properties and form a qualitative model quality evaluation. Such an assessment compares whether the quantitative model predictions properly reflect the influence of the excitation /

ancillary features, the uncertainties that they introduce and the character of the asset time-dependent process.

6.4. Estimation, calibration and corroboration of the models

The statistical models for the asset time-dependent process developed in the conceptualisation phase require parameter specification, i.e. estimation and calibration. Additionally, the quality of the external properties of the statistical models needs to be assessed, see figure 6.1. This assessment is made in the light of both the task specification of the individual asset time-dependent process and that of the overarching performance criteria, i.e. corroboration. In this case no sharp division is made between parameter estimation and calibration on one hand and corroboration on the other hand.

This section deals in other words with the quantitative model quality evaluation. As mentioned before, sections 6.3, 6.2 and 6.1 formulate a systematic modelling methodology to develop statistical models for asset time-dependent processes. The results from the conceptualisation analysis, figure 6.2, can be used as a qualitative model quality evaluation. A comparison can be made between the quantitative results and the findings on the excitation / ancillary features, the uncertainties that they introduce and the character of the asset time-dependent process.

6.4.1. Task specification at the individual asset time-dependent process level

Firstly, some general comments on the task specification at the individual asset time-dependent process level are given, relating to figure 6.1. Secondly, parameter estimation, calibration and corroboration methods for the quantitative testing of the statistical models for asset time-dependent processes are described in general. Thirdly, some implications are discussed for the calibration and corroboration of the asset time-dependent statistical models. Finally, four different practical situations in terms of data availability are brought forward. The data availability on asset time-dependent processes is often limited or related to the variables in the model rather than the asset time-dependent quantity.

General comments on the task specification at the individual asset time-dependent process level

There are several angles to the task specification of the individual asset time-dependent process. The main task specification for an asset time-dependent process model in this thesis is a realistic quantitative estimate of the asset time-dependent process in time. According to figure 6.1 the asset time-dependent process model needs to build on both existing / historical information and future information. Historical observations and future observations are defined with respect to the moment of implementation of the maintenance framework, see figure 6.3. The type of information available to enable a realistic quantitative estimate is field data, expert elicitation and, if relevant, information related to other requirements that the task specification might encompass.

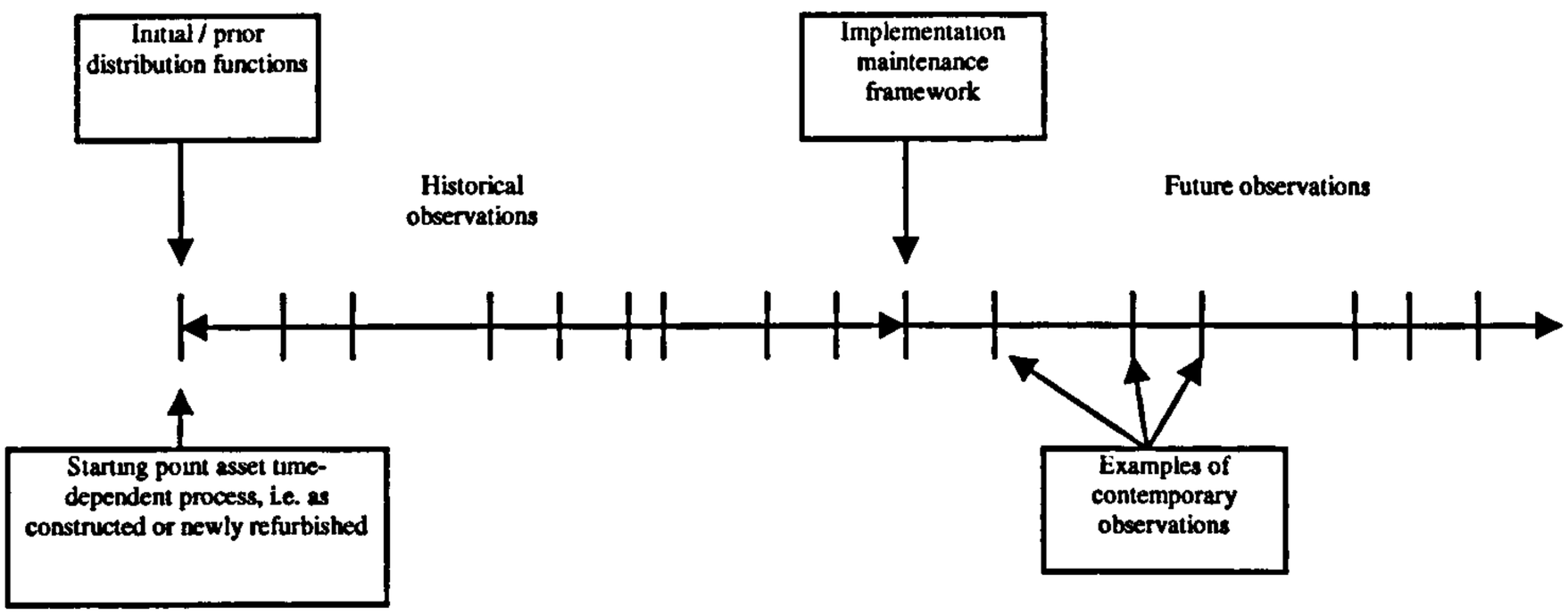

Figure 6.3 Timeline defining the base or prior distributions, the historical and future observations with respect to the maintenance framework implementation.

The incorporation of future or historical observations relates to for example whether the quantitative maintenance framework is based on the Markovian property or on the Bayesian decision-making approach. Section 3.2.1 deals with the advantages and disadvantages of both types of quantitative decision-making approaches. The Bayesian posterior updating approach allows internalisation of future observations into the time-dependency model. Alternatively, the Markovian property restricts its future predictions conditional on the contemporary standing of the process. In section 3.2.1 the Bayesian approach is chosen over the Markovian approach. Basic theory

about posterior updating of the statistical distributions of **d** or the overall quantity $X_i(t)$ is given in section 3.2.1, expression (3.1). More details are provided in e.g. Bernardo & Smith (2003), Pratt et al. (1995) and Van Gelder (1999).

Parameter estimation, calibration and corroboration methods

The next step is the estimation of the parameters of the statistical model of the asset time-dependent process, based on the available information. The asset time-dependent processes are defined according to figure 5.1. $X_i(t)$ represents the asset time-dependent quantity. The random variables in the hierarchical or parametric process model are represented by **d**. The parameters of the statistical distribution functions of **d** or of stochastic processes $d_i(t)$ or $X_i(t)$ are represented by θ.

The main methods supporting parameter estimation based on datasets of field measurements are given in e.g. Casella & Berger (2002), Van Gelder (1999) or Pratt et al. (1995): point estimation, hypothesis testing and interval estimation. Point estimation formulates a statistic that is operated as an estimator of the parameters of the statistical model based on the available dataset. The estimator is the single estimate of the parameter of interest. Point estimation methods are for instance the method of moments or maximum likelihood estimation. Hypothesis testing formulates the null hypothesis, H_0: $\theta \in \Theta_0$, and the alternative hypothesis, H_1: $\theta \in \Theta_0{}^c$ for a parameter set Θ_0 and its complement $\Theta_0{}^c$ in the parameter space θ. The acceptance or rejection criterion for Θ_0 is usually defined based on a test statistic as a function of the available data sample. Examples are likelihood ratio tests or Bayesian tests. Interval estimation involves the estimation of a set of parameters θ whereby $L(\mathbf{x}) \leq \theta \leq U(\mathbf{x})$, in which $L(\mathbf{x})$ and $U(\mathbf{x})$ are the interval estimators. Interval estimation usually accompanies point estimation. In the absence of data the estimation of parameters based on expert elicitation might be preferable.

A detailed approach to derive expert elicited parameter sets is discussed in e.g. Cooke (1991) and Cooke & Goossen (2004).

The calibration tunes the statistical model predictions to the available data on historical time series samples of $X_i(t)$. During this process different sets of parameter distributions are investigated. The corroboration of the statistical model of the asset time-dependent process amounts to an overall assessment and testing of the statistical model. The corroboration can lead to the acceptance or rejection of a

conceptual model structure. Hypothesis or significance testing are suitable methods to support the calibration and corroboration of the statistical model.

Some implications of scarce data availability

Unfortunately, historical time series samples of the asset time-dependent quantity $X_i(t)$ are usually scarcely populated. Calibration is then supported by checking whether the time series samples of the asset time-dependent quantity $X_i(t)$ are in a sensible order of magnitude and display a sensible variation. Corroboration of the model is supported by comparing the qualitative behaviour of the process following from the modelling methodology with the behaviour of the time series samples. Such an analysis is advisable in any case as a form of qualitative evaluation (figure 6.1).

The increasing availability of future observations can either be used for further calibration and corroboration or for Bayesian updating of the prior distributions. The necessity of further calibration and corroboration depends on several issues. A first issue is the complexity of the asset time-dependent process. A second issue is the influence of the statistical properties of the asset time-dependent process on those of the affected feature. The asset time-dependent process might e.g. be very complex. However, the rate of the process might be very low and the amount of uncertainty contributed to the initial variation of the affected feature might be negligible. A third issue is the influence of the asset time-dependent process on the flood defence reliability, risk and life cycle cost in the context of the overarching maintenance optimisation model. This influence can be measured with importance measures as developed in chapter 4.

If the process is relevant, it can be decided to choose for state-dependent maintenance in figure 3.5 until the statistical model provides satisfactory asset time-dependent predictions. Moreover, the qualitative decomposition of the asset time-dependent process into excitation, ancillary and affected features supports practical maintenance purposes. Two examples are given. *Example 1:* An asset time-dependent process statistical model which is not properly calibrated and corroborated might not be qualified as 'Good description of course of strength' in figure 3.5. However, if it concerns an asset time-dependency that is mainly driven by recurrent events (e.g. storms or trafficking events), then the process can be organised under 'Load dependent maintenance'. Depending on the type of process it might suffice to roughly estimate the amount of damage given a recurrent event and carry out

maintenance once a certain number of events have occurred. A process driven by a continuous excitation would in the same circumstances be categorised under 'State dependent maintenance' or 'Time-dependent maintenance', depending on the cost of the inspection. *Example 2:* The qualitative decomposition of the asset time-dependent process guides to which flood defence features should be paid most attention to during monitoring, in addition to the overall time-dependent quantity $X_i(t)$.

Discussion of a number of practical situations

The following discussion illustrates how to populate the parameters of the asset time-dependent statistical model in six different practical situations. Table 6.5 contains an overview of the six situations, depending on: whether the data availability is ample or scarce, whether the data availability is on **d** or $X_i(t)$ and in the latter case whether $X_i(t)$ is modelled as a stochastic process or as a parametric or hierarchical process. The definitions of $X_i(t)$, **d**, stochastic, hierarchical process and parametric process are according to section 5.1.1 and figure 5.1.

Situation 1 in table 6.5 has ample data availability on a stochastic process $X_i(t)$. In this case the parameters of the statistical model of $X_i(t)$ can be estimated with point estimation methods. The future observations as they become available can be incorporated by posterior updating.

Situation 2 in table 6.5 has ample data availability in the form of observations of $X_i(t)$ on parametric or hierarchical process $X_i(t)$. The initial distribution functions of variables **d** can be estimated by expert elicitation. Historical time series observations can be used for the calibration of the statistical distributions of **d** so that the model predictions of $X_i(t)$ correspond with the observations. Under ample data availability, the historical observations can also be used for corroboration of the statistical model. Hypothesis or significance testing are useful methods for calibration or corroboration. Future observations are incorporated with posterior updating.

Situation 3 in table 6.5 has scarce data availability on a stochastic process $X_i(t)$. Point estimation of the parameters based on a scarcely populated time series sample might lead to a large number of credible parameter sets. The large number of sets is brought on by the fact that different types of curves fit through the same scarcely populated time series sample. This problem is illustrated by Bakker & Van Noortwijk (2004) and Pandey & Van Noortwijk (2004), who discuss fitting methods of gamma

process models to scarcely populated data samples. The maximum likelihood method is applicable, but will be accompanied with very wide confidence intervals. For some stochastic process models such as the gamma process model expert elicitation on average deterioration rates and their standard deviation is optional. It is possible to calibrate the expert elicited parameters with a hypothesis or significance test against the scarce historical observations. The future observations can be used to further improve the statistical model by a better underpinned maximum likelihood parameter estimation or further calibration of the expert elicited parameters. If the quality of the statistical model is satisfactory, posterior updating can be applied.

Situation 4 in table 6.5 has scarce data availability in the form of observations of $X_i(t)$ on parametric or hierarchical process $X_i(t)$. The initial distribution functions of variables **d** can be estimated by expert elicitation. Historical time series observations can be used for the calibration of the statistical distributions of **d** so that the model predictions of $X_i(t)$ correspond with the observations. Hypothesis or significance testing are useful methods in this context. Future observations can be used for further calibration and corroboration of the statistical model of the asset time-dependent process (referred to with hypothesis or significance testing in table 6.5). If the quality of the parameters and structure of the statistical model is satisfactory the increasing data availability can be used in a posterior analysis.

Situation 5 in table 6.5 has ample data availability on the variables **d** in the statistical model of the asset time-dependent process $X_i(t)$. The statistical distribution functions of the random variables **d** can then be established with point estimation. Future or historical observations on **d** can be incorporated with posterior analysis. The absence of field observations on $X_i(t)$ do not allow further calibration or corroboration of the statistical model of the asset time-dependent process.

Situation 6 in table 6.5 has scarce data availability on the variables **d** in the statistical model of the asset time-dependent process $X_i(t)$. The statistical distribution functions of the random variables **d** can then be established with expert elicitation. Similar comments as in the fifth situation apply to the incorporation of future or historical observations and the corroboration of the statistical model.

In situations 2 and 4 in table 6.5 it is possible that there is ample data availability on the variables **d**, enabling point estimation of the distribution functions of **d**.

In situations 3 and 4 the transition between further calibration of the statistical model given future observations and posterior analysis depends on the necessity to further improve the statistical model. Three issues related to the necessity for further calibration and corroboration are mentioned under the previous heading of parameter estimation, calibration and corroboration methods.

*Table 6.5 How to derive and update distribution functions for the parameters **d** and the overall quantity $X_i(t)$, for six practical situations in a Bayesian decision-making framework.*

		Data availability			
		Ample		Scarce	
Data on $X_i(t)$ (asset time-dependent quantity)		***Situation 1:*** $X_i(t)$	***Situation 2:*** $X_i(t) = f(\mathbf{d},t)$	***Situation 3:*** $X_i(t)$	***Situation 4:*** $X_i(t) = f(\mathbf{d},t)$
	Initial / prior distributions of parameters		Expert elicitation on prior distributions of **d**	Maximum likelihood / Expert elicitation on prior distribution of $X_i(t)$	Expert elicitation on prior distributions of **d**
	Historical observations	Point estimation of statistical model parameters θ of $X_i(t)$.	Calibration and corroboration of the statistical model	Maximum likelihood / Hypothesis or significance testing of the expert elicited distribution of $X_i(t)$ above	Hypothesis or significance testing of the expert elicited distributions of **d**
	Future observations	Posterior updating of $X_i(t)$	Posterior updating of $X_i(t)$	Maximum likelihood / Hypothesis testing or significance test of expert elicited distributions of $X_i(t)$ / posterior updating of $X_i(t)$	Hypothesis or significance testing of the expert elicited distributions of **d** / posterior updating of $X_i(t)$
Data on **d** (random variables in hierarchical or parametric process model)	Initial / prior distributions of parameters	***Situation 5:*** Point estimation for parameters of the distributions of **d**		***Situation 6:*** Expert elicitation on prior distributions of **d**	
	Historical observations	Posterior updating of **d**		Posterior updating of **d**	
	Future observations	Posterior updating of **d**		Posterior updating of **d**	

6.4.2. Task specification at the overarching maintenance framework level

The statistical model of the asset time-dependent process affects the performance criteria in the overarching quantitative maintenance framework, see figure 6.1. As mentioned above, the overarching maintenance optimisation framework can be based on the Markovian property or the Bayesian decision-making approach. Performance criteria refer to for instance life cycle cost, risk and reliability. Data on such performance criteria are usually not available in the flood defence industry, which is why they are simulated by means of a probabilistic model, see section 5.2. The quality of the internal properties of a maintenance framework model is therefore underpinned by systematic rational methods. One way of ensuring the quality of the external properties of the maintenance framework model is by ensuring the quantitative quality of model properties at the roots of the model. For model properties such as flood defence properties, operational activities and costs, data acquisition is feasible. An appropriate quantitative quality of those model properties is achieved by point estimation, hypothesis testing, expert elicitation or Bayesian updating. A second way to provide feedback on the quality of the probabilistic predictions within the maintenance framework is to conduct expert elicitation on the performance criteria themselves (Cooke & Goossen, 2004 and Slijkhuis et al., 1998). The simulated reliability, risk or life cycle cost is then compared to the expert elicited values. A third way of ensuring the quality of both the internal and the external properties of the overarching maintenance framework is by sensitivity analysis, Beck & Jining Chen (2000).

The sensitivity analysis may be carried out in different phases of the modelling process, e.g. to identify important model properties, to eliminate irrelevant activities, processes or flood defence sections, to focus on important model predictions, to compare alternative model structures or to establish where the model provides a prediction contrary to the expected prediction. Flood defence system life cycle cost models are complex and have not been fully developed and populated at this stage. Importance measures to indicate the influence of asset time-dependent processes and operational activities on performance criteria such as reliability, risk and life cycle cost provide a starting point for such a sensitivity analysis. Chapter 4 develops these importance measures. In addition, the sensitivity analysis should ideally be directed at

properties (e.g. flood defence properties, cost, operational activities or alternative conceptual model structures) that are meaningful to the quality assessment of the life cycle cost model. In addition to an often used method such as variance decomposition a sensitivity analysis investigates e.g. the sensitivity to expert elicited performance values, other definitions of the quality requirements, different conceptual model structures, different scenarios.

6.5. Review

The modelling methodology for statistical models of asset time-dependent processes consists of the following main phases: problem formulation, conceptualisation and parameter estimation, calibration and corroboration of the model. The quality evaluation of the statistical model of an asset time-dependent process relates to its internal properties, qualitative evaluation, and its external properties, quantitative evaluation (figure 6.1). The internal model properties are formed by the model structure. Their quality is supported by an appropriate problem formulation and a systematic conceptualisation phase. The external model properties deal with the quantitative predictions of the model. The quality of model predictions is analysed against the task specification on an individual process level and in the context of an overarching maintenance optimisation model. The external model properties are analysed in the parameter estimation, calibration and model corroboration phase.

The problem formulation defines the expectation about the performance of the asset time-dependent process statistical model, on the level of the process and of the overarching maintenance optimisation framework. This task specification forms the basis of the overall model quality evaluation, consisting of a qualitative and quantitative quality evaluation. The steps in the analysis of the asset time-dependent process in the conceptualisation phase are shown in figure 6.2. The five-step analysis of the asset time-dependent process in the conceptualisation phase of the modelling methodology develops assessable, and hence less subjective, internal model structures. The conceptualisation firstly starts with a review of existing scientific understanding and the availability of field information. The second step is to identify the flood defence properties that are involved with the asset time-dependent process in some way: the excitation, ancillary and affected features. This provides insight in the features driving the time-dependency (excitation), the features that contribute in

another way (ancillary) and the features that are subject to the time-dependency (affected). The third step is to describe the character of the asset time-dependent process conditional on the excitation. For example, the process can be represented by a stochastic process, a parametric process or a hierarchical process. The process may be history dependent or display cumulative, intermittent or cyclical behaviour. The fourth step is to analyse the dependencies among different asset time-dependent processes. Some examples of the type of dependencies are given. The correlation is one alternative structure to represent these dependencies. Subsequently, the alternative statistical models are formulated. Finally, the parameter estimation, calibration and corroboration of the asset time-dependent process statistical model is evaluated against the task specification at a process and maintenance optimisation level. At an individual process level appropriate parameter estimation, calibration and corroboration methods are discussed.

Unfortunately, historical time series are often scarcely populated making the quantitative quality evaluation of the model difficult. Additionally, even process models based on abundant historical observations do not guarantee appropriate extrapolations in the future. Calibration is then supported by checking whether the time series samples of the asset time-dependent quantity $X_i(t)$ are in a sensible order of magnitude and display a sensible variation. Corroboration of the model is supported by comparing the qualitative behaviour of the process following from the conceptualisation phase with the behaviour of the time series samples. Such an analysis is advisable in any case as a form of qualitative evaluation (figure 6.1). The increasing availability of future observations can either be used for further calibration and corroboration or for Bayesian updating of the prior distributions. The necessity of further calibration and corroboration depends on several issues. A first issue is the complexity of the asset time-dependent process. A second issue is the influence of the statistical properties of the asset time-dependent process on those of the affected feature. The asset time-dependent process might e.g. be very complex. However, the rate of the process might be very low and the amount of uncertainty contributed to the initial variation of the affected feature might be negligible. A third issue is the influence of the asset time-dependent process on the flood defence reliability, risk and life cycle cost in the context of the overarching maintenance optimisation model. This influence can be measured with importance measures as developed in chapter 4. Six practical situations of ample or scarce data availability on the variables **d** or the asset

time-dependent quantity $X_i(t)$ with the latter being a stochastic process or a parametric / hierarchical process are discussed. Appropriate parameter estimation, calibration and model corroboration methods are suggested.

If the process is relevant, state-dependent maintenance in figure 3.5 can be adopted until the statistical model provides satisfactory asset time-dependent predictions. Moreover, the qualitative decomposition of the asset time-dependent process into excitation, ancillary and affected features supports practical maintenance purposes. It is possible to decide on a state-dependent, time-dependent, load-dependent or fault-dependent maintenance approach. Additionally, the decomposition in flood defence features steers the information retrieved from monitoring the asset time-dependent process.

The modelling methodology is demonstrated in chapter 7 on the Dartford Creek to Swanscombe Marshes flood defence system.

7. Time-dependent reliability of the Dartford Creek to Swanscombe Marshes flood defence system

The time-dependent reliability methods developed in the previous chapters are demonstrated on the Dartford Creek to Swanscombe Marshes flood defence system along the Thames Estuary. Chapter 7 sets up the time-dependent reliability analysis of the Dartford Creek to Swanscombe Marshes flood defence system. This chapter starts with an introduction to the Dartford Creek to Swanscombe Marshes flood defence system and the steps to set up a flood defence reliability analysis, section 7.1. The information sources relating to the case study site are given in section 7.2. The time-dependent reliability analysis of earth embankments, reinforced concrete walls and anchored sheet pile walls is described in sections 7.3 to 7.5. The flood defence system reliability analysis is discussed in section 7.6.

7.1. Introduction

In the late 1970s and beginning 1980s the flood defences along the Thames Estuary were subject to a major improvement scheme. After 30 years of service it takes approximately another 20 years before systematic refurbishment of the current flood defence system is required. The next generation of flood defences, ideally in place in 2030, will be designed to last beyond 2100. The Environment Agency launched the Thames Estuary 2100 project (TE2100 project) to initiate the design of these large scale refurbishment works. Part of the feasibility stage of the TE2100 project is to carry out flood risk assessments to identify the most flood prone areas. The results serve to compare the costs and risk reduction of different maintenance intervention or improvement options. To enable life-cycle costing, insight is required in the time-

dependent reliability of the defences. This research project is conducted in that context.

The location of the Dartford Creek to Swanscombe Marshes flood defence system along the Thames Estuary is shown in figure 7.1. The flood defence line between Dartford Creek and Swanscombe Marshes has a length of 10.6 km. Of the total flood defence line, approximately 63% is made up by earth embankments, 17% by reinforced concrete walls and 20% by anchored sheet pile walls. The frontage also consists of a large variety of composite reinforced concrete and anchored sheet pile walls. In addition, there are over 25 floodgates with widths varying between 2.5 and 12 meter. However, both the floodgates and the composite structures are not considered in the research project. Figure 7.2 presents the elevation of the defence line and the division into the main defence types. The elevation is compared between those recently surveyed and those indicated on as designed / constructed drawings of

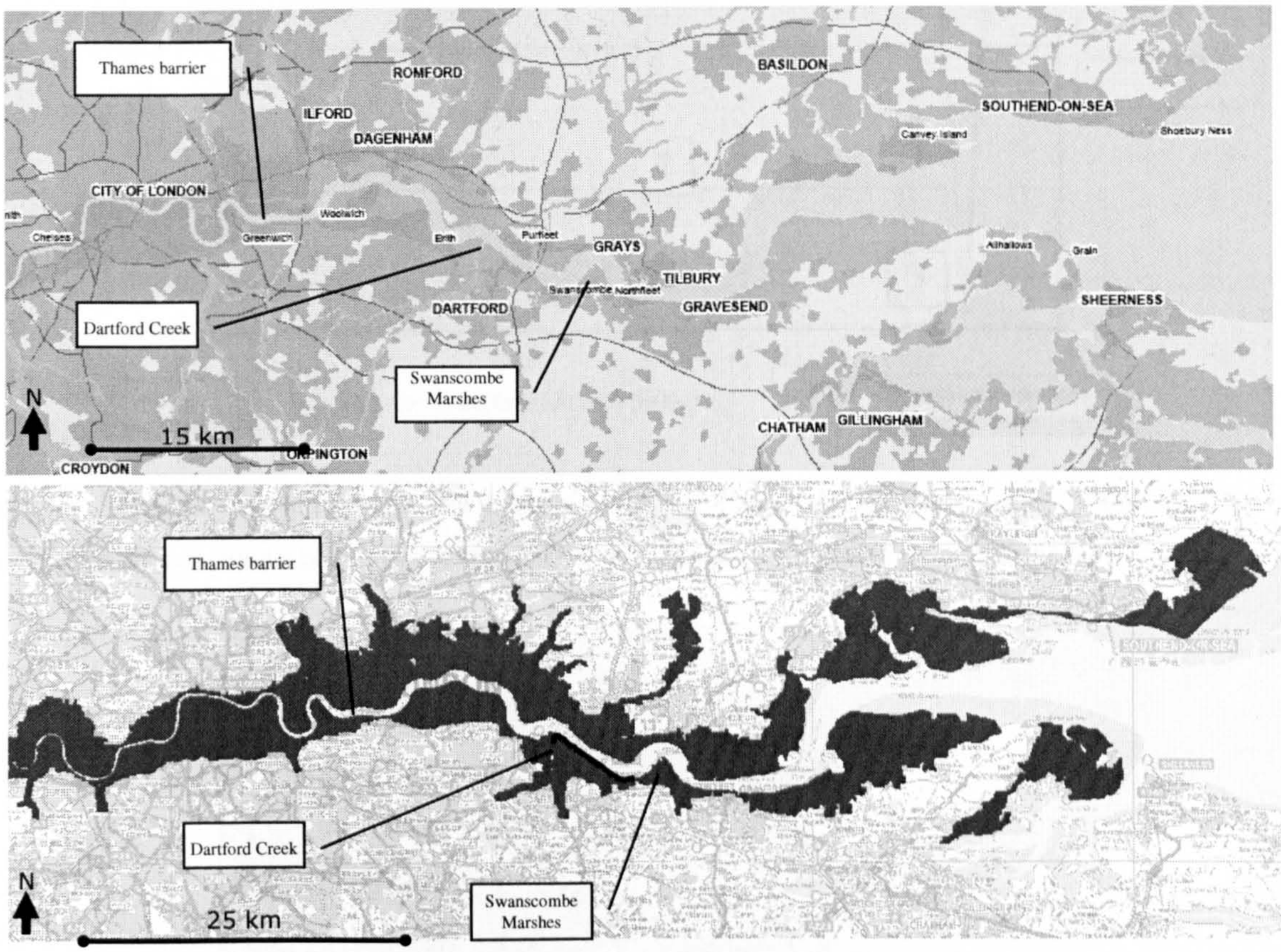

Figure 7.1 The location of Dartford Creek and Swanscombe Marshes as well as the Thames barrier at Greenwich in the Thames Estuary (top). An indication of flood contours along the Thames Estuary and the location of the Dartford Creek to Swanscombe Marshes flood defence system (bottom).

the improvements in the '70s and '80s. These crest levels relate to a floodplain elevation of between OD+0m and OD+2m.

An indication of the tide levels are given by a highest recorded water level of about OD+4.9m downstream near Swanscombe Marshes and of about OD+5.1m upstream near Erith.

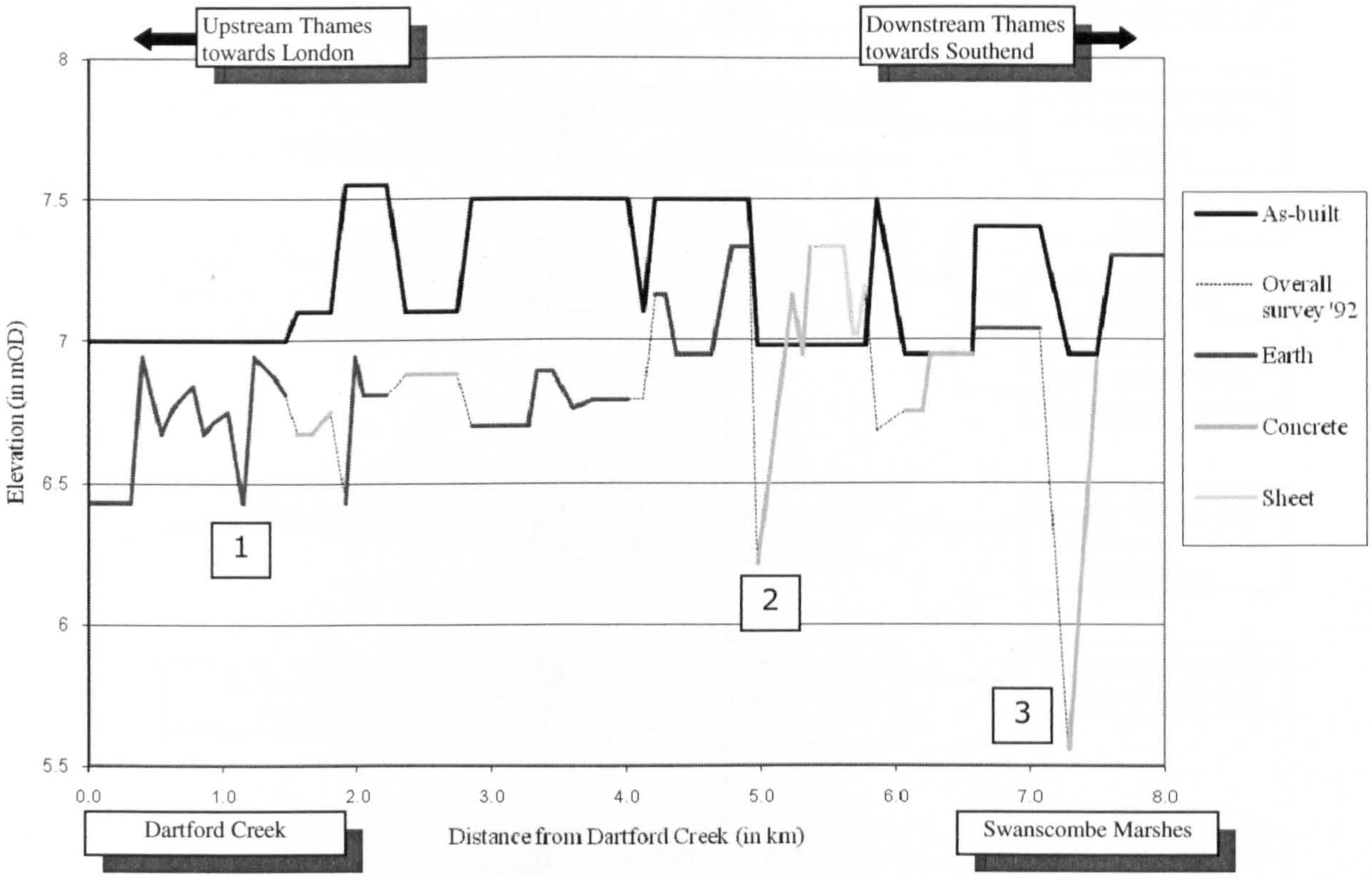

Figure 7.3 Elevation of the defence line between Dartford Creek to Gravesend: after '70s / '80s improvements (in continuous black) versus the recently surveyed defence line (light and dashed).

Figure 7.2 Example of a longitudinal crack in an earth embankment in 1955, with in the background Littlebrook powerstation.

The '70s and '80s improvements to the Thames Estuary flood defences were triggered by the storm that took place in January 1953. During this storm earth embankments

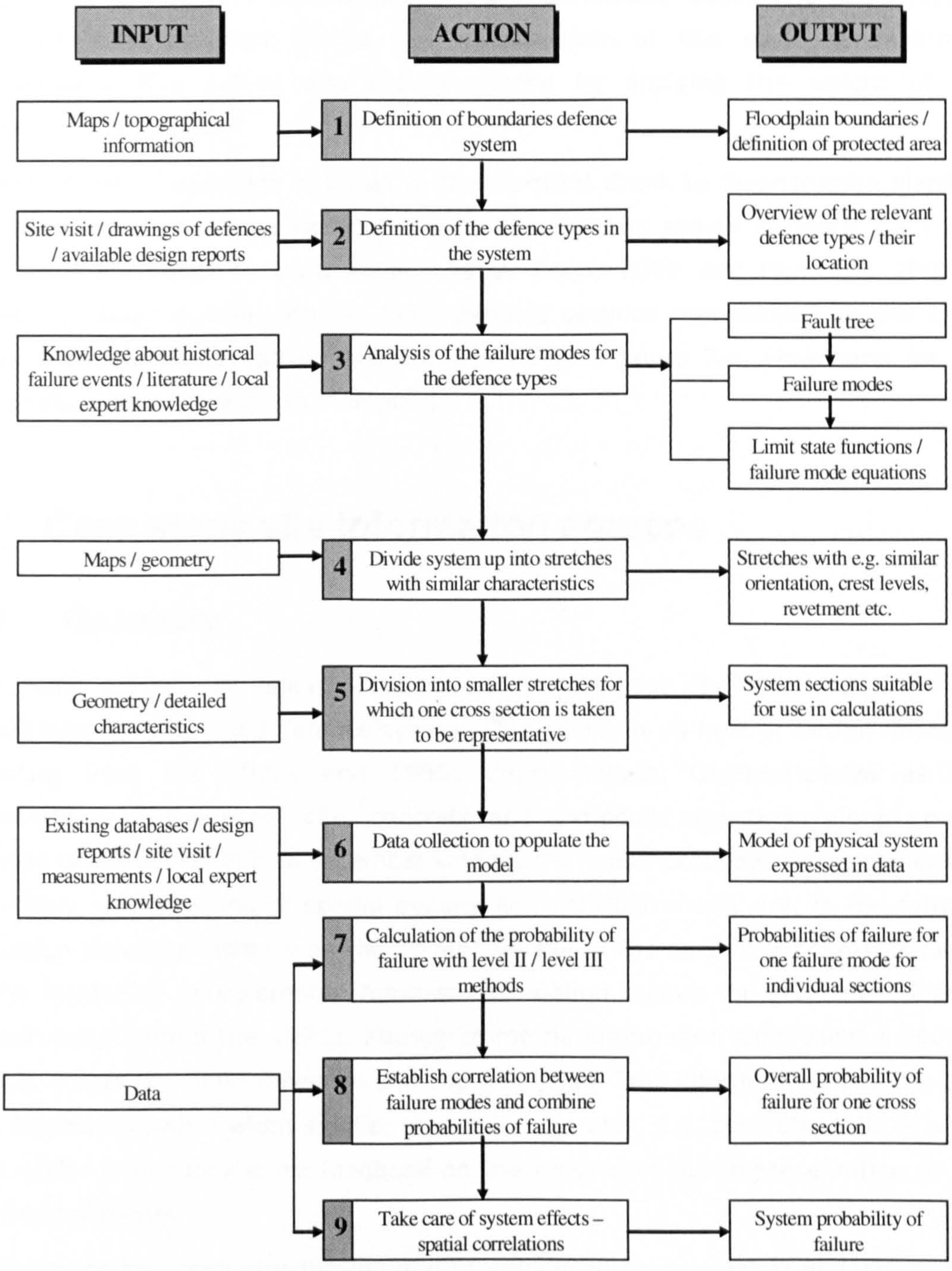

Figure 7.4 Flow chart of activities to calculate flood defence system reliability including examples of the type of input source material and the output products.

failed due to overtopping of the crest, seepage into fissures and cracks (figure 7.3) followed by slope instability. Another type of failure was brought on by uplifting and piping behind the earth embankments of the impermeable clayey and peaty layers. Slope instability occurred during the construction of the earth embankment improvements. This failure was mainly caused by applying the weight of the improvement too quickly.

The time invariant reliability analysis of the Dartford Creek to Swanscombe Marshes flood defence system is set up according to the method shown in figure 7.4 (after CUR, 1990, illustrated in Buijs et al., 2003, Buijs, 2006 and Floodsite, 2007). Appendix A shows a map with the flood defence sections represented by one cross section in the system reliability analysis according to figure 7.4. Flowcharts for the calculations in step 7 are given in appendix E.

7.2. Case study site information sources

7.2.1. Geometry

Three main information sources serve as a basis for the Dartford Creek to Swanscombe Marshes flood defence system. One source is as-built or design drawings originating from the 1970s and 1980s improvements. Comprehensive as-built documentation of the sheet pile, concrete and composite structures along private frontages is available. For earth embankments the cross sectional representation is qualitatively less in terms of spatial density and conclusiveness, e.g. in the form of final design drawings rather than the as-built versions. The earth embankments are in addition harder to georeference. Another information source for geometry is crest level surveying during the 1990s. Photogrammetric information from 2000 / 2001 is available across the flood defences and the floodplain. This information does not pick up on structures with a width smaller than 0.5 – 1 meter, e.g. concrete walls or wave return walls. It provides extra feedback on the cross sectional representation of the earth embankments.

The quality of the geometry information is influenced by a number of factors. One factor is the measurement error. In figure 7.2 for example, a recent survey shows an improvement in crest level at a sheet pile frontage compared to its as-constructed

level. Another factor is whether the geometry is derived from as designed or as-built drawings and whether these drawings can be georeferenced. Design drawings tend to be less accurate than as-built drawings. A third factor is the spatial resolution of available as-built or design drawings. The resolution of flood defence cross sections along private frontages tends to be quite dense. The availability of design drawings on the other hand tends to be spatially less dense and the quality limited. A last factor is the ability to capture three dimensional effects such as bends in the alignment of the flood defences. Such three dimensional effects lead to e.g. the concentration of flow or wave impact.

7.2.2. Soil conditions

The sources of information on soil conditions used in this Dartford Creek to Swanscombe Marshes reliability analysis consist of: borehole data; design of settlement and instability of earth embankments along Dartford Creek to Greenhithe; some lab tests of samples at various locations; investigation of tidal uplift pressures in gravel layer underlying the impermeable layers and some sparse information on grain sizes.

The information is fairly limited and the spacing of the locations with information is quite big. Interpolation is therefore necessary to obtain an indication of the soil properties between the locations with information. The procedure consists of three main steps. Firstly, the borehole data from the design drawings need to be georeferenced. The second step is the classification of the soil layers from the borehole descriptions into a limited number of generic types. Thirdly, the borehole and soil classification are interpolated to cover the whole defence line.

The quality of the soil property representation is determined by a number of issues. Firstly, georeferencing of boreholes or lab tests turns out to be not straightforward. Additionally, the results from lab tests require additional work to derive soil properties for the reliability analysis. Secondly, it is expected that the presence of peat lenses is insufficiently picked up due to the large spacing of borehole locations. Thirdly, generic classification is necessary as the financial feasibility of testing soil layers is restricted. However, the use of generic soil types to capture a class of similar soils does not provide a specific representation of soil properties. A fourth issue is errors introduced by measurements and the need to work the measurements into useful soil

information. Most of these quality issues are resolved by an increased amount of soil measurements and more comprehensive testing.

7.2.3. Hydraulic boundary conditions

A joint probability study of water levels and wind speeds was carried out for the sea conditions at the mouth of the Thames Estuary, HR Wallingford (2004d). This study provides a Monte Carlo simulation of joint couples of wind speed and water level based on the method according to Hawkes et al. (2002), see also HR Wallingford (1998). The simulations are based on joint water level and wind speed data sets that cover a period of about thirty years. According to HR Wallingford (2004d), the effect of the river discharge on the local water levels is negligible downstream of Tilbury. The discharge is therefore not taken into account in the Dartford Creek to Swanscombe Marshes flood defence reliability analysis. The Monte Carlo simulation provides an advanced representation of the correlation structure between wind speeds and tide levels. However, a disadvantage is that, as with any Monte Carlo simulation, the sample has a limited size. The limited sample size restricts the ability to investigate flood risk or importance measures for extremes. Additionally, the parameters of the bivariate normal correlation structure underlying the Monte Carlo simulation are not available for this study. The absence of these parameters restricts the ability to derive very small probabilities of failure as well as direction cosines (section 7.3.3).

Local water levels given a number of different sea water levels at the mouth of the Thames Estuary were provided from TUFlow / Isis calculations. Several locations along the Dartford Creek to Swanscombe Marshes flood defence system are represented in those results. The local water levels are provided in case the Thames barrier is closed and in case the Thames barrier is not closed. The sea water levels span a sufficiently large range to represent extreme sea water levels.

The two information sources described above are combined to find local water levels during the reliability calculations. A simulation of a water level at one of the locations along the defence line can be derived through linear interpolation between water levels and defined locations.

To derive local wave conditions a simple shallow water wave prediction model (formulae according to Bretschneider) is used. That prediction is based on the local water level, bathymetrical information, fetch and reduced estuarial wind speeds

according to HR Wallingford (1999). Local bathymetrical information was derived from a larger bathymetry study carried out for the TE2100 project covering the Thames River over the course of the twentieth century. Fetches were measured from a map. Being quite far upstream of the Thames Estuary, the local wave climate is not severe. The wave conditions thus calculated are in the order of magnitude of those presented in HR Wallingford (1999) for the Dartford Creek to Swanscombe Marshes flood defence system.

The quality of the local water level representation depends on the quality of the statistical wind speed / water level model and the quality of the local water level predictions as a function of sea water levels and river bathymetry. The quality of the statistical wind speed / water level model is determined by a number of issues. A first issue is the availability of data to fit the statistical model to, in case of the Thames Estuary the data cover a sufficiently long period of about thirty years. A second issue is the quality of the representation in the extreme tails of the statistical distribution. A third issue is the choice of dependency structure and distribution function. It is finally noted that the quality of the statistical model is often hard to judge for more extreme values as these events tend to be less populated with data. The quality of the local water level predictions is determined by a number of factors. One factor is the detail of representation of the river bathymetry and the physical processes. A second factor is the data availability at different locations along the Thames to calibrate and validate the numerical model against, especially for more extreme water levels sufficient data availability is questionable. A third factor is the applicability of the physical relations to more extreme local water level predictions. A fourth factor is the approximation made by applying the linear interpolation between the local water levels at two locations, depending e.g. on the variability in vegetation or foreshores, the slope along the river, the distance between two defined locations, etc. Another factor is the approximation by linear interpolation between two simulated water levels at one location. Finally, local surge effects and funnelling effects causing extra surge due to a wind field directed upstream (westward) of the Thames Estuary are not taken into account.

The quality of the representation of local wave conditions is determined by several issues. One issue is the quality of the water level predictions along the river. Secondly, it is determined by the quality of the wave prediction model. Thirdly, it depends on the data availability to calibrate and validate the wave prediction model against. A fourth issue is whether a detailed representation of the river bathymetry is applied. A fifth

issue is whether depth limited effects on waves are taken into account. Finally, the quality of the model of the local wave conditions depends on the appropriateness of the local wind field model.

7.2.4. Economic damages inundation

Detailed flood risk calculations are not the scope of this research project. Economic damages from a broadscale flood risk assessment of the Thames Estuary are therefore taken as an indication. The density of the local water level and the flood risk are shown in table 7.1. The economic damages in table 7.1 are build up of the joint probability of independent flood defence failure scenarios and the corresponding economic damages. The table illustrates that only a small range of local water levels introduce flood risk.

A cost-benefit based importance measure requires the calculation of the change in flood risk due to an operational activity or a deterioration process. As mentioned above, the joint probability of failure of flood defence failures is based on independent flood defence sections. The broadscale flood risk assessment in table 7.1 is dominated by a limited selection of flood defence failure scenarios. As a simplification, a change in the probability of failure of a flood defence section is assumed to lead to a proportional change of the joint probability of failure.

Table 7.1 Economic damages and local water level densities.

Annual probability of water level h (in mOD)		£ Annual flood risk
$P(h \leq 3.7)$	= 0.9510975	0
$P(4.3 \leq h < 4.5)$	= 0.034755	0
$P(4.5 \leq h < 4.7)$	= 0.00269	25903
$P(4.7 \leq h < 4.9)$	= 0.00125	139072
$P(4.9 \leq h < 5.1)$	= 0.0000775	3571438
$P(5.1 \leq h < 5.3)$	= 0.000035	9925149
$P(5.3 \leq h < 5.5)$	= 0.000025	20082748
$P(5.5 \leq h < 5.7)$	= 0.00002	53532469
$P(h \geq 5.7)$	= 0	102,736,040

7.3. Time-dependent reliability of earth embankments

7.3.1. Description of the structure type

The earth embankments along the Dartford Creek to Gravesend defence line typically have two crests (figure 7.5). In the late '70s and early '80s the Thames Estuary defences were improved. The lower riverward crest is the pre-improvement defence line, the higher landward crest has been constructed as part of the improvements. The defences are founded on weak clayey and peaty soil layers with a thickness in the order of magnitude 14 to 20 m.

Those impermeable layers are in turn founded on a water conductive layer formed by

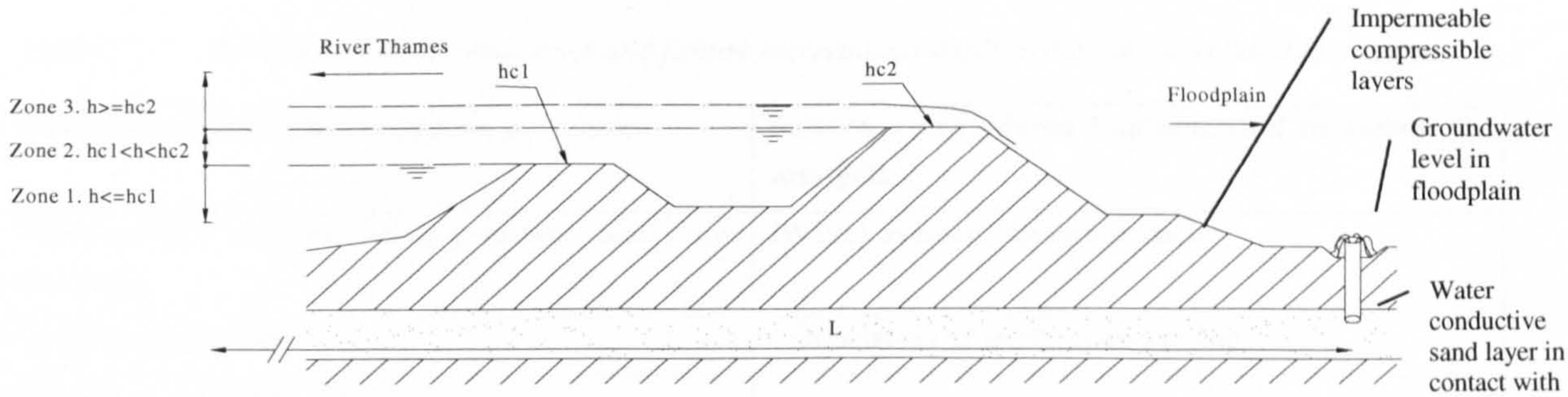

Figure 7.5 Typical cross section of earth embankments between Dartford Creek to Gravesend

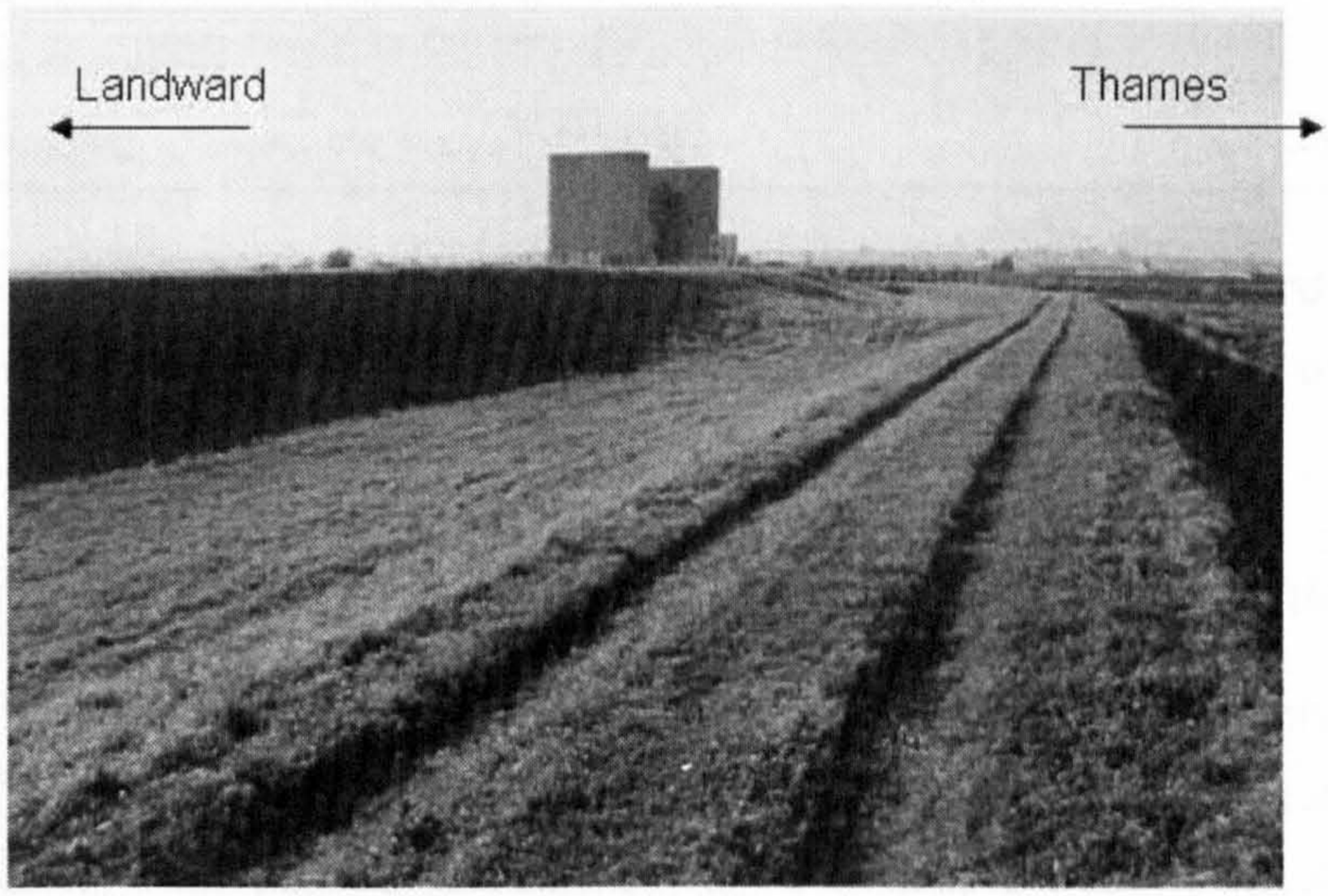

Figure 7.6 View along the current embankment just downstream of Dartford Creek, in the background the Dartford Creek barrier can be seen

sandy or chalky layers. To avoid the occurrence of deep seated slip circles during and after construction, berms were applied on the inside and outside toes of the defences to provide for sufficient stabilising weight. See figure 7.5 for an example cross section and a picture in figure 7.6. Table 7.2 contains an overview of the failure processes encountered at the Dartford Creek to Swanscombe Marshes flood defence system and the failure mechanisms implemented in the reliability analysis. Generally mentioned time-dependent processes for earth embankments are, Environment Agency (2004a & 2004b): settlements or compaction of the embankment foundation, cracking / fissuring, seepage, animal infestation, damage to vegetation, deteriorating revetment material, vandalism, heavy trafficking, the presence of foreign objects. This research project is restricted to settlements, damage due to trafficking and seepage length reduction due to internal erosion in the water conductive layer.

Table 7.2 Site specific failure processes and failure mechanisms implemented in the reliability analysis

Overview of site specific failure processes	**Failure mechanisms implemented in reliability analysis**
Overtopping / overflow causing erosion and slope instability	(Wave) overtopping and erosion
Uplifting and piping	Combination of uplifting and piping
Fissuring / cracking	
Long term crest level settlements: compressible layers and estuarial settlements 0.5 to 1 meter	
Short term crest level settlements: off-road cycling	
Bathymetrical changes of Thames	
Third party activities loading embankment slopes	

The primary function of the earth embankments along the Dartford Creek to Swanscombe Marshes flood defence line is protecting against flooding by retaining water.

7.3.2. Fault tree, failure mechanisms and limit state equations

Failure, or the top event in the fault tree, is defined here if the earth embankment fails to fulfil its primary function. Excessive overtopping discharges which cause damage are not considered in this study. The top event related to an earth embankment is therefore limited to structurally breaching and subsequent flooding. Failure

mechanisms are the chains of events leading up to the top event, see definitions in section 3.1.2. The accompanying limit state equations are provided in appendix B.

Fault tree

Figure 7.7 illustrates the simplified fault tree for double crested earth embankments used in the reliability calculations. The fault tree approach changes for water levels lower and higher than the riverward crest level. Two comments are made with regard to the fault tree for double crested earth embankments. Firstly, for water levels lower than the riverward crest level, failure of both of the two embankments must occur

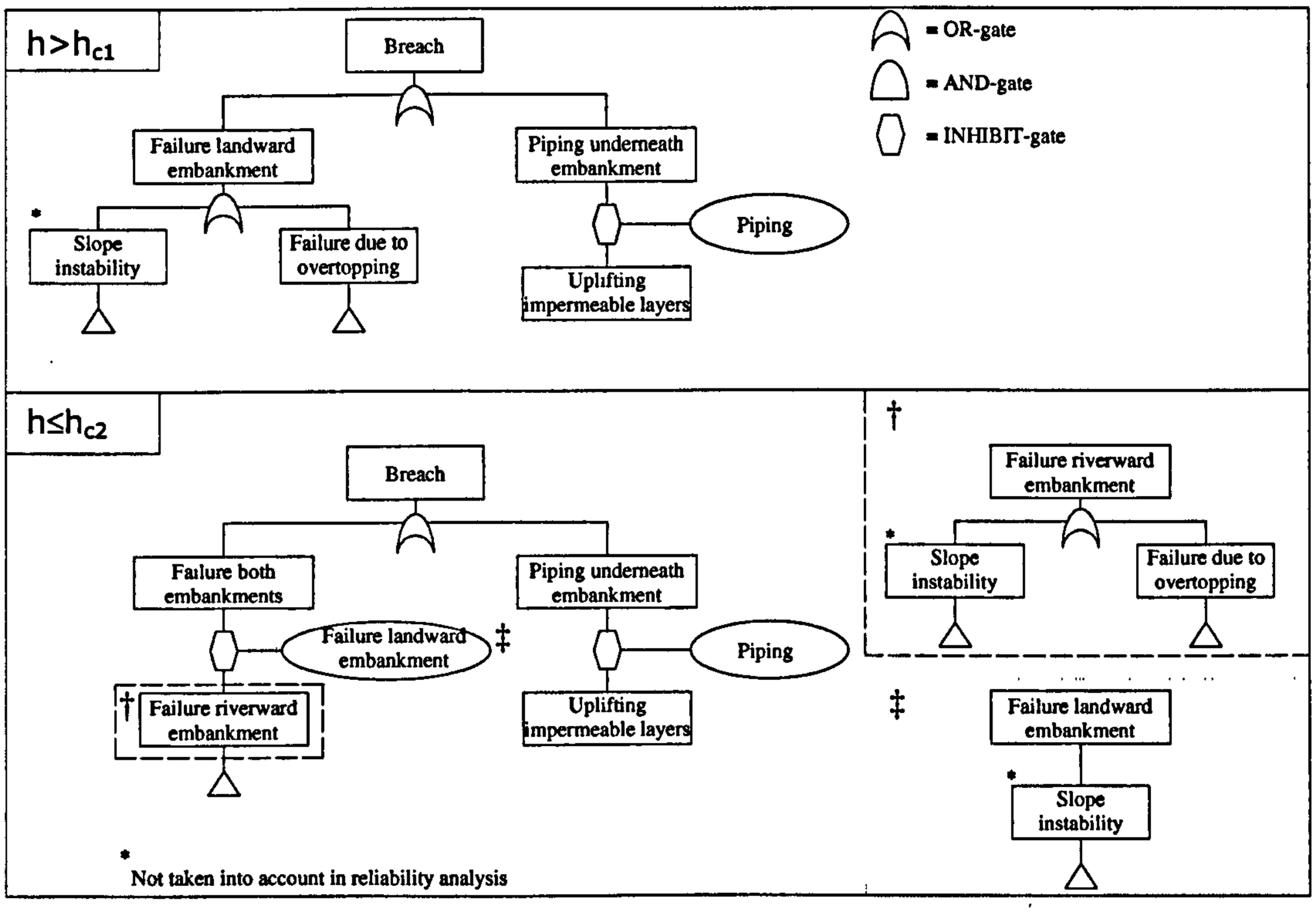

Figure 7.7 Fault trees for double crested earth embankments underpinning the reliability analysis.

Explanation to top fault tree: if the water level is higher than the riverward crest level, h_{c1}, then the water level directly loads the landward embankment, h_{c2}. Inundation occurs in that case if the landward embankment fails, hence those failure mechanisms are relevant. Explanation to bottom fault tree: If the water level is lower than the riverward crest level, h_{c1}, then inundation occurs if either the total structure fails due to undermining by uplifting and piping or both embankments fail. In the latter case inundation occurs if the landward embankment fails after the riverward embankment fai., h_{c1} and h_{c2} as indicated in figure 7.5.

before breach occurs. Secondly, for water levels higher than the riverward crest level only failure of the landward embankment is required for breach. In this case it still matters whether the riverward embankment has failed prior to the second. The presence of the riverward embankment affects e.g. the wave overtopping conditions or the pore pressures of the landward embankment. This effect is not taken into account in the calculations in this study.

Description of the failure mechanisms

As indicated in table 7.2 and appendix B the following failure mechanisms are part of the reliability analysis: wave overtopping / overflow and erosion, uplifting and piping. Inside slope instability is briefly mentioned since it is a relevant failure mechanism. However, slope instability is too computationally intensive to include in the scope of this thesis.

Wave overtopping / overflow followed by erosion involve water discharges due to wave overtopping or overflow that respectively hit or scour the inside slope of the embankment. The loading of the inside slope damages the grass turf. After the grass has been damaged, the embankment body is exposed to the overtopping/overflowing water. In the end, if this erosion process continues long enough, the embankment breaches. The duration of this erosion process depends on the duration of the overtopping discharges during the storm.

In the Thames Estuary an embankment is often founded on a pack of impermeable layers overlaying a water conductive sand or gravel layer. Uplifting occurs when the upward hydraulic force in the water conductive layer exceeds the cumulative weight of the impermeable layers. The hydraulic force bursts the impermeable layer upward. In the Thames Estuary, pipes applied in ditches behind the embankment relieve the upward hydraulic force (Marsland & Randolph, 1979).

Bursting by uplifting of the impermeable layers opens the doorway for the water in the water conductive layers. Water then seeps up, driven by the hydraulic head between the water level outside the embankment and in the floodplain, and erodes particles from the water conductive sand layer. If this process can carry on long enough, pipes form underneath the embankment undermining the foundation. This can eventually lead to collapse of the embankment. The initiation of a piping process depends on whether the water conductive layer is connected to the water level at the

Thames – defining the seepage length. For the Dartford Creek to Swanscombe Marshes site this seepage length depends on the bathymetry of the river as well as the variability of the thickness of impermeable layers.

Slope instability can be initiated in many different ways, e.g. by an increase in pore pressures. The increase in pore pressures can have several causes, e.g. rainfall over a longer period of time, rising river water levels, rapidly receding tides, overtopping discharges seeping into fissures, etc. The characterisation of the pore pressure distribution depends on the situation of interest. As a first estimate of factor of safety of slopes often Bishop's slip circle method is used. Bishop's factor of safety approach can also be set up in a probabilistic model, although that brings some complications. The grid encapsulating the pool of more likely slip circles needs to be located beforehand. Once the optimal grid is found, the method is computationally intensive and takes a long time to run.

7.3.3. Importance measures for earth embankments

The importance measures developed in section 4.3 are calculated for earth embankments along the Dartford Creek to Swanscombe Marshes flood defence line.

Indicate the influence of variables on the reliability

The influence of the variables on the reliability is indicated by the direction cosines, expression (2.11), and the partial derivative based concept introduced in expression (4.11). These indicators are derived from the time invariant reliability analysis and presented in table 7.3 for flood defence section 4 and water level OD+7.5m. As mentioned in section 7.2.3, the absence of the parameters of the bivariate normal distribution of wind speeds and water levels restricts the ability to derive direction cosines. The statistical distributions of the random variables are given in appendix C. It is noted that the sensitivity indicators do not show a major shift in importance given different water levels in the fragility curve. One water level therefore suffices to demonstrate the interpretation of these indicators.

The direction cosines α and partial derivative based concept PD_X show a different emphasis in importance for all three failure mechanisms. The model uncertainty, m_{qe}, and in the second place the storm duration, t_s, contribute most to the probability of failure due to overtopping as indicated by the direction cosines. This importance is

complemented by the PD_X which show that the ratio between the water level, h, and the crest level, h_c, are relevant to consider in improvement or maintenance. The direction cosines for uplifting point out that the uncertainty in the thickness of the impermeable layers, d, and in the second place the density of the impermeable layers contribute, γ_s, most to the probability of failure. The PD_X point out that the uplifting model is mainly sensitive to the density, γ_s. The direction cosines for piping indicate that the permeability of the sand in the water conductive layer, k_s, contributes most to the probability of failure. It is noted that there was difficulty to iterate the FORM procedure to a probability of failure, hence the quality of these direction cosines is doubtful.

Table 7.3 Direction cosines α and partial derivative based concept PD_X for the random variables in the failure mechanisms of flood defence section 4, water level OD+7.5m.

		Flood defence section 4					
		α			PD_X		
		Overtopping	Uplifting	Piping	Overtopping	Uplifting	Piping
h =	water level (mOD)	0	0	0	-0.493	-0.028	-0.019
H_s =	significant wave height (m)	0	-	-	0	-	-
T_p =	Peak wave period (s)	0	-	-	0	-	-
h_c =	crest level (mOD)	0	-	-	0.493	-	-
c_w =	crest width (m)	0.065	-	-	0.242	-	-
tan_o =	tan outside slope (-)	0	-	-	0	-	-
tan_i =	tan inside slope (-)	-0.068	-	-	-0.173	-	-
c_g =	erosion strength grass (ms)	0	-	-	0.145	-	-
c_{RK} =	erosion strength core (ms)	0	-	-	0.242	-	-
d_w =	depth grass roots (m)	-0.24	-	-	-0.239	-	-
P_t =	pulsating percentage (-)	0	-	-	-0.287	-	-
r_i =	roughness inside slope (-)	0.12	-	-	0.058	-	-
t_s =	storm duration (h)	-0.39	-	-	-0.287	-	-
m_{qe} =	model uncertainty erosion model (-)	0.88	-	-	0.348	-	-
d =	thickness impermeable layer (m)	-	0.769	-	-	0.063	-
γ_s =	Volumetric weight saturated soil (kN/m^3)	-	0.568	0	-	0.707	0
h_b =	ground water level (mOD)	-	0.033	0	-	0.050	0.038
m_u =	model uncertainty uplifting (-)	-	0.261	-	-	0.063	-
L =	seepage length (m)	-	-	0.005	-	-	0.239
η =	constant of White (-)	-	-	0.006	-	-	0.216
d_{70} =	d70 of sand (m)	-	-	0.006	-	-	0.216
k_s =	permeability of sand (m/s)	-	-	-1	-	-	-0.072
m_p =	model uncertainty piping (-)	-	-	0.005	-	-	0.244
θ =	angle piping model (°)	-	-	0.005	-	-	0.454
D =	Thickness water conductive sand layer(m)	-	-	0	-	-	-0.067
γ_{sand} =	Volumetric weight sand in water conductive layer (kN/m^3)	-	-	0	-	-	0.537

The PD_X show that the piping model is additionally sensitive to the friction angle, θ, the model uncertainty, m_p, the seepage length, L, the constant of White, η, and the representative grain size of the sand d_{70}. Improvement measures and maintenance should be focused on the failure mechanisms uplifting and piping. The failure mechanisms are the most prominent combination if the probability distribution of water levels is taken into account. Monitoring which aims to achieve a precise description of the uncertainties in the random variables should be directed at the random variables highlighted by both the α, and the PD_X indicators.

Highlight time-dependent processes

Section 4.3.3 introduces a suitable importance measure to highlight relevant time-dependent processes in the form of expression (4.5) and (4.7). The time-dependent processes that are investigated are: settlement of the crest level due to compation of the foundation, crest level and vegetation damage due to trafficking and seepage length reduction in the water conductive layer underneath the embankment. The change in probability of failure given different water levels is calculated for an asset time-dependent process and combined with the economic damages. The cost benefit ratio is derived by calculating additionally the cost of remediation of the asset time-dependent process in consideration. The cost information is derived e.g. from sources accompanying Environment Agency (2006). The probability density of local water levels above OD+5.7 meter is negligible, see table 7.1. Economic damages are relevant for water levels larger than OD+4.5m. However, the probability of flood defence failure given water levels between OD+4.5m and OD+5.7m is negligible. The importance measure would then equal zero. Instead, as a basis of comparison the flood risk at OD+7 meter is chosen, a design water level of the earth embankments 30 years ago. The Burden to risk Importance Ratios (BIRs) are given in table 7.4 for three different asset time-dependent processes: settlements due to compaction, trafficking and seepage length reduction. A lower BIR implies a more relevant asset time-dependent process as either the cost of the remediation is relatively lower or the impact on the flood risk is relatively higher. The change in flood risk per year is calculated to take different rates of time-dependency into account. Trafficking is according to these calculations given a water level of OD+7m the most relevant asset time-dependent process.

Table 7.4 Burden to risk Importance Ratios given h=OD+7m for flood defence section 4 in case of three asset time-dependent processes: settlements, trafficking and seepage length reduction.

Asset time-dependent process	Burden (£)	Change in flood risk (£ / year)	BIR/year
Settlement	65504	43355	1.5
Trafficking	91008	2927977	0.031
Seepage length reduction	896124	329	2726

Indicate the flood risk reduction impact of operational activities

Section 4.3.4 presents a suitable importance measure to indicate the flood risk reduction impact of different operational activities. An often applied improvement measure is raising the crest level by one or several meters. Improvement options inspired on the sensitivity indicators are increasing the thickness of the impermeable layers or ground improvement thus increasing the soil density. Routine inspection and specific inspection are only considered in the context of the reduction of statistical uncertainty. The benefits of knowledge about the development of condition levels in time or the discovery of failure mechanisms are not taken into account. The results for routine and specific inspection in table 7.5 are therefore of limited significance and are indicated with the suffix – statistical uncertainty. In this context, routine inspection only increases the precision of the uncertainty representation of external properties such as the geometry. Specific inspection increases in addition the precision of internal properties such as soil properties. The thickness of the impermeable layers also falls under this type of inspection as a borehole is necessary to establish its size rather than external methods like remote sensing.

Table 7.5 Benefit to risk Importance Ratios of five maintenance intervention options given OD+7 meter for flood defence section 4

Intervention options	Burden (£)	Change in flood risk (£)	BIR
Raising crest level 1 meter	91008	850654	0.11
Raising crest level 4 meter	244031	867092	0.28
Ground improvement	896124	4109	218
Routine inspection – statistical uncertainty	1515	8218883	$0.18 \cdot 10^{-3}$
Specific inspection – statistical uncertainty	7534	8250074	$0.9 \cdot 10^{-3}$

The impact of operational activities on the flood risk reduction, in table 7.5, is compared on the basis of the flood risk at a water level in the order of magnitude of the original design level, OD+7m. The same deliberations apply as encountered above

when highlighting the relevant asset time-dependent processes. Namely, the probability density of local water levels above OD+5.7 meter is negligible, hence the water levels below OD+5.7 meter mainly contribute to the annual average flood risk. Therefore a water level is chosen for which the probability of flood defence failure is significant in order to study the impact of different operational activities.

The improvement options considered are raising the crest level by one meter, raising the crest level by four meter and ground improvement of the impermeable layers behind the embankment. The inspection options which are included in the comparison are routine inspection and specific inspection. Section 4.3.4 contains a discussion on the comparability of physical improvement activities versus the reduction of epistemic uncertainty. The Benefit to risk Importance Ratios are tabulated for these options in table 7.5.

According to table 7.5 routine inspection reducing statistical uncertainty in the flood risk assessment is worth considering compared to the investment. According to this result similar conclusion applies to specific inspection. Raising the crest level one meter is the most cost beneficial physical improvement measure. Settlements over the first twenty years due to crest level raising by one or four meter are taken into account.

It is noted that these results merely serve to illustrate a comparison of a number of intervention options. These options and importance measures do not provide a complete impression, as the following will clarify. Firstly, routine inspection often monitors a long stretch of flood defence line for one investment, e.g. remote sensing. The increase in knowledge achieved on a system scale given one routine inspection is not taken into account. Specific inspection on the other hand involves a higher cost and is very localised. Failure mechanisms on which this type of inspection would have a large impact, e.g. slope instability, are not taken into account. An additional benefit of specific inspection compared to routine inspection is also not incorporated in the results, i.e. detecting a problem which either does or does not lead to repair, figure 2.8. Secondly, the assumption underlying the BIR of routine inspection in table 7.5 is that the inspection leads to a reduction in uncertainty. The added benefit of reducing statistical spatial uncertainty diminishes after a number of inspections, as discussed in section 2.1.

7.3.4. Asset time-dependent process: settlements

The modelling methodology outlined in figure 6.2 is followed to define a statistical model of settlements as an asset time-dependent process. Appendix E provides flowcharts for the simulations of asset time-dependent processes and their incorporation in time-dependent fragility and probability of failure in a time interval of interest.

Problem formulation and identification of existing knowledge

The task specification of the settlements statistical model at an individual process level is to quantitatively express settlements in time corresponding with experience and field measurements. The task specification at an overarching maintenance level is to realistically represent the influence of the settlements on the overarching performance indicators such as reliability, risk and life cycle cost. The latter is not further investigated in the Dartford Creek to Swanscombe Marshes system reliability analysis.

The existing knowledge on settlements is twofold. Firstly, the design crest levels and a survey in the early 2000s are known. Secondly, it is possible to calculate settlements by means of finite element methods or fairly straightforward process-based models exist, such as expressions (7.1) to (7.3).

$$\frac{\Delta h_p}{h} = \frac{C_c}{1+e_0}\log\left(\frac{\sigma_i' + \Delta\sigma'}{\sigma_i'}\right)\cdot[U(t_{i+1}) - U(t_i)] \tag{7.1}$$

$$\frac{\Delta h_s}{h} = C_\alpha[\log(t_{i+1}) - \log(t_i)] \tag{7.2}$$

$$U(t) = \sqrt[6]{\frac{T^3}{T^3+0.5}}; \qquad T = \frac{c_v(t)}{(ah)^2} \tag{7.3}$$

in which Δh_p is the primary compression increment over a period t_{i+1}-t_i due to the consolidation process, h_s is the secondary compression increment over a period t_{i+1}-t_i, C_c is the compression index, e_0 is the ratio between the volume of pores and of the total soil volume at the start of the compression process, σ_i' is the grain stress in soil strata i, $\Delta\sigma'$ is the change in grain stress caused by superimposed loading on the earth embankment for example induced by raising the crest level, $U(t_{i+1}$-$t_i)$ is the degree of consolidation in the form of the ratio between the excess in water pressure

and the actual water pressure as a function of time, C_α is the secondary compression index representing creep in the grain structure after the primary compression has taken place, t is the time duration in days after the superimposed loading has been applied, c_v is the vertical consolidation coefficient, a is a coefficient indicating the type of outflow, whereby 1.0 is single-sided outflow and 0.5 is two-sided outflow, and h is the thickness of the loaded soil strata.

Excitation, ancillary and affected features

The excitation, ancillary and affected features are tabulated in table 7.6.

Table 7.6 Excitation features, ancillary features and affected features in case of settlements

Excitation features	**Uncertainty**
Superimposed load on the embankment causing grain stress increase $\Delta\sigma'$ and an excess in pore pressures p_l	Inherent uncertainty in space for $\Delta\sigma'$ and p_l Constant in time for the superimposed loading Inherent uncertainty in time for pore pressures p_l – rainfall and environment → seasonality
Ancillary features	**Uncertainty**
The grain stress $\sigma_l' = \sigma_l - p_l$	Inherent uncertainty in space for ground pressures and pore pressures p_l Inherent uncertainty in time for pore pressures p_l only – rainfall and environment → seasonality
The compression index C_c	Inherent uncertainty in space
Void ratio e_0	Inherent uncertainty in space
Secondary compression index C_α	Inherent uncertainty in space
Vertical consolidation constant c_v	Inherent uncertainty in space
Outflow constant a	A deterministic constant which is 0.5 for two-sided outflow and 1.0 for one-sided outflow
Thickness of the loaded strata h	Inherent uncertainty in space
Affected features	**Uncertainty**
Crest level of embankment h_c / overall geometry of the embankment	Stochastic process introduces inherent uncertainty in time and space

Character of the asset time-dependent process

The character of the asset time-dependent process conditional on the constant excitation in time is logarithmic. It is driven by the excess in pore pressures created by the constant superimposed loading. The development in time of the pore pressures is a function of this difference in water pressures. The pore pressures are subject to seasonal and environmental fluctuations, for example due to rainfall and drought seasons.

Dependencies between asset time-dependent processes

The asset time-dependent process trafficking affects the same flood defence property as the settlement process, i.e. the crest level. However, the trafficking process mainly affects the upper layer of the embankment whereas the settlements compress the layers in the embankment and those forming the foundation. The two asset time-dependent processes can therefore be superposed.

Development of alternative statistical models

The three main alternative statistical models mentioned in section 6.3.4 are considered for settlements: parametric process, gamma process and a hierarchical process.

The parametric process for settlements consists of equations (7.1) to (7.3) as a deterministic function in time and random variables for e.g. C_c, e_0, etc. Corresponding with figure 5.2 (left) such a parametric process consists of a large number of logarithmic time paths. For one sample of the random variables the logarithmic development in time is fixed.

The hierarchical process model takes the inherent uncertainty in time into account. The feature responsible for introducing this inherent uncertainty in time is the pore pressure, which is subject to seasonality and environmental fluctuations. The pore pressures occur in two places in equation (7.1), through the grain stress $\Delta\sigma_i$ and the degree of consolidation $U(t_i)$. It is suggested to model this influence by modifying equation (7.1) to:

$$\frac{\Delta h_p}{h} + \frac{\Delta h_s}{h} = s_1 \cdot \left(\frac{C_c}{1+e_0} \log\left(\frac{\left(\sigma_i - \gamma_w\left(s_2 \cdot h_g - l_i\right)\right) + \Delta\sigma'}{\left(\sigma_i - \gamma_w\left(s_2 \cdot h_g - l_i\right)\right)} \right) \cdot \left[U(t_{i+1}) - U(t_i)\right] + C_\alpha \left[\log(t_{i+1}) - \log(t_i)\right] \right) \quad (7.4)$$

The primary compression Δh_p and secondary compression Δh_s are increments over a period of a quarter of a year: t_{i+1} - t_i. The total compression at a moment in time is found by accumulating the increments in the preceding period. In (7.4) σ_i is the ground pressure in strata i in kN/m^2, γ_w is the density of water in kN/m^3, h_g is the freatic surface in the embankment, l_i is the level of strata i in meter OD. s_1 is a model uncertainty capturing the inherent uncertainty in time introduced by seasonality and

environmental fluctuations in the consolidation process. s_1 also covers the secondary settlements since the pore pressures influence the structure of the grain skeleton. s_2 is a model uncertainty capturing the inherent uncertainty in time introduced by seasonality and environmental fluctuations directly in the freatic surface in the embankment. The expressions for s_1 and s_2 are modeled after Vrouwenvelder (2005):

$$s_1 = s_{11} - s_{12} \tag{7.4.1}$$

$$s_2 = s_{21} + s_{12} \tag{7.4.2}$$

In which s_{11} =1.0, a random variable with mean value 1.0 and a standard deviation representing the time-independent model uncertainty due to e.g. discontinuities in the granular structure. The seasonal effects in the model uncertainty are related to the outflow process in the consolidation process or the limitations to fully model this process. This uncertainty is reflected by s_{12}, a wave renewal model with a statistical distribution function and constant intervals, e.g. a normal distribution function with mean value 0, standard deviation 0.1 and intervals of 0.25 years. Both s_1 and s_2 share the same wave renewal process s_{12}, as they capture the same seasonal fluctuations. s_{12} can be both positive and negative. s_{12} in s_2 is meant to represent a seasonal variation in the freatic surface. Higher pore pressures relate to less outflow in the consolidation process, therefore s_{12} in s_1 is negative when s_{12} in s_2 is positive.

The gamma process model assumes that there is insufficient information available on the soil properties to populate the process-based model. An average settlement rate μ with a standard deviation σ is estimated with expert judgement and implemented in the form of a gamma process.

$$\begin{aligned} p_{X(t)} &= Ga(x|a,b) = Ga\left(x\middle|\left[\mu^2 t\right]/\sigma^2, \mu/\sigma^2\right) \\ E(X(t)) &= \mu t \\ Var(X(t)) &= \sigma^2 t \end{aligned} \tag{7.5}$$

The gamma process in this form is suitable for a settlement process that has progressed through its steep initial development. A non-linear model is proposed by Speijker et al. (2000), but is in this case not further explored.

Estimation, calibration and corroboration

The mean values of the random variables in equations (7.1) to (7.4) are populated with field measurements on variables such as C_c, e_0, etc, from Halcrow (2006) and Soil Mechanics (2006). Insight in the statistical properties of these random variables

can be acquired from e.g. Baecher & Christian (2003), Vrouwenvelder et al. (2001b) or CUR 162 (1999). The prior distributions of the variables in equations (7.1) to (7.4) are tabulated in table 7.7. The situation corresponds with situation 4 in table 6.5. It is noted that for the Dartford Creek to Swanscombe Marshes flood defence system the data availability is good. However, for statistical point estimation methods a much larger sample is required on **d** and the time series samples on the settlements need to be denser populated, hence 'scarce data availability'.

Table 7.7 Prior distributions of the random variables in the hierarchical process, gamma process and parametric settlement models the right column contains the coefficients of influence corresponding with FORM. The bottom row contains a description of the distribution types. V is the coefficient of variation: σ/μ.

		Description		Unit	Dist. type	μ	σ	V	Direction cosines eqn. (2.11)
γ_w	=	Volumetric weight water		kN/m³	N	10	0.01	-	0.016
l_l	=	Soil layer levels		mOD	N	defined per soil layer	0.2	-	0.15
γ_s	=	Volumetric weight saturated soil		kN/m³	N	defined per soil layer	-	0.05	0.070
γ_d	=	Volumetric weight dry soil		kN/m³	N	defined per soil layer	-	0.05	0.035
C_p	=	Primary compression indices total contribution	Clay	-	LN	0.86	-	0.25	-0.24
			Peat	-	LN	0.90	-	0.25	
			Sand	-	LN	0.004	-	0.25	
h_c	=	Original crest level		mOD	N	4	0.1	-	-0.034
e_0	=	Void ratio total contribution	Clay	-	LN	1.667	-	0.25	0.16
			Peat	-	LN	1.848	-	0.25	
			Sand	-	LN	-	-		
C_α	=	Secondary compression indices total contribution	Clay	-	LN	0.085	-	0.25	-0.93
			Peat	-	LN	0.016	-	0.25	
			Sand	-	LN	-	-	-	
h_g	=	Freatic surface in embankment		mOD	N	4	0.1	-	-0.012
$\Delta\sigma'$	=	Weight of superimposed loading		kN/m²	N	30	-	0.1	-0.16
s_{11}	=	Time-independent model uncertainty		-	LN	1	0.05	-	N/A
s_{12}	=	Seasonality in consolidation process		-	WR 0.25	0	0.1	-	N/A
s_{21}	=	Seasonality in embankment pore pressures		-	WR 0.25	0	0.1	-	N/A
$dh_{s;gam}$	=	Average settlement in one year, gamma process model		m	Ga	0.018	0.01	-	N/A
N = Normal distribution function LN = Lognormal distribution function WR 0.25 = Wave Renewal model with constant intervals of 0.25 years, I.e. seasons Ga = Gamma process									

The data availability on historical observations is not much. The design crest levels in the 1970s and a field survey in the early 2000s are known. This allows a limited significance test on the initially established expert elicited parameter set, see for more details the analysis described below. The parameters in equation (7.5) are populated by making an estimate on the average settlement rate and its standard deviation. A significance test is made against the measurements in 2000. This significance test is based on only one observation and is of limited value. However, it provides an indication of the suitability of a parameter set.

Analysis

The results of the simulations with the hierarchical process (with seasonal components s_{21} and s_{12}), the parametric process (without seasonal components s_{21} and s_{12}) and gamma process models are shown in figure 7.8. These simulations are based on the distribution functions in table 7.7. The start of the plot t=0 is taken 25 years earlier than the observation made in the period 2000 to 2003. The parametric process model displays a slightly larger variance in the simulations than the hierarchical process model, i.e. including seasonality. The gamma process model is in this case compared to the predictions with equations (7.1) to (7.4) from t=20 over

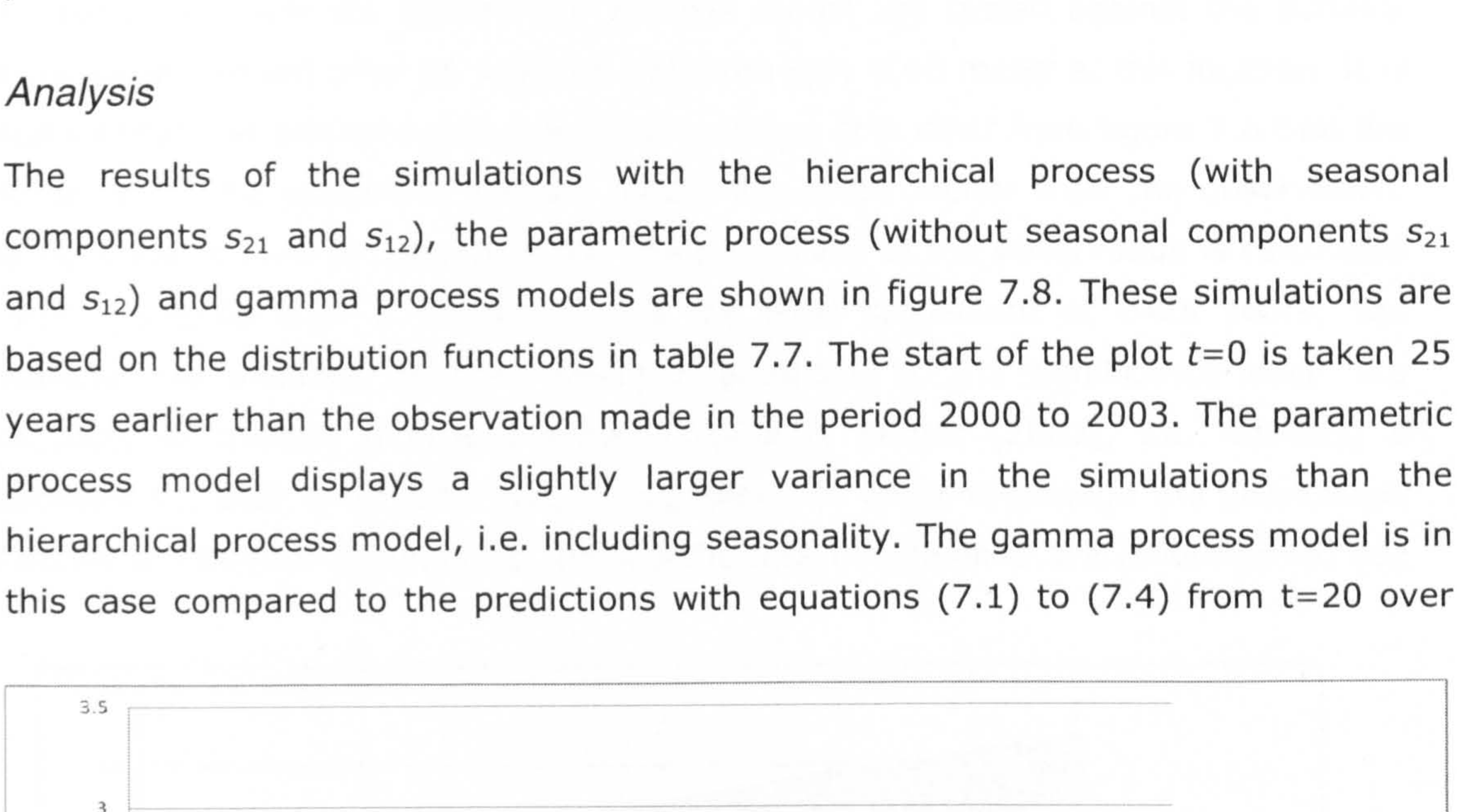

Figure 7.8 Time series sample of a hierarchical process, parametric process and gamma process model for settlements

the next 30 years of lifetime. The variance of the gamma process model is therefore not comparable with that of the other models.

The quality of the models are evaluated and improved in the following way. Firstly, a significance test is carried out on the parameter set in table 7.7. Secondly, a sensitivity analysis points out which parameters are contributing most to the settlement model. Literature is then consulted to make a new estimate on the rejected parameter set. The results are tested against the available observation.

The predictions with the hierarchical process model are tested against the actually measured settlement after 25 years of approximately 0.60 meter at this location. It is assumed that this settlement is due to compaction. It is clear from figure 7.8 that the predictions of the stochastic process model are much higher than the observation. The significance level is taken at 0.05. The probability of the observation is calculated at $P(S \leq s=0.60\ m) \approx 0$. In which s is the total settlement at t=25 years. The parameter set therefore requires rejection according to the significance level. The probability of making a type I error, Casella & Berger (2002), i.e. rejecting a parameter set that is actually true, is negligible. In order to change the distribution functions of relevant parameters, the coefficients of influence are investigated, see

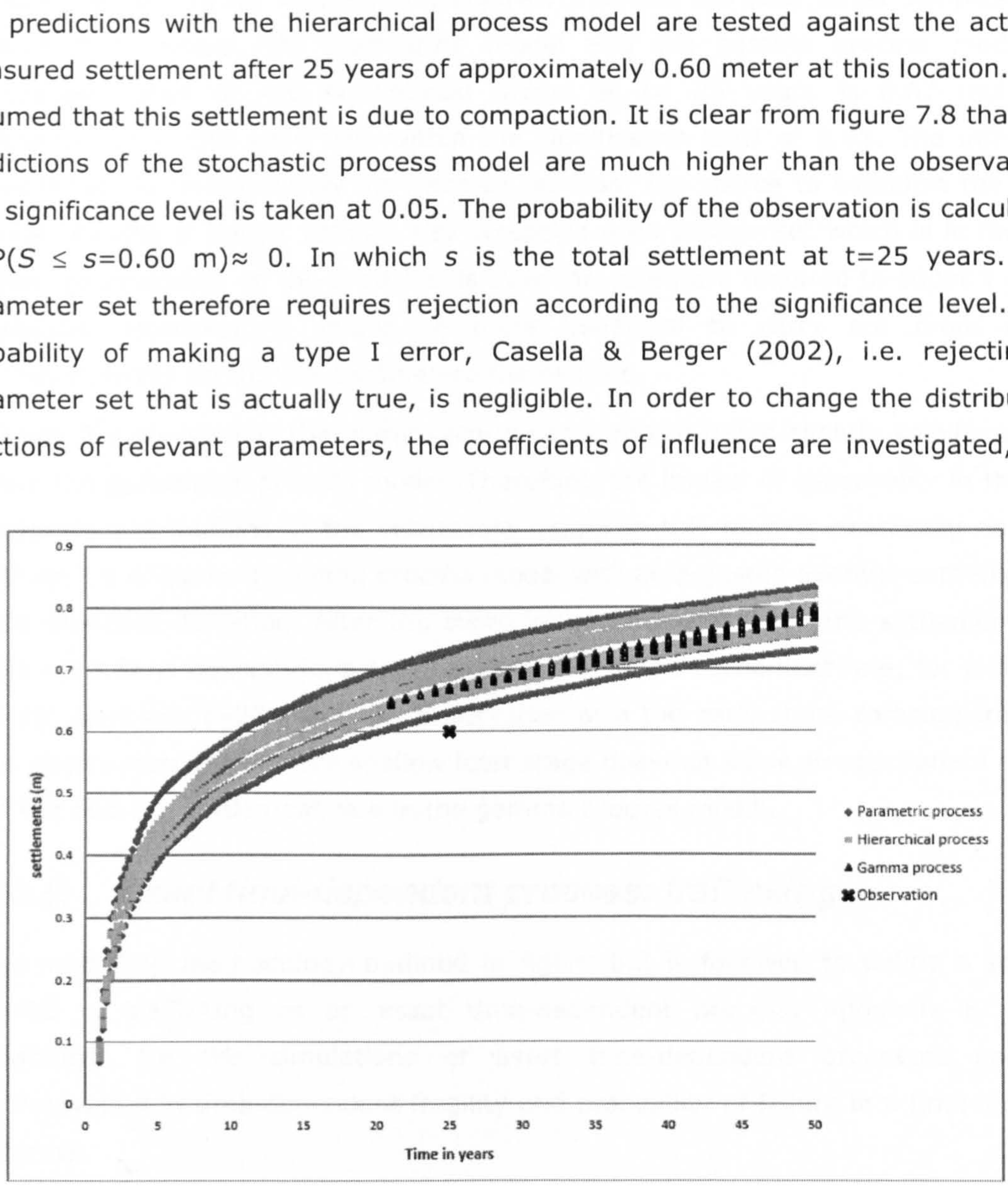

Figure 7.9 Hierarchical process, parametric process and gamma process model with adjusted parameter set: C_α for clay is 0.023.

right column in table 7.7. The largest coefficient of influence is associated with the secondary compression indices. The value indicated in table 7.7 is the aggregate coefficient of influence for C_α over all soil layers. The parameters of the distribution function of C_α for clay layers in the first analysis are derived from field measurements according to Halcrow (2006). They are adjusted based on CUR 162 to C_α=0.023. This value corresponds with very organic clay layers. Additionally, it is assumed that the new landward embankment corresponds with a layer thickness of approximately 2.5 meter, leading to $\Delta\sigma'$ =45 kN/m3. Figure 7.9 shows the time series samples for the hierarchical model, the parametric model and the gamma process model. The expected value of the hierarchical model at t= 25 years is 0.67 meter, the observation in this case falls within the significance level of 0.05. The information availability is unfortunately very scarce, at least too scarce to establish the type II error, Casella & Berger (2002), i.e. accepting a parameter set which is in fact false. More observations on the crest levels over the years are required to support such an analysis. Moreover, it might be more beneficial to carry out more detailed measurements on the soil parameters themselves.

Figure 7.9 shows that the hierarchical process model has a slightly smaller variance than the parametric process model. Therefore, the impact of seasonality in the water pressure distributions in the settlement model in this form is practically negligible. Figure 7.9 contains a gamma process model with an adjusted average settlement rate and standard deviation. After the steep initial development of the settlement model two crest level observations allow an estimate of the settlement rate, for example at t=20 years and t=25 years. An observation at a too early stage complemented with an observation at the more shallow later stage does not allow an appropriate estimate of the average settlement rate in the gamma process model.

7.3.5. Asset time-dependent process: trafficking

The modelling methodology outlined in figure 6.2 is followed to define a statistical model of trafficking as an asset time-dependent process. Appendix E provides flowcharts for the simulations of asset time-dependent processes and their incorporation in time-dependent fragility and probability of failure in a time interval of interest.

Problem formulation and identification of existing knowledge

The task specification is to quantitatively express the damage to the crest level and vegetation in time corresponding with experience and field measurements. The task specification at an overarching maintenance level is to realistically represent the influence of trafficking on the overarching performance indicators such as reliability, risk and life cycle cost.

A process model to quantify the damage to the crest level and vegetation due to trafficking is not available. Site specific field measurements are not around either. Expert elicitation on damage rates of the crest level and vegetation is possible.

Excitation, ancillary and affected features

The excitation, ancillary and affected features related to trafficking are listed in table 7.8.

Character of the asset time-dependent process

The asset time-dependent process of trafficking causing crest level settlement is characterised by: a stochastic process consisting of recurrent damage events, with nonlinear settlement behaviour during each event and nonlinear behaviour between successive events. The settlement during an event and between successive events is influenced by the seasonality in moisture content in the embankment. The trafficking asset time-dependent process is dependent on its own development history. I.e. the impact of the trafficking event diminishes with the number of events due to compaction in the embankment surface.

The asset time-dependent process of trafficking causing vegetation damage is characterised by: a stochastic process consisting of recurrent damage events, nonlinear behaviour during the trafficking event depending on a combination of excitation and ancillary features. The pore pressures in the embankment surface influence the strength of the vegetation and that of the soil and roots in the turf. The asset time-dependent process is therefore influenced by seasonality.

Dependencies between asset time-dependent processes

The asset time-dependent processes crest level settlement and vegetation damage are caused by the same excitation, i.e. recurrent trafficking events. The relationship

between the singular asset time-dependent processes and the characteristics of the trafficking event does not entirely overlap – see excitation block in table 7.8.

Settlements due to trafficking and settlements due to compaction affect different layers of the earth embankments. The total crest level settlement is found by superposition of the two processes. Compaction is a process in the soil layers underneath the earth embankments. Trafficking damages the upper layer of the earth embankment by spraying and partly by compressing the upper layer.

Table 7.8 Excitation features, ancillary features and affected features in case of trafficking

Excitation features	**Uncertainty**
Recurring trafficking events damaging crest level, with the following characteristics: • Tyre width, profile and number of tyres on vehicle • Vehicle weight • Number of vehicles in the trafficking event and the spread of the damage • The number of different types of vehicles and their characteristics • Duration of the trafficking • The rate of recurrence of trafficking events • The recurrence of different groups of vehicles	Inherent uncertainty in time introduced by the recurrent trafficking events Inherent uncertainty in space
Recurrent trafficking events damaging vegetation, with the following characteristics: • Tyre width, profile and number of tyres on the vehicle • Number of vehicles in the trafficking event and the spread of the damage • Duration of the trafficking event • The rate of recurrence of the trafficking events • The recurrence of different groups of vehicles	Inherent uncertainty in time introduced by the recurrent trafficking events Inherent uncertainty in space
Ancillary features	**Uncertainty**
Soil type Compressibility Grain size Pore pressures near the embankment surface Cohesion Angle of internal friction	Inherent uncertainty in space Inherent uncertainty in time, e.g. soil properties vary with moisture content
Vegetation root depth, length, strength Soil type Grain size Cohesion Angle of internal friction Pore pressure near the embankment surface	Inherent uncertainty in space Inherent uncertainty in time, e.g. soil properties vary with moisture content, vegetation grows
Affected features	**Uncertainty**
Crest level, h_c	Inherent uncertainty in time and space
Vegetation, c_g	Inherent uncertainty in time and space

Development of alternative statistical models

The parametric process model is not applicable to trafficking as it concerns a shock damage process. Below the hierarchical process model is given and subsequently the gamma process model is described.

The hierarchical process models the arrival of trafficking events with a Poisson distribution, whereby the number of trafficking events is N_t. The damage to the crest level is then modelled as follows.

$$Z_{\Delta h} = \sum_{i=1}^{N_t} W_i \qquad (N_t = 1,2,\ldots),$$
$$= 0 \qquad (N_t = 0) \tag{7.6}$$

$$W_i = \Delta h_{s;i} + \Delta h_{c;i} \tag{7.7}$$

In which W_i is the increment caused by trafficking event i, and is broken down into a spray component $\Delta h_{s;i}$ and a compaction component $\Delta h_{c;i}$ both in meter. The compaction component is a function of the previous compaction increments:

$$\Delta h_{c;i} = m_{com} \cdot c_{com} \cdot \log\left(1 + \sum_{j=1}^{i-1} \Delta h_{c;j}\right) \tag{7.8}$$

In which m_{com} is the modelling uncertainty associated with compaction due to trafficking and c_{com} is a coefficient involved with the compaction of the top layer of the embankment. m_{com} takes seasonality in the moisture in the top layer of the embankment into account. The damage to the vegetation is caused by the same Poisson distributed trafficking events. The total damage to the vegetation at a moment in time is given by:

$$Z_{cg} = \sum_{i=1}^{N_t} \Delta c_{g;i} \qquad (N_t = 1,2,\ldots),$$
$$= 0 \qquad (N_t = 0) \tag{7.9}$$

In which Δc_g is the damage to the vegetation resulting from one trafficking event.

The gamma process model for the correlated asset time-dependent processes crest level settlements, Δh_{gamma}, and damage to the vegetation, $\Delta c_{g;gamma}$, is developed according to Buijs et al. (2005). Each singular asset time-dependent process is modelled with the gamma process model according to equation (5.25) allowing estimates for the mean rates of deterioration and standard deviations. The correlations between the processes are represented by a double-gamma distribution, Kotz et al. (2000), and simulated with trivariate reduction methods according to Devroye (1986). An overview of the double-gamma model is given below.

The procedure requires the scale and shape parameters of the marginal distributions of $X_1 \sim \text{Ga}(x_1|a_1,b_1)$, and $X_2 \sim \text{Ga}(x_2|a_2,b_2)$, and the mutual correlation ρ, which must lie between $0 \leq \rho \leq \min(a_1/\sqrt{(a_1a_2)},a_2/\sqrt{(a_1a_2)})$. The trivariate reduction method is carried out by the following procedure:

Generate $Y_1 \sim \text{Ga}(a_1 - \rho\sqrt{(a_1a_2)},1)$

Generate $Y_2 \sim \text{Ga}(a_2 - \rho\sqrt{(a_1a_2)},1)$

Generate $Y_3 \sim \text{Ga}(\rho\sqrt{(a_1a_2)},1)$

Return $(X_1,X_2)=(b_1(Y_1+Y_3),b_2(Y_2+Y_3))$

In this procedure Y_1, Y_2 and Y_3 are independent gamma distributed random variables. The correlated variables X_1 and X_2 are a linear function of two of those three variables Y_1, Y_2 and Y_3, each sharing Y_2. The model assumes that an exchangeable sequence of loading can be assembled into three independent sets of loading characteristics Y_1, Y_2 and Y_3. The deterioration increments X_1 and X_2 are modelled with a linear function of those loading characteristics and share a set of overlapping characteristics Y_2. The model in case of trafficking events damaging the crest level and the vegetation works out as follows. In this case study, the exchangeable sequence of loading is represented by the trafficking events. The condition variables subject to damage are: the crest level and the vegetation (resp. X_1 and X_2). It is assumed that the damage due to the trafficking is (linearly) proportional to three sets of independent characteristics, indicated with Y_1, Y_2 and Y_3, representing characteristics of the vehicles (e.g.: weight of the vehicles, tyre width and number of vehicles). These assumptions enable the application of trivariate reduction methods as described above. The average rates of deterioration for the marginal gamma processes of the crest level and of the vegetation are separately estimated based on a reasonable judgment. The mutual correlation between the two deterioration processes given the same underlying sequence of loading events can be estimated similarly.

Estimation, calibration and corroboration

There are no field measurements for the settlements and vegetation damage due to trafficking and the scientific understanding is limited. The prior distributions of the variables in the hierarchical process, equations (7.6) to (7.9), and the mean value and standard deviation of the marginal distributions in the double-gamma model are tabulated in table 7.9. The situation corresponds with situation 4 in table 6.5.

Historical observations are not available to carry out a significance test. Future observations are expected on the overall quantity.

Table 7.9 Prior distributions of the random variables in the trafficking hierarchical process model and the gamma process model. The bottom row contains a description of the distribution types. V is the coefficient of variation: σ/μ

			Description	Unit	Dist. type	μ	σ	V	ρ
N_t		=	Number of trafficking events	-	Po	3/year	-	-	-
dh_s		=	Spraying settlement due to trafficking	m/event	LN	0.01	-	0.5	-
dh_c	m_{com}	=	Model uncertainty associated with compaction	-	WR 0.25	1	-	0.1	-
	c_{com}	=	Top layer compaction coefficient	-	LN	0.3	-	0.1	-
Δc_g		=	Damage to vegetation	m·s / event	LN	1000	-	0.1	-
Δh_{gamma}		=	Total trafficking settlement in one year	m	DGa	0.5	0.12	-	0.8
$\Delta c_{g;gamma}$		=	Incremental damage to the vegetation due to trafficking in one year	m·s	DGa	500	50	-	0.8

Po = Poisson distribution function with mean value μt and standard deviation $\sqrt{\mu t}$
LN = Lognormal distribution function
WR 0.25 = Wave Renewal model with constant intervals of 0.25 years, normally distributed
DGa = Double-gamma distribution function

Analysis

As mentioned above, a significance test is not applicable as there are no historical observations. The comparison of the hierarchical process model and the double-gamma model for settlements and vegetation damage due to trafficking is therefore only a qualitative one. Figure 7.10 contains some time series samples of the hierarchical process model as well as the double-gamma model. The hierarchical process model samples clearly reflect the shock damages introduced by the trafficking events.

The hierarchical process model is advocated over the double-gamma process model in this case. This choice is argued based on the consideration of three aspects. The first aspect is the appropriate representation of the stochastic process. The hierarchical process model portrays the shock damages due to trafficking events more appropriately than the double-gamma process model. The spread in the time series samples is also larger than those simulated with the double-gamma model.

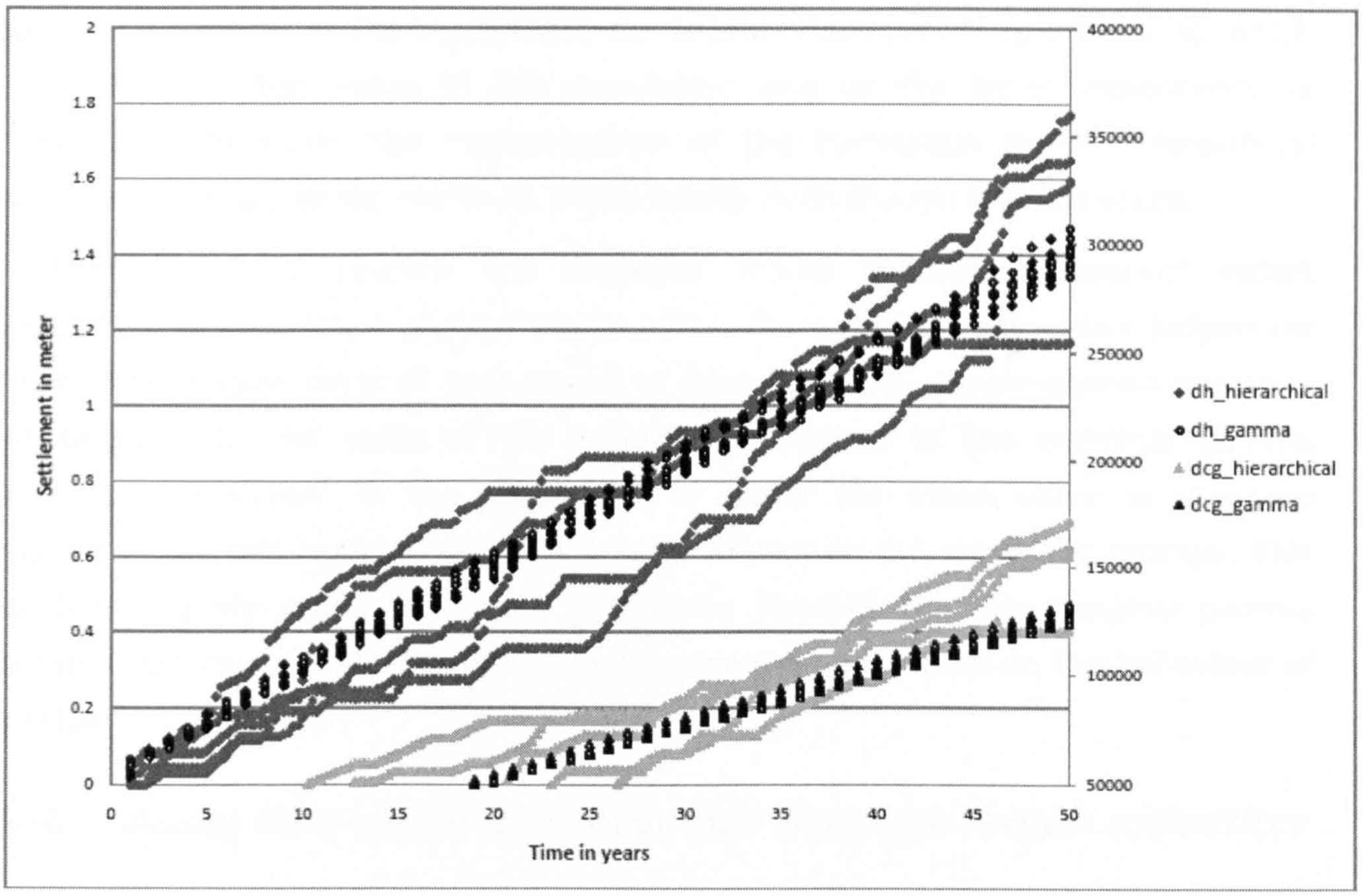

Figure 7.10 Some time series samples of hierarchical process model and double-gamma process model for settlements and vegetation damage due to trafficking

The second aspect is the appropriate representation of the dependency between the two deterioration processes. The evaluation of this aspect is not straightforward. The dependency between settlements and damage to the vegetation due to trafficking is twofold. The first type of dependency is the fact that both damages are caused by the same number and timing of trafficking events. The hierarchical process model picks up on this dependency by calculating the cumulative damages over the same number of trafficking events. In figure 7.10 similar behaviour of the hierarchical process model samples for the settlements and vegetation damage can be seen. The double-gamma model does not explicitly deal with this type of dependency. The second type of dependency is that the damages during one trafficking event are caused by the same loading properties. The absence of a process-based model does not allow capturing this dependency in the form of shared function properties. This type of dependency should therefore be reflected by means of mutual correlation. This correlation is not picked up by the hierarchical process model, whereas it is by the double-gamma model. Estimation of the correlation coefficient covers both

dependency aspects in the double-gamma model. However, it is unclear to which extent and by what value of the correlation one or the other dependency is represented. Therefore, the representation of the correlation by the hierarchical process model is preferred due to its transparency even though it is one-sided.

The third aspect is whether the statistical model enables transparent expert elicitation. The hierarchical process model allows more transparent expert judgement on the deterioration rates of both types of damages. The double-gamma model is very sensitive to the value of the variation coefficient in the marginal gamma processes. A deviation in the judgement of either the mean value or standard deviation of the deterioration rate has a large impact on the stochastic process. This sensitivity is pronounced due to the correlation between the two marginal gamma processes. Change in judgement on one marginal has an impact on the behaviour of the other.

7.3.6. Asset time-dependent process: seepage length reduction

The modelling methodology outlined in figure 6.2 is followed to define a statistical model of long-term internal erosion in the water conductive layer as an asset time-dependent process. Appendix E provides flowcharts for the simulations of asset time-dependent processes and their incorporation in time-dependent fragility and probability of failure in a time interval of interest.

Problem formulation and identification of existing knowledge

The task specification of the seepage length reduction statistical model at an individual process level is to quantitatively express the reduction in seepage length in time. The task specification at an overarching maintenance level is to realistically represent the influence of the seepage length reduction on the overarching performance indicators such as reliability, risk and life cycle cost.

Earth embankments along the Dartford Creek to Swanscombe Marshes flood defence line are susceptible to uplifting and piping. To relieve the uplift pressures underneath the impermeable foundation, the earth embankment is equipped with drainpipes in the ditch behind the embankment. These drainpipes are directly reaching into the water conductive layer underneath the embankment. A storm with a water level higher than the drainpipe level produces flow and allows for the initiation of internal

erosion of the water conductive layer. Internal erosion reduces the seepage length in the piping failure mechanism. There is no field information about the occurrence of such a time-dependent process. However, it is reasonable to consider this process since the drainage pipes do not contain a filter or any other device preventing the wash out of fines. Sellmijer (1988) formulates a process model for the piping process leading up to structural failure given a water head difference. However, the gradual loss of fines as a consequence of a sequence of storms over the years is not included in this model. The analysis below aims to provide an indicative model of the gradual loss of fines over the years.

Excitation, ancillary and affected features

Table 7.10 presents the excitation, ancillary and affected features for the asset time-dependent process reduction in seepage length.

Table 7.10 Excitation, ancillary and affected features for the reduction in seepage length asset time-dependent process

Excitation features	**Uncertainty**
The water head difference between the river level and the upper end of the drainage pipe initiates flow through the water conductive layer underneath the embankment.	Inherent uncertainty in space due to differences in water levels Inherent uncertainty in time as the water levels are a stochastic process
Ancillary features	**Uncertainty**
The density of the sand / gravel	Inherent uncertainty in space
The size of the sand / gravel particles	Inherent uncertainty in space
The grading of the sand / gravel particles	Inherent uncertainty in space
The diameter of the drainage pipes	Inherent uncertainty in space
The height of the drainage pipes	Inherent uncertainty in space
The seepage length	Inherent uncertainty in space
Affected features	**Uncertainty**
Seepage length, *L*	Stochastic process introduces inherent uncertainty in time and space

Character of the asset time-dependent process

The seepage length reduction asset time-dependent process is a recurrent process since it is driven by the water head between the river and the drainage pipe. The amount of reduction in the seepage length during a storm event is in addition a function of the seepage length itself. The amount of seepage length reduction therefore depends on the preceding sequence of storms and is history dependent.

Dependencies between asset time-dependent processes

The seepage length reduction asset time-dependent process is assumed to be a singular process. Dependencies with other asset time-dependent processes are not considered.

Development of alternative statistical models

The statistical model is in this case clearly a stochastic process as the asset time-dependent process of the seepage length is driven by the storm water level and storm duration. The parametric process model is therefore not considered among the statistical models.

The hierarchical process model is built up as follows.

$$L_{i+1} = L_i - \Delta L_i \tag{7.10}$$

In which L_{i+1} is the seepage length at $t=i+1$ and L_i is the seepage length at $t=i$. ΔL_i is the deterioration of the seepage length between $t=i$ and $t=i+1$. This quantity is roughly estimated by:

$$\Delta L_i = c \cdot k \cdot \frac{\Delta h}{L_i} t_s \tag{7.11}$$

In which c is a dimensionless coefficient, k is the permeability of the water conductive layer, t_s is the storm duration, $\Delta h=h-h_p$ in which h is the water level and h_p is the level of the drainpipe. L_i is the seepage length at $t=i$.

This expression is a function of the water level, the storm duration and the time-dependent seepage length. This introduces a dependency on the sequence of storms. How this is implemented is described in the following. The number of storms N_{st} in an interval dt is modelled with a Poisson distribution. Each storm is represented by a pair

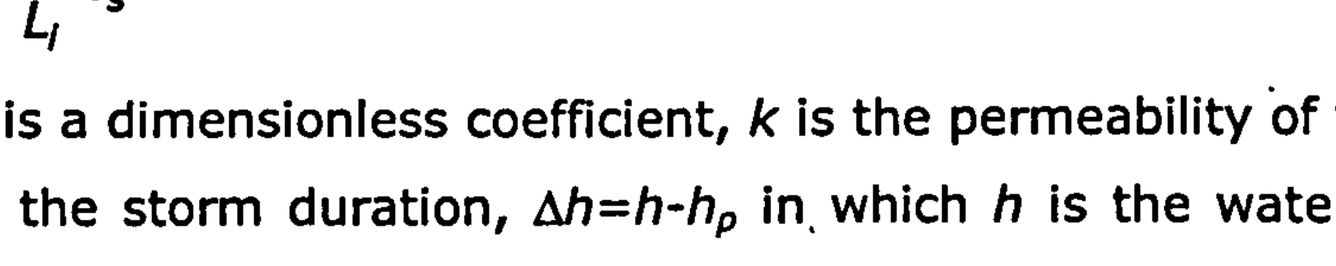

Figure 7.11 *A sequence of storms and the pairs of water level and storm duration that represent each storm*

of a water level, h, and a storm duration, t_s (figure 7.11).

N_{st} storms give $N_{st}!$ sequences which is computationally impossible to simulate for high numbers of N_{st}. There is a probability of $1/N_{st}$ that each of the pairs occurs first, a probability of $1/(N_{st}-1)$ that one of the remaining events occurs secondly, $1/(N_{st}-2)$, etc. The procedure is then as follows:

1. Establish a number of storms N_{st} that is Poisson distributed.
2. For 1, .., N_{st} randomly draw a pair of h_l and $t_{s;l}$ providing:

$$\begin{bmatrix} h_1 & t_{s;1} \\ & \vdots \\ h_{N_{st}} & t_{s;N_{st}} \end{bmatrix} \tag{7.12}$$

3. Select the first pair with probability $1/N_{st}$ and eliminate it from the matrix, calculate the corresponding ΔL, determine $L=L-\Delta L$
4. Select the second pair from the remaining matrix with probability $1/(N_{st}-1)$
5. Etc. until N_{st} , L is carried on to the next time interval dt.
6. Select a new N_{st} for dt and carry out the same procedure with the resulting L from the previous round.

Estimation, calibration and corroboration

There is no knowledge about the occurrence of seepage length reduction along this site. The prior distributions of the variables in the hierarchical process, equations (7.10) to (7.12), and the mean value and standard deviation are tabulated in table 7.11. This table also contains the mean value and standard deviation of the internal erosion rates in a gamma process model. The situation corresponds with situation 4 in table 6.5. Historical observations are not available to carry out a significance test. Future observations are expected on the variables in the model.

Analysis

The time series samples of the hierarchical process model and the gamma process model for seepage length reduction are displayed in figure 7.12. The model intends to provide an indication of the reduction in seepage length due to the presence of open drainage pipes. An experimentally underpinned detailed process model for the threshold of piping failure under impervious structures is described in Sellmijer (1988). Observations of the seepage length in time are not available. Hence, a

significance test on the parameter set in table 7.11 is not applicable, nor any other kind of quantitative quality assessment of the statistical model.

Table 7.11 *Prior distributions of the random variables in the internal erosion hierarchical process model and the gamma process model. The bottom row contains the description of the distribution types.*

		Description	Unit	Dist. type	μ	σ	V
N_{st}	=	Number of storms	-	Po	20/year	-	-
k	=	Permeability	m/s	LN	0.01	-	0.1
h	=	Local water levels	mOD	Joinsea simulations	Transformation to local water levels	N/A	N/A
h_p	=	Level of the top of the drainage pipe	mOD	N	3	0.01	-
L	=	Seepage length	m	LN	Width embankment	-	0.1
t_s	=	Storm duration	hours	LN	5	-	0.25
c	=	Coefficient for internal erosion	-	LN	2	-	0.1
ΔL_{gamma}	=	Reduction in seepage length gamma process model in one year	m/year	Ga	0.06	0.02	-

N = Normal distribution function
LN = Lognormal distribution function
Ga = Gamma process
Po = Poisson distribution with mean value μt and standard deviation $\sqrt{\mu t}$

The chance of improving the opportunity for such a quality assessment is small, as the size of the seepage length as a function of time is hard to measure. The water conductive layer is over 10 meter from the ground surface and the erosion process is three dimensional. Posterior updating on the parameters on the other hand is a possibility under increasing information in the future.

Figure 7.12 presents time series samples for the hierarchical model and the gamma process model based on the parameter distributions in table 7.11. The seepage length L is considered as a deterministic variable, "L_det_hier" and "L_det_gamma", as well as a random variable, "L_var_hier" and "L_var_gamma". In this model the initial variance in the seepage length overshadows the variance introduced by the erosion process. The gamma process model provides a good approximation of the hierarchical process model.

7.3.7. Time-dependent fragility for earth embankments

Figure 7.12 shows the time-dependent fragility for flood defence section 4 along the Dartford Creek to Swanscombe Marshes flood defence line. Appendix E provides

flowcharts for the simulations of asset time-dependent processes and their incorporation in time-dependent fragility and probability of failure in a time interval of interest.

Flood defence section 4 is the section of the earth embankments that has the lowest

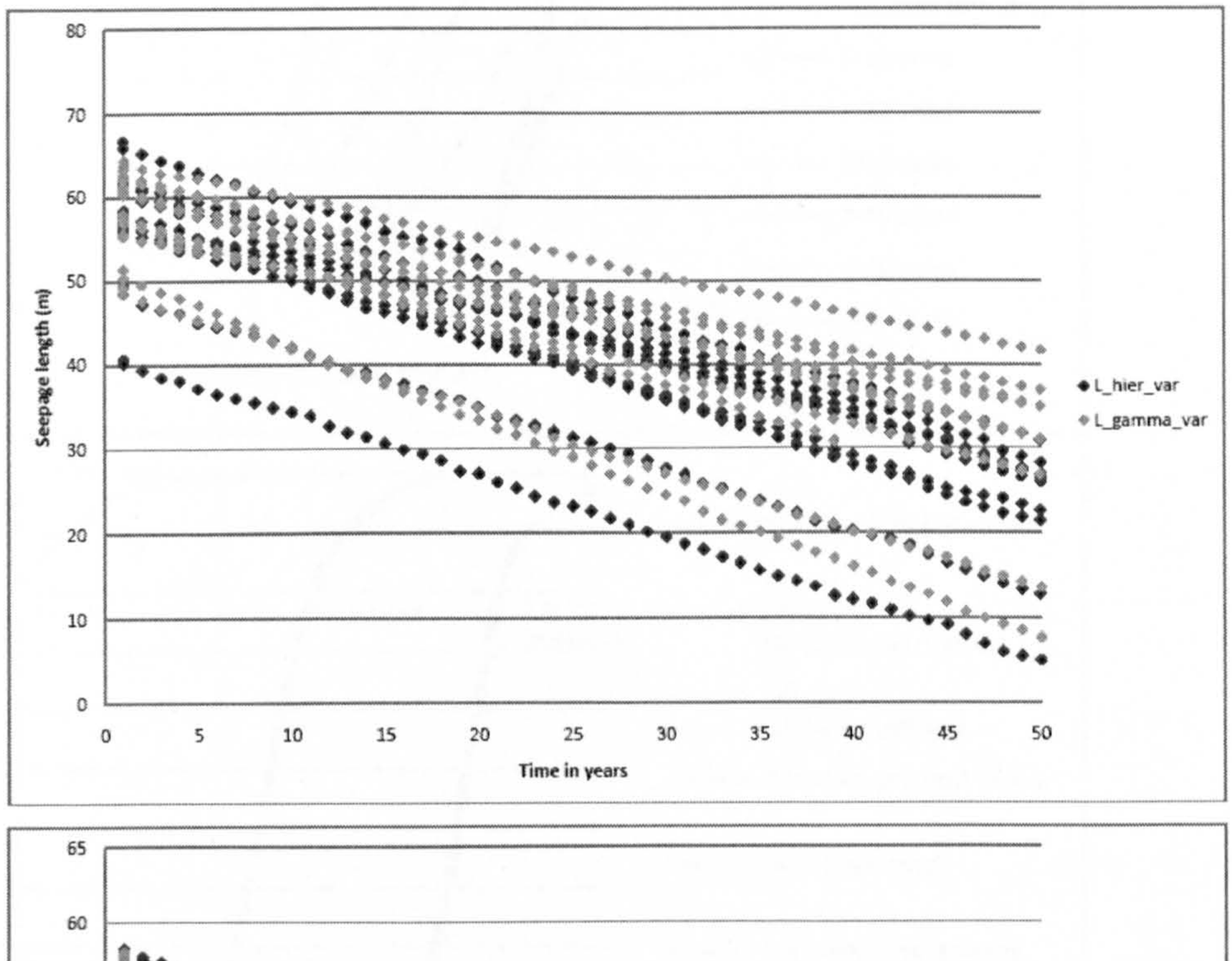

Figure 7.12 *Hierarchical process and gamma process model for seepage length with in bottom plot: L is deterministic, "L_det_hier" and "L_det_gamma", top plot: L is a random variable, "L_var_hier" and "L_var_gamma".*

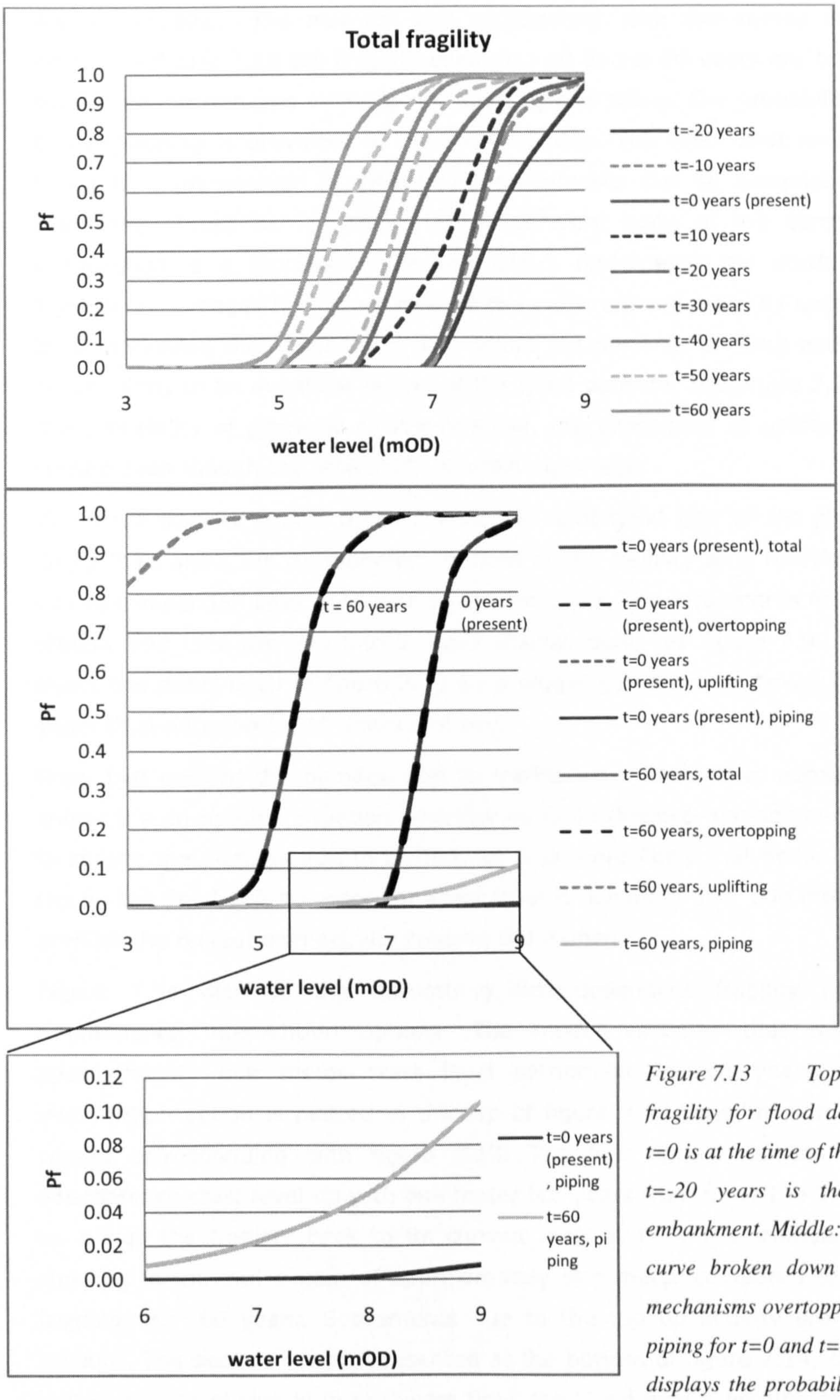

Figure 7.13 Top: time-dependent fragility for flood defence section 4, t=0 is at the time of the survey in 2001, t=-20 years is the as-constructed embankment. Middle: the total fragility curve broken down into the failure mechanisms overtopping, uplifting and piping for t=0 and t=60 years. Bottom: displays the probability of failure due to piping.

annual reliability. The moment t=0 corresponds with the survey in 2001. At the bottom of figure 7.13 the fragility curve at t=0 and t=60 years are broken down into the failure mechanisms overtopping, uplifting and piping. The probability of failure due to overtopping is prevalent in the total fragility. The total crest level settlement is found by superposition of crest level settlements due to compaction and due to trafficking. These two processes affect different parts of the earth embankment. Compaction is a process in the soil layers underneath the earth embankments. Trafficking damages the upper layer of the earth embankment by spraying and partly by compressing the upper layer. The failure mechanisms uplifting and piping need to occur jointly in an event for failure of the flood defence, see figure 7.7. Therefore, as the probability of piping is relatively small, the probability of uplifting and piping is limited even though the probability of uplifting is high.

The three fragility curves up to t=0 at the right hand side of the plot at the top of figure 7.13 show the development in time of the fragility as a function of settlement due to compaction after construction around 1980. The settlements first increase fairly steeply and then develop into a more shallow part, see figure 7.9. This logarithmic effect translates itself in figure 7.13 by a bigger gap between t=-20 years and t=-10 years than between t=-10 years and t=0.

From t=0 onward the damage due to trafficking is taken into account. Figure 7.13 shows the do-nothing situation whereby no flood defence management is undertaken to reduce the damage due to trafficking. It is more likely that action will be taken to top up the flood defence once the crest level is damaged over one meter or to limit or prohibit the recreational activity causing the damage.

Figure 7.14 displays the do-nothing time-dependent fragility in case of two maintenance intervention options. The model assumes that trafficking causes approximately one meter crest level settlement in ten years time. The first intervention option is plotted in the top of figure 7.14 together with the do-nothing curves corresponding with figure 7.13. The first option consists of topping the flooddefence crest level up with one meter ten years from now. The 1m crest level top up brings the fragility back to its current level at t=0. The trafficking is continued showing in the end a gain of approximately one meter compared to the do-nothing fragility at t=60 years. Settlements due to the top up activity are also taken into account. The second option, presented at the bottom of figure 7.14, consists of a one meter crest level top up in ten years time combined with a prohibit of trafficking. The

fragility is brought back to its current level. The shift in the curves up to t=60 years is in this option only caused by compaction of the soil in the foundation. The last option is similar to an improvement in the form of a one meter top up in the current situation.

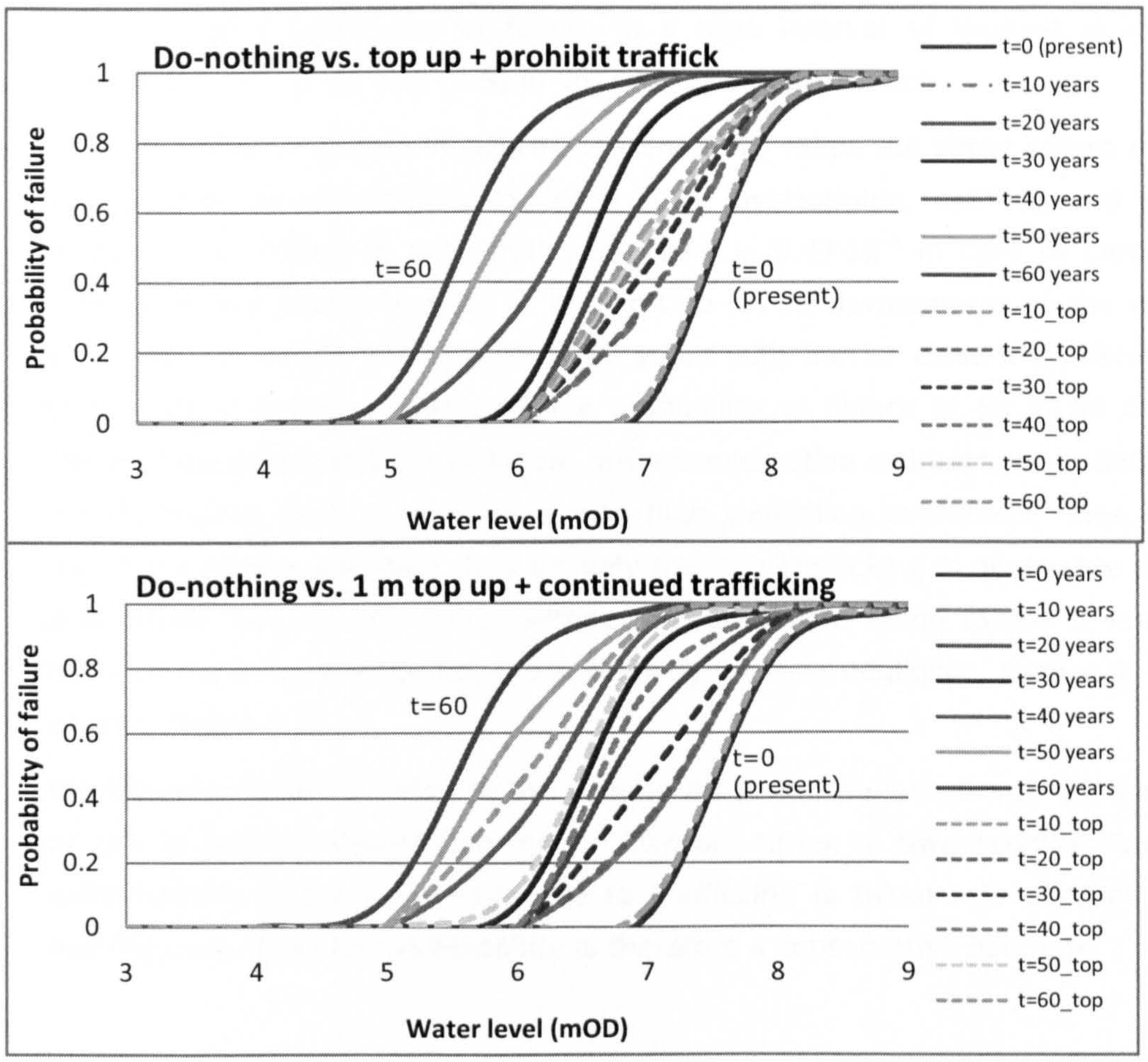

Figure 7.14 *Two examples of maintenance interventions compared to do-nothing time-dependent fragility. Top plot: topping up the crest level by one meter without taking measures against trafficking. Bottom plot: topping up the crest level by one meter and instating a prohibit on trafficking. The dotted lines refer to the time in years and fragility in case of topping up the crest level, e.g. t=10_top represents time is 10 years after topping up.*

7.3.8. Lifetime probability of failure for earth embankments

Figure 7.15 displays the annual probability of failure as a function of time for flood defence section 4 in case of Thames barrier closure during all the tides and in case

there is no barrier closure during any of the high tides. The location of the Thames barrier at Greenwich is indicated in figure 7.1. Appendix E provides flowcharts for the simulations of asset time-dependent processes and their incorporation in time-dependent fragility and probability of failure in a time interval of interest. The relevance of a probability of failure in a time interval of interest is indicated by equations (3.7), (3.8) and (3.9) in life cycle cost optimisation.

The probability of failure in figure 7.15 and 7.16 takes the same failure mechanisms into account as the fragility in figure 7.13: overtopping, uplifting and piping. The probability of failure in the coming 50 years is $0.47 \cdot 10^{-3}$ in case of barrier closure. Closure of the barrier results in higher tide levels downstream of the barrier. The probability of failure in the coming 50 years with barrier closure is therefore higher than without barrier closure, with a probability of failure in 50 years of $0.47 \cdot 10^{-4}$. These lifetime probabilities of failure are a conservative estimate, as in both situations the do-nothing case is considered with high trafficking settlement rates. As pointed out in the previous section, it is unlikely that the trafficking is allowed to damage the crest levels beyond one meter without any measures being taken. If measures are taken in the form of a top up, the probability remains negligible, similar to the first 40 years in figure 7.15.

The lifetime reliability index in the coming 80 years, derived from equation (2.22) or (2.27), is given in figure 7.16 for the Dartford Creek to Swanscombe Marshes earth embankment sections. Damage due to trafficking is taken into account in the do-nothing case. The lifetime reliability is therefore a conservative estimate.

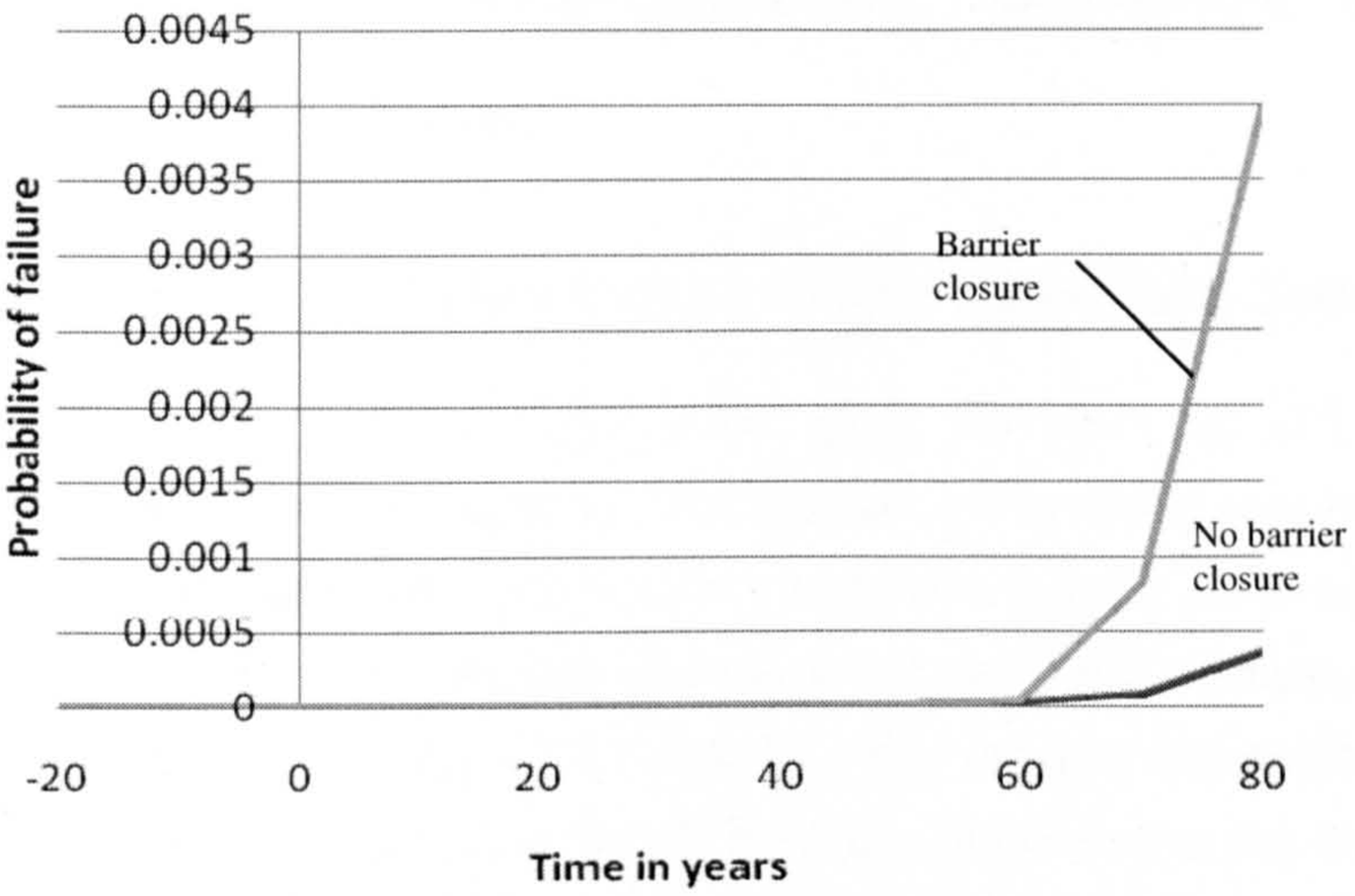

Figure 7.15 *The do-nothing probability of failure as a function of time for flood defence section 4, in case of closure of the Thames barrier at Greenwich (figure 7.1) or no barrier closure.*

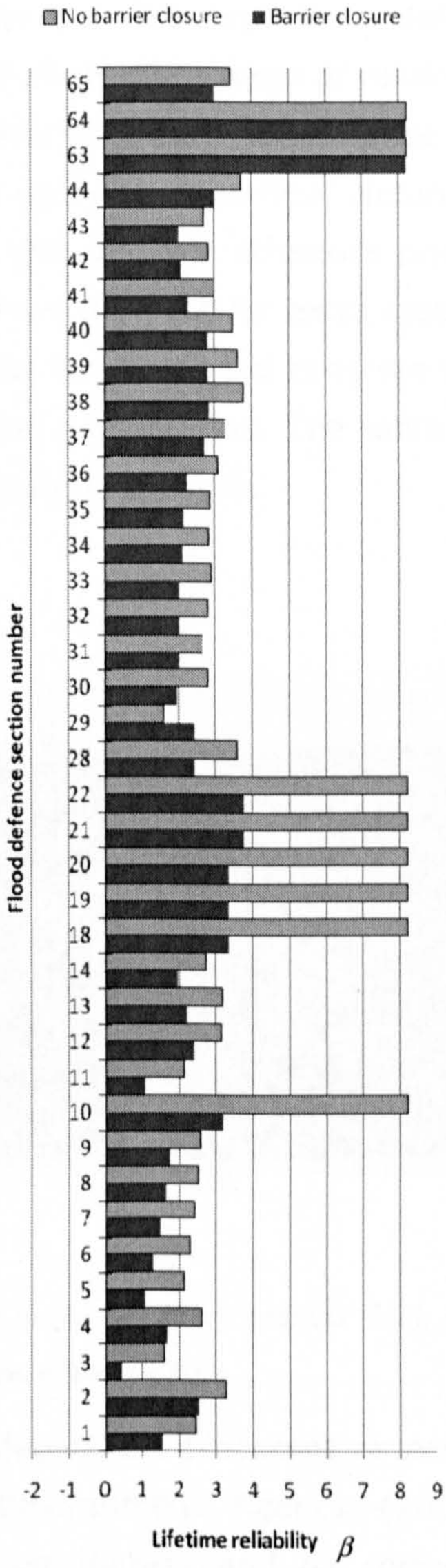

Figure 7.16 *Lifetime reliability index for the earth embankment flood defence sections*

7.4. Time-dependent reliability of reinforced concrete walls

7.4.1. Description of the structure type

The concrete walls were built as part of the Thames Estuary flood defence improvements in the '70s and '80s. There are a number of different types of reinforced concrete walls along the Dartford Creek to Swanscombe Marshes flood defence line. The three types considered in the reliability analysis as well as a superficial picture are shown in figure 7.17. Sheet piles applied underneath the concrete structure prevent seepage/piping or in some cases mobilise the soil between the piles for extra stability. Table 7.12 contains an overview of the failure processes for reinforced concrete walls along the Dartford Creek to Swanscombe Marshes flood defence line. The table also indicates the failure mechanisms incorporated in the reliability analysis.

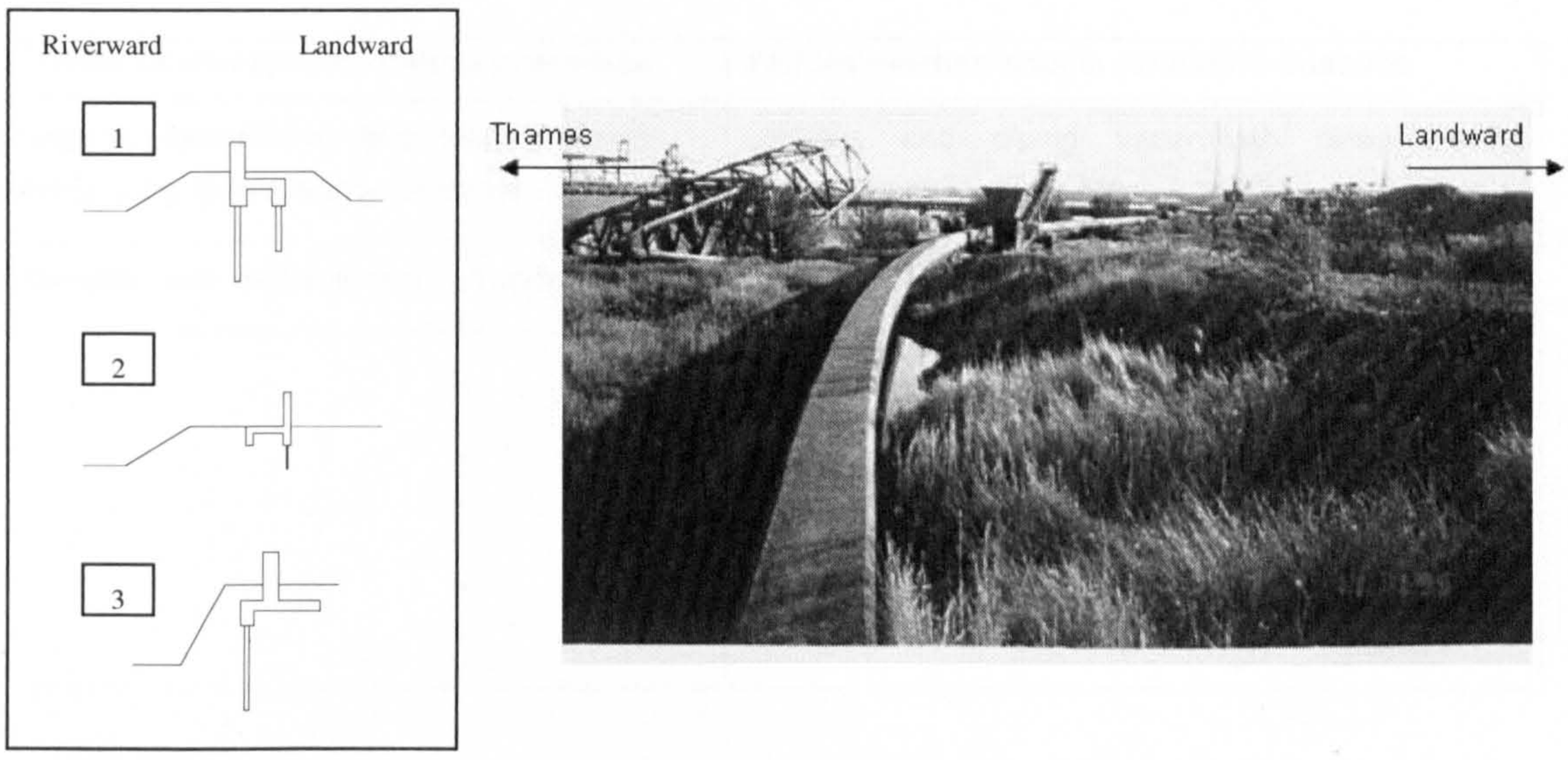

Figure 7.17 The three reinforced concrete wall types implemented in the reliability analysis (left), a picture of reinforced concrete walls along the flood defence line (right).

Commonly considered concrete material related time-dependent processes associated with reinforced concrete walls are for example, Environment Agency (2004b), Concrete society (1995), BRE (2000 & 2001): chloride ingress and pit corrosion, carbonation and (pit) corrosion possibly in combination with sulphate attack, freeze-thaw deterioration or alkali-silica attack. Other time-dependent processes of reinforced

concrete walls are: abrasion of concrete material, deterioration of joint material between concrete units, toe erosion or leakage underneath the concrete wall.

This research project is restricted to carbonation and reinforcement corrosion as it is a time-dependent process for which a process model is available and expected to occur at the case study site. Chloride ingress is unlikely as the Dartford Creek to Swanscombe Marshes flood defence system is quite upstream in the estuary, even though the water levels are driven by tidal discharges rather than fluvial discharges. Other concrete material related processes either have a very site specific nature or are not captured by process models. Similar constraints apply to the other time-dependent processes which are mentioned above.

The primary function of the concrete walls along the Dartford Creek to Swanscombe Marshes flood defence line is protecting against flooding by retaining water. In most cases the concrete wall is combined with a larger earth embankment structure.

Table 7.12 Site specific failure processes and failure mechanisms implemented in the reliability analysis

Overview of site specific failure processes	**Failure mechanisms in reliability analysis**
Damage by residential developments: concrete cracking, joint failure and settlements	Uplifting and piping underneath overall earth embankment (only for types 1 and 2)
Carbonation and reinforcement corrosion	Sliding of the concrete wall
	Overturning of the concrete wall
	Reinforcement failure in the vertical concrete slab
	Shear failure in the vertical concrete slab
	Piping directly underneath concrete / sheet pile toe

7.4.2. Fault tree, failure mechanisms and limit state equations

Failure, or the top event in the fault tree, is defined here if the reinforced concrete wall structurally fails and flooding occurs. Excessive overtopping discharges which cause damage are not considered in this study. It is additionally noted that the Dartford Creek to Swanscombe Marshes reinforced concrete walls are part of a larger earth embankment structure. Structural failure of the concrete wall alone may not in all cases lead to a full breach.

Figure 7.18 illustrates the fault tree implemented for concrete walls along the Dartford Creek to Swanscombe Marshes flood defence line. Failure mechanisms are the chains of events leading up to the top event, see definitions in section 2.1.2. The accompanying limit state equations are provided in appendix B.

Fault tree

Figure 7.18 contains the simplified fault tree for reinforced concrete walls. This fault tree is applicable to each of the three types of concrete walls. The selection of failure mechanisms and the formulation of the limit state equations may differ among the types.

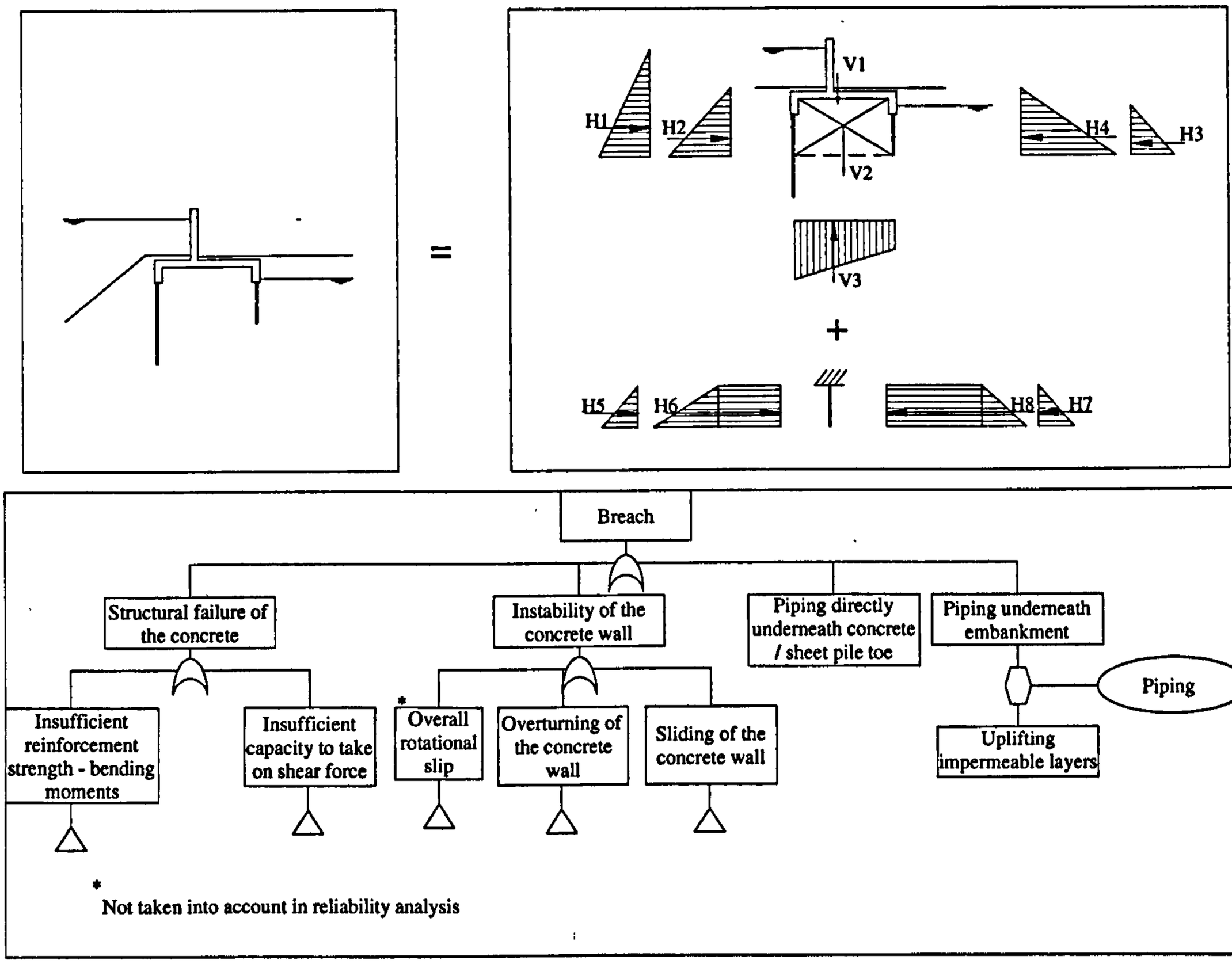

Figure 7.18 *Simplified fault tree for reinforced concrete wall as applied in reliability analysis (top). Decomposition of concrete wall in case of mobilised foundational soil (bottom). The horizontal grain forces on the main structure are active and passive on respectively the river- and landside. The horizontal grain forces on the sheet pile wall extension are active and passive on respectively the land- and riverside.*

Description of the failure mechanisms

Table 7.12 indicates the failure mechanisms which are taken into account in the reliability analysis in the form of limit state equations. The descriptions below include two extra failure mechanisms: (wave) overtopping followed by erosion and overall rotational instability.

(Wave) overtopping followed by erosion has not been incorporated for these concrete walls. Firstly, the concrete walls are part of a very wide earth structure which is extensively protected by asphalt / concrete pavements or roads. Secondly, the nature of the failure mechanism is different from that applied to earth embankments: the erosion process undercuts the foundation of the concrete wall leading to instability. Appropriate representation requires further investigation.

Uplifting and piping underneath the earth embankment is more appropriate at some locations than at others. For example along the frontage at Greenhithe the failure mechanisms are not incorporated. The frontage of the village of Greenhithe can be considered as high ground. However, at other locations the concrete wall forms part of a wider earth embankment and is the combination of uplifting and piping relevant.

Sliding of the reinforced concrete wall is relevant if the water level or wave impact exert horizontal pressures on the concrete wall. These forces can initiate sliding of the concrete structure. Resisting forces are the weight of the structure and the pressures of the ground keeping the structure into place.

Overturning of the concrete wall is relevant if the water level or wave impact exert horizontal pressures on the concrete wall. These forces can overturn the concrete structure. Resisting forces are the weight of the structure and the pressures of the ground keeping the structure in place.

Overall rotational instability of the concrete wall can become relevant under horizontal pressures due to wave impact or the water level. These forces exert a destabilising force against the concrete structure. Depending on the geotechnical properties of the foundational soil and the pore pressures, an overall slip circle can initiate, leading to instability of the wall. As a simplified analysis Bishop's slip circle analysis can be used to estimate a factor of safety. Intersection of simulated slip circles with one of the sheet pile cut-off / concrete extensions should be avoided and therefore poses a minimum restraint on the radii of the slip circles. Given the time-consuming nature, these calculations are not carried out.

Failure of vertical concrete slab due to bending moments is relevant under horizontal pressures due to a water level, wave impact and the active and passive ground pressures. The concrete structure consists of units of a length of for instance 10 meter long, sealed by joints. These joints are not designed to transfer forces between the blocks of concrete structure. The vertical slabs are therefore only supported by the foundational slab of the structure. The bending moment for which the reinforcement should be designed is then present at the base of the vertical slab. See figure 7.19. Failure of the vertical slab occurs when there is insufficient reinforcement to take on the tensile stress due to the bending moment.

Failure of the vertical concrete slab due to shear stress is relevant under horizontal pressures due to a water level, wave impact and the active and passive ground pressures. The concrete structure consists of units of a length of for instance 10 meter long, sealed by joints. These joints are not designed to transfer forces between the blocks of concrete structure. The vertical slabs are therefore only supported by the foundational slab of the structure. The horizontal force is therefore transferred at the base of the vertical slab. See figure 7.19.

Failure of the vertical slab occurs if the concrete cross section has insufficient width or shear strength to take on the horizontal force. Concrete slabs are usually not

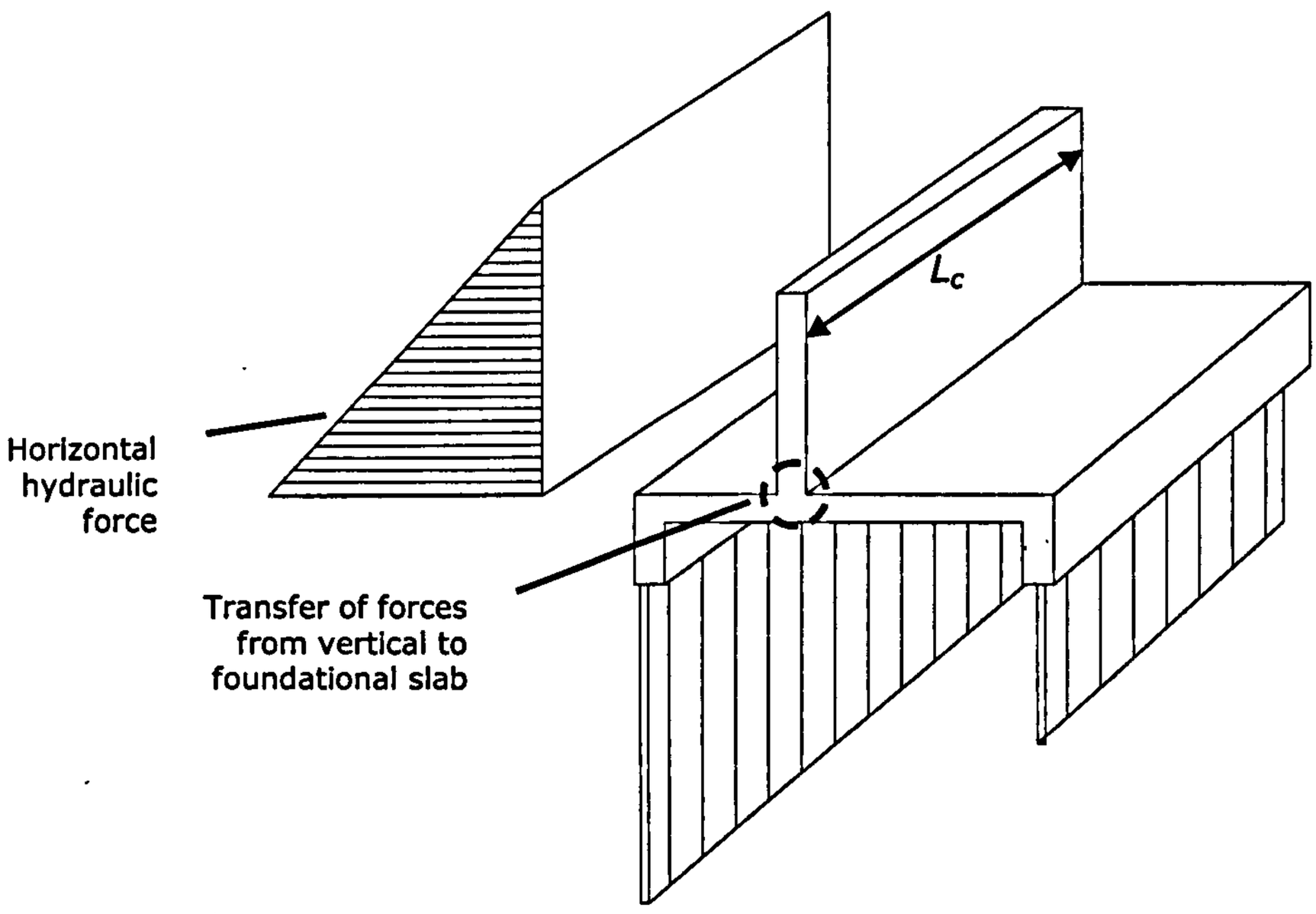

Figure 7.19 One unit of concrete wall structure indicating location of transfer of forces between vertical slab to foundational concrete slab.

equipped with reinforcement for shear stress, that is confirmed by technical drawings of the Dartford Creek to Swanscombe Marshes concrete walls.

Failure due to piping directly underneath the sheet pile cut-off is taken into account if the water level exceeds the ground water level in the earth bank behind the wall. This ensures a positive water head over the concrete structure, which drives the piping process. One of the requirements is that the water level persists long enough for the piping process to initiate. In this context two issues are worth noting. Firstly, the local water levels in this study represent the high water level during a storm. It depends per storm or surge situation how long such a high water level prolongs. Secondly, whether or not the piping process initiates depends amongst other factors on the permeability of the soil / the presence of permeable strata underneath the concrete or sheet pile toe. This is currently not taken into account in the model.

7.4.3. Importance measures for reinforced concrete walls

The importance measures developed in section 4.3 are calculated for reinforced concrete walls along the Dartford Creek to Swanscombe Marshes flood defence line.

Indicate the influence of variables on the reliability

The influence of the variables on the reliability is indicated by the direction cosines (2.11) and the partial derivative based concept introduced in (4.11). These indicators are derived from the time invariant reliability analysis and are tabulated for flood defence section 26 in table 7.13, corresponding with concrete wall type 1 in figure 7.17. In the calculation of the direction cosines the influence of the wave impact model is not taken into account. Appendix C contains the statistical distribution functions of the random variables. The form in which the statistical distribution of the wave conditions is available is not suitable for this type of analysis. Still, the direction cosines provide insight in the sensitivity of the results to the flood defence properties in the strength model. The PD_X do not properly capture the sensitivity of the reliability to the wave conditions either. The local wave conditions are derived with a formula as a function of the fetch and the wind speed. It is clear from the influence of the wave obliquity β that the influence of wave impact on structural failure is high. See figure 7.20 for generic dimensions of the reinforced concrete walls. The asset time-dependent process of interest is carbonation of the concrete setting off reinforcement corrosion in the carbonated concrete. This process is assumed to mainly affect the

properties A_s, area of the reinforcement bars, and d_s, distance between the top of the concrete cross section and the heart of the reinforcement bars.

Table 7.13 The direction cosines α and the PD_X for the failure mechanisms of a reinforced concrete wall. Not all failure mechanisms are relevant at each location and water level. The indicators are specified for the flood defence sections: 26 and 48, given a water level of OD+6.5m.

		Direction cosines α					Partial derivative based PD_X				
		Reinforcement failure (csn 26)	Shear failure (csn 26)	Sliding failure (csn 26)	Overturning failure (csn 26)	Piping toe (csn 26)	Reinforcement failure (csn 26)	Shear failure (csn 26)	Sliding failure (csn 26)	Overturning failure (csn 26)	Piping toe (csn 26)
h	= Water level (mOD)	0	0	0	0	0	0	0	0.061	0.057	0.060
H_s	= Significant wave height (m)	0	0	-	-	-	0	0	-	-	-
T_p	= Peak wave period (s)	0	0	-	-	-	0	0	-	-	-
h_c	= Crest level (mOD)	0	0	0	0	-	0.049	0.026	0	0	-
β	= Wave obliquity (°)	0	0	-	-	-	0.9	0.96	-	-	-
l_l_1	= Transition between top level and 2nd strata (mOD)	0	0	0	0	-	0	0	0.004	0.006	-
l_l_2	= Transition between 2nd strata and 3rd strata (mOD)	0	0	0	0	-	0	0	0	0	-
γ_{s1}	= Saturated volumetric weight of top strata (kN/m³)	-0.001	0	0.027	0.073	-	0	0	0.357	0.176	-
γ_{s2}	= Saturated volumetric weight of 2nd strata (kN/m³)	0	0	0	0.002	-	0	0	0.001	0.007	-
γ_{d1}	= Dry volumetric weight of top strata (kN/m³)	0.009	0	0	0.014	-	0	0	0.012	0.025	-
K_a	= Active horizontal grain stress coeff. (-)	-0.001	0	0	-0.008	-	0	0	-0.016	-0.008	-
K_p	= Passive horizontal grain stress coeff. (-)	0.018	0	0	0.049	-	0	0	0.101	0.049	-
m_R	= Model uncertainty strength model (-)	0	0	0	0.6	0	0.000	0.001	0.076	0.064	0
m_S	= Model uncertainty loading model (-)	0	0	0	-0.6	0	-0.096	-0.102	-0.101	-0.158	0
γ_c	= Volumetric weight of concrete (kN/m³)	-	0	0.053	0.002	-	0	0	0.075	0.072	-
δ	= Friction angle (°)	-	-	0	-	-	-	-	0.109	-	-
$d1$	= Dimension concrete wall (m)	-	-	-0.034	0.001	0	-	-	0.036	-0.067	0
$d2$	= Dimension concrete wall (m)	-	-	0.011	-0.003	0	-	-	0.024	-0.028	0
$d3$	= Dimension concrete wall (m)	-	-	0.014	0	0	-	-	0.000	0.000	0
$d4$	= Dimension concrete wall (m)	0	0	0.014	-0.004	-	0	0	0.020	-0.028	-
$d5$	= Dimension concrete wall (m)	0	0	0.006	0	0	0	0	0.015	0.014	0
$d6$	= Dimension concrete wall (m)	-	-	0.012	0.003	0	-	-	0.008	0.042	0
$d7$	= Dimension concrete wall (m)	-	-	0.012	0.002	-	-	-	0.008	0.027	-
$d8$	= Dimension concrete wall (m)	-	-	0.006	-0.003	-	-	-	0.008	-0.021	-
$d9$	= Dimension concrete wall (m)	-	-	-0.297	-0.001	0	-	-	0.008	-0.012	0
$L1$	= Riverward toe level (mOD)	-	-	0	0.312	-0.231	-	-	0.492	0.460	-0.169
$L3$	= Landward toe level (mOD)	-	-	0	-0.285	-0.231	-	-	-0.454	-0.427	-0.169
Lc	= Length of concrete wall unit (m)	-0.238	0	-0.302	0	-	-0.096	0	0	0	-
g_w	= Ground water level in floodplain (mOD)	0	0	0	-0.135	0.677	0	0	-0.064	-0.318	0.930
h_1	= Ground level floodplain side	0	0	0.901	0.068	0	0.401	0.220	0.310	0.118	0.000
h_2	= Top of horizontal concrete slab floodplain side (mOD)	0.95	0.547	0	0.265	0	0	0	0.227	0.574	0.000
h_3	= Ground level riverward side (mOD)	0.159	0	0	0.008	0.231	0	0	-0.014	0.005	0.169
A_s	= Area reinforcement (mm²)	0.063	0	-	-	-	0	0	-	-	-
f_s	= Yield stress reinforcement steel (N/mm²)	0.063	-	-	-	-	0	0	-	-	-
f_b'	= Cubic pressure strength concrete (N/mm²)	0.005	0	-	-	-	0	0	-	-	-
f_b	= Tensile strength concrete (N/mm²)	-	0.835	-	-	-	0	0.001	-	-	-
d_s	= Distance top of pressure zone concrete cross section to heart reinforcement (m)	0.064	0.037	-	-	-	0	0.101	-	-	-
ε_{bu}	= Limit strain concrete for breaking (-)	0	-	-	-	-	0	0	-	-	-
ε_b	= Plasticity strain concrete (-)	0	-	-	-	-	0	0	-	-	-
E_c	= Elasticity modulus (N/mm²)	0	-	-	-	-	0	0	-	-	-
L_h	= Seepage length around concrete structure (-)	-	-	-	-	0.085	-	-	-	-	0.029
c_T	= Terzaghi creep coefficient piping (-)	-	-	-	-	-0.102	-	-	-	-	-0.150
m_t	= Model uncertainty piping toe model	-	-	-	-	0.603	-	-	-	-	0.152

Table 7.13 shows that the sensitivity both in terms of α and PD_X is mainly to the wave impact loading. The most important flood defence properties as indicated by the direction cosines in the failure mechanism reinforcement failure are: the top of the horizontal concrete slab on landward side, h_2, the length of a concrete wall unit L_c, and the ground level at landward side, h_3. The PD_X indicate as relevant flood defence properties the wave obliquity, β, and the ground level in the floodplain, h_3. In failure

due to high shear stress in the concrete cross section the direction cosines indicate that the tensile stress, f_b, and the top of the horizontal concrete slab on the landward side, h_2, are relevant properties. The PD_X highlight the wave obliquity, β, and the ground level in the floodplain, h_3. The flood defence properties h_1, ground level at the riverside, and the length of the concrete wall unit, L_c, contribute most uncertainty to failure due to sliding of the reinforced concrete wall. The depth of the seepage screens, L_1 and L_3, the ground level in the floodplain, h_3, and the ground level in front of the concrete wall, h_1, have high PD_X indicators in this failure mechanism. It is noted that flood defence section 26 is a type 2 concrete wall according to figure 7.20.

The type of concrete wall determines whether or not a seepage screen is present at both toes. If not, either L_1 or L_3 represent the toe level of the concrete wall instead. In case of failure due to overturning of the reinforced concrete wall the direction cosines point out that the depth of the seepage screens L_1 and L_3 contribute most uncertainty. The PD_X point out that this failure mechanism is in addition sensitive to the depth of the seepage screens, L_1 and L_3, the ground level in the floodplain, h_3, and the ground level in front of the concrete wall, h_1. In case of failure due to piping directly underneath the concrete toe the largest direction cosine is associated with the groundwater level, g_w. The PD_X point out that this failure mechanism is mainly sensitive to the groundwater level, g_w.

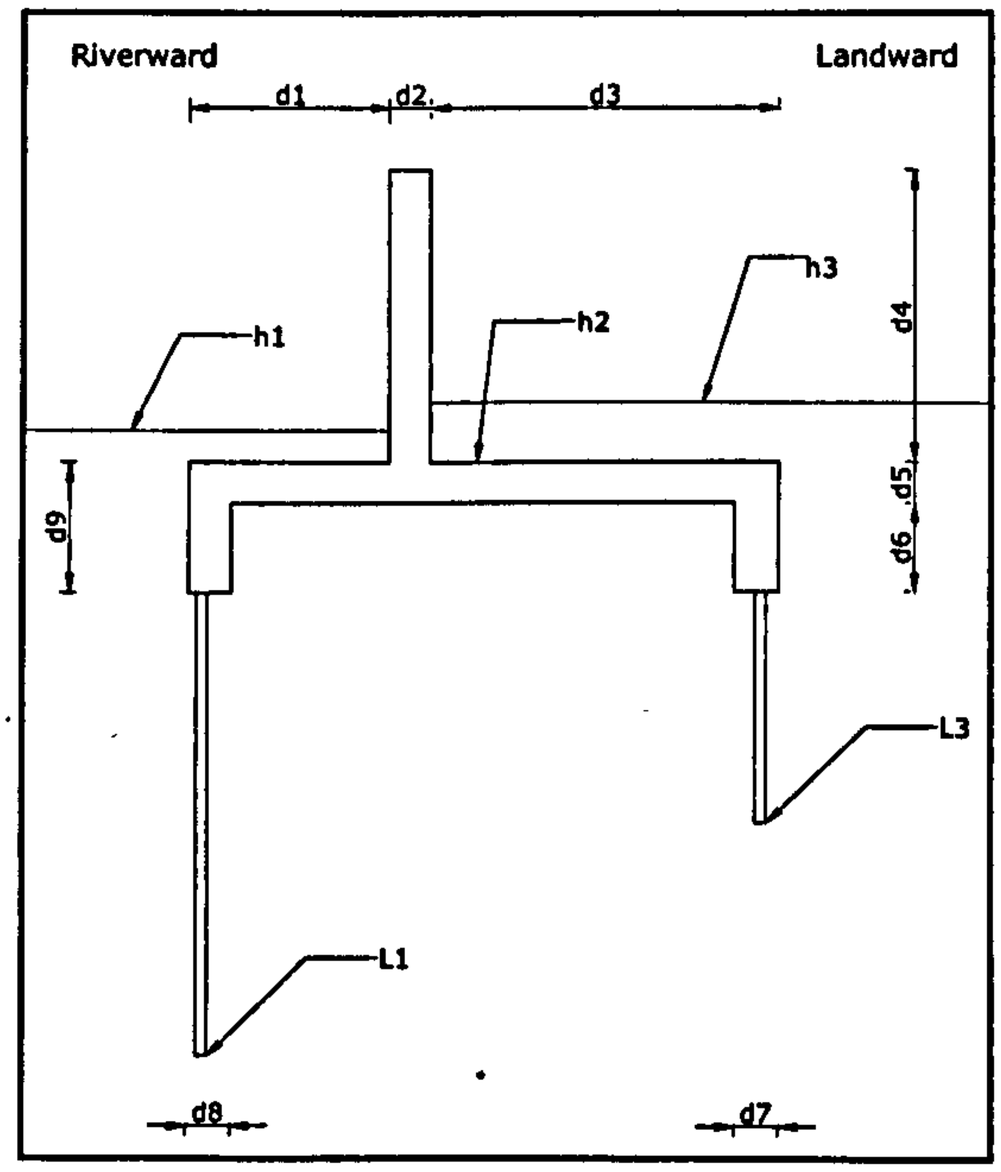

Figure 7.20 Generic dimensions of the concrete wall types.

Highlight time-dependent processes

The asset time-dependent processes in consideration are carbonation and the reinforcement corrosion set off by the carbonation. These asset time-dependent processes are coupled. A comparison of these processes is in this context irrelevant.

Indicate the flood risk reduction impact of operational activities

Three different types of operational activities are compared according to the importance measures developed in section 4.3.4. The first one is based on the assumption that section 16, a reinforced concrete wall type 1, is damaged by cracks over half the width of the vertical concrete slab. The cracks are present at several points along the approximately 140 meter long flood defence stretch. The operational activity is full repair of these cracks. The crack damage leads to an increased probability of failure due to bending moments. Reinforcement corrosion is increased due to cracking. The cost of repair is derived from Spon (2005). The probability of failure of the concrete wall is investigated around the design water level of about OD+7m at the original time of construction 30 years ago. The choice for the design water level is for the same reason as in section 7.3.3 in case of earth embankments.

The second operational activity is routine inspection specifically directed at statistical uncertainty reduction, i.e. changing the knowledge basis about the external dimensions of the reinforced concrete wall. The third operational activity is a specific inspection which increases the knowledge about some important internal properties, in addition to the knowledge about the external properties. It is noted that routine and specific inspection have other benefits such as monitoring time-dependent behaviour of condition levels and the discovery of failure mechanisms. Such benefits are not represented in table 7.14.

Table 7.14 Burden to risk Importance Ratios of three maintenance intervention options given OD+7 meter for flood defence section 26

Intervention options	Burden (£)	Change in flood risk (£)	BIR
Repair of cracks in concrete	1257	1027360	$1.2 \cdot 10^{-3}$
Routine inspection – statistical uncertainty	1515	210991	$7.2 \cdot 10^{-3}$
Specific inspection – statistical uncertainty	7534	205369	$3.7 \cdot 10^{-2}$

The Burden to risk Importance Ratios of the three maintenance intervention options mentioned above are listed in table 7.14. According to table 7.14 repair of cracks in the reinforced concrete wall is more beneficial than routine or specific inspection. It is noted that the comparison merely serves as an illustration. Not all benefits are reflected by the BIRs in the table. Routine inspection e.g. often provides information on a system scale rather than covering one flood defence stretch. Specific inspection is localised, but brings faults to the surface that might otherwise have remained unnoticed. More in general, the added benefit of reducing epistemic spatial uncertainty diminishes after a number of inspections.

7.4.4. Asset time-dependent process: carbonation and reinforcement corrosion

The modelling process in figure 6.2 is followed to define a statistical model for carbonation and reinforcement corrosion. Appendix E provides flowcharts for the simulations of asset time-dependent processes and their incorporation in time-dependent fragility and probability of failure in a time interval of interest.

Problem formulation and identification of existing knowledge

The task specification of the carbonation and reinforcement corrosion statistical model is to quantitatively express the carbonation and corrosion depth as a function of time. The task specification at an overarching maintenance level is to realistically represent the influence of the carbonation and reinforcement corrosion on the overarching performance indicators such as reliability, risk and life cycle cost.

Carbonation and reinforcement corrosion are commonly considered processes associated with concrete structures. According to The Concrete Society (2000) reinforcement corrosion due to carbonation or chloride ingress can be split into two parts. The initiation phase during which the carbonation or chloride ions ingress the concrete; and the propagation phase during which corrosion damages the reinforcement bars. Faber et al. (1999) consider chloride ingress in three phases. The first phase is the initiation phase during which the chloride ions penetrate the concrete. The second phase is the corrosion initiation phase which is demarked by a threshold of chloride concentration. The third phase is corrosion of the reinforcement bars. As mentioned before, chloride ingress is not taken into account in this analysis.

Carbonation is a process whereby the carbon dioxide in the environment reacts with the calcium hydroxide in the cement paste, The Concrete Society (2000). Calcium carbonate is a product of carbonation and lowers the pH to about 9. pH values lower than 10 cause the protective oxide layer around the reinforcement bars to break down. Without this protective oxide layer the reinforcement bars are susceptible to corrosion. The Concrete Society (2000) points out that the moisture content in the concrete is important to the development of the carbonation process. The moisture content needs to be sufficiently high for the carbonation reaction to occur, as the reaction of carbon dioxide and calcium hydroxide only occurs in solution. Carbonation in very dry concrete will therefore be slow. In saturated concrete, on the other hand, the moisture presents a barrier to the penetration of carbon dioxide and again carbonation will be slow. The most favourable condition for the carbonation reaction is when there is sufficient moisture for the reaction, but not enough to act as a barrier. This usually occurs when the concrete is in an environment with a relative humidity of 50 – 70% or in wetting and drying conditions. Quillin (2001) provides the following factors influencing the onset of carbonation-induced corrosion: depth of concrete cover, concrete mix design and materials, execution, curing time and conditions, exposure environment including relative humidity, atmospheric CO_2 concentration and the use of additional protection strategies such as coatings. Quillin (2001) suggests equation (7.13) below for the carbonation depth. This simplified equation is derived from experimental results, whilst Fick's 2nd law shows a similar dependence on time. A simplifying assumption underpinning this equation is for instance that the porosity, permeability and moisture content of the concrete and the atmospheric CO_2 concentration are constant over time (or can be represented by single values).

$$d_c = C_c t^{\frac{1}{2}} \tag{7.13}$$

In which d_c is the average carbonation depth in mm, t is the time in years and C_c is a rate determining constant determined by the permeability of the concrete (which is in turn dependent upon the mix design, curing conditions and level of workmanship), the buffering capacity of the cement and the atmospheric concentration of CO_2.

Equation (7.13) can be used to estimate the remaining character of the carbonation process for existing structures based on measured carbonation depths. However, there are problems in relating carbonation depth to either the type of cement and mix design, or to measurable properties of the concrete at early ages. As an indication for

C_c the table given in Holický (2000) can be used. This table for the coefficient C_c is based on a large number of samples. The reaction involved with corrosion is defined as follows, Quillin (2001):

Anodic reaction: $Fe \rightarrow Fe^{2-} + 2e^-$

Cathodic reaction: $H_2O + \frac{1}{2} O_2 + 2e^- \rightarrow 2OH^-$

The corrosion reaction is therefore enabled both by the availability of oxygen and by the presence of moisture on the surface of the reinforcement or in the adjacent concrete. The corrosion reaction takes place fairly uniformly over the length of the reinforcement bars, though severe localised corrosion can occur on isolated bars with low cover. This contrasts with the corrosion in the presence of chloride ions, which is characterised by local, rapidly corroding areas of bars. A consequence of corrosion additional to damage to the reinforcement bars is the onset of concrete cracking. Steel corrosion ('rust') usually occupies a much larger volume than the uncorroded steel and results in bursting stresses that can cause cracking and spalling of the concrete cover. These cracks bring the oxygen and water closer to the reinforcement and accelerate the corrosion. The understanding of corrosion of reinforcement in carbonated concrete is not far advanced. Edvardsen et al. (1999) provide the parameters in table 7.15 for different environment exposure classes.

Table 7.15 Parameters for corrosion rates of reinforcement in carbonated concrete, from Edvardsen et al. (1999)

Exposure classes		V_{corr} [µm/year]		W_t [-]	
		Mean	Stdv	Mean	Stdv
0	No risk of carbonation	0	-	0	-
Totally carbonated					
XC1	Dry	0	-	0	-
XC2	Wet, rarely dry (unsheltered)	4	3	1	-
XC3	Moderate humidity (sheltered)	2	1	0.5	
XC4	Cyclic wet-dry (unsheltered)	5	3	0.75	
Chloride-induced corrosion					
XD1	Wet rarely dry	4	3	1	
XD2	Cyclic wet-dry	30	20	0.75	
XS1	Airborne sea water	30	20	0.5	
XS2	Submerged	Not expected except bad concrete / low cover			
XS3	Tidal zone	70	40	1	

Excitation, ancillary and affected features

Table 7.16 presents the excitation, ancillary and affected features associated with carbonation and reinforcement corrosion.

Table 7.16 Excitation, ancillary and affected features for the carbonation and reinforcement corrosion asset time-dependent process

Excitation features	**Uncertainty**
Carbonation:	
The atmospheric CO_2 concentration in the exposure environment which drives the diffusion of CO_2 into the concrete.	Inherent uncertainty in time in the form of seasonality and daily fluctuations. Inherent uncertainty in space.
The presence of moisture allowing the carbonation to take place in solution, yet not too much as to block the CO_2 from ingressing. The presence of moisture depends on the relative humidity in the exposure environment.	Inherent uncertainty in time in the form of seasonality and daily fluctuations. Inherent uncertainty in space.
Reinforcement corrosion:	
Carbonation that breaks down the protective oxide layer around the reinforcement bars.	Inherent uncertainty in time in the form of the stochastic process of carbonation. Inherent uncertainty in space.
The presence of oxygen and water near the reinforcement bars.	Inherent uncertainty in time in the form of seasonality and daily fluctuations. Inherent uncertainty in space.
Ancillary features	**Uncertainty**
Carbonation	
Depth of concrete cover	Inherent uncertainty in space.
Concrete mix design and materials	Inherent uncertainty in space.
Execution of the concrete, determines the concentration of CO_2 in the concrete in advance	Inherent uncertainty in space.
Curing time and conditions	Inherent uncertainty in space and time.
The use of additional protection strategies such as coatings	Inherent uncertainty in space.
Reinforcement corrosion	
The size of the reinforcement bars	Inherent uncertainty in space.
The resistivity of the concrete, which depends on the moisture content in the concrete. The more moisture, the less the resistivity and the higher the corrosion current. However, the presence of too much moisture blocks the oxygen from the reinforcement bars and stops the corrosion reaction.	Inherent uncertainty in space and time.
The temperature	Inherent uncertainty in space and time
The presence of cracks providing easier access for oxygen and water to the reinforcement bars	Inherent uncertainty in space and in time as the cracks grow or increase due to corrosion
Affected features	**Uncertainty**
The effective width of the concrete cross section, expressed in the distance between the top of the concrete slab and the heart of the reinforcement d_s	Inherent uncertainty in time and space
Reinforcement bar, expressed in reinforcement area, A_s	Inherent uncertainty in time and space

Character of the asset time-dependent process

The character of the carbonation as an asset time-dependent process is described as follows. The diffusion of CO_2 and the presence of water start off a continuous chemical reaction. However, the concentration CO_2 at the surface and the presence of water are determined by the environment and therefore subject to dry – wet cycles and seasonal effects. Several models are available to predict the development of the carbonation depth. Equation (7.13) provides the simplest model, proportional to a square root relationship with time.

The character of reinforcement corrosion as an asset time-dependent process is described as follows. The chemical reaction leading to corrosion is continuous and depends on the presence of oxygen and water. The presence of the latter two depends on the exposure to the environment. Corrosion is therefore subject to dry-wet cycles and seasonal effects.

Dependencies between asset time-dependent processes

Carbonation breaks down the protective oxide layer at the surface of the reinforcement bars. After this protective layer has been broken down, the corrosion process starts. Carbonation therefore forms the excitation of the corrosion process. The assumption is that once the carbonation frontier has reached the reinforcement bars, the corrosion process initiates.

Development of alternative statistical models

The parametric process model of carbonation corresponds with the conventional carbonation model in equation (7.13). The comparison of C_c values among different tests shows a large variation. This large variation is a combination of model uncertainty, inherent uncertainty in time and inherent uncertainty in space. C_c is a variable with a variation which equals that found among the different tests. This variation is then meant to represent all three sources of uncertainties (model, time and space). It is actually inappropriate to represent inherent uncertainties in time in such a manner, unless the influence of this uncertainty is negligible.

In the hierarchical process model the uncertainties are introduced to express these different sources of uncertainty more transparently, after Vrouwenvelder (2005):

$$d_c = m \cdot C_c t^p = (m_1 + m_2 + m_3) \cdot C_c t^p \quad (7.14)$$

In which m_1 is a constant model uncertainty, m_2 is a model uncertainty capturing seasonality, m_3 is a model uncertainty covering the environmental fluctuations, C_c is the carbonation coefficient and p is the power. Two different types of model approaches are considered. One approach, referred to with "carb_hier_base" and "rcor_hier_base", applies m_1 as a model uncertainty in the form of a wave renewal model, m_2 as short term fluctuations and C_c to capture the inherent uncertainty in space. The second approach, referred to with "carb_hier_coeff" and "rcor_hier_coeff", assumes that the variation measured in C_c reflects both seasonality and spatial variation. C_c is then modelled with a wave renewal model and with the model uncertainty m_3 to cover the environmental fluctuations. The choice for one of these two approaches depends on the available measurements underpinning the carbonation coefficient. If these measurements contain mainly spatial uncertainties then the first model is applicable

The gamma process model represents the carbonation and the corrosion rate according to (7.5). Time-independent model uncertainties and inherent variations in space are therefore not separated and dealt with separately. For carbonation the mean value μ and standard deviation σ are expressed as suggested by Van Noortwijk & Klatter (1999):

$$\mu = a_{carb} t^b \quad (7.15)$$

$$\sigma^2 = \theta_{carb} a_{carb} t^b \quad (7.16)$$

With $a_{carb}=C_c$ and $b=0.5$, and in which θ_{carb} is a coefficient expressing the uncertainty in the $a_{carb}t^b$ model.

The parametric process model for reinforcement corrosion is a function of a random variable for the corrosion rate and a deterministic time t.

The hierarchical process model of the reinforcement corrosion rate applies a model uncertainty to capture seasonality in the moisture in the concrete adjacent to the reinforcement.

The corrosion rate and its standard deviation are applied in a linear gamma process model such as (7.5).

Estimation, calibration and corroboration

The prior distributions of the variables in the hierarchical process, equations (7.14) to (7.16), and the mean value and standard deviation are tabulated in table 7.17. The prior distribution of C_c is estimated based on Holický (2000). The corrosion rate of the reinforcement is taken from table 7.10.

Table 7.17 Prior distributions of the random variables in the carbonation and reinforcement hierarchical process model and the gamma process model.

Symbol		Description	Unit	"carb_hier_base" and "rcor_hier_base"				"carb_hier_coeff" and "rcor_hier_coeff"			
				Dist.	μ	σ	V	Dist.	μ	σ	V
m_1	=	Constant model uncertainty in carbonation	-	LN	1	-	0.05	-	-	-	-
m_2	=	Model uncertainty capturing seasonality in carbonation	-	WR 0.25	0	0.1	-	-	-	-	-
m_3	=	Model uncertainty capturing environmental fluctuations in carbonation	-	BM	0	0.1	-	BM	0	0.1	-
C_c	=	Carbonation coefficient	mm/ year	LN	6	1.14	-	WR 0.25	6	1.14	-
p	=	Power in the carbonation equation	-	LN	0.5	-	0.05	LN	0.5	-	0.05
a_{carb}	=	Coefficient in gamma process model	$mm/year^{0.5}$	Ga	6						
θ_{carb}	=	Coefficient expressing uncertainty	-	Ga	0.2						
$m_{1;r}$	=	Constant model uncertainty in corrosion rate	-	LN	1	0.05	-	LN	1	0.05	-
$m_{2;r}$	=	Model uncertainty capturing seasonality in corrosion rate	-	WR 0.25	0	0.1	-	WR 0.25	0	0.1	-
$m_{3;r}$	=	Model uncertainty capturing environmental fluctuations in corrosion rate	-	BM	0	0.1	-	BM	0	0.1	-
r_{cor}	=	Reinforcement corrosion rate	µm/ year	LN	5	3	-	LN	5	3	-
$r_{cor;gam}$	=	Reinforcement corrosion in gamma process model for a period of one year	µm	Ga	5	3	-				

N = Normal distribution function
LN = Lognormal distribution function
WR 0.25 = Wave Renewal model with constant intervals of 0.25 years, normally distributed
BM = Brownian Motion with constant renewal of one year
Ga = Parameter in gamma process model

Analysis

Some simulations of the time series samples for the hierarchical process model, the parametric process model and the gamma process model are displayed in figure 7.21. The bottom plot contains the development of the expectation and standard deviation

in time of the carbonation depth. As mentioned previously, the hierarchical process model is represented in two different forms. The first approach distributes the variability among a constant model uncertainty, a model uncertainty for seasonality, a model uncertainty for environmental fluctuations and a carbonation coefficient covering the spatial uncertainty. Series "carb_hier_base" and "rcor_hier_base" represent this model. The second approach distributes the variability over a model uncertainty for the environmental fluctuations and the carbonation coefficient, which captures both the variation in time due to seasonality and the variation in space.

There are no field measurements of the carbonation depth or reinforcement corrosion for the Dartford Creek to Swanscombe Marshes flood defence line. A quantitative quality assessment cannot be made at this point in time.

The two hierarchical model approaches illustrate the situations whereby the variability in the measurements of C_c is mainly attributed to spatial variations, indicated by suffix "_base", or to variability in time, indicated by suffix "_coeff". The development of the standard deviation in time and the time series samples in figure 7.21 shows that the ranking in the amount of variance in the carbonation depth is as follows: hierarchical model with time variability in model uncertainty ("carb_hier_base"), parametric process model ("carb_para"), hierarchical model with seasonality in C_c ("carb_hier_coeff") and gamma process model ("carb_gamma").

The variance in the carbonation depth model strongly influences the time of initiation of reinforcement corrosion and therefore increases the likelihood of corrosion damage. Figure 7.21 shows that at a carbonation depth of around 50mm, corresponding with the concrete cover, the corrosion time series samples are initiated. Choices about whether to attribute the variance in carbonation depth mainly to spatial uncertainty or variability in time therefore impact on the likelihood of corrosion of the reinforcement.

7.4.5. Time-dependent fragility for reinforced concrete walls

The time-dependent fragility therefore does not show a shift in time in these calculations. Reinforcement corrosion is set off by the carbonation process and therefore starts quite late in the lifetime of the concrete structure, see figure 7.21. The influence of reinforcement reduction on the fragility is negligible in the time scope considered in the calculations. Maintenance intervention options are therefore not

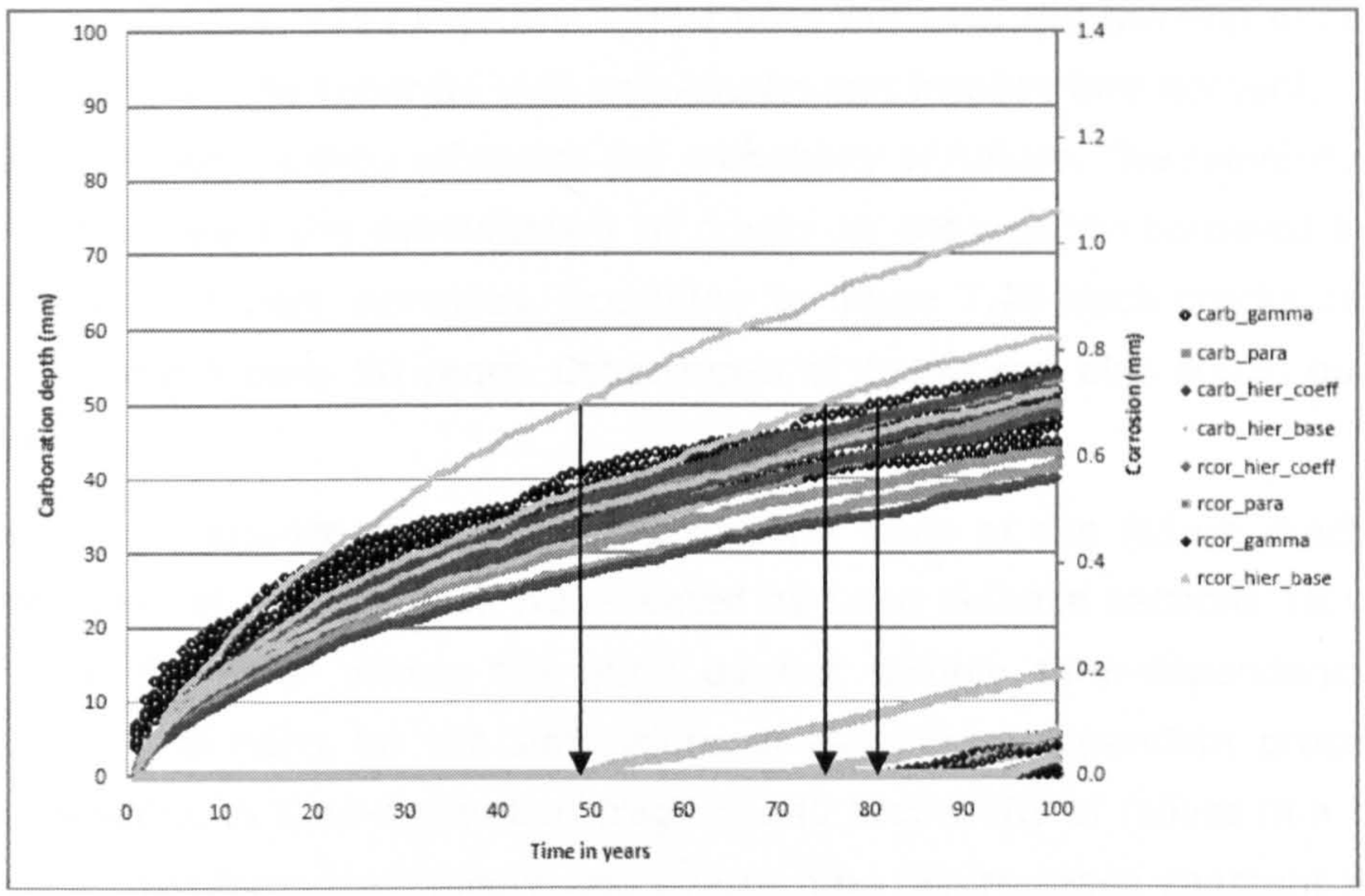

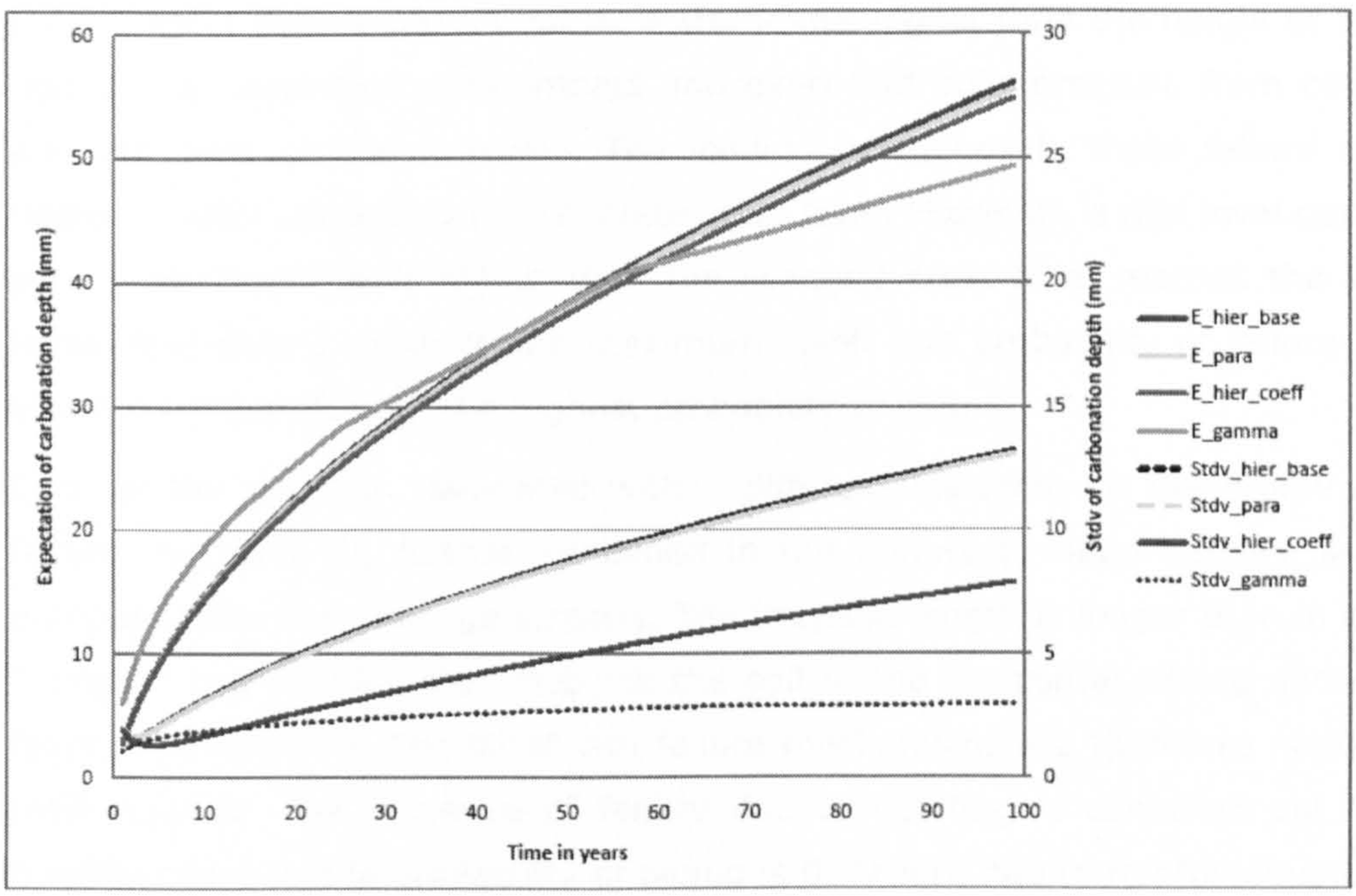

Figure 7.21 *Some time series samples of carbonation and reinforcement corrosion for the hierarchical process model – with seasonality in the model uncertainty ("carb_hier_base" and "rcor_hier_base") or in the carbonation coefficient ("carb_hier_coeff" and "rcor_hier_coeff") – for the parametric process model ("carb_para" and "rcor_para") and for the gamma process model ("carb_gamma" and "rcor_gamma").*

considered. It is noted that this model does not take the development and the effect of cracking on the concrete wall time-dependent fragility into account. The presence of cracks can significantly influence the probability of failure. The reinforcement corrosion process initiates the development of cracks as the volume occupied by the corroded reinforcement bars increases. According to figure 7.21 such cracks can be expected after approximately 50 years. Other types of cracks can also occur, due to e.g. shear force.

Figure 7.22 provides the fragility curves for each of the failure mechanisms of the three types of concrete wall represented by flood defence sections 16, 26 and 48. For reasons described above the plots do not display time-dependency. Appendix E provides flowcharts for the simulations of asset time-dependent processes and their incorporation in time-dependent fragility and probability of failure in a time interval of interest. Reinforcement failure and overturning failure reach constant levels for water levels higher than a certain value. Water levels higher than the height of the concrete wall do not introduce wave impact and exert hydraulic pressure from both the front and the back of the structure. The loading conditions in these failure mechanisms decrease after exceeding the concrete crest level. However, a tide level during a storm with a maximum level higher than the concrete crest level reaches the lower water levels first before rising to the maximum level. The probability of failure during that storm corresponds with the highest probability of failure.

Each of the types is associated with a different hierarchy in the prominence of the failure mechanisms, further explained in the following. Flood defence section 26 is equipped with two seepage screens. The seepage length is longer than in case of type 2 and 3. The screens also mobilise the soil in the horizontal sliding and overturning failure mechanisms. The latter two failure mechanisms are therefore negligible in the total fragility. The influence of failure due to uplifting is cancelled out in the total fragility curve as the probability of piping is 0. Failure due to reinforcement is for flood defence section 16 relatively higher than for section 48. The slope in front of section 48 is practically horizontal, whilst the slope in front of both section 16 and 26 is much steeper. The wave impact is higher in the latter two instances. The rest of the total fragility curve is governed by piping directly underneath the toe of the reinforced concrete wall. The condition for this failure mechanism is that the high tide event persists long enough for the piping process to develop.

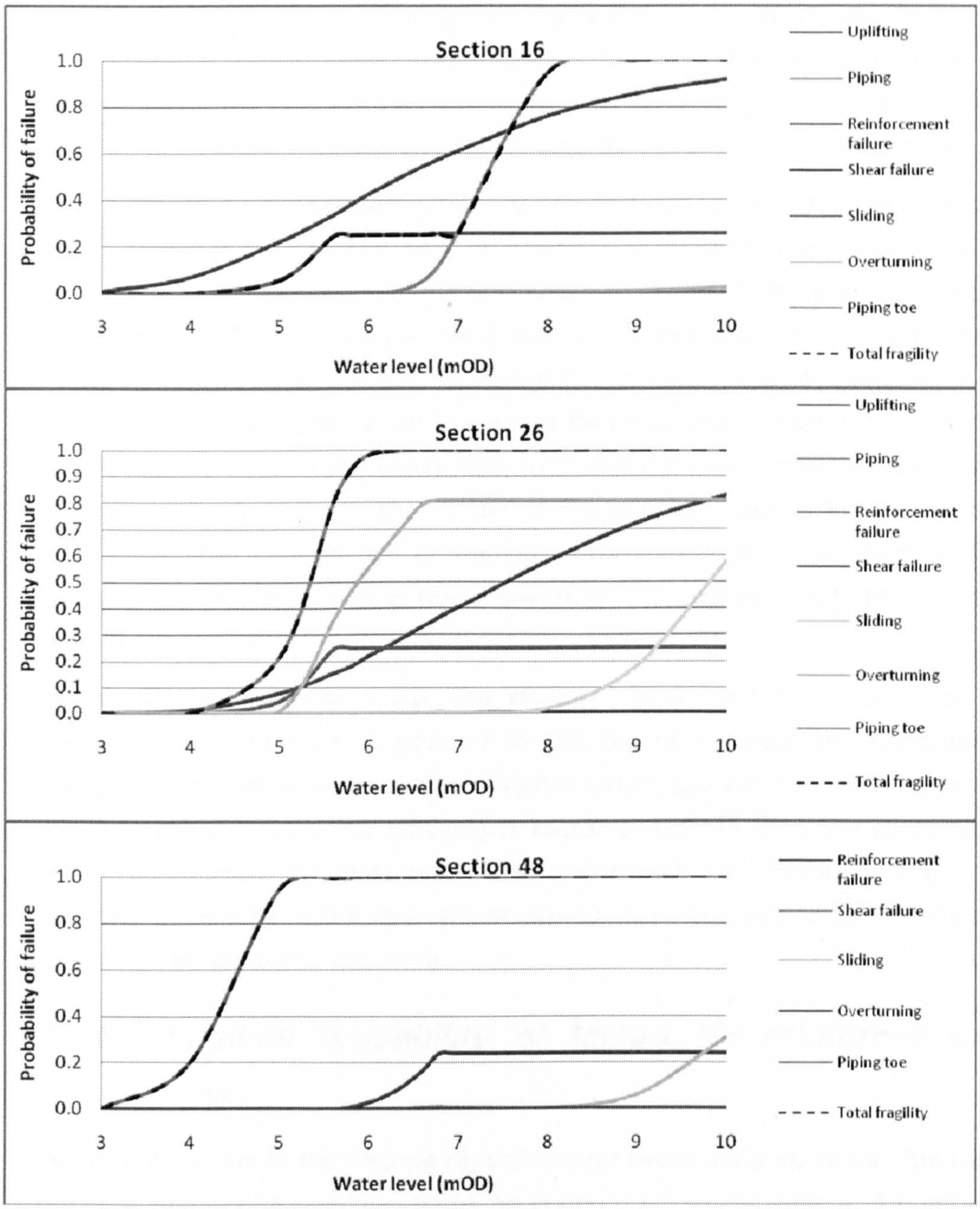

Figure 7.22 *The total fragility curve broken down into the individual failure mechanisms for the flood defence sections 16, 26 and 48.*

Flood defence section 26 is equipped with only one seepage screen. This type of structure is less stable than type 1, as the probability of failure of the mechanisms overturning and horizontal sliding appear on the plot. The probability of reinforcement failure is in the same order of magnitude as for flood defence section 16. These sections have a

similar slope in front of the structure. Failure due to piping underneath the toe is prominent in the total fragility curve. The shorter seepage length is the main cause for the prominence of this failure mechanism. The same condition as above applies, i.e. the high tide needs to persist sufficiently long for the piping process to develop.

Flood defence 48 is equipped with only one seepage screen, but the implementation depth is deeper than section 26. The structure is therefore more stabile than section 26, shown by the fact that overturning does not appear in the plot. The probability of sliding appears for very high water levels, and is driven by the hydraulic uplift force. However, at those water levels the economic damage due to overtopping is expected to prevail. The probability of reinforcement failure is smaller than in case of section 16 and 26, as the slope is practically horizontal and the wave impact smaller. Failure due to piping directly underneath the toe of the concrete wall is the prominent failure mechanism. The development of this failure mechanism starts at relatively low water levels as the ground level in at the riverward side is relatively lower than in case of the other two sections.

As mentioned in section 7.4.3, the effect of reinforcement corrosion on concrete cracking is not taken into account in the failure mechanisms. Corrosion on the reinforcement bars involves a larger reinforcement bar volume and introduces tensile stress in the concrete. The cracking is better detectable than the susceptibility of a reinforced concrete wall section to piping underneath the concrete wall toe. The latter is poorly detectable in the operational management and should be of concern during the design phase of the structure.

7.4.6. Lifetime probability of failure for reinforced concrete walls

Figure 7.23 presents the lifetime reliability over the coming 50 years. The locations of the flood defence sections can be found in figure A.1 in appendix A. A number of flood defence sections have a very low lifetime reliability. Appendix E provides flowcharts for the simulations of asset time-dependent processes and their incorporation in time-dependent fragility and probability of failure in a time interval of interest. The relevance of a probability of failure in a time interval of interest is indicated by equations (3.7), (3.8) and (3.9) in life cycle cost optimisation.

The low results are attributable to piping underneath the toe of the concrete structure or the wave impact model in structural failure. The persistence of the storm is not taken into account in the piping underneath the toe of the concrete wall failure mechanism. The wave impact model provides relatively high impact forces. A more detailed model will lead to a better represented lifetime reliability for the very weak flood defence sections. Even though the reliability model requires more refinement, figure 7.23 provides a useful basis for comparison of the different flood defence sections. The lifetime reliability and time-dependent fragility suggest that once the water level has reached the reinforced concrete wall the probability of failure is much higher than in case of earth embankments.

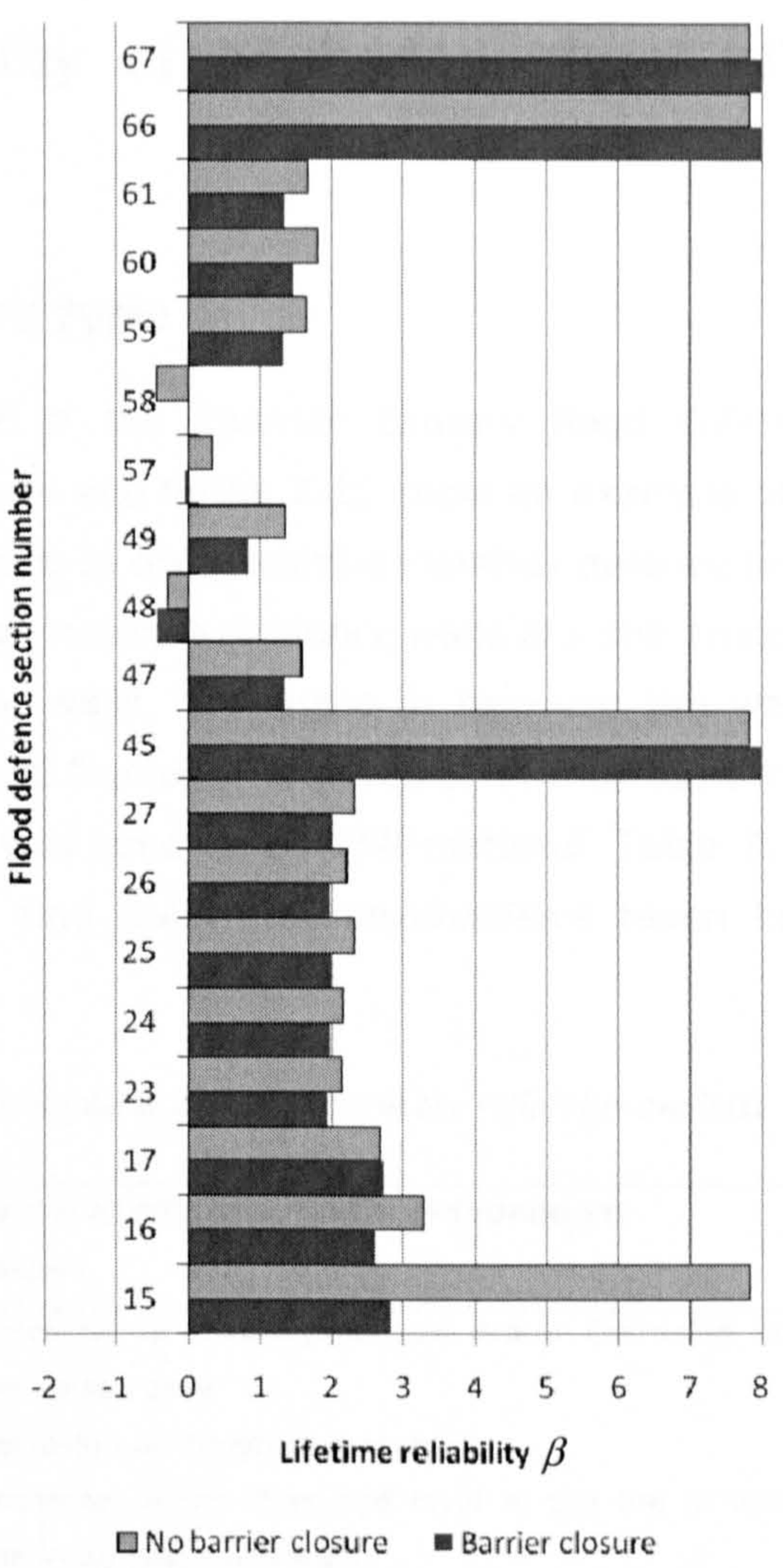

Figure 7.23 *Lifetime reliability of the reinforced concrete wall flood defence sections*

7.5. Time-dependent reliability of anchored sheet pile walls

7.5.1. Description of the structure type

Sheet pile walls were refurbished as part of the Thames Estuary flood defence improvements in the '70s and '80s. Figure 7.24 and figure 7.25 show an example of a sheet pile wall applied along the Dartford Creek to Swanscombe Marshes defence line. In some cases old frontages in the form of for instance masonry walls are still present in the ground behind the current sheet pile walls, the space in between the walls backfilled with concrete. In other cases, the old frontage was used to anchor the sheet pile walls or the rubble of the old frontage was used as backfill material. Table 7.18 presents the site specific failure processes and the failure mechanisms taken into account in the reliability analysis.

Table 7.18 Site specific failure processes and failure mechanisms implemented in the reliability analysis

Failure mechanisms in reliability analysis	**Overview of site specific time-dependent processes**
• Breaking of the ground anchor • Sliding of the ground anchor due to insufficient shear strength of the soil • Breaking of the sheet pile cross section • Rotational failure of the sheet pile after failure of the ground anchor	• Corrosion or Accelerated Low Water Corrosion in the splash zone • Corrosion of the ground anchors • Accretion of the river bed level at the toe of the anchored sheet pile wall.

At the time of the construction of the defence improvements, parts of the frontage between Dartford Creek and Swanscombe Marshes were docks. Because of the function as a dock, besides the typical sheet pile wall a large variation of sheet pile wall cross sections and combinations with concrete structures occur. By now, the frontages are not in use as docks anymore.

The primary function of the sheet pile walls along the Dartford Creek to Swanscombe Marshes flood defence line is retaining ground. Protection against overtopping is a secondary function as the sheet pile frontages border high grounds and rather fulfilled a role as part of dock frontages.

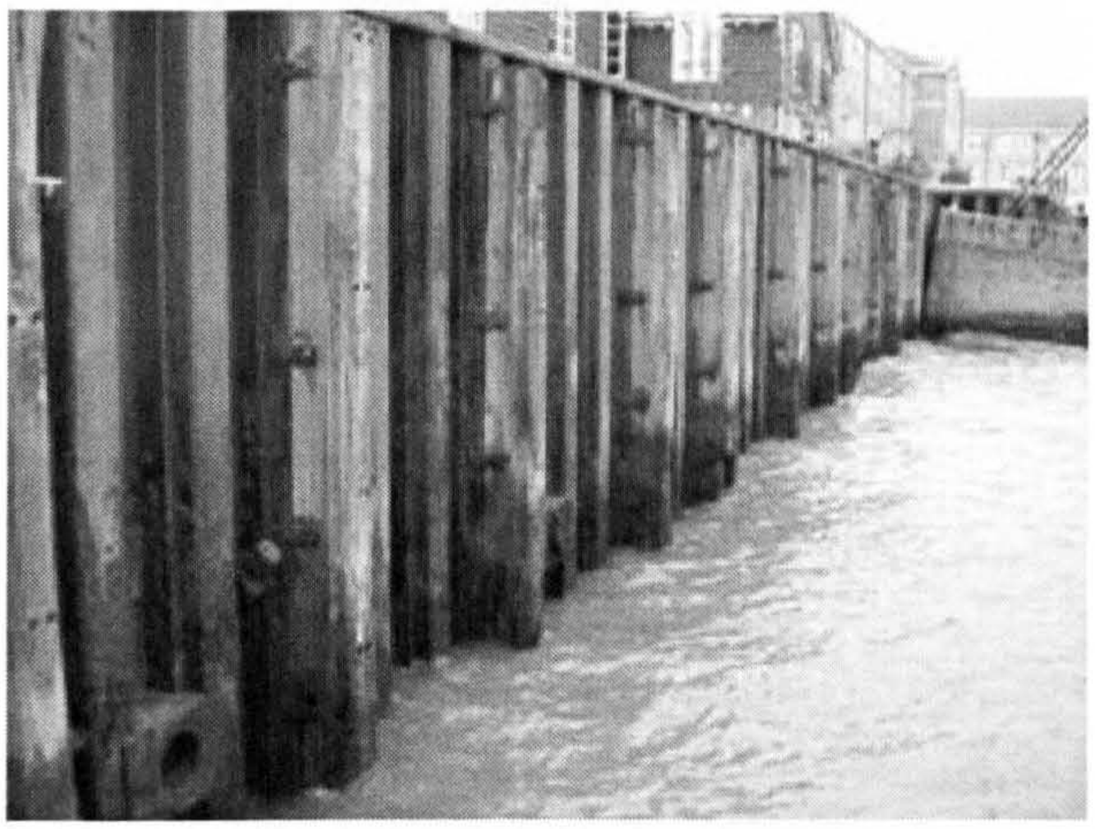

Figure 7.24 Example of a sheet pile wall along the Dartford Creek to Gravesend defence line. The corrosion appears clearly in the picture.

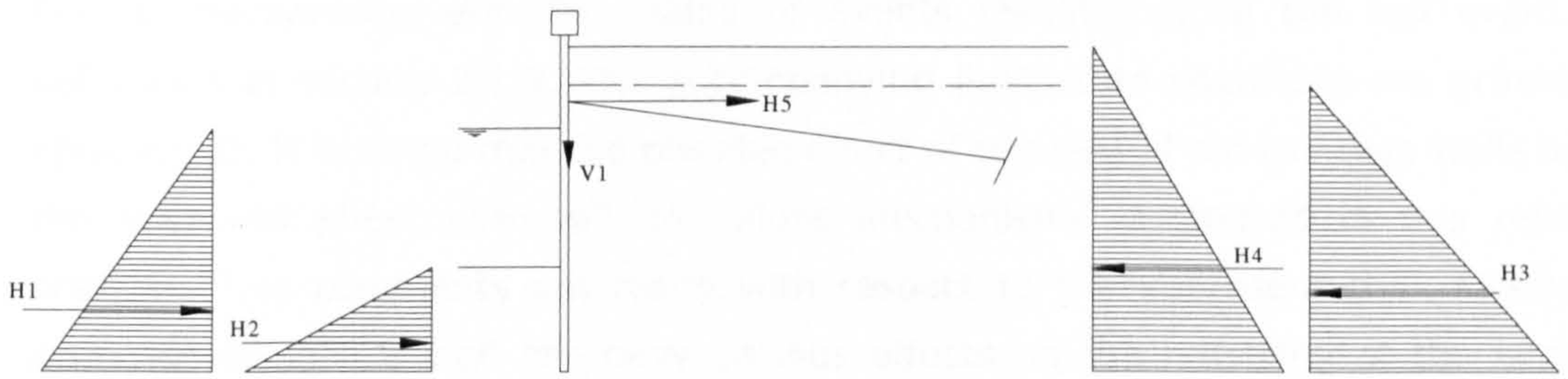

Figure 7.25 Representation of forces acting at anchored sheet pile structure. Passive pressures at the river toe of the sheet pile and active ground pressures on the landward side of the sheet pile.

7.5.2. Fault tree, failure mechanisms and limit state equations

Failure, or the top event in the fault tree, is here defined when the sheet pile wall structurally fails and therefore does not retain the ground it was designed to. The probability of failure is therefore not representative of the probability of breach. The latter is not applicable as the sheet pile walls protect high grounds. However, structural failure of the sheet pile walls does imply less protection against overtopping during high water events. Overtopping without structural failure leading to flooding is not considered in this reliability analysis.

Fault tree

Figure 7.26 illustrates the fault tree implemented for anchored sheet pile walls along the Dartford Creek to Swanscombe Marshes flood defence line.

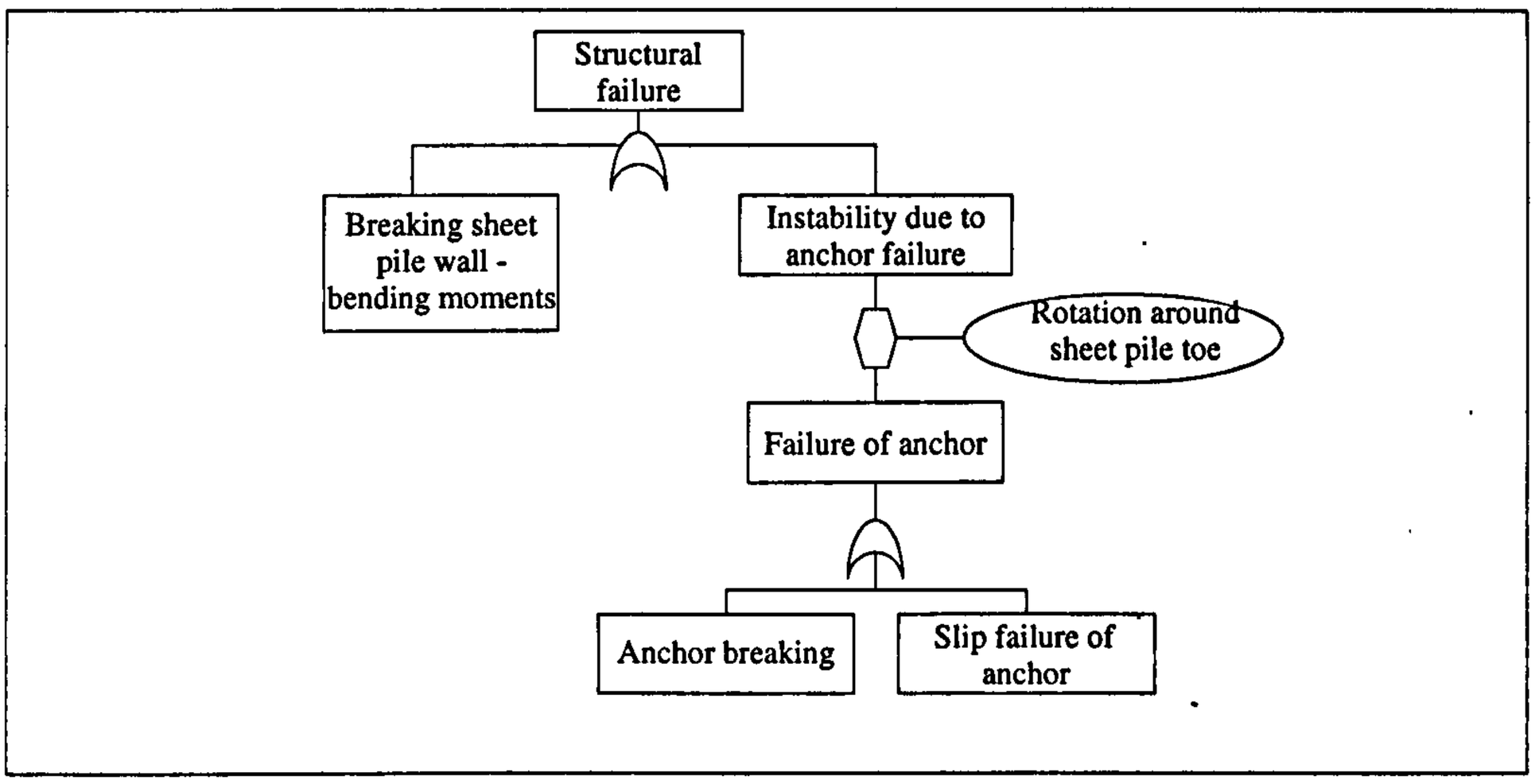

Figure 7.26 Simplified fault tree for anchored sheet pile wall as applied in reliability analysis

Failure mechanisms are the chains of events leading up to the top event, see definitions in section 2.1.2. The accompanying limit state equations are provided in appendix B. It is noted that the possible effect of remains of old frontage walls behind the anchored sheet pile wall on failure mechanisms is ignored in this reliability analysis. Two comments are made with respect to this representation. Firstly, the presence of such a wall can have various effects on the reliability of the anchored sheet pile wall. If the old wall e.g. still partly has a retaining function, it relieves the sheet pile wall. In other cases the old wall can introduce backfill pressures in the form of rubble. Secondly, in some cases old river frontages have been used to anchor the tie rod of the sheet pile wall. In such a case the failure mechanism of anchor failure due to insufficient shear strength in the soil is irrelevant.

Description of the failure mechanisms

Table 7.18 provides an overview of the failure mechanisms that are incorporated in the reliability analysis. The description of the failure mechanisms below contain two extra failure mechanisms: (wave) overtopping followed by erosion and overall rotational instability.

Overtopping followed by erosion has not been incorporated for these anchored sheet pile walls. The anchored sheet pile walls are per definition part of a very wide earth structure which provides support to the tie rod. These banks can usually be considered as high ground.

Breaking of sheet pile wall due to bending moments is a function of pressures exerted on the sheet pile wall by the ground that is retained, the groundwater, the river water level and the tie rod. Those pressures cause bending moments in the sheet pile wall. Failure occurs if the capacity of the sheet pile cross section is exceeded by the actually occurring bending moments. From the maximum occurring bending moment in the anchored sheet pile a maximum tensile stress in the sheet pile wall can be derived, using the moment of inertia and the height of the section. That maximum occurring tensile stress is compared against the tensile strength of the sheet pile steel.

Sliding of the anchor due to insufficient shear strength of the soil near the anchorhead in combination with rotational failure of the sheet pile wall leads to structural failure. Tie rods of the Dartford Creek to Gravesend anchored sheet pile walls are usually anchored in the soil using an anchor head. The anchor head transfers the force from the tie rod to the soil. Failure occurs if the stress exerted by the anchor head exceeds the shear strength of the soil. The shear strength of the soil depends on e.g. the depth of the anchor head, the size of the anchor head and the soiltype.

Breaking of the anchor due to insufficient strength of the tie rod in combination with rotational failure of the sheet pile wall leads to failure. The tie rod supports the sheet pile wall in taking on the forces. Failure of the tie rod occurs if the stress occurring in the tie rod exceeds the tensile strength of the steel. Corrosion can play a large role in reducing the tie rod cross section near the connection with the sheet pile wall.

Whether the sheet pile wall collapses after failure of the tie rod depends on the moment equilibrium around the toe of the sheet pile. Rotational failure occurs if the moments as a result of the ground and groundwater pressures are larger than those as a result of the ground and water level on the river side.

Overall rotational failure of the anchored sheet pile takes place if a slip circle occurs encapsulating both the anchor and the sheet pile. Bishop's slip circle method can be used to make an estimation of the factor of safety. The slip circles cannot intersect with the tie rod and the toe of the sheet pile, this poses a constraint on the choice of slip circle radius. Given the time-consuming nature, these calculations are not carried out.

CIRIA (2006) mentions that as a consequence of sheet pile corrosion the sheet pile can break due to bending moments, as described above. However, it is more common

that fines behind the sheet pile wash out through the holes in the sheet pile caused by corrosion. The washed out fines lead to instability of the structure or of collapse of the retained ground. The probability that the corrosion depth exceeds the sheet pile thickness is taken into account in the time-dependent fragility.

7.5.3. Importance measures for anchored sheet pile walls

The importance measures developed in section 4.3 are calculated for anchored sheet pile walls along the Dartford Creek to Swanscombe Marshes flood defence line.

Indicate the influence of variables on the reliability

Table 7.19 contains the direction cosines, α, and partial derivative based indicators, PD_X, for the failure mechanisms of the anchored sheet pile wall. Appendix C contains the statistical distribution functions of the random variables. Figure 7.27 presents some of the dimensions and properties of the anchored sheet pile structure. The PD_X are not included for failure due to sheet pile breaking as Monte Carlo sampling delivers a probability of failure of 0. FORM provides a low probability of sheet pile breaking and due to the relative complexity of the process model the direction cosines are regarded with some scepticism (possibly iteration problems). Still, they are an indication of the differences in uncertainty contributions among the flood defence properties.

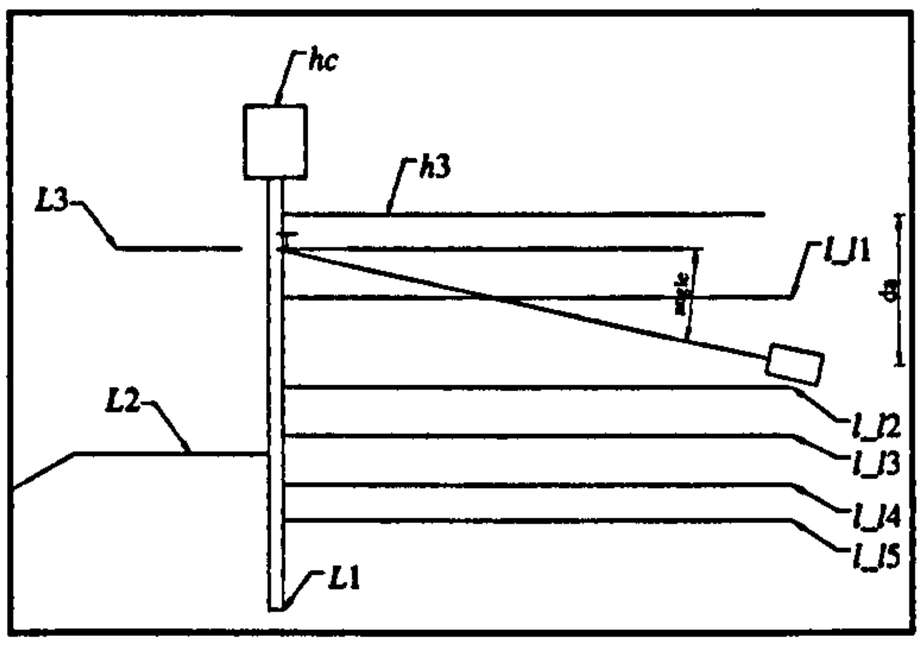

Figure 7.27 Some dimensions and properties associated with the anchored sheet pile wall.

The sheet pile properties that contribute most uncertainty to the probability of failure due to anchor breaking are: the model uncertainty of the strength, m_R, and the loading model, m_S, the active and passive horizontal grain stress coefficient, K_a and K_p, the river bed level, L_2, and the ground water level, g_w. The probability of failure due to anchor breaking is additionally sensitive to the river bed level L_1 and the groundwater level, g_w. The sheet pile properties that contribute most uncertainty to the probability of failure due to anchor sliding are: the model uncertainty of the strength, m_R, and the loading model, m_S, the active and passive horizontal grain stress coefficient, K_a and K_p. The probability of failure due to anchor sliding is

additionally sensitive to the river bed level L_1 and the groundwater level, g_w. The uncertainty contribution in the probability of failure due to rotational failure can be attributed to the active horizontal grain stress coefficient, K_a, the river bed level, L_2, and the ground water level, g_w. The probability of rotational failure is additionally sensitive to the river bed level L_1 and the groundwater level, g_w. The sheet pile properties that contribute most uncertainty to the probability of sheet pile breaking are: the yield stress of the steel, f_s, the active and passive horizontal grain stress coefficients, K_a and K_p, the sheet pile toe level, L_1 and the river bed level, L_2.

Table 7.19 Direction cosines, α, and partial derivative based indicators, PD_X, for the failure mechanisms of the anchored sheet pile wall.

			α				PD_X		
			Anchor breaking	Anchor sliding	Rotational failure	Sheet pile breaking	Anchor breaking	Anchor sliding	Rotational failure
h	=	Water level (mOD)	0	0	0	0	-0.17	-0.23	-0.31
h_c	=	Crest level (mOD)	0	0	0	-0.009	0	0	0
l_l_1	=	Transition between top level and 2nd strata (mOD)	0.044	0.016	-0.005	-0.03	0.10	0.01	-0.01
l_l_2	=	Transition between 2nd and 3rd strata (mOD)	0.118	0.067	-0.014	-0.077	0.25	0.18	-0.02
l_l_3	=	Transition between 3rd and 4th strata (mOD)	-0.083	-0.051	-0.053	0.063	-0.20	-0.15	-0.09
l_l_4	=	Transition between 4th and 5th strata (mOD)	0.029	0.02	0.026	-0.023	0.07	0.07	0.04
l_l_5	=	Transition between 5th and 6th strata (mOD)	0	-0.031	0	0	0.00	-0.18	0.00
γ_{s1}	=	Saturated volumetric weight of top strata (kN/m³)	0.107	0.068	0.164	-0.088	0.12	0.11	0.11
γ_{s2}	=	Saturated volumetric weight of 2nd strata (kN/m³)	0.089	0.074	0.252	-0.087	0.11	0.16	0.18
γ_{s3}	=	Saturated volumetric weight of 3rd strata (kN/m³)	0.115	0.087	0.088	-0.09	0.12	0.15	0.06
γ_{s4}	=	Saturated volumetric weight of 4th strata (kN/m³)	-0.007	0.007	0.002	0.003	0.00	0.03	0.00
γ_{s5}	=	Saturated volumetric weight of 5th strata (kN/m³)	-0.002	0.002	0	0.001	0.00	0.01	0.00
γ_{d1}	=	Dry volumetric weight of top strata (kN/m³)	-0.024	-0.007	0	0.015	-0.02	0.00	0.00
γ_{d2}	=	Dry volumetric weight of 2nd strata (kN/m³)	-0.08	-0.035	-0.001	0.053	-0.08	-0.02	0.00
K_a	=	Active horizontal grain stress coeff. (-)	-0.345	-0.265	-0.156	0.229	-0.25	-0.27	-0.05
K_p	=	Passive horizontal grain stress coeff. (-)	0.381	0.247	0.6	-0.314	0.21	0.21	0.21
d_a	=	Depth anchor head underneath ground level (m)	0	-0.003	-	0	-0.29	-0.36	-
α_{an}	=	Angle anchor with horizontal (°)	-0.016	0.009	-	0.008	-0.04	0.11	-
m_R	=	Model uncertainty strength model (-)	0.506	0.594	0	0	0.07	0.13	0
m_S	=	Model uncertainty loading model (-)	-0.506	-0.594	0	0	-0.12	-0.15	0
q	=	Superimposed loading behind sheet pile wall (kN/m²)	0	0	0	0	-0.08	-0.11	0
L_1	=	Level of the sheet pile toe (mOD)	-0.115	-0.068	-0.2	0.104	-0.24	-0.21	-0.25
L_2	=	River bed level (mOD)	0.247	0.164	0.419	-0.199	0.61	0.59	0.67
L_3	=	Connection anchor with sheet pile (mOD)	0	0	-	0	0	0	-
g_w	=	Ground water level (mOD)	-0.27	-0.201	-0.537	0.187	-0.26	-0.28	-0.38
A_s	=	Area sheet pile cross section (mm²)	-	-	-	0	-	-	-
h_a	=	Height anchor head (m)	0	-0.024	-	0	0	0	-
b_a	=	Width anchor head (m)	0	-0.024	-	0	0	0	-
h_3	=	Ground level behind the sheet pile wall (mOD)	-0.099	-0.028	0.001	0.067	-0.27	-0.02	0
A_a	=	Area of the anchor cross section (mm²)	0.011	0.246	-	0	0.07	0	-
x_a	=	Distance between centres of the anchors (m)	-0.011	-0.013	-	0	-0.12	-0.13	-
f_s	=	Yield stress steel (N/mm²)	0.011	-	-	0.848	0.07	-	-
z	=	Section modulus (mm³/m)	-	-	-	-0.006	-	-	-

In summary, the most relevant anchored sheet pile properties are the active and passive grain stress coefficients, the river bed level and the groundwater level. The relevance of the active and passive grain stress coefficients both implies the importance of the soil density of the retained ground as well as the quality of the model of the horizontal grain stresses. The latter is represented in a fairly simplified way, as reflected by the model uncertainty of the strength and the loading model.

Highlight time-dependent processes

The asset time-dependent processes that are modelled for the anchored sheet pile walls are listed in table 7.18: sheet pile corrosion, anchor corrosion and toe accretion. Section 4.3.3 introduces a suitable importance measure to highlight relevant time-dependent processes in the form of expression (4.5) and (4.7). The change in probability of failure given different water levels is calculated given an asset time-dependent process and combined with the economic damages. These damages are in case of the anchored sheet pile wall caused by the instability of the retained ground on which residential properties are founded. The cost benefit ratio is derived by calculating additionally the cost of remediation of the asset time-dependent process in consideration. The cost information is derived from Spon (2005).

Remediation is in case of anchor corrosion excavation and replacement of the corroded ground anchors. In case of sheet pile corrosion remediation consists of the refurbishment of the sheet pile wall. The situation is slightly more complicated for accretion of the river bed level at the toe of the anchored sheet pile structure. Dredging activities bring the toe level down, thereby increasing the instability and thus the probability of failure of the sheet pile wall. The cost associated with the dredging activity plus the increase in risk due to increased instability together need to be compensated by another important benefit of the dredging activity: e.g. navigation or the morphological balance of the river. Otherwise dredging is not worth it. The cost benefit ratios, referred to as the Burden to risk Importance Ratios (BIRs) are summarised in table 7.20.

According to table 7.20 sheet pile corrosion is the most relevant asset time-dependent process for this particular anchored sheet pile wall structure. Three comments are made with regard to this result. Firstly, in table 7.20 the BIR is calculated per year in order to compare the deterioration processes on the same timescale. A quicker deterioration process associated with the same remediation cost is then more relevant. The anchor corrosion and sheet pile corrosion is considered between now and the damage in 50 years time. Secondly, the increase in probability of failure due to anchor breaking is partly reduced in the past few decades due to the increase in river bed level caused by toe accretion. The river bed level is highlighted as an important structural property influencing the reliability of the sheet pile wall. Secondly, sheet pile corrosion merely considers the probability of a hole in the sheet

pile wall structure. It therefore does not factor in the remaining stability of the retained ground behind the holed sheet pile. The probability of failure is therefore expected to be smaller, the BIR in table 7.20 would then be higher.

Table 7.20 Burden to risk Importance Ratios of three asset time-dependent processes of the anchored sheet pile wall. Toe accretion refers to the price of the benefit which the dredging at least needs to compensate.

Asset time-dependent processes	Burden (£)	Change in flood risk (£/year)	BIR/year
Sheet pile corrosion	15000	31538	$9.5 \cdot 10^{-3}$
Anchor corrosion	17340	1125	0.31
Toe accretion (in £ of required benefit)	15000	7808	22808

Indicate the flood risk reduction impact of operational activities

Four different types of operational activities are compared according to the importance measures developed in section 4.3.4: sheet pile refurbishment, replacement of the ground anchors, specific inspection and routine inspection. It is noted that routine and specific inspection are only considered in the capacity of statistical uncertainty reduction. Benefits of routine or specific inspection in the form of monitoring the time-dependent behaviour of condition levels and identifying failure mechanisms are not taken into account. The change in risk in case of the operational activities is considered at the present moment. The timescale of the process is therefore the period between the last sheet pile refurbishment or anchor replacement and now. The cost of replacement or refurbishment is estimated according to Spon (2005). Table 7.21 summarises the Burden to risk Importance Ratios (BIRs) for the four operational activities.

Table 7.21 Burden to risk Importance Ratios of four maintenance intervention options on the anchored sheet pile wall.

Asset time-dependent processes	Burden (£)	Change in flood risk (£)	BIR
Sheet pile refurbishment	15000	37.5	400
Anchor replacement	17340	182	95.2
Specific inspection – statistical uncertainty	7534	4755	1.6
Routine inspection – statistical uncertainty	1515	3293	0.46

In the current situation anchor replacement is actually preferable over sheet pile refurbishment. The increase in probability of failure in the coming 50 years is higher for sheet pile holing than for anchor breaking, which is why the preference in table 7.20 is the other way around. Specific inspection monitors the crest level and ground level at the landward side behind the sheet pile wall, as well as the active and passive horizontal grain stress coefficients and the groundwater level. The specific inspection activity performs well against sheet pile refurbishment or anchor replacement. As mentioned before, the increase in knowledge diminishes with an increasing number of monitoring activities. On the other hand, the benefit of discovering a failure process or other problem with a specific inspection is not taken into account. Routine inspection monitors the crest level as well as the ground level behind the anchored sheet pile wall. Cost benefit wise routine inspection is in table 7.21 the preferable activity. The benefit of routine inspection is actually larger as it usually covers a longer flood defence stretch for the same activity cost. This extra benefit is not taken into account. The increase in knowledge diminishes with an increasing number of monitoring activities.

7.5.4. Asset time-dependent process: sheet pile corrosion

The sheet pile corrosion is modelled according to the modelling process in figure 6.2. Appendix E provides flowcharts for the simulations of asset time-dependent processes and their incorporation in time-dependent fragility and probability of failure in a time interval of interest.

Problem formulation and identification of existing knowledge

The task specification of the sheet pile corrosion statistical model is to quantitatively express the corrosion depth as a function of time for the different exposure zones on the sheet pile wall. The task specification at an overarching maintenance level is to realistically represent the influence of the sheet pile corrosion on the overarching performance indicators such as reliability, risk and life cycle cost.

Existing knowledge about sheet pile corrosion is available through general sources such as British Steel (1997) and CIRIA (2005). Southern Water (1989) and Halcrow (2006) provide sheet pile thickness measurements specifically at several locations along the Greenhithe anchored sheet pile frontage in the Dartford Creek to Swanscombe Marshes flood defence system.

CIRIA (2005) distinguishes between 'traditional' corrosion and Accelerated Low Water Corrosion (ALWC). '*Traditional' marine corrosion* occurs according to CIRIA (2005) on unprotected steel structures, which varies in intensity depending on the position on the structure. This type of corrosion appears in the form of customary, usually adherent, hydrated iron oxide deposits on exposed steel, or 'rust'. The 'traditional' corrosion is controlled by the concentration of dissolved oxygen available at the steel surface.

The rate of corrosion is usually governed by the rate of diffusion of oxygen through the layers of dust and/or marine biofouling that build up on unprotected surfaces over time. The rate of such oxygen diffusion to the surface tends to reduce in time reaching a steady state value as the thickness of the deposits increases. Factors influencing the 'traditional' corrosion rates or significantly accelerating them are mentioned under the ancillary features. CIRIA (2005) describes *ALWC* as a particularly aggressive form of localised corrosion associated with unusually high rates of metal wastage and holing on unprotected, or inadequately protected, steel maritime structures. Average corrosion rates are reported in the order of magnitude of 0.3 to 1.0 mm/wetted side/year. ALWC is most commonly found just above LAT (Lowest Astronomical Tide) on sheet maritime structures in tidal waters. There is no definitive agreement about the detailed mechanism of ALWC, some claim that it is an

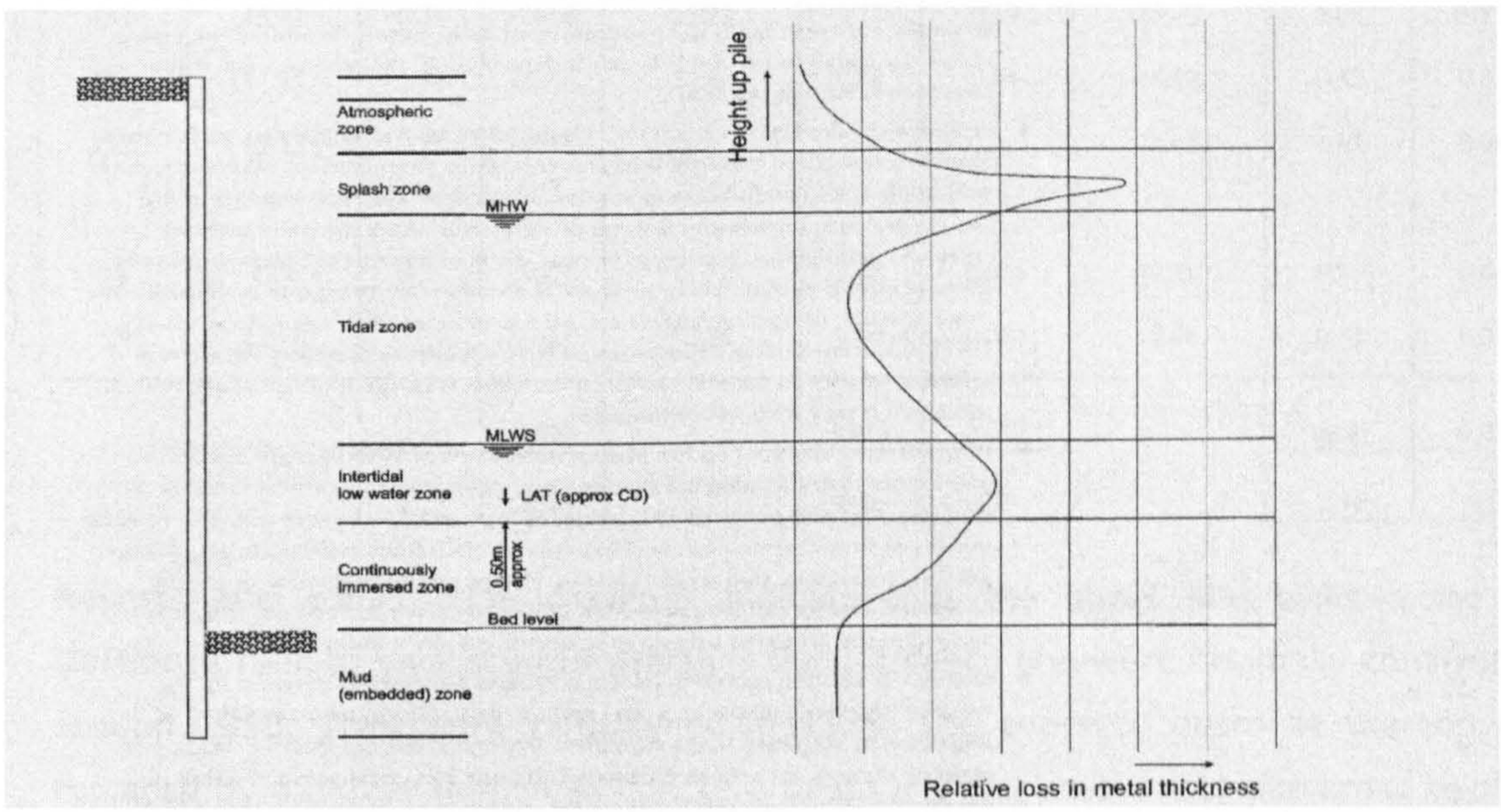

Figure 7.28 Definition of 'traditional' corrosion zones for the anchored sheet pile wall, and typical profile for 'traditional' corrosion behaviour (from CIRIA, 2005)

extension of traditional corrosion in the form of oxygen concentration cells. However, evidence from research associates it with bacterial activity which makes it a form of microbially influenced corrosion (MIC). ALWC is a discrete corrosion form typically occurring in the form of patches of lightly adherent, bright orange and black (iron sulphide rich) deposits over a clean, shiny and pitted steel surface. The pits deepen, become more numerous and overlap. This process produces a dishing effect in the metal surface, which ultimately develops in a hole.

The site specific field measurements presented in Southern Water (1989) and Halcrow (2006) provide no evidence about the occurrence of ALWC. The analysis is therefore restricted to 'traditional' corrosion (referred to as corrosion). British Steel (1997) defines different exposure zones, figure 7.28, and indicative corrosion rates. British Steel (1997) also provides the reduction in the sheet pile section modulus as a function of the thickness loss due to corrosion for different types of sheet piles.

Table 7.22 Sheet pile thickness measurements in 2006. 'Traditional' corrosion rates are based on the assumption that full restoration was achieved in 1989.

Site investigation 2006 Assuming lifetime 17 years									
Design thickness (mm)	Bottom			Middle			Top		
	Remaining measured thickness (mm)	Reduction (mm)	Rate (mm /year)	Remaining measured thickness (mm)	Reduction (mm)	Rate (mm /year)	Remaining measured thickness (mm)	Reduction (mm)	Rate (mm /year)
15.5	15.23	0.27	0.016	12.23	3.27	0.19	15.45	0.05	0.0029
15.5	14.75	0.75	0.044	14.82	0.68	0.04	14.98	0.52	0.031
15.5	15.23	0.27	0.016				14.03	1.47	0.086
13	12.1	0.9	0.053	11.72	1.28	0.075	12.29	0.71	0.042
13	12.76	0.24	0.014	12.34	0.66	0.039	12.46	0.54	0.032
		mean	0.029		mean	0.087		mean	0.039
		stdv	0.076		stdv	0.3		stdv	0.12

Reports and construction drawings indicate that the sheet pile walls along the Dartford Creek to Swanscombe Marshes flood defence line were originally constructed around 1950. They were refurbished in 1979: the concrete beam at the top was replaced by a higher reinforced concrete beam and the steel sheet pile cross sections were patched and sealed until 1 meter in the mud. In the period from 1979, two sets

of sheet pile thickness measurements for the Dartford Creek to Swanscombe Marshes anchored sheet piles are available: in 1989 and 2006. Each of those measurements was followed by remediation activities. The extent of these activities is not clear. The second set, dating from 2006, targets the top, middle and bottom zones of the sheet pile walls and is applied as the basis for the statistical model. Table 7.22 presents the corrosion rates assuming that restoration to its original thickness was achieved in 1989. The influence of measurement errors is not further investigated.

Table 7.23 Excitation, ancillary and affected features for the sheet pile corrosion asset time-dependent process

Excitation features	**Uncertainty**
The presence of oxygen and water.	Inherent uncertainty in time in the form of seasonality and daily fluctuations. Inherent uncertainty in space.
Oxygen diffusion through dust or marine biofouling layer, possibly stimulated due to: • Different environmental exposures • Erosion corrosion, when the velocity of seawater (due to river currents, tidal currents, ships, wave action, etc.) over the steel surface is sufficiently fast to periodically or continually remove semi-protective surface deposits.	Inherent uncertainty in time in the form of seasonality and daily fluctuations. Inherent uncertainty in space.
Ancillary features	**Uncertainty**
Steel composition	Inherent uncertainty in space.
Surface condition, I.e. bare patches in sheet pile protective surface layer	Inherent uncertainty in space.
Nature of surface deposits	Inherent uncertainty in space and time
Local variation in exposure conditions	Inherent uncertainty in space and time
Local and/or repeated stresses	Inherent uncertainty in space and time
Mechanical working, such as a bending of steel plate	Inherent uncertainty in space and time
Local differences in dissolved oxygen availability, due to differences in low water or tidal zones, the presence of marine organisms or crevices in the steel surface.	Inherent uncertainty in space and time
The presence of a connection between two different metals, leading to bimetallic corrosion.	Inherent uncertainty in space and time
The presence of e.g. improperly grounded welding generators, ship service systems, electric crane installations, etc. Leading to stray current corrosion.	Inherent uncertainty in space and time
Corrosion caused or accelerated by microbiological organisms on a steel surface, particularly under conditions of stagnation or restricted water movement. The MIC mechanism of attack is to develop a unique inorganic environment close to the metal surface that is highly aggressive.	Inherent uncertainty in space and time
Affected features	**Uncertainty**
Sheet pile thickness	Inherent uncertainty in time and space

Excitation, ancillary and affected features

The excitation, ancillary and affected features of sheet pile corrosion are tabulated in table 7.23.

Character of the asset time-dependent process

Many factors influence the corrosion of sheet piles. It is difficult to describe the corrosion process in much detail. The corrosion rates in table 7.22 provide a site specific indication of how the corrosion develops in time.

Dependencies between asset time-dependent processes

Corrosion of the sheet pile cross section is considered independently of other asset time-dependent processes of the steel sheet pile.

Development of alternative statistical models

The main sources of uncertainty underlying the variation among the corrosion rates in table 7.22 are: measurements at different locations, inherent uncertainties in time at one location due to seasonality and daily fluctuations (different environmental fluctuations for each location), non-linear behaviour of the corrosion process.

In the hierarchical process model, the corrosion depth is represented as follows:

$$d(t) = m_c c_d t \tag{7.17}$$

In which m_c is the model uncertainty, c_d is the corrosion rate and t is the time. Two different approaches of distributing the uncertainties over the model uncertainty and the corrosion rate are considered. In the first case, the corrosion rate is represented by a wave renewal model capturing seasonality. A lognormal distribution with a mean value and standard deviation according to table 7.22 are applied to the corrosion rates. The model uncertainty is broken down into a constant factor and a Brownian motion to represent environmental fluctuations. Each realisation of the stochastic process captures both the differences in corrosion rates during different time intervals and the differences in spatial properties. Figure 7.29 refers to this model with "Coefficient seasons". In the second case, the corrosion rate is a random variable with a lognormal distribution and mean value and standard deviation according to table 7.22. The model uncertainty is broken down into three different factors. One factor is

a constant model uncertainty, a second factor picks up seasonality and a third factor captures the environmental fluctuations. These simulations are referred to as "Model seasons".

In the "Coefficient seasons" approach therefore the variance found in table 7.22 is attributed to inherent uncertainty in time. In the "Model seasons" approach the variability in the corrosion rate is mainly treated as an inherent uncertainty in space and the variability in time is distributed over the model uncertainty, see table 7.24.

The parametric process model applies (7.17) whereby the corrosion rate is modelled with a lognormal distribution and a mean value and standard deviation according to table 7.22. The parametric process applies a constant model uncertainty without time variability $m_{c;1}$ as in table 7.24. These simulations feature in figure 7.29 as "Parametric process".

The gamma process model estimates an average corrosion rate and a standard deviation in equation (7.5). The gamma process model does not distinguish between time independent and time dependent model uncertainties. The way in which the variation in the time-dependent process is modelled is therefore different from the hierarchical process.

Estimation, calibration and corroboration

The prior distributions of the variables in the hierarchical process, parametric process and gamma process model for sheet pile corrosion are tabulated in table 7.24. The prior distributions of the corrosion rates are based on table 7.22. The mean value of the average corrosion in one year for the gamma process equals that of the middle sheet pile area in table 7.22; the standard deviation is at least higher than that presented in table 7.22.

Analysis

The observation of the corrosion thickness serve to establish site specific corrosion rates. A significance test or posterior updating is therefore not applicable. Figure 7.29 displays some time series samples of the hierarchical process (two approaches), parametric process and the gamma process model. The largest variation is associated with the "Model seasons" and the parametric process models. These models are very similar as most variation is represented through the corrosion rates in the form of a

spatial uncertainty. The additional seasonality and daily fluctuations in "Model seasons" do not provide a much different variation in the time series samples. "Coefficient seasons", i.e. seasonality in the corrosion rates, shows a much smaller variation. The gamma process model provides similar results, with a slightly larger variation in the time series samples.

Table 7.24 Prior distributions of the random variables in the sheet pile corrosion hierarchical process model, parametric model and the gamma process model. The bottom row contains the description of the distribution functions.

Symbol		Description	Unit	"Coefficient seasons"				"Model seasons"			
				Dist. type	μ	σ	V	Dist. type	μ	σ	V
$m_{c;1}$	=	Constant model uncertainty	-	LN	1	-	0.05	LN	1	-	0.05
$m_{c;2}$	=	Model uncertainty capturing seasonality in corrosion	-	-	-	-	-	WR 0.25	0	0.1	-
$m_{c;3}$	=	Model uncertainty capturing environmental fluctuations in corrosion	-	BM	0	0.1	-	BM	0	0.1	-
c_d	=	Corrosion	mm/ year	WR 0.25	Table 7.22	Table 7.22	-	LN	Table 7.22	Table 7.22	-
c_{ga}	=	Average corrosion in one year, gamma process model	mm	Ga	0.087 Table 7.22	0.3 Table 7.22	-				
N = Normal distribution function LN = Lognormal distribution function WR 0.25 = Wave Renewal model with constant intervals of 0.25 years BM = Brownian Motion with constant renewal of one year Ga = Gamma process											

The field observations in table 7.22 already serve to derive the corrosion rates and cannot be used for a quantitative quality evaluation. Still, the prediction of the different models at t=17 years is compared with table 7.22 to get an impression of whether the order of magnitude of the variation is appropriate. The actual sheet pile corrosion depth measurements have a variation coefficient of V=0.84 (mean value of 1.5 mm and standard deviation of 1.24 mm). The parametric process model implies that one realisation of the corrosion rate remains constant throughout the 50 year simulated lifetime. The time series samples have a variation coefficient of V=0.76 at t=17 years, calculated from the mean value and standard deviation of the process at t=17 years. The "Coefficient seasons" simulations applies the same variation to the corrosion rate c_d, however, each season (one quarter of a year) a new corrosion rate is randomly drawn. In addition, environmental fluctuations are represented by a

Brownian motion. The variation coefficient after 17 years is V=0.062. This variation coefficient corresponds most closely to table 7.22. As mentioned before, the "Model seasons" simulations show great similarity to the parametric process model and has a variation coefficient of V=0.77.

The difference between the "Coefficient Seasons" and "Model seasons" approach is the distribution of the uncertainty introduced by time variability and by spatial uncertainty. It depends on the situation which one of these models is most appropriate.

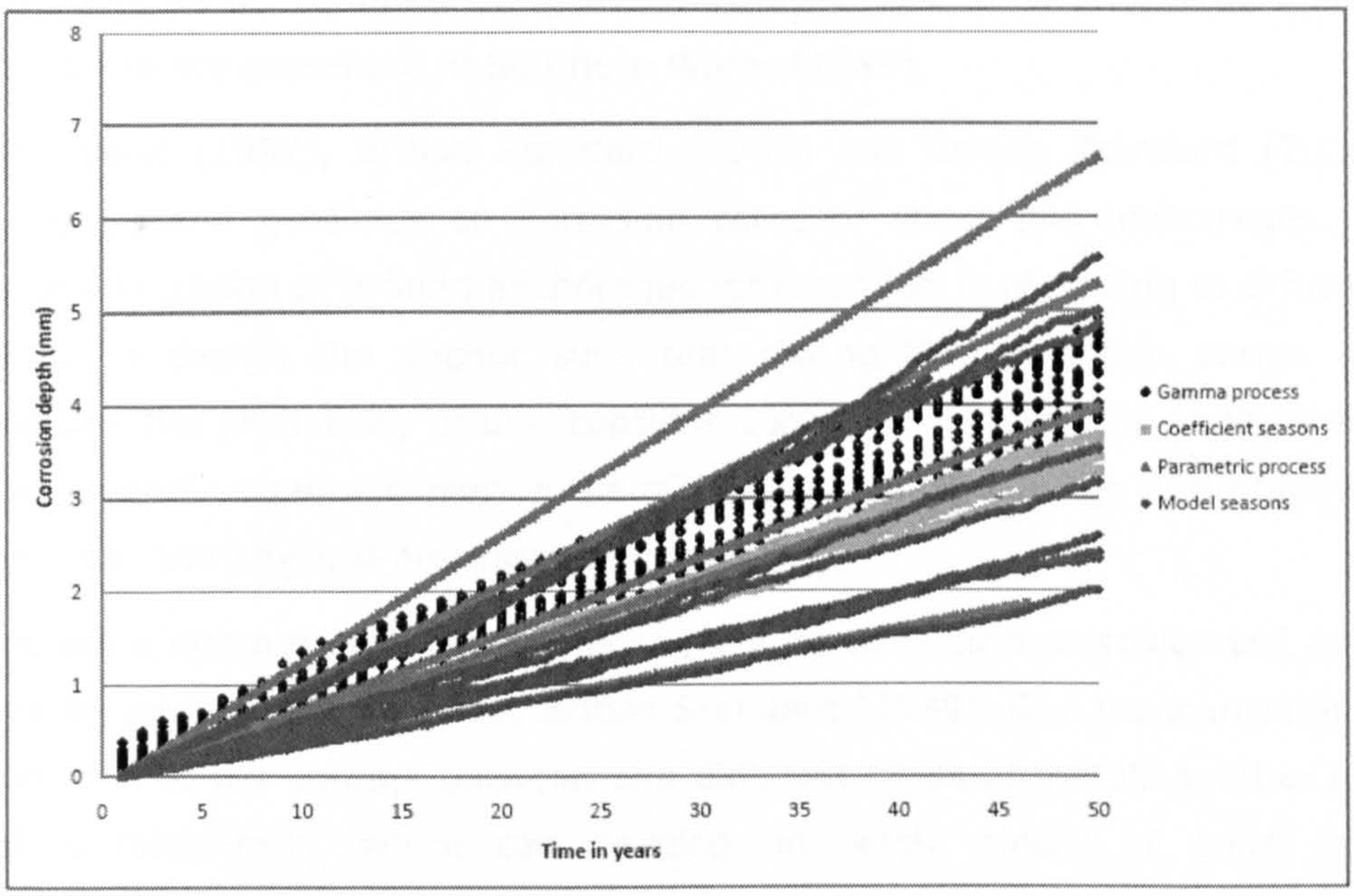

Figure 7.29 *Some time series samples for sheet pile corrosion hierarchical process, "model seasons" and "Coefficient seasons", parametric process, "Parametric", and gamma process model, "Gamma process".*

7.5.5. Asset time-dependent process: anchor corrosion

Anchor corrosion is modelled according to the modelling process in figure 6.2. Appendix E provides flowcharts for the simulations of asset time-dependent processes and their incorporation in time-dependent fragility and probability of failure in a time interval of interest.

Problem formulation and identification of existing knowledge

The task specification of the anchor corrosion statistical model is to quantitatively express the reduction of the anchor cross section as a function of time. The task specification at an overarching maintenance level is to realistically represent the influence of the anchor corrosion on the overarching performance indicators such as reliability, risk and life cycle cost.

There are general sources covering the design of anchors against corrosion, British Steel (1997), British Standard (1989) and British Standard (2000). Specific field measurements at locations along the Dartford Creek to Swanscombe Marshes flood defence line are presented in Southern Water (1989).

British Steel (1997), British Standard (1989) and British Standard (2000) do not provide general guidance on corrosion rates of sheet pile anchorages. The main objective in design of ground anchorages for corrosion is according to British Standard (1989): to design the anchor such that during the economic design life of the anchorage the probability of unacceptable corrosion occurring is small. The design of ground anchors against corrosion therefore goes into the design of protective systems rather than the physical processes of corrosion.

There are a number of different mechanisms to develop a corrosion cell as a process driven by oxygen and moisture, British Standard (1989). One mechanism is bimetallic action, due to the contact between two different types of metal. Another mechanism involves micro-cells, which can develop on single pieces of metal or alloy in appropriate environments, e.g. due to inhomogeneities in metal composition (especially applicable to alloys). A third mechanism consists of the development of differential aeration cells, due to e.g. a transition from disturbed soil to undisturbed soil. A fourth mechanism is differential concentration cells, due to variations in ionic concentrations, e.g. differing pH. A last example is differential embedment, e.g. at the passage of a gravel layer to a clay layer.

Given the mechanisms to develop a corrosion cell, British Standard (1989) describes a number of main types of corrosion. The first type is generalised attack, whereby a general film is formed on the ground anchor. The second type is localised attack or corrosion pitting, whereby separate corrosion cells can be distinguished by variations of the electrode potential over the metal surface. This type of corrosion is generally associated with the presence of a protective oxide film on the metal or alloy and a

mechanism of pitting or crevice corrosion occurring due to the presence of aggressive ions such as chloride. The third type is bacterial attack, the most common form of bacterial attack results from the metabolic processes of sulphate-reducing bacteria utilizing sulphate in anaerobic conditions. The fourth type is stress corrosion cracking (SCC), which is a combination of internal or external static tensile stress and localised corrosion. High tensile steels are for instance susceptible to this type of corrosion. This type of corrosion is not thought to be a problem for this case study. The fifth type is corrosion fatigue, which is the result of conjoint action of corrosion and cyclic stresses, e.g. alternating tensile and compressive stresses. The sixth type is stray current corrosion, which can occur in the neighbourhood of e.g. electrified tram or railways. The seventh type is fretting corrosion, a surface wear phenomenon occurring between two contacting surfaces having a small amplitude oscillating relative motion.

As mentioned in section 7.5.4, the anchored sheet pile frontage along Greenhithe was originally constructed in 1950/1951. In 1979 improvement and maintenance of this frontage was carried out. There is no mention of work undertaken on the anchorages as part of this remediation scheme. It is therefore assumed that these were not replaced or repaired. The site investigation in 1989 of the sheet pile frontage involved excavation of the anchors at several sites in addition to sheet pile thickness measurements. The propagation of the corrosion was measured at three places along the anchor: near the wall, midway and at the connection with the anchor block.

Three types of anchor corrosion appear to be relevant from these observations. The first type of observed corrosion is generalised corrosion occurring uniformly over the tie rods, with the highest rates close to the wall. This type of corrosion is therefore dependent upon the environment, i.e. the exposure to oxygen and moisture. A second type of observed corrosion is localised corrosion / corrosion pitting occurring at most of the observed locations. It is assumed that this pitting corrosion can best be attributed to bacterial attack. This type of corrosion is very local and the influence of environmental exposure is negligible. A third type of observed corrosion is accelerated corrosion occurring midway of the anchorages due to the presence of turnbuckles. This type of corrosion is attributed to bimetallic corrosion. The location of these turnbuckles is midway of the anchors where the influence of environmental exposure is considered to be negligible. It is likely that at the locations where the corrosion at

the turnbuckles was observed to be very low, the ground anchor was submerged under the groundwater level.

Excitation, ancillary and affected features

The excitation, ancillary and affected features of sheet pile corrosion are tabulated in table 7.25.

Table 7.25 Excitation, ancillary and affected features for anchor corrosion.

Excitation features	**Uncertainty**
Generalised corrosion:	
The presence of oxygen and moisture is a function of the exposure to the environment in the ground close to the wall.	Inherent uncertainty in time in the form of seasonality. Inherent uncertainty in space.
Corrosion at turnbuckles:	
The presence of oxygen and moisture midway of the ground anchor is more or less constant and is not considered to be significantly influenced by the environment.	Inherent uncertainty in space.
Corrosion pitting:	
Bacterial attack, pitting can then occur in an anaerobic environment, e.g. when the anchor is submerged	Inherent uncertainty in space, equal probability of a pit occurring along the length of the anchor.
Ancillary features	**Uncertainty**
Generalised corrosion:	
The type and properties of the metal.	Inherent uncertainty in space.
The presence of corrosion acceleration factors such as: aeration differences, micro-cells, differential embedment etc.	Inherent uncertainty in space and time.
The presence of a protective layer on the ground anchor.	Inherent uncertainty in space and time.
Corrosion at turnbuckles:	
The presence of a turnbuckle to provide two different connecting metals.	-
The cross section of the ground anchor.	Inherent uncertainty in space.
The types and properties of the metal of both the turnbuckle and the ground anchor.	Inherent uncertainty in space.
The presence of a protective layer on the ground anchor.	Inherent uncertainty in space and time.
Corrosion pitting:	
The presence of a protective layer on the ground anchor.	Inherent uncertainty in space and time.
The type and properties of the metal.	Inherent uncertainty in space.
Favourable circumstances for bacterial activity.	Inherent uncertainty in space and time.
Affected features	**Uncertainty**
Anchor cross section	Inherent uncertainty in time and space

Character of the asset time-dependent process

The generalised corrosion is uniformly distributed over the cross section of the anchor. The corrosion rate is assumed to be applicable to one third of the distance of

the ground anchor. The corrosion rate is subject to seasonal and daily differences in oxygen and moisture concentration in the ground adjacent to the anchor.

The corrosion at turnbuckles occurs midway of the anchor and is uniformly distributed along the cross section of the ground anchor. The corrosion rate is assumed to be subject to seasonal changes in oxygen and moisture concentration.

The corrosion pitting problem is approached as follows. The arrival of a corrosion pit initiation anywhere along the anchor surface is considered as a Poisson process. The corrosion rate is high compared to the generalised corrosion and corrosion at the turnbuckles. However, bacterial attack also occurs in an anaerobic environment and is thus uninfluenced by exposure to the environment.

Dependencies between asset time-dependent processes

The generalised corrosion, corrosion at turnbuckles and corrosion pitting are considered to be independent. The loading and strength properties of the sheet pile anchors are fully correlated over the length of the anchor. The location with the highest anchor cross section reduction therefore dominates the probability of failure.

Development of alternative statistical models

The general corrosion rate affects the part of the anchor directly behind the waterfront and is therefore subject to seasonality and environmental fluctuations. The corrosion at the turnbuckles affects the anchor more landward and is only assumed to be subject to seasonal differences in corrosion rate. Both types of corrosion uniformly affect the cross section of the anchor, such as depicted left in figure 7.30.

$$\phi(t) = \phi_0 - m_g c_g t \tag{7.18}$$

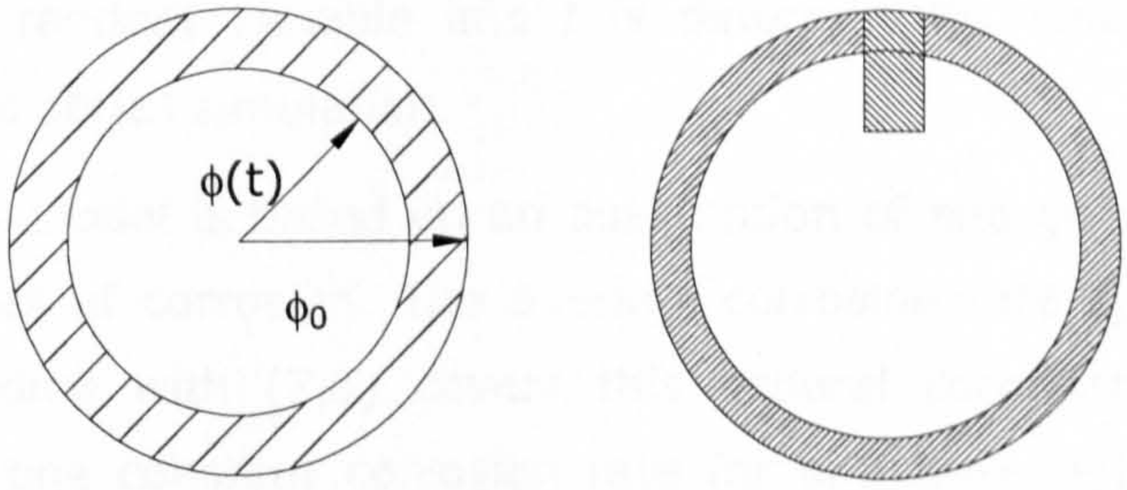

Figure 7.30 *Left: generalised corrosion uniformly affecting the anchor cross section. Right: a combination of a uniformly by corrosion affected anchor cross section and a corrosion pit.*

$$A(t) = \pi(\phi(t))^2 \tag{7.19}$$

In which $\phi(t)$ is the radius of the anchor cross section in time, ϕ_0 is the initial anchor radius, m_g is the model uncertainty, c_g is the generalised corrosion rate, t is the time in years $A(t)$ is the anchor cross section in time and A_0 is the initial anchor cross section. The model uncertainty m_g is for generalised corrosion broken down into a constant model uncertainty, a seasonality model uncertainty and a model uncertainty capturing daily fluctuations. Turnbuckle corrosion is derived with similar expressions as (7.18) and (7.19), but associated with a rate c_{tb} and a model uncertainty m_{tb}. The model uncertainty is broken down into a constant and seasonality component. The arrival of corrosion pits is assumed to be Poisson distributed. The effect of corrosion pitting on the performance of the anchor can manifest itself in different ways. The effect is in this model simplified with a rectangular shaped pit with a depth $d(t)$ and a width of $0.5 \cdot d(t)$, see figure 7.30. The hatched area is subtracted from the original area A_0. The corrosion pit can occur at any point in the anchor cross section and develop in any direction. It is unclear how the location and development direction of the corrosion pit affects the distribution of stress in the anchor cross section. This effect is therefore not taken into account. The corrosion rates associated with corrosion pitting are usually high. The model uncertainty of pit corrosion rates are broken down into a constant model uncertainty and a model uncertainty capturing fluctuations introduced in the corrosion by other factors related to the bacterial attack.

The parametric process model does not include the arrival of corrosion pits but assumes one corrosion rate affecting the anchor cross section. This corrosion rate then represents all types of corrosion.

$$\phi(t) = \phi_0 - c_{para}t \tag{7.20}$$

In which c_{para} is a random variable and t is deterministic. One corrosion rate is sampled for one time series simulation.

The gamma process model is based on an assumption of one general corrosion rate representing all types of corrosion. The average corrosion rate c_{gamma} and standard deviation corresponding with (7.5) covers this general corrosion rate. Instead of randomly sampling one constant corrosion rate for one time series simulation, the corrosion process is represented by a stochastic process. The simulations of the

gamma process model are different from the hierarchical process model. The arrival of pit corrosion is not taken into account.

Estimation, calibration and corroboration

Southern Water (1989) contains measurements of the corrosion depth of sheet pile anchors at several locations along the Greenhithe frontage, at the Dartford Creek to Swanscombe Marshes flood defence system. This information is used to establish the prior distributions of the generalised corrosion, turnbuckle corrosion and pit corrosion rates. The details of these distribution functions are presented in table 7.26.

Table 7.26 Prior distributions of the random variables in the anchor corrosion hierarchical process model, parametric model and the gamma process model. The bottom row contains the description of the distribution functions.

Symbol		Description	Unit	Dist. type	μ	σ	V
$m_{g;1}$	=	Constant model uncertainty	-	LN	1	-	0.05
$m_{g;2}$	=	Model uncertainty capturing seasonality	-	WR 0.25	0	0.2	-
$m_{g;3}$	=	Model uncertainty capturing environmental fluctuations	-	BM	0	0.1	-
c_d	=	Generalised corrosion	mm/year	LN	0.06	-	1.4
$m_{tb;1}$	=	Constant model uncertainty	-	LN	1	-	0.05
$m_{tb;2}$	=	Model uncertainty capturing seasonality	-	WR 0.25	0	0.2	-
c_d	=	Turnbuckle corrosion	mm/year	LN	0.16	-	1.1
m_p	=	Constant model uncertainty	-	LN	1	-	0.05
c_p	=	Pit corrosion	mm/year	LN	0.1	0.09	
N_{plt}	=	Arrival of corrosion pit	pit/year	Po	0.5	-	-
c_{para}	=	Overall corrosion rate in parametric model	mm/ year	LN	0.06	0.05	-
c_{gamma}	=	Average corrosion in one year, gamma process model	mm	Ga	0.06	0.05	-

N = Normal distribution function
LN = Lognormal distribution function
WR 0.25 = Wave Renewal model with constant intervals of 0.25 years, normally distributed
BM = Brownian Motion with constant renewal of one year
Po = Poisson distribution with mean value μt and standard deviation $\sqrt{\mu t}$
Ga = Gamma process

Analysis

Figure 7.31 displays the time series samples for the hierarchical process, the parametric process and the gamma process model. Currently, there is insufficient

information to carry out a significance test on the statistical models. Such tests can be carried out under increasing information in the future.

The time series samples of the parametric process and gamma process model all display linear behaviour. The hierarchical model shows time series samples whereby the reduction in anchor cross section due to a generalised or turnbuckle corrosion rate is complemented by the arrival of corrosion pits. The hierarchical process model shows a large variation as the variability in time is mainly attributed to the model uncertainty rather than the corrosion rates. As can be seen in case of the sheet pile corrosion time series samples such a distribution of uncertainty in time has a significant impact on the spread in the time series samples. A different distribution of the variation in time should then lead to a smaller variation in the time series samples of the hierarchical process model. This aspect is not further investigated here. To demonstrate the difference between the linear parametric and gamma process models and the curved hierarchical model the development of the expectation in time is given in figure 7.32.

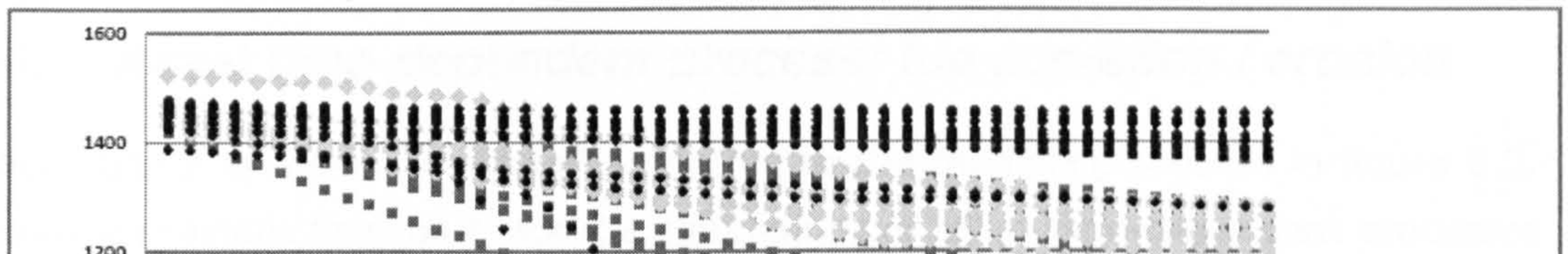

Figure 7.31 Hierarchical process, parametric and gamma process model for anchor corrosion.

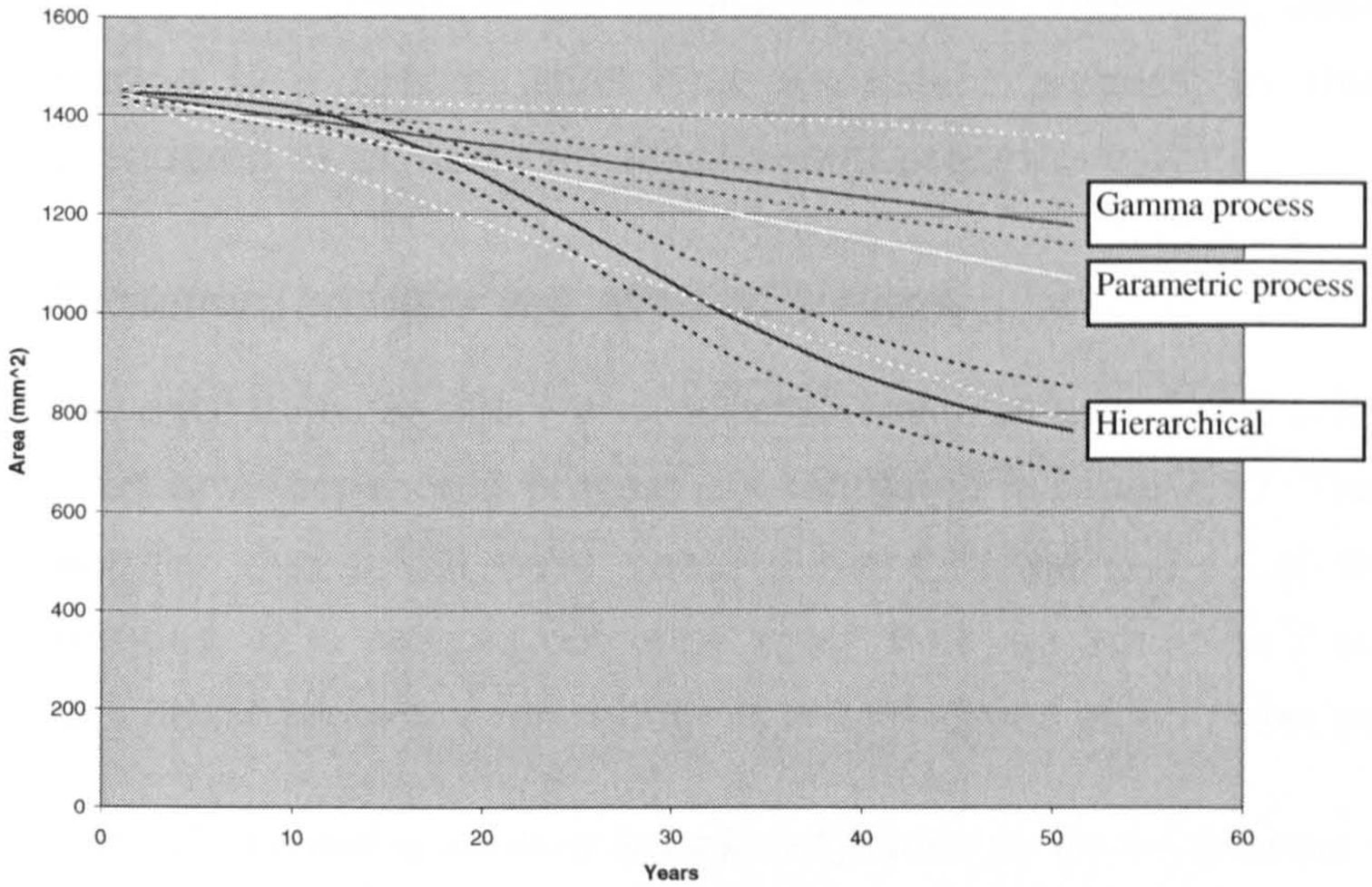

Figure 7.32 *Development of the expectation in time of the hierarchical process, the parametric process and gamma process model. An indication of the variation in the time series samples is*

7.5.6. Asset time-dependent process: toe accretion / erosion

Toe accretion / erosion is modelled according to the modelling process in figure 6.2. Appendix E provides flowcharts for the simulations of asset time-dependent processes and their incorporation in time-dependent fragility and probability of failure in a time interval of interest.

Problem formulation and identification of existing knowledge

The task specification of the toe accretion / erosion statistical model is to quantitatively express the toe level as a function of time. The task specification at an overarching maintenance level is to realistically represent the influence of the toe accretion / erosion on the overarching performance indicators such as reliability, risk and life cycle cost.

Toe accretion / erosion is in fact a system time-dependent process as it is driven by river morphology. The river bathymetry has been monitored regularly over the past century. Comparisons between river bed levels in the 1910s and the 1990s have been made. These comparisons point out that along the Greenhithe frontage (figure A.1, appendix A) the toe level has increased with 1.5 to 2 meter and is therefore worth

taking into account in the reliability analysis. Therefore, even though toe accretion / erosion is a system level time-dependent process, in this research project it is considered as an asset time-dependent process.

Excitation, ancillary and affected features

The excitation, ancillary and affected features associated with toe accretion / erosion asset time-dependent process are tabulated in table 7.27. The excitation and ancillary features that might have been relevant in the course of the last century are also included. It is pointed out once again that toe accretion / erosion is a system time-dependent process even though it is considered as an asset time-dependent process.

Table 7.27 Excitation, ancillary and affected features for the toe accretion / erosion asset time-dependent process

Excitation features	**Uncertainty**
Tidal currents	Inherent uncertainty in space and time
River discharge, which is negligible at this point of the Thames Estuary	Inherent uncertainty in space and time
Local wave climate	Inherent uncertainty in space and time
Dredging activities, in the Thames Estuary	Inherent uncertainty in space and time
Naval activity, it is noted that the frontage is not in use as a dock facility anymore	Inherent uncertainty in space and time
Ancillary features	**Uncertainty**
Bathymetry of the river as a system	Inherent uncertainty in space and time
The shape and type of frontage in relation to the tidal currents or wave reflection, e.g. vertical sheet pile wall structure, or sloped foreshore	Inherent uncertainty in space
Local sheltering due to the alignment of the frontage	Inherent uncertainty in space
Affected features	**Uncertainty**
Toe level	Stochastic process introduces inherent uncertainty in time and space

Character of the asset time-dependent process

The character of the erosion or accretion at the toe of the anchored sheet pile wall is an accumulation of several effects. Tidal currents and the river discharge have a more gradual effect. The local wave climate is mainly relevant during storm conditions and therefore introduces a recurrent component. Dredging activities are not recurrent or gradual. They have a short term abrupt effect and a larger scale influence on the river bathymetry, which has a longer term morphological effect. If the frontage is used as a dock facility the naval activity has a recurrent erosion effect.

It is assumed that along Greenhithe the changes of the river bed level at the toe of the anchored sheet pile wall are mainly driven by tidal currents and the local wave climate during storm conditions. The river discharge at this point of the Thames Estuary is negligible. Dredging activities have taken place in the past but it is not clear whether and in which way it is a regularly recurring activity in the future. Naval activity has played a role in the past, but the frontage does not have a naval function anymore. Analysis of changes in bathymetry between the 1910s and 1990s is available. The resulting accretion / erosion over those years is also determined by the effect of naval and dredging activity. Naval activity is assumed to be negligible in future predictions. Finally, it is noted that all effects need to be considered in the light of the overall morphological behaviour of the river.

Dependencies between asset time-dependent processes

Even though toe accretion / erosion is part of the morphological system formed by the Thames Estuary it is considered in this research project as an independent asset time-dependent process.

Development of alternative statistical models

The hierarchical process model of the accretion / erosion process is still simplified as it does not consider the overall morphological system.

$$dh_t = dh_a - dh_w \tag{7.21}$$

In which dh_t is the change in toe level, dh_a is the change in river bed level due to continuous accretion / erosion and is modelled with a Brownian motion. dh_w is the change in river bed level caused by erosion due to the wave climate in storms. The arrival of storms is Poisson distributed. The storms cause a lognormally distributed erosion dh_w. This approach allows time series samples resulting in a negative as well as a positive development of the toe level in time.

The parametric process model applies one overall accretion rate.

$$dh_t = r_a t \tag{7.22}$$

In which r_a is the accretion rate. This model assumes that one draw for an accretion rate is representative of one time series. It does not represent the variability in time.

The gamma process model builds on (7.5) and specifies an average toe accretion rate for $dh_{t;gamma}$ and a standard deviation. The gamma process model does not distinguish between an accretion rate due to morphological development and the erosion caused by recurrent storms.

Estimation, calibration and corroboration

As mentioned above, there is an indication of the total change in toe level over the last century. However, the influence of the different contributors in this process is not specified. In addition, it unclear to which extent the same contributors will remain influential in the future, e.g. dredging activities and the cease of naval activities in this area of the river. The prior distributions of the statistical models are tabulated in table 7.28.

Analysis

Figure 7.33 displays some time series samples of the hierarchical process, the parametric process and the gamma process model for toe accretion / erosion. The parametric process and gamma process models model a strictly increasing toe level. Figure 7.33 shows that the hierarchical process model allows erosion, accretion as well as alternating erosion and accretion of the toe level.

Table 7.28 Prior distributions of the random variables in the toe accretion / erosion hierarchical process model, parametric model and the gamma process model. The bottom row contains the description of the distribution functions.

Symbol		Description	Unit	Dist. type	μ	σ	V
dh_a	=	Change in bed level due to accretion	meter	BM	0.28	0.015	-
dh_w	=	Change in bed level due to wave action given a storm	meter	LN	0.08	0.01	-
N_{storms}	=	Number of storms	storms / year	Po	3	-	-
r_a	=	Accretion rate in parametric process model	m/year	LN	0.04	0.03	-
$dh_{t;gamma}$	=	Change in toe level in one year in gamma process model	m	Ga	0.04	0.015	-
LN	= Lognormal distribution function						
BM	= Brownian Motion with drift						
Po	= Poisson distribution with mean value μt and standard deviation $\sqrt{\mu t}$						
Ga	= Gamma process						

It is noted that without a morphological model it is hard to make definitive statements about the quality of such predictions. The toe level increased 2 meter in the past

century, but it is unclear whether it will develop in the same fashion over the next decades.

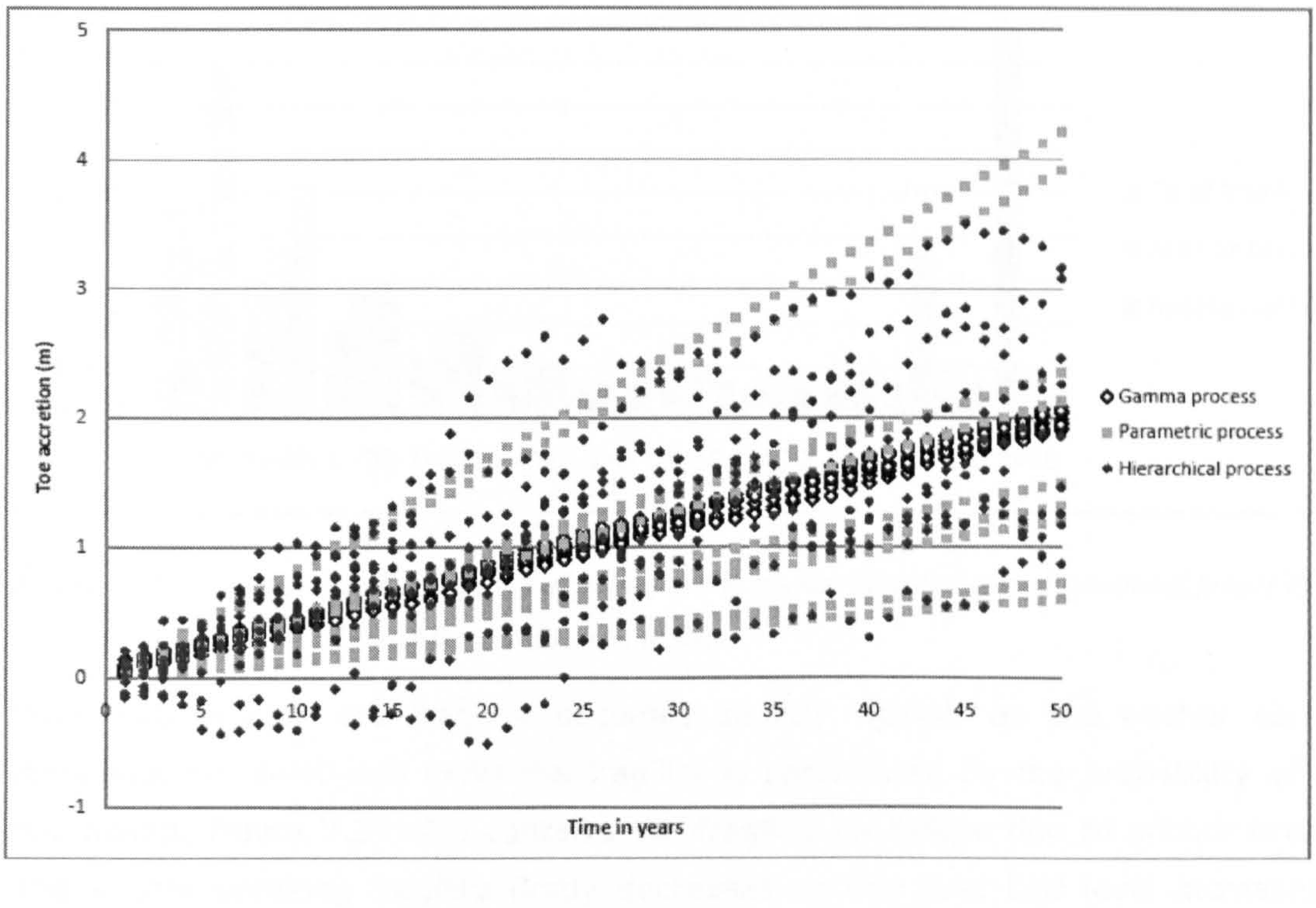

Figure 7.33 *Some time series samples of the hierarchical process, the parametric process and the gamma process model.*

7.5.7. Time-dependent fragility for anchored sheet pile walls

In case of a sheet pile wall, the lowest water levels are associated with the highest probability of failure. A storm is therefore dominated by the probability of failure at the lowest water level rather than the peak of the high water event. The fragility curve is consequentially a horizontal line. Figure 7.34 shows the constant probability of failure for fragility of anchor breaking, rotational failure and the total fragility value for ten moments in time for anchored sheet pile wall section 53 (appendix A, figure A.1). Appendix E provides flowcharts for the simulations of asset time-dependent processes and their incorporation in time-dependent fragility and probability of failure in a time interval of interest. The moment in time indicated with t=-50 years represents the time of construction of the sheet pile walls, t=0 is present time. The assumption in figure 7.34 is that the river bed level rises from t=-50 until t=0, and that from that

moment onward the river bed level remains more or less equal. Until t=0 the total fragility becomes stronger as the river bed level in front of the structure increases.

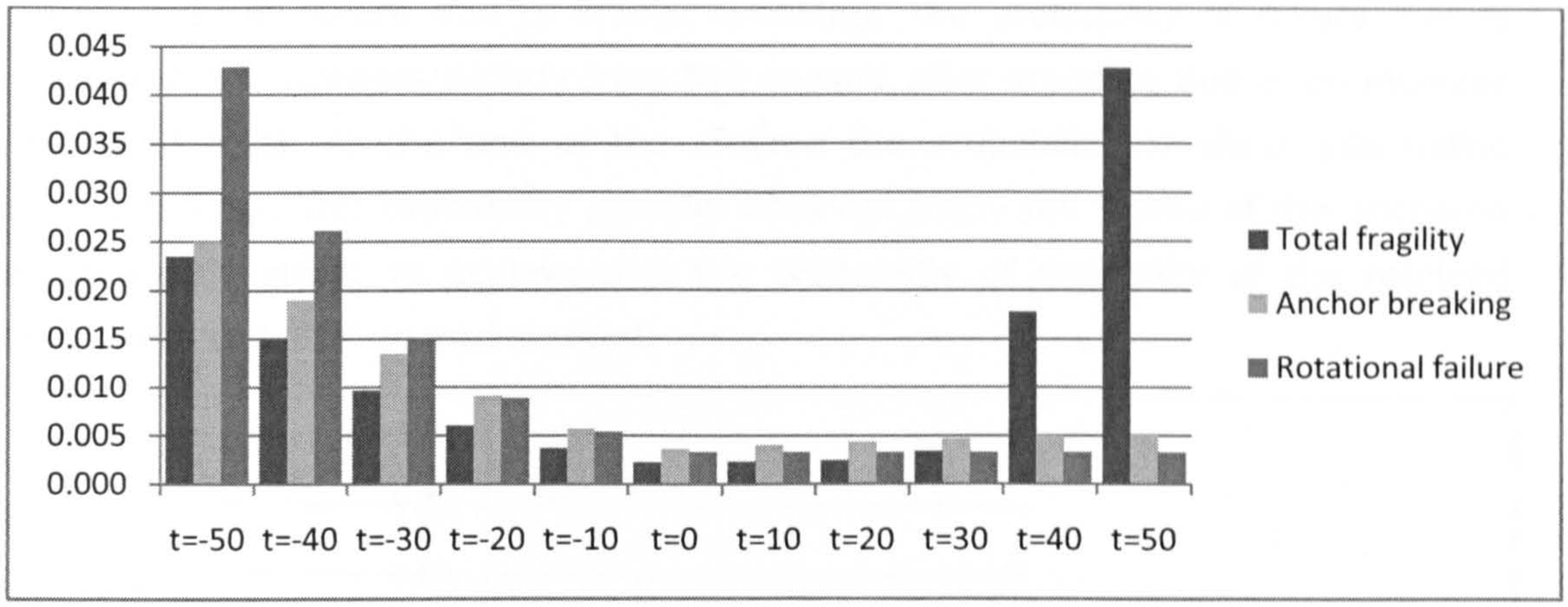

Figure 7.34 *Total fragility, fragility of failure due to anchor breaking and of rotational failure of the sheet pile wall for ten moments in time.*

From t=0 onward the fragility becomes slightly weaker as the anchor corrosion increases. For t=40 and t=50 the fragility is determined by the probability of sheet pile holing. Figure 7.34 also contains the fragility for failure due to anchor breaking. The anchor breaking fragility firstly decreases as the river bed level increases and subsequently from t=0 goes slightly up as the anchor corrosion increases. The stabilising influence of the toe accretion brings the anchor breaking fragility down more than that the anchor corrosion increases it.

7.5.8. Lifetime probability of failure for anchored sheet pile walls

Figure 7.35 contains the total probability of failure in time for flood defence section 53. The total probability of failure in time is broken down in the probability of failure of the individual failure mechanisms. Appendix E provides flowcharts for the simulations of asset time-dependent processes and their incorporation in time-dependent fragility and probability of failure in a time interval of interest in life cycle cost optimisation. The relevance of a probability of failure in a time interval of interest is indicated by equations (3.7), (3.8) and (3.9).

The moment in time indicated with t=-50 years represents the time of construction of the sheet pile walls, t=0 is present time. The anchored sheet pile wall only completely

fails in case of failure due to anchor breaking if the structure subsequently fails due to rotational failure. Figure 7.35 therefore shows a lower total probability of failure than the probability of failure due to anchor breaking. The probability of failure due to anchor breaking increases slightly from t=0 onward after dropping due to an increase in river bed level. At the end of the lifetime the probability of sheet pile holing increases steeply. This probability actually does not imply full failure of the anchored sheet pile wall either; to achieve that the probability of instability of the retained ground needs to be taken into account.

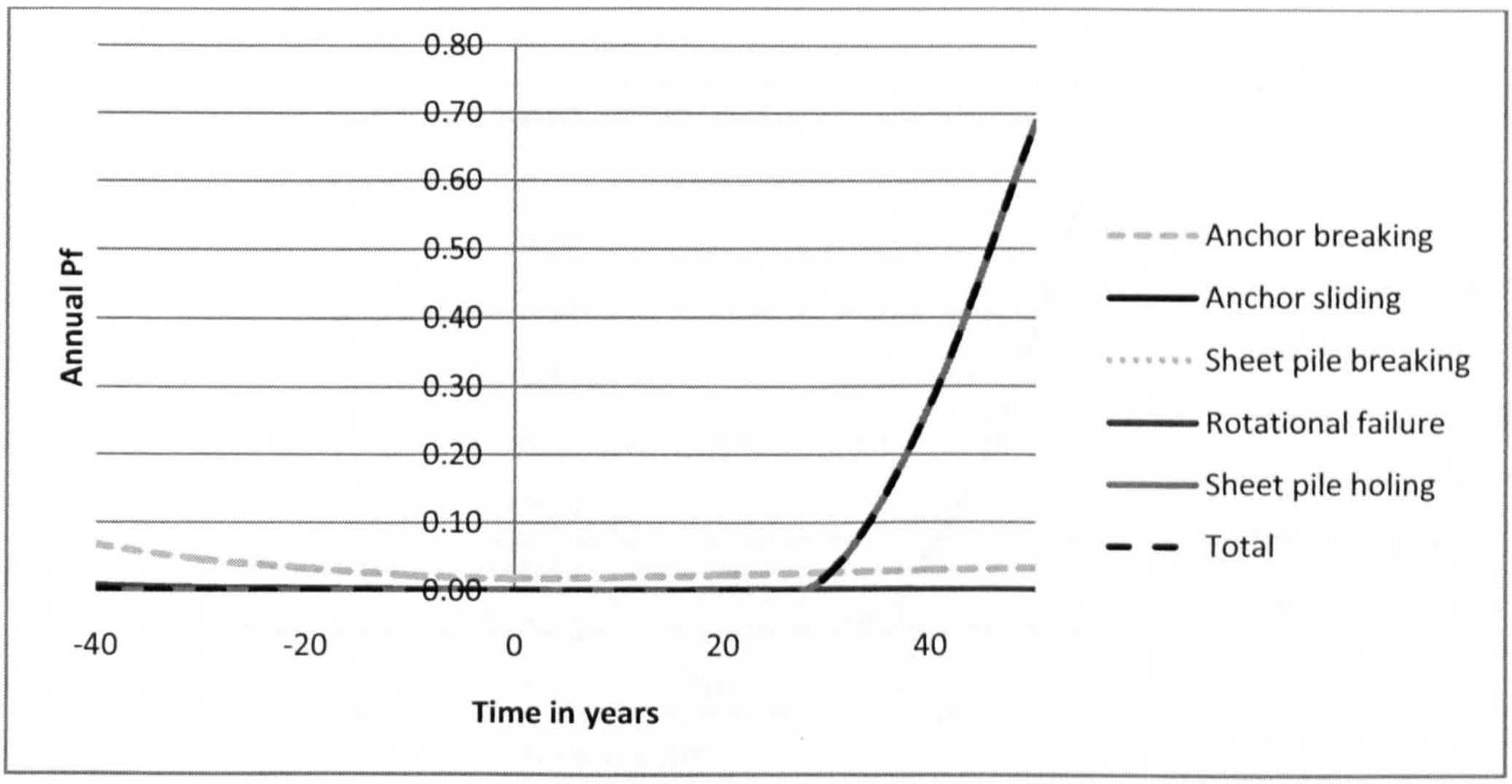

Figure 7.35 *The total probability of failure in time for flood defence section 53 and the breakdown in failure mechanisms.*

Figure 7.36 shows the probability of failure in time in case of dredging activities lowering the river bed level with one meter at t=10 years and t=30 years. The development of the overall probability of failure is unchanged compared to figure 7.35 due to the dredging activity. The probability of rotational failure increases at those moments, followed by a decrease in probability as the river bed level starts to rise again. The probability of anchor breaking also increases at the moment of dredging, and decreases as soon as the river bed level rises afterward.

Figure 7.37 shows the total probability of failure in time in case of anchor replacement at t=30 years and sheet pile refurbishment at t=40 years. The probability of anchor breaking then hardly rises from t=0 onward, after dropping due to an increasing river

bed level. The probability of sheet pile holing is not significant compared to figure 7.35.

Figure 7.38 presents the total probability of failure in time for five anchored sheet pile wall flood defence sections: number 53, 46, 50, 54 and 55. For the location of these flood defence sections see figure A.1 in appendix A. The increase in total probability of failure at a later stage in the lifetime is caused by the increasing probability of sheet pile holing. The probability of sheet pile holing becomes relevant for flood defence sections 46 and 50 in about 10 years time, whilst sections 50, 54 and 55 can carry on for another 30 years.

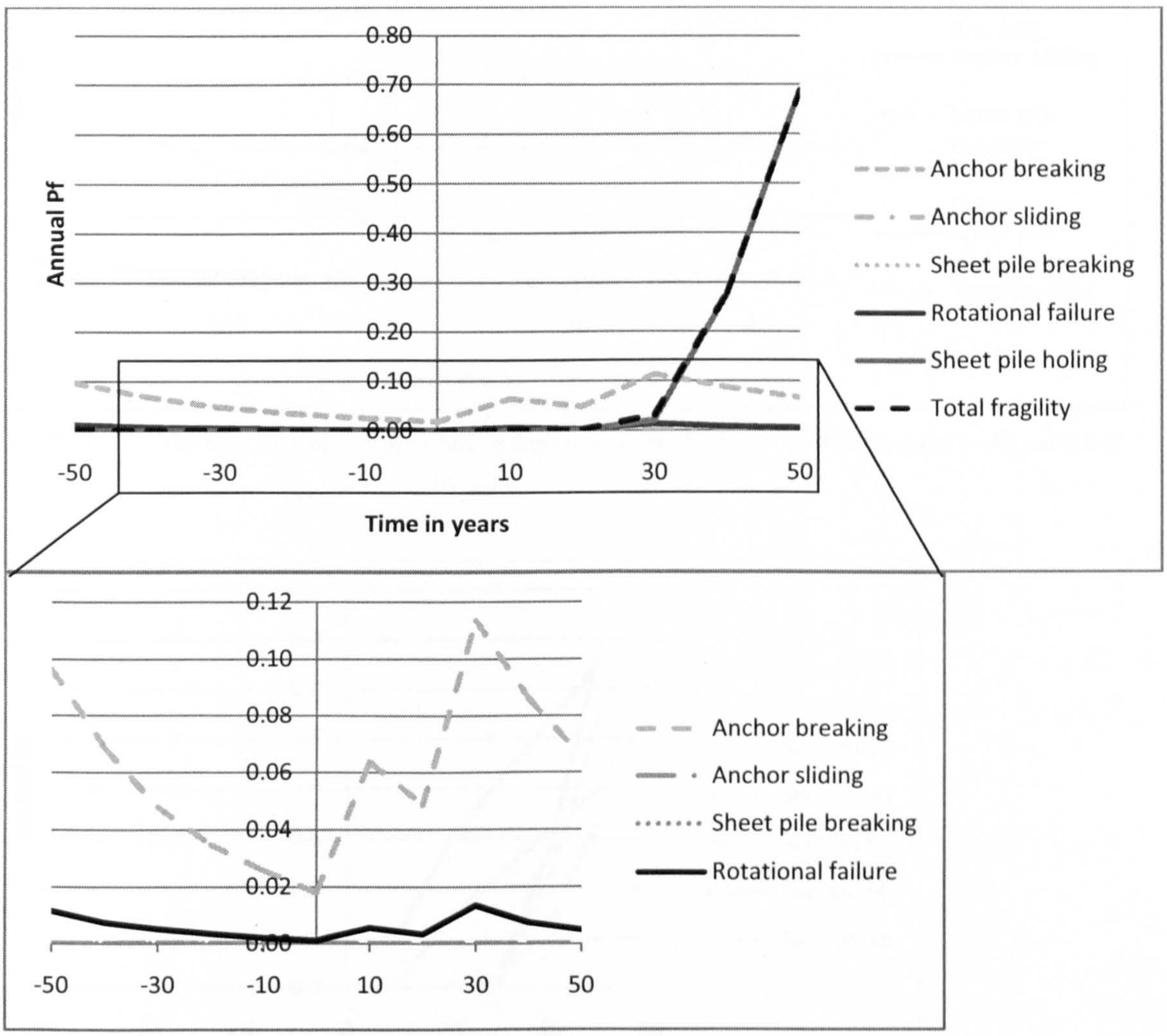

Figure 7.36 The total probability of failure in time in case of dredging (top) and more enlarged for anchor breaking, rotational failure, anchor sliding and sheet pile breaking (bottom).

Figure 7.39 shows that the lifetime reliability taking sheet pile holing into account is low for the anchored sheet pile walls. However, instability of the retained ground behind the sheet pile wall is a condition for sheet pile holing to lead to full failure of the structure. The total probability of failure is therefore lower than may seem from figure 7.39. The second series of lifetime reliability is the reliability of the anchored sheet pile walls if refurbishment is undertaken.

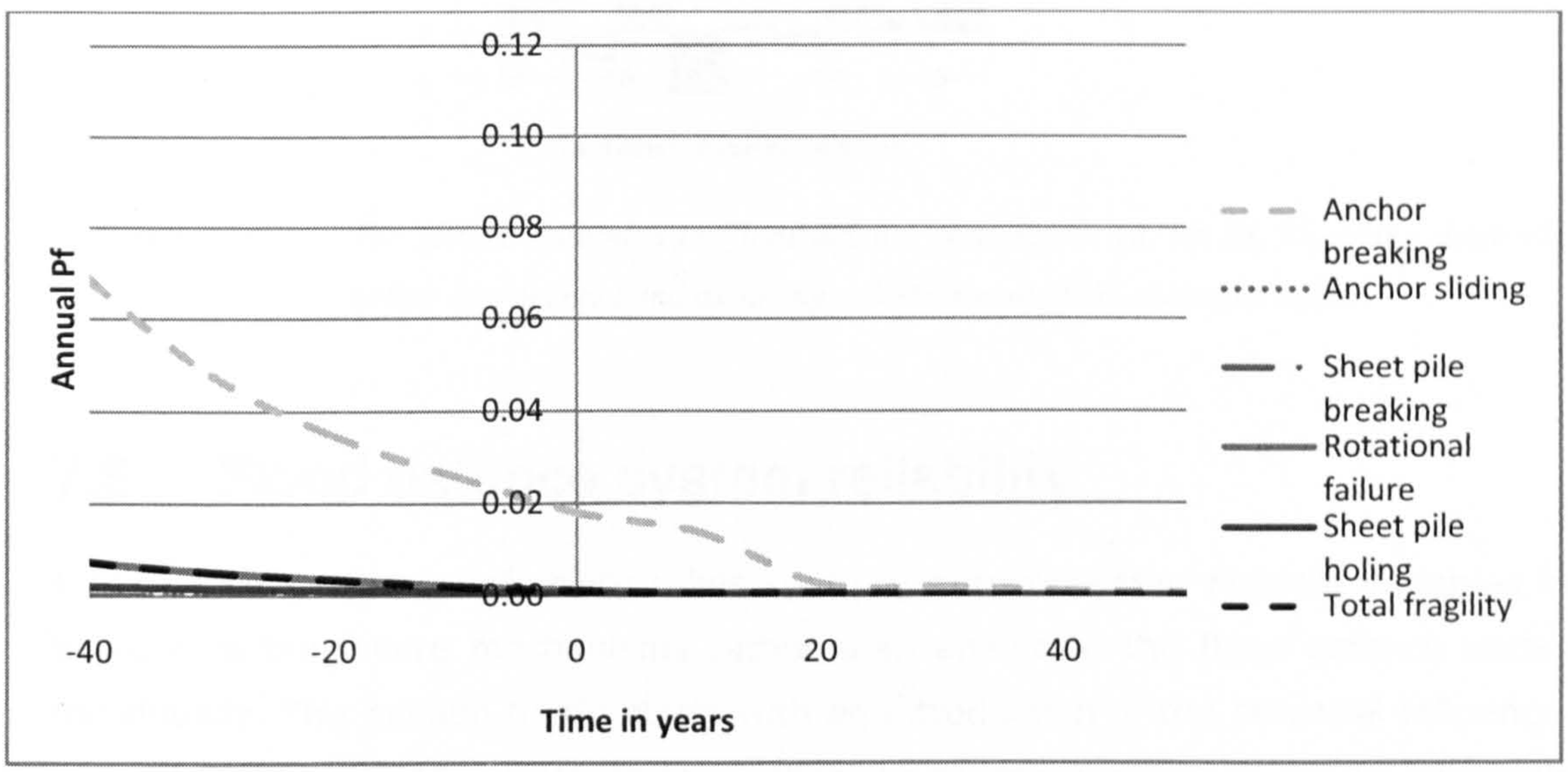

Figure 7.37 *The total probability of failure in time in case of sheet pile refurbishment at t=40 years and anchor replacement at t=30 years.*

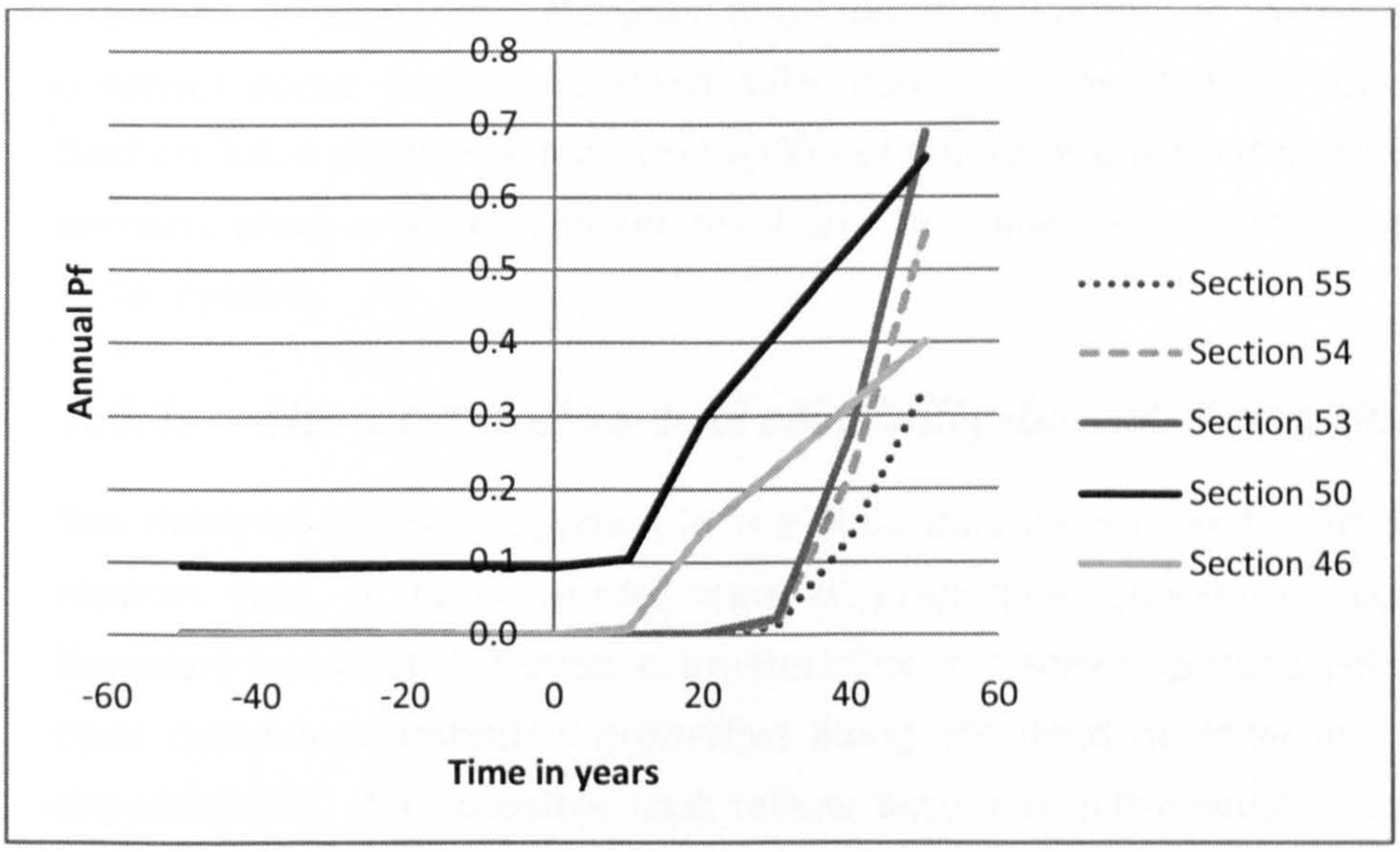

Figure 7.38 *The total probability of failure in time for flood defence sections 53, 46, 50, 54, 55.*

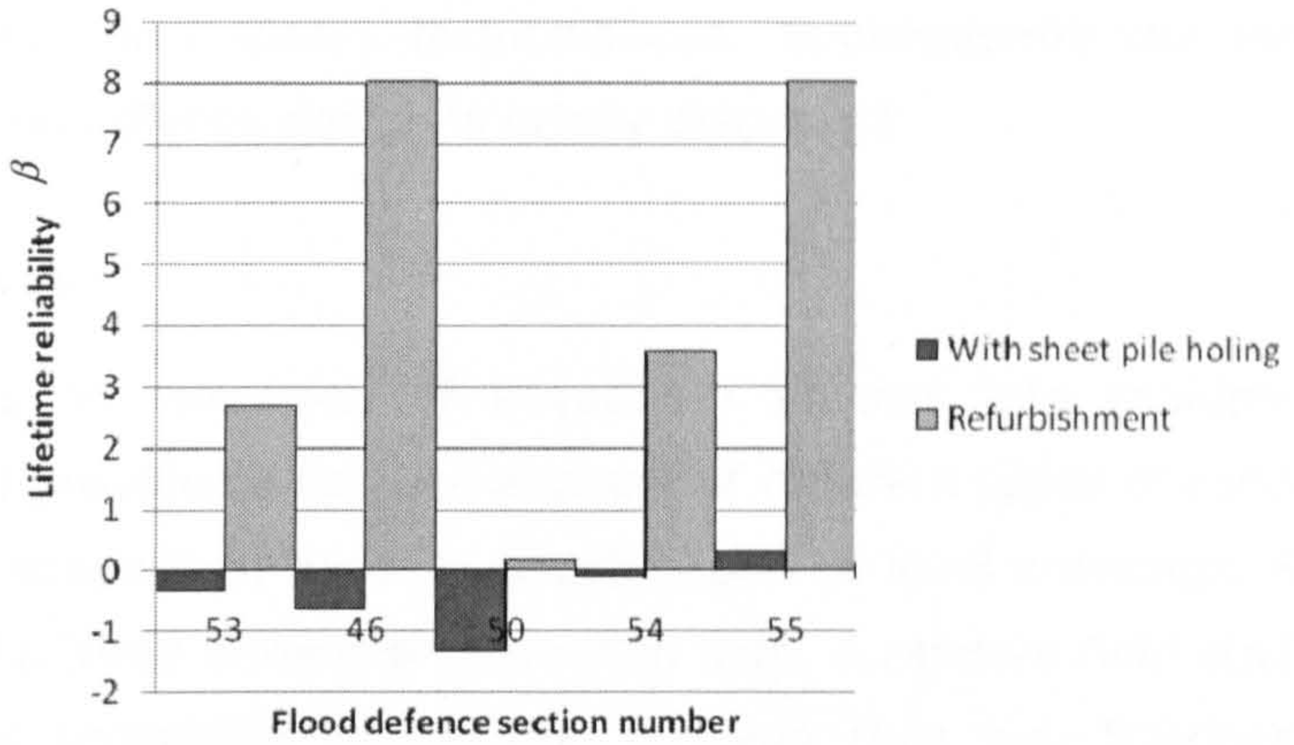

Figure 7.39 *The lifetime reliability for flood defence sections 53, 46, 50, 54, 55, taking sheet pile holing into account and assuming refurbishment of the sheet pile walls.*

7.6. Flood defence system reliability

Flood defence system reliability takes spatially autocorrelated random variables into account in the failure mechanisms rather than analysing the flood defence sections individually. This section firstly starts with an introduction in the potential influence of autocorrelated random variables in a reliability or risk analysis in 7.6.1. Approaches that have been implemented in flood defence system reliability are also briefly introduced. In section 7.6.2 the system reliability model developed for the Dartford Creek to Swanscombe Marshes flood defence system is described. Section 7.6.3 presents some results obtained with correlated asset time-dependent processes. Section 7.6.4 shows the joint probability of failure of a limited number of flood defence sections given a specific water level and the time-dependent system reliability as a serial system.

7.6.1. Random fields and reliability-based flood defence design

The material or soil properties in the flood defence line and in its foundation form a random field. In other words, material properties, geometry, vegetation, hydraulic boundary conditions or other characteristics that make up flood defence reliability can have dependent statistical properties along the flood defence line. Because of these dependencies, it is possible that failure occurs simultaneously over certain defence stretches and breach locations tend to be spatially related.

Below firstly random field theory is introduced. Subsequently the length effect in reliability-based flood defence design is briefly discussed.

Random field theory

A random field is an extension of a random process into multiple dimensions. Vanmarcke (1983) provides a detailed account of different types of random fields and e.g. their spectral properties, parameter estimation or level crossings. Soil properties are an example of a three dimensional random field. A random field $z(\mathbf{x})$ is defined by the following joint probability distribution function (see e.g. Baecher & Christian, 2003):

$$F_{x_1,..,x_n}(z_1,..,z_n) = P\{z(x_1) \le z_1,..,z(x_n) \le z_n\} \quad (7.23)$$

in which $z(x_i)$ is a stochastic process. The mean or trend and subsequently the variance of $z(\mathbf{x})$ are given by:

$$E[z(\mathbf{x})] = \mu(\mathbf{x}) \quad (7.24)$$

$$Var[z(\mathbf{x})] = \sigma^2(\mathbf{x}) \quad (7.25)$$

The covariance between $z(x_1),..., z(x_n)$ is represented by:

$$Cov[z(x_i), z(x_j)] = E[(z(x_i) - \mu(x_i)) - (z(x_j) - \mu(x_j))] \quad (7.26)$$

Stationarity and ergodicity for stochastic processes are discussed in section 5.1.1. Table 7.29 summarises the stationary, ergodic, isotropic and homogeneous properties for random fields (from Baecher & Christian, 2003).

Table 7.29 Stationarity, ergodicity, istropic property and second-order stationarity (from Baecher & Christian, 2003).

Property	Explanation
Homogeneous, stationary	Joint probability distribution functions are invariant to translation; joint probability distribution function depends on the relative, not absolute locations.
Isotropic	Joint probability distribution functions are invariant to rotations.
Ergodic	All information on joint pdf's can be obtained from a single realisation of the random field.
Second-order stationary	For all $x \in S$: $E[z(\mathbf{x})] = \mu(\mathbf{x})$ For all $x_1, x_2 \in S$: $Cov[z(x_i), z(x_j)] = C(x_1, x_2)$

Gaussian random fields have convenient statistical properties and are representative of a large number of distribution functions of properties in nature. Gaussian random fields are used in models of autocorrelation structures between soil properties (Baecher & Christian, 2003). The random field is Gaussian if the joint distribution function given by (7.23) is multivariate normally distributed. A vector **X** of *M* Gaussian random variables is characterised by the multivariate normal pdf:

$$f_{\mathbf{x}}(\mathbf{x}) = (2\pi)^{-M/2}|\mathbf{B}|^{-1/2}\exp\left\{-\tfrac{1}{2}(\mathbf{x}-\mathbf{m})^t\mathbf{B}^{-1}(\mathbf{x}-\mathbf{m})\right\} \quad (7.27)$$

in which **m** is the vector of mean values and **B** is the *M* by *M* covariance matrix.

$$\mathbf{B} = [B_{kl}] \equiv [Cov[X_k, X_l]] \equiv [\rho_{kl}\sigma_k\sigma_l] \quad (7.28)$$

B can be broken down into a unique lower triangular matrix by a Cholesky decomposition:

$$\mathbf{B} = \mathbf{C}\mathbf{C}^T \quad (7.29)$$

in which **C** is the Cholesky factor. A random sample of independent identically distributed variables $Z_1, .., Z_n \sim N(0,1)$ is transformed into a correlated random vector as follows:

$$\mathbf{X} = \mu + \mathbf{C}\mathbf{Z} \quad (7.30)$$

Other examples of random fields can be found in Vanmarcke (1983).

Length effect in flood defence design

The material or soil properties in the flood defence line and in its foundation form a random field. In other words, material properties, geometry, vegetation, hydraulic boundary conditions or other characteristics that make up flood defence reliability can have dependent statistical properties along the flood defence line. Because of these dependencies, it is possible that failure occurs simultaneously over certain defence stretches and breach locations tend to be spatially related. In the integration of the economic damages over different breach combination scenarios correlated breach scenarios have a higher joint probability than independent breaches. The economic damages related to the correlated breach combinations therefore gain more emphasis than in an independent model.

Correlated flood defence failures are referred to as the length effect. Expression (2.28) allows an illustration of the length effect in addition to the approximation of the autocorrelation at two moments in time introduced in chapter 2. Expression

(7.31) below is a simplification for the correlation between Z_i and Z_j at a location i and a location j along the flood defence line. In this expression the distance between two flood defence sections i and j is assumed to be such that the autocorrelation between strength variables R_i and R_j is negligible. The autocorrelation between the loading S_i and S_j is assumed to be 1. These assumptions lead to (7.31).

$$\rho(Z_i, Z_j) = \frac{\rho_{R_i,R_j}\sigma_{R_i}\sigma_{R_j} + \rho_{S_i,S_j}\sigma_{S_j}\sigma_{S_i}}{\sigma_{Z_i}\sigma_{Z_j}} = \frac{\sigma_S^2}{\sigma_R^2 + \sigma_S^2} \qquad (7.31)$$

in which ρ_{R_i,R_j} is the correlation between the strength R at location i and location j, σ_{R_i} is the standard deviation of the strength at location i, σ_{R_j} is the standard deviation of the strength at location j, ρ_{S_i,S_j} is the correlation between the loading S at location i and at location j, σ_{S_i} is the standard deviation of the loading at $t=i$ and σ_{S_j} is the standard deviation of the loading at $t=j$.

If the variation in the loading, σ_S, is much larger than the variation in the strength, σ_R, then the correlation between failure at location i and at location j, $\rho(Z_i, Z_j) \approx 1$. The next challenge is to describe the autocorrelation between material and soil properties with a correlation function such as introduced in (2.31). The shape of the correlation function is a factor in whether the serial probability of failure of flood defence section converges to a stabile value given finer discretisation grids (Chun-Ching LI & Der Kiureghian, 1993). Correlation functions that are convex at distances of $x \downarrow 0$, where x is the distance between two autocorrelated properties, do not converge to a stabile value. Correlation functions that are concave do converge.

Vrouwenvelder (2001b) defines the autocorrelation between flood defence properties by (2.31). Vrouwenvelder (1999) describes a method based on the formulation of the limit state function in the standard normal space corresponding with (2.12), see figure 7.39. The limit state functions of the failure mechanisms for each flood defence section are combined to form one equivalent limit state function. Each flood defence section along the flood defence line of interest is then represented by one equivalent limit state function in the form of (2.12), referred to in figure 7.40 by Z_{Ae}. The reliability indices of the flood defence sections are modelled with a Gaussian random process. The correlation matrix is derived as indicated in the right hand box in figure 7.39. $\rho_{A,B,k}$ in those expressions is the spatial autocorrelation of random variable k in the limit state function. The Gaussian random field is in this model applied to the random variables of the limit state functions in the design point. The bivariate and

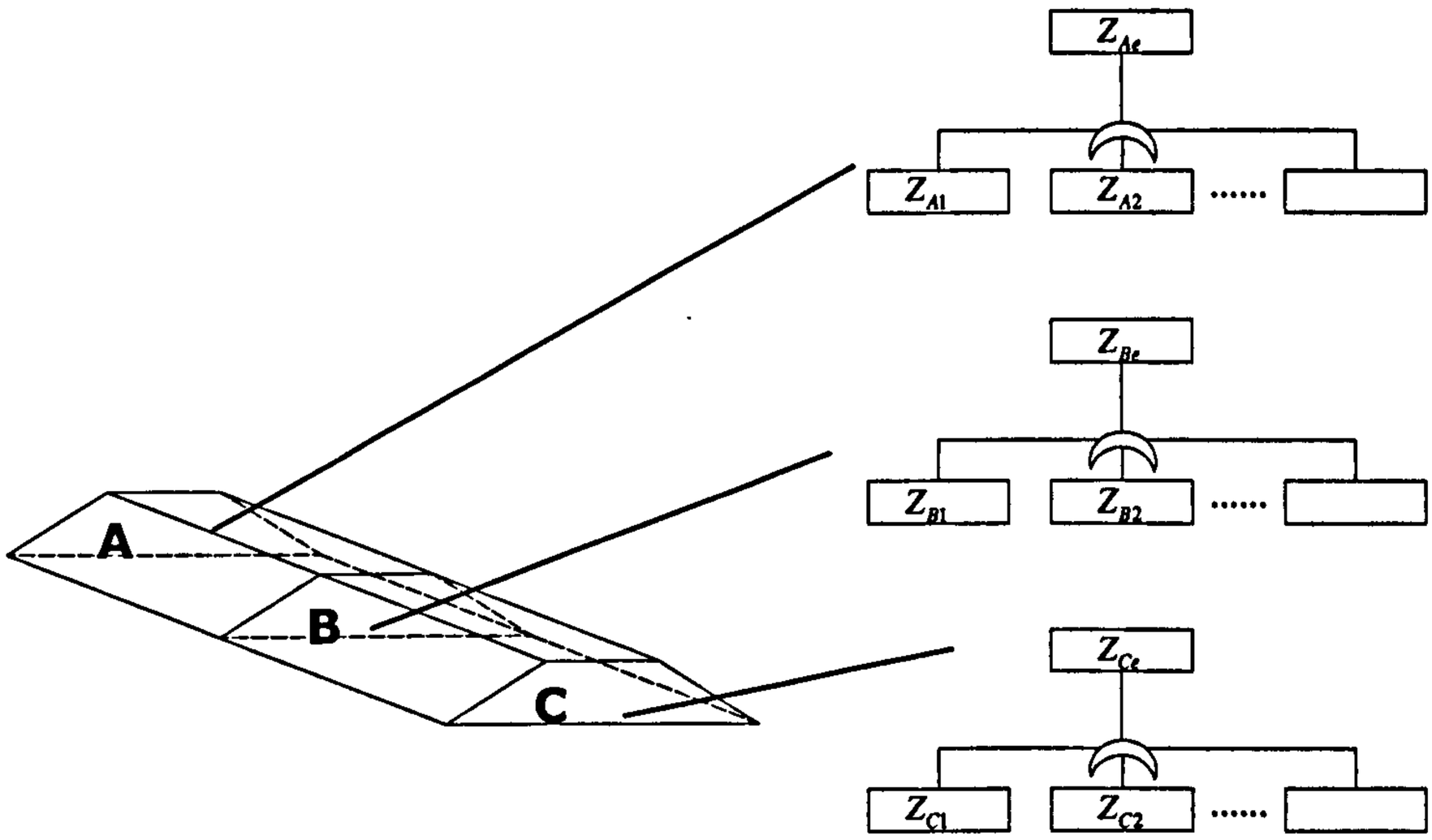

Derivation of equivalent limit state function for one flood defence section

$$Z_{A1} = \beta_{A1} + \alpha_{A11}u_{A11} + \alpha_{A12}u_{A12} + \ldots = \beta_{A1} + \sum_{k=1}^{n} \alpha_{A1k}u_{A1k}$$

$$Z_{A2} = \beta_{A2} + \alpha_{A21}u_{A21} + \alpha_{A22}u_{A22} + \ldots = \beta_{A2} + \sum_{k=1}^{n} \alpha_{A2k}u_{A2k}$$

$$\rho_{Z_{Ai}Z_{Aj}} = \sum_{k=1}^{n} \alpha_{Aik}\alpha_{Ajk}\rho_{Aijk}$$

$$\Phi(-\beta_{Ae}) = \Phi(-\beta_{A1}) + \Phi(-\beta_{A2}) - BVN(-\beta_{A1}, \beta_{A2}, \rho_{Z_{A1}Z_{A2}}).$$

$$Z_{Ae} = \beta_{Ae} + \alpha_{Ae1}u_{Ae1} + \alpha_{Ae2}u_{Ae2} + \ldots = \beta_{Ae} + \sum_{k=1}^{n} \alpha_{Aek}u_{Aek}$$

Derivation of joint probability of failure

$$\rho_{Z_{Ae}Z_{Be}} = \sum_{k=1}^{n} \alpha_{Aek}\alpha_{Bek}\rho_{A,B,k}$$

$$\mathbf{R}_{A,B,C} = \begin{bmatrix} 1 & \rho_{Z_{Ae}Z_{Be}} & \rho_{Z_{Ae}Z_{Ce}} \\ \rho_{Z_{Be}Z_{Ae}} & 1 & \rho_{Z_{Be}Z_{Ce}} \\ \rho_{Z_{Ce}Z_{Ae}} & \rho_{Z_{Ce}Z_{Be}} & 1 \end{bmatrix}$$

$$\Phi_{Joint}(-\beta_{Joint}) = MVN(-\beta_{Ae}, -\beta_{Be}, -\beta_{Ce}, \mathbf{R}_{A,B,C})$$

Z_{Ai}	= Limit state equation for failure mechanism *I* of flood defence section *A*.
β_{Ai}	= Reliability index for failure mechanism *I* of flood defence section A.
α_{Aik}	= Direction cosine for random variable *k* in failure mechanism *I*, of flood defence section A.
u_{Aik}	= Standard normal representation for random variable *k* in failure mechanism *I*, of flood defence section A.
$\rho_{Z_{Ai}Z_{Aj}}$	= The correlation between failure mechanism *I* and *J* of flood defence section A.
Z_{Ae}	= Equivalent limit state equation for flood defence section A, amalgamating the rest of the failure mechanisms.
β_{Ae}	= Equivalent reliability index of flood defence section A
α_{Aek}	= Equivalent direction cosine of random variable *k*, amalgamating the direction cosines of *k* in the failure mechanisms of defence section *k*.
u_{Aek}	= Equivalent standard normal representation for random variable *k*, of flood defence section A.
$\rho_{Z_{Ae}Z_{Be}}$	= The correlation between the equivalent limit state functions of flood defence section A and B.
$\rho_{A,B,k}$	= Autocorrelation of random variable *k* between flood defence sections A and B, expression (2.31)
$\mathbf{R}_{A,B,C}$	= Correlation matrix between flood defence sections A, B and C

Figure 7.40 *Derivation of an equivalent limit state function and the joint probability of failure of flood defence sections according to Vrouwenvelder (1999).*

multivariate normal distributions are calculated according to Hohenbichler & Rackwitz (1983). The method in figure 7.40 is a computationally feasible method in the context of large scale flood risk assessments. The method subdivides a flood defence section into slices with the size of an equivalent correlation distance. The equivalent correlation distance entails a rough approximation. It would be interesting to know whether it captures the discretisation grid for which stabilisation of the serial system probability is achieved. This method is not further investigated in this context.

7.6.2. Definition of the time-dependent system reliability model

This section describes the time-dependent system reliability model applied to the Dartford Creek to Swanscombe Marshes flood defence system, see figure 7.41. It is an

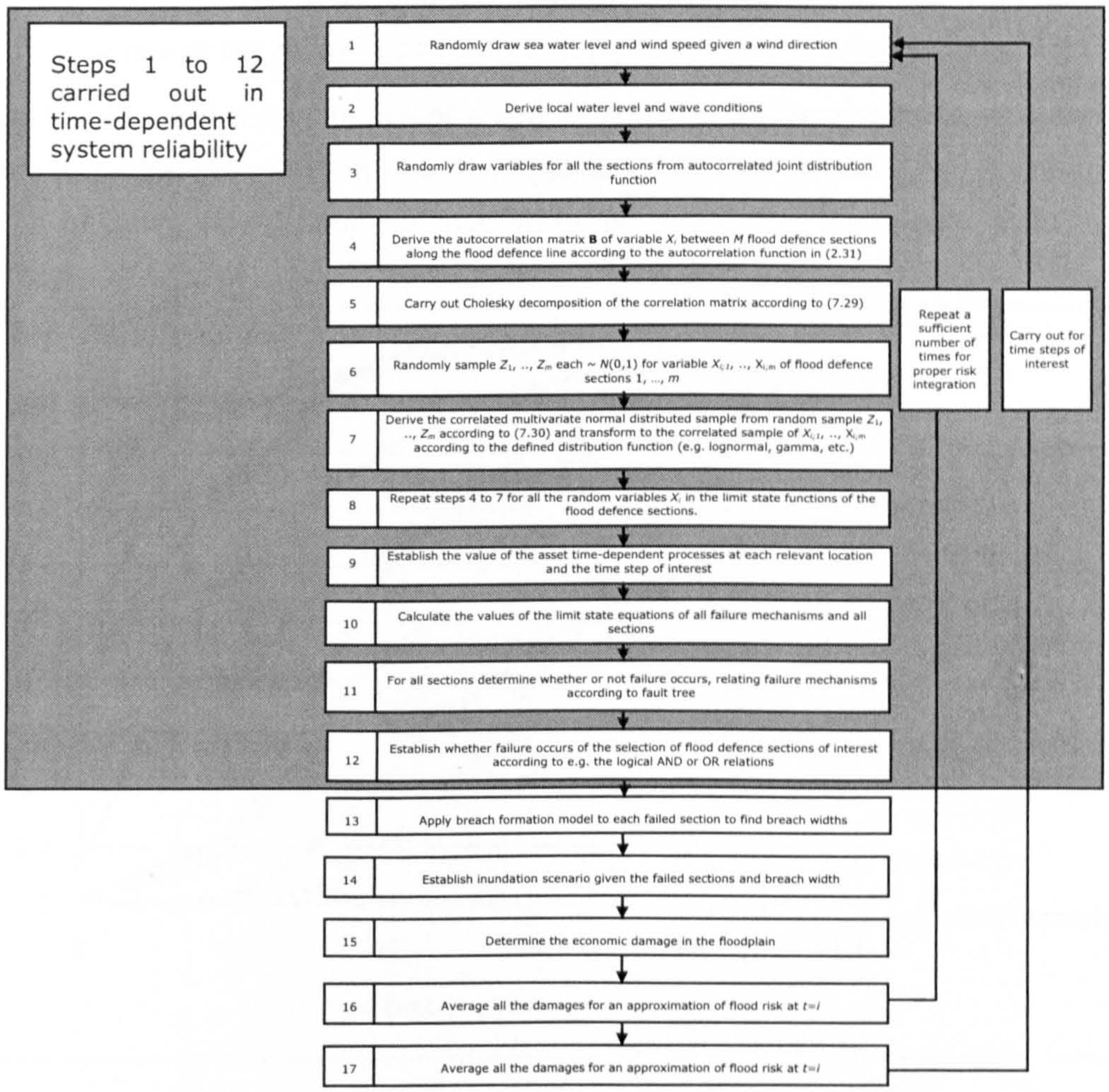

Figure 7.41 *Steps in time-dependent system reliability calculations in the perspective of a flood risk assessment. Steps 1 to 12 are carried out for the Dartford Creek to Swanscombe Marshes flood defence system.*

alternative system reliability approach to that shown in figure 7.40 after Vrouwenvelder (1999). The advantage of the model presented in figure 7.41 is that it allows a detailed representation of the Gaussian correlation structure of the variables in the limit state functions between different locations of interest. The autocorrelation model is not specifically related to the formulation of the limit state functions in the design point in the standard normal space. Neither does the method require the derivation of equivalent limit state functions or an approximation of equivalent direction cosines. However, the method in figure 7.41 is computationally intensive and the Cholesky factor is sensitive to the correlation values in the correlation matrix. In order to achieve a Cholesky decomposition the correlation matrix must be positive definite. A positive definite correlation matrix has positive eigenvalues. Appendix D contains the autocorrelations and correlation distances which are applied to the random variables in the model according to equation (2.31) in step 4 figure 7.41.

Section 7.6.3 shows the influence of a spatial autocorrelation structure on asset time-dependent processes. Section 7.6.4 compares the joint probability of failure of a selection of independent flood defence sections with that of correlated flood defence sections.

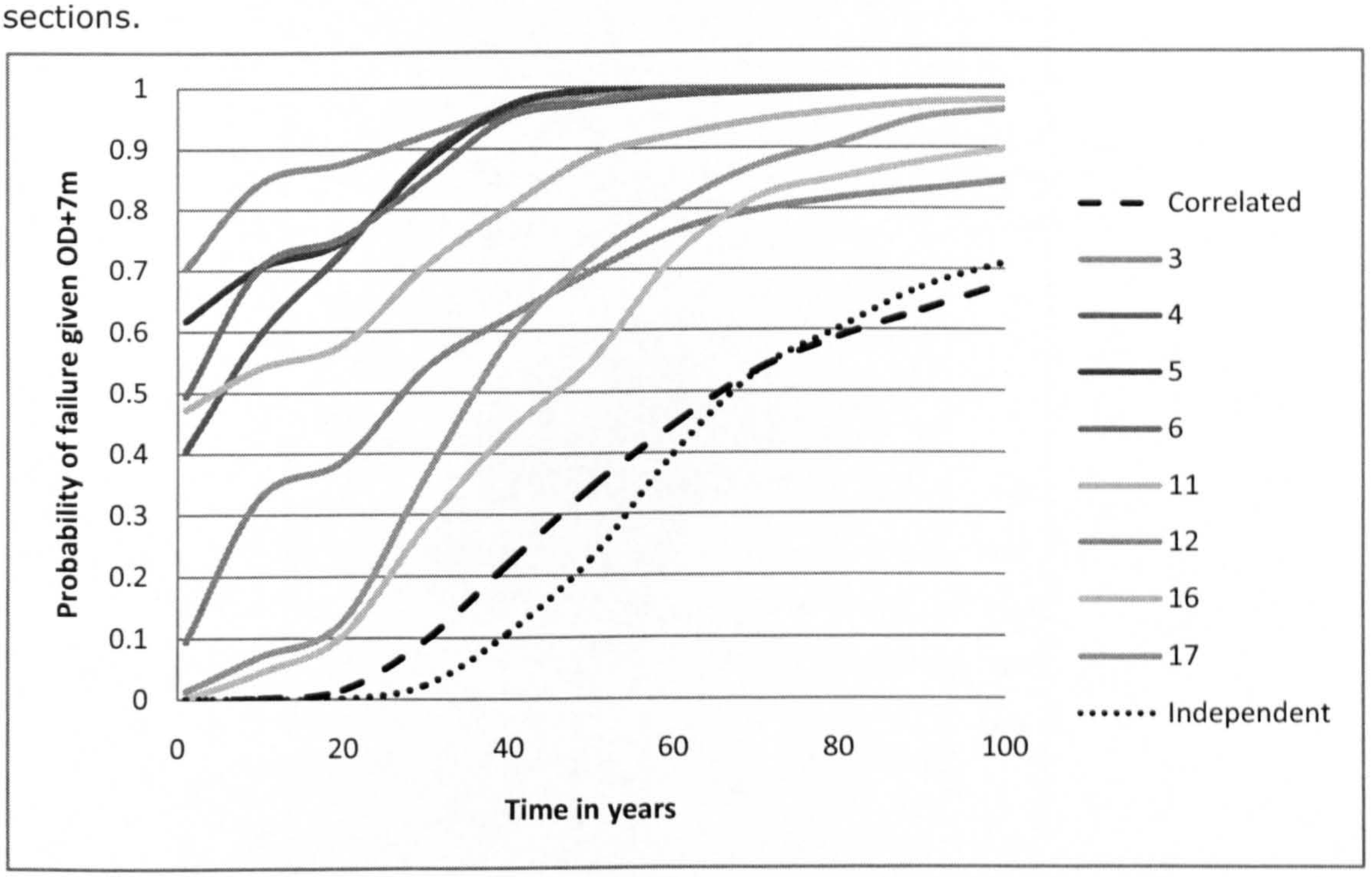

Figure 7.42 *The correlated and independent joint probability of failure of flood defence sections 3, 4, 5, 6, 11, 12, 16 and 17.*

7.6.3. Time-dependent system reliability analysis

Figure 7.42 presents the joint probability of failure of an arbitrary selection of flood defence sections given a water level of OD+7m. The joint probability of failure taking autocorrelations into account is compared to independent flood defence sections. The number of simulations is limited which may explain why the independent joint probability of failure is higher than the correlated joint probability of failure for t>70.

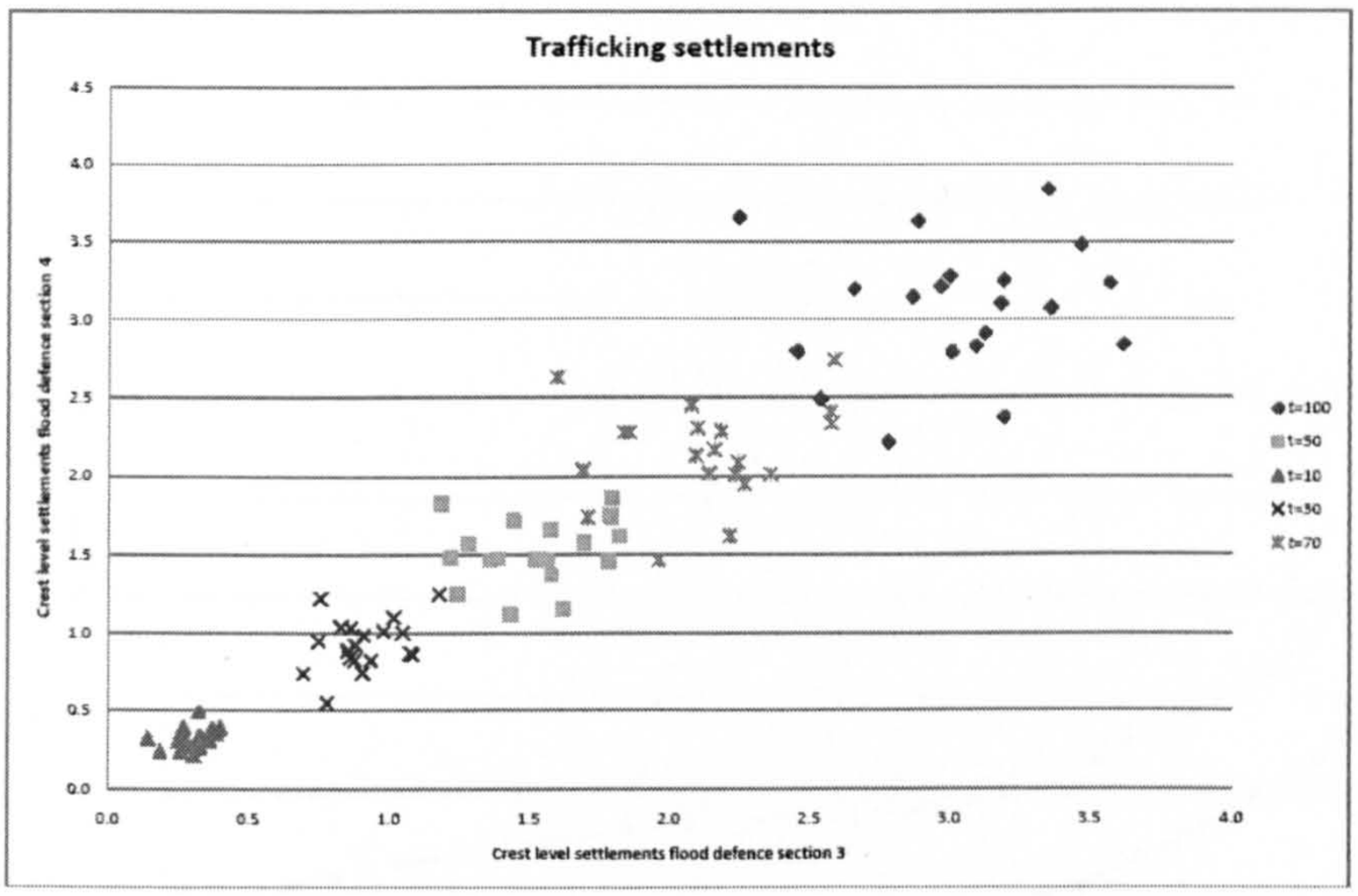

Figure 7.43 *The crest level settlements for flood defence section 3 and 4 due to trafficking (top) and due to compaction (bottom).*

Crest level settlements determine the time-dependency in the probability of failure for OD+7m. The asset time-dependent processes trafficking and settlements show spatially no autocorrelation as a correlation distance smaller than the flood defence length has been applied (figure 7.43). The spatial autocorrelation between the reliability of the flood defence sections therefore decreases while the influence of the time-dependency increases with time.

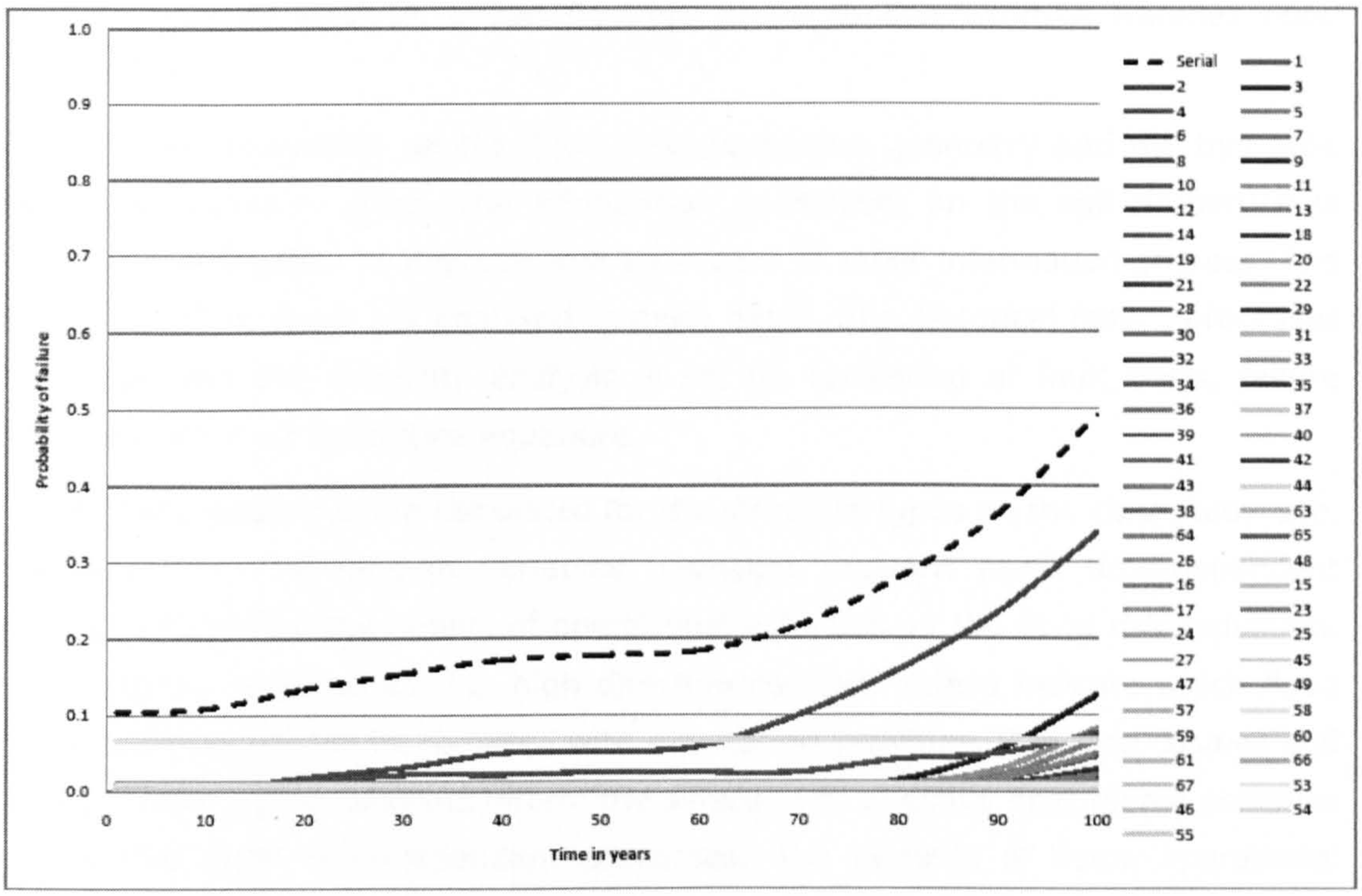

Figure 7.44 *The probability of serial system failure and the probability of the individual flood defence sections.*

Figure 7.44 shows the time-dependent probability of serial system failure taking autocorrelation into account. The flood defence sections with the highest probability of failure dominate the serial system probability of failure. The probability of serial system failure is higher than the flood defence section with the highest probability of failure.

The probability of serial system failure is quite high. The probability of failure of the reinforced concrete wall sections are causing the high probability in the first 60 years of the system calculation. The high probability of reinforced concrete wall failure is dominated by piping directly under the toe of the wall. This failure mechanism is a

simplified model not taking remaining strength into account. The storm level needs to persist long enough to initiate piping and the permeability is modelled conservatively.

7.7. Review

The theory presented and developed in chapters 2 to 7 are demonstrated in a time-dependent reliability analysis of the Dartford Creek to Swanscombe Marshes flood defence system.

The information availability on the flood defence system geometry and the hydraulic boundary conditions is good. The information availability on the soil properties is patchy, but it is possible to improve that by means of other information sources. The individual structure types are analysed in more detail. The historical failure processes are collected and the reliability analysis is set up consisting of fault trees, failure mechanisms and their limit state equations.

The importance measures are calculated for the structure types on the case study site, i.e. sensitivity to the random variables, highlight relevant asset time-dependent processes and indicate the impact of operational activities on the flood risk reduction. High uncertainty contributors, i.e. high direction cosines, indeed indicate which flood defence properties should be targeted with monitoring activities. Direction cosines and partial derivative based concepts inform the selection of effective operational activities and influential asset time-dependent processes. The benefits of some operational activities, such as dredging, can only be properly captured at a system level.

Subsequently, the asset time-dependent processes of the structure type are analysed according to the modelling methodology outlined in chapter 5. Due to the limited information availability all the asset time-dependent processes fall in situation 4 in table 6.5: scarce data availability on asset time-dependent quantity $X_i(t)$ represented by a hierarchical process model. The opportunities for parameter estimation, calibration and model corroboration are therefore limited. In case a process model is available, it depends on the emphasis of the inherent uncertainties in time whether a parametric process model suffices or whether a hierarchical process model is required. In this context, two different situations are brought forward. Firstly, settlements due to compaction are e.g. driven by a load which is static in time, whilst ancillary pore pressures are subject to inherent uncertainty in time. The influence of the pore

pressures is such that the statistical properties of the hierarchical model are nearly equal to those of the parametric process model. Secondly, in some cases, the attribution of variation in measurements to inherent uncertainty in time or space affects the variation in the predictions of the hierarchical process model. If the attribution is mainly to inherent spatial uncertainty, the hierarchical process model predictions are similar to those of a parametric process model. Finally, it is noted that the gamma process model provides an approximation to the hierarchical process model for most of the asset time-dependent processes. However, the asset time-dependent processes seepage length reduction and anchor corrosion are not properly represented by a parametric process model. It is also difficult to approximate the hierarchical process model predictions closely by a gamma process model.

Based on the asset time-dependent analysis, time-dependent fragility and lifetime probability of failure is calculated. Time-dependent fragility and lifetime probability appropriately reflect the influence of the asset time-dependent processes and the impact of operational activities. The influence of the processes and activities is also expressed in the probabilities of individual failure mechanisms. The flood defence sections with a higher lifetime probability relative to other sections are not necessarily the sections with a higher initial annual probability of failure. The rate and influence of the asset time-dependent processes can increase the probability of failure of some sections faster than others. The fragility of the reinforced concrete walls is not time-dependent in this thesis. The influence of carbonation and reinforcement corrosion on the performance of the wall is negligible. The prominent failure mechanism in the reliability model is piping directly underneath the reinforced concrete wall. The toe depth of the wall is mainly a design concern. The wall is not strong once the water level reaches the reinforced concrete wall. Two failure processes are not taken into account in the time-dependent fragility of reinforced concrete walls, i.e. deterioration of joints between reinforced concrete wall units and cracking of the reinforced concrete. Joint failure between reinforced concrete wall units is not taken into account. A failure mechanism for increased flow velocity through the gaps in the joints initiating piping underneath the reinforced concrete wall is not available. Cracking of reinforced concrete due to an increased volume of corroded reinforcement bars is not taken into account. It is expected that cracking has a significant effect on the performance of the reinforced concrete wall. The fragility of anchored sheet pile walls balances the destabilising influence of anchor corrosion by the stabilising influence due to toe level

accretion. Sheet pile holing due to corrosion leads to a high probability of failure in 50 years time. However, this probability of failure does not include the remaining strength represented by the stability of the soil behind the anchored sheet pile wall. The economic damage of e.g. collapsing assets on the instable ground caused by failure of the anchored sheet pile is not taken into account in the flood risk assessment.

Finally, the time-dependent system reliability model for the flood defence system is defined and the time-dependent system reliability results are produced. The system reliability model represents the autocorrelation structure in a detailed way, see figure 7.40. However, the method is computationally intensive and the Cholesky factor is not always convenient with the representation of higher autocorrelations. The time-dependent probability of failure of jointly failing flood defence sections shows a correlation for lower time steps. The correlation becomes smaller while the influence of the asset time-dependent processes increases. This effect is explained by the fact that the autocorrelation applied in the asset time-dependent process models is such that the simulations between flood defence sections are independent.

The autocorrelation structure therefore has an influence on jointly failing flood defence sections at a distance of a flood defence length. A further subdivision in smaller slices of the flood defence sections itself will therefore have an influence on the reliability of one flood defence section. This influence has not been further explored in this thesis.

The probability of serial system failure appropriately provides a higher probability of failure than that of the weakest flood defence section. The high results are explained by the failure mechanism piping underneath the toe of the reinforced concrete wall. The condition that the storm level must persist sufficiently long and the conservative estimate of the permeability are both sources of more piping resistance than is taken into account.

The following chapter contains the conclusions and recommendations of the thesis.

8. Brief overview, conclusions and recommendations

This chapter starts in section 8.1 with a brief overview of the research aim and objectives and the research contributions made in each chapter. The conclusions are presented in section 8.2 according to the objectives. The recommendations are discussed in section 8.3 according to the objectives.

8.1. Brief overview

Chapter 1 introduced the research aim and objectives in section 1.3. The research aim is to investigate how the time-dependent behaviour of flood defence properties can be appropriately characterised and incorporated in a reliability-based approach. The investigation in this research project is restricted to flood defence asset time-dependent processes. Flood defence asset time-dependent processes can be simulated for individual assets in contrast to system time-dependent processes which require simulation at a flood defence system level. An example of an asset time-dependent process is crest level settlements. An example of a system time-dependent process is sea level rise due to climate change.

The aim is achieved by the following 4 research objectives:

1. Review existing time-dependent structural reliability methods, maintenance optimisation frameworks and statistical models for time-dependent processes in the engineering industry.
2. Develop a method to highlight relevant time-dependent processes and maintenance operations in the context of a rational maintenance framework.
3. Provide a systematic methodology to develop alternative statistical models for time-dependent processes at the flood defence individual asset level.

4. Incorporate the statistical models for time-dependent processes in the reliability analysis of the Dartford Creek to Swanscombe Marshes flood defence line.

A brief overview is given of the research contributions made in each chapter. The relations between the research objectives and the thesis chapters are given in figure 1.6 and as part of the brief overview shown in figure 8.1 below.

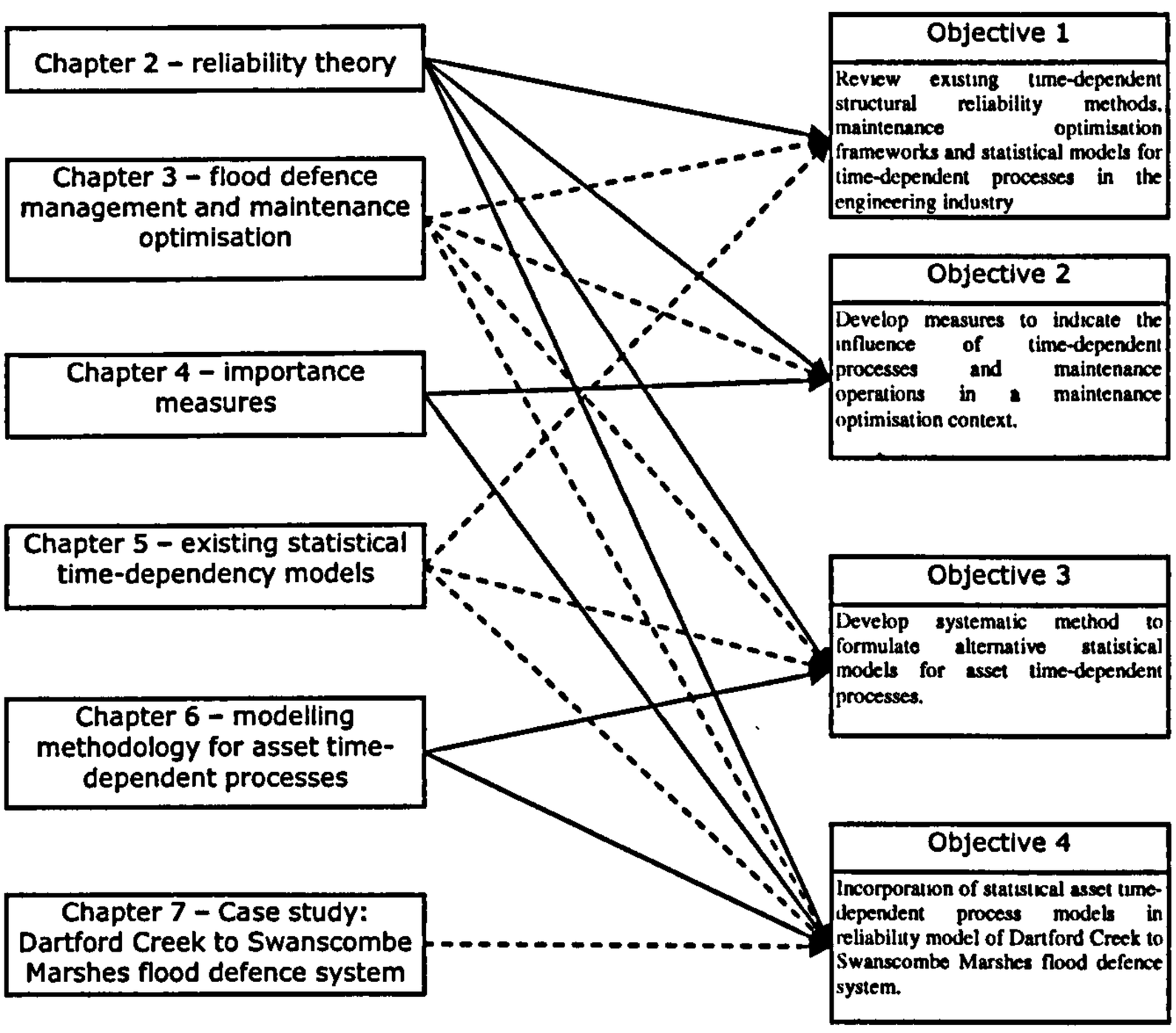

Figure 8.1 The relations between the chapters and the research objectives (also figure 1.6)

Chapter 2 is an overview of existing structural reliability theory. Chapter 3 describes current flood defence management practice and quantitative, qualitative and mixture rational maintenance optimisation frameworks. Chapter 4 develops the importance measures for asset time-dependent processes and maintenance operations in the context of the overarching maintenance optimisation context. These Importance measures correspond with objective 2 in this thesis. Chapter 5 gives additional theoretical background to existing statistical models for time-dependent processes. Chapter 6 sets out the modelling methodology for statistical models of asset time-dependent processes, corresponding with objective 3 in this thesis. Chapter 7

demonstrates the methods with a time-dependent (system) reliability model on the Dartford Creek to Swanscombe Marshes flood defence system, objective 4.

8.2. Conclusions

Sections 8.2.1 to 8.2.4 present the conclusions according to the 4 research objectives mentioned above in section 8.1.

8.2.1. Objective 1: review

The following conclusions are drawn with respect to the review of structural reliability methods in chapter 2.

1.a. The uncertainty classification in reliability-based flood defence design (figure 2.1) is a suitable framework to analyse the uncertainties involved with asset time-dependent processes.

1.b. Reliability theory and probabilistic calculation methods to incorporate statistical models for asset time-dependent processes are available. The time-dependent reliability approach rather than the time-integrated reliability approach is applied in the calculations.

1.c. Existing risk-based methods for flood defence systems are suitable to support large scale flood risk assessments. These methods allow the extension with asset time-dependent processes.

The following conclusions are relevant with respect to the review of current flood defence management practice and rational maintenance decision-making frameworks in chapter 3.

1.d. A quantitative rational maintenance optimisation framework has not yet been specified for flood defence management, though significant progress has been made in the definition of parts of the building blocks (table 3.4). Such a quantitative rational maintenance framework generally consists of four building blocks: a functional system model, a risk and reliability system model, an operational management model and a calculation optimisation model. The existing components are drawn together in this thesis in an overarching rational maintenance approach and where possible complemented with theory from other fields in the engineering industry.

1.e. It is expected that a mixture between a quantitative and qualitative maintenance decision-making framework is practically the most attractive approach. A mixture approach combines the computational feasibility of a qualitative approach with the objective prioritisation enabled by a quantitative approach.

1.f. The discussion of the quantitative rational maintenance optimisation framework is of relevance for this thesis for several reasons. The framework firstly shows the overarching context of time-dependent system reliability analysis. Secondly, that framework is the context of the risk-based importance measures in objective 2. Thirdly, in such a maintenance optimisation framework the asset time-dependent processes can be modelled with a Bayesian or a Markovian approach. This choice has two implications for the maintenance framework. Firstly, it determines the type of statistical models for the asset time-dependent processes. It is noted that the Bayesian maintenance optimisation framework also allows the incorporation of Markovian asset time-dependent process models. Secondly, it determines how the information from monitoring (experiments) is taken into account in the maintenance optimisation model. The Bayesian approach is in this thesis favoured over the Markovian decision process approach as it internalises rather than discards historical time series observations and dependencies.

The following conclusions are made with respect to the review of existing statistical models for time-dependent processes in chapter 5.

1.g. The statistical models for asset time-dependent processes are categorised according to three main compositions: a stochastic process for an overall asset time-dependent quantity; a hierarchical process model consisting of a function of random variables and one or more stochastic processes; a parametric process model consisting of a function of random variables and a deterministic time.

1.h. A stochastic process for an overall asset time-dependent quantity is in some cases favoured over a more detailed hierarchical process model. Lack of scientific understanding or the unavailability of field information are for example reasons to choose for such an approximation. It is also possible that due to financial and time constraints in some situations a detailed approach is not feasible.

1.i. There is a collection of existing suitable stochastic process models to model different types of asset time-dependent processes e.g. recurrent shock damages or gradual continuously developing processes.

1.j. Suitable multivariate distributions to represent correlations between asset time-dependent processes exist.

8.2.2. Objective 2: importance measures

The following conclusions are made with respect to risk-based importance measures for flood defence management in chapter 4:

2.a. Sensitivity analysis methods point out the sensitivity of flood defence reliability to the random variables in the reliability model. Direction cosines point out the highest uncertainty contributing flood defence characteristics. Partial derivative based concepts provide additional sensitivity information. Such information indicates which random variables might introduce time-dependency or a significant change in reliability due to operational activities. It needs to be placed in a cost benefit context to provide a basis for rational comparison of the impact of asset time-dependent processes or of operational activities.

2.b. The cost benefit ratio is suitable to highlight relevant asset time-dependent processes. The cost of remediation of the time-dependency is divided by the rate in flood risk change due to the asset time-dependent process. This knowledge enables targeting monitoring activities or eliminating irrelevant processes from the life cycle optimisation model. A life cycle model needs to be populated with field information and scientific understanding about the asset time-dependent processes before it can be used. The monitoring intends to improve the scientific understanding of time-dependency, populate and update the optimisation model or to identify trigger condition levels for more detailed inspection or repair.

2.c. There are two types of monitoring. *The first type* is monitoring that intends to collect information to populate the maintenance optimisation model, increase the scientific understanding of time-dependency or to identify trigger condition levels for further maintenance operations. The value of this type of monitoring must be established in the context of life cycle optimisation. It is therefore difficult to compare its value to that of repair or improvement activities in advance of or without full life cycle optimisation. It is possible to target this type of monitoring to relevant asset time-dependent processes, see conclusion 2.b. *The second type* of monitoring increases the confidence about the random variables in the reliability model. The cost-benefit ratio enables an approximate comparison of the value of more precise knowledge about the flood risk level, irrespective of

whether the level turns out higher or lower, to the value of a repair or improvement activity.

2.d. The cost-benefit ratio provides a suitable basis for comparison of operational activities. The cost of a repair or improvement activity is compared to the decrease in flood risk achieved by the activity. As mentioned in conclusion 2.c, monitoring aiming to increase the level of knowledge about the reliability model can also be compared with repair or improvement operational activities. The cost of the monitoring activity is divided by the change in flood risk due to increased knowledge. The effect on the flood risk of monitoring to increase the level of knowledge diminishes with an increasing amount of monitoring activities. There are two benefits that are not quantified in this thesis. The first benefit is that routine inspection activities often increase the knowledge about the whole flood defence system for the same cost. This thesis only considers individual flood defence sections. The second benefit is that specific inspection detects ongoing failure processes in addition to increasing the level of knowledge.

8.2.3. Objective 3: modelling methodology asset time-dependency

The following conclusions are made with respect to the development of the modelling methodology for statistical models of asset time-dependent processes in chapter 6.

3.a. The modelling methodology proposed in chapter 6 provides a structured approach to build statistical models of asset time-dependent processes. The methodology deals with both a qualitative and quantitative quality evaluation of the statistical model at the level of the asset time-dependent process as well as at the level of the overarching maintenance optimisation model.

3.b. The five-step analysis of the asset time-dependent process in the conceptualisation phase of the modelling methodology (figure 6.2 and 8.2) develops assessable, and hence less subjective, internal model structures. The analysis appropriately captures: existing field information or scientific understanding about the process; the flood defence properties driving or involved with the process and the uncertainties that they introduce; the behaviour of the process conditional on the excitation; the dependencies among

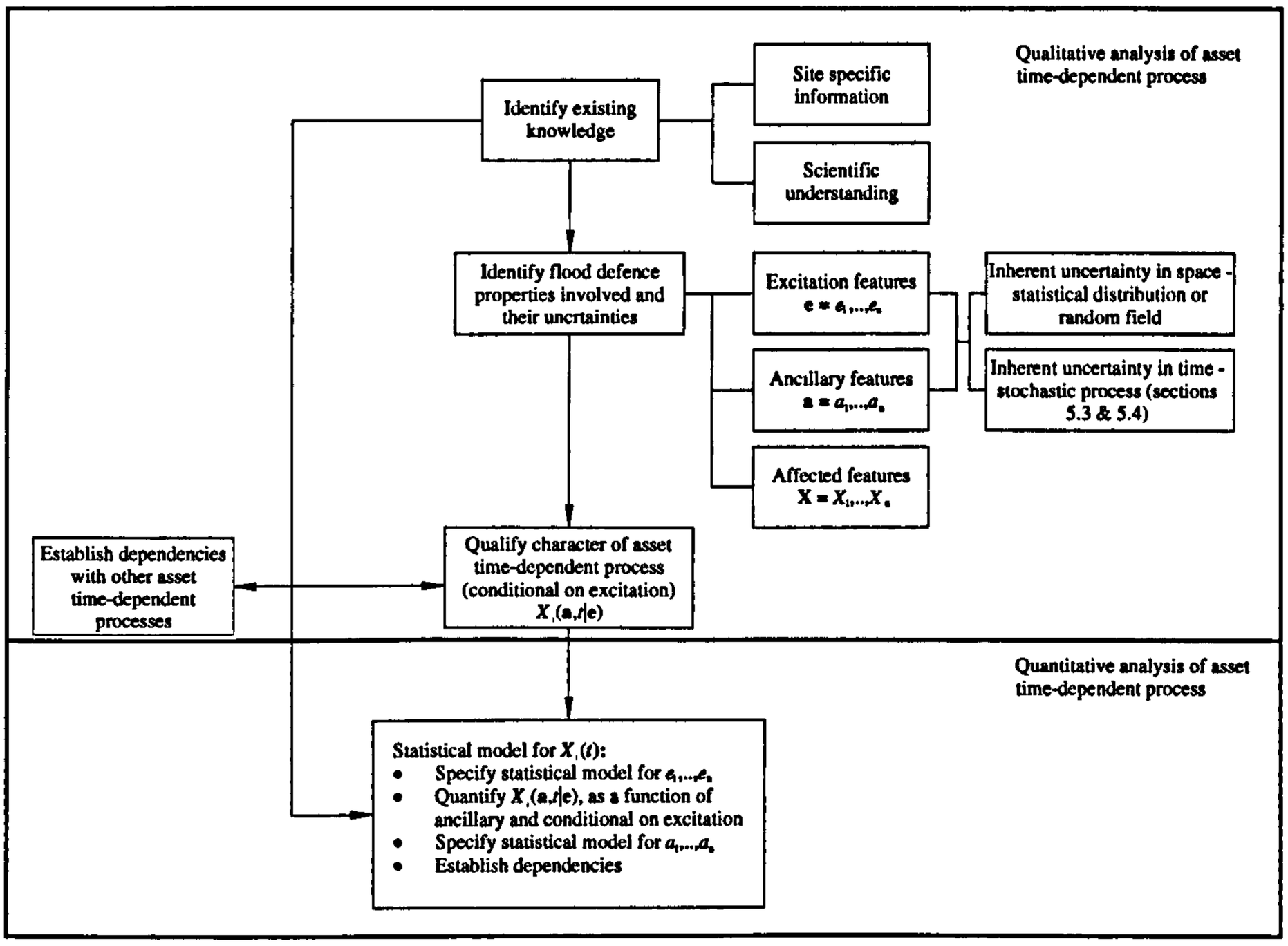

Figure 8.2 Qualitative and quantitative evaluation of an asset time-dependent process and the sequence of steps to take in the modelling process(figure 6.2).

different asset time-dependent processes; the formulation and motivation of alternative statistical models of the process.

3.c. Statistical parameter estimation, calibration and corroboration methods are available for statistical models of asset time-dependent processes. However, the data availability is often limited and even process models based on abundant historical observations do not guarantee appropriate extrapolations in the future. The opportunities to carry out calibration and corroboration of statistical time-dependency models are therefore limited.

3.d. The five-step internal model structure analysis allows additional calibration or corroboration in the form of: checking whether the order of magnitude, the variation in and the behaviour of the predictions correspond with the expectations emerging from the analysis.

3.e. The way in which future observations are incorporated in the statistical model, i.e. further calibration/corroboration or Bayesian posterior analysis, depends on the following issues. A first issue is the complexity of the asset time-dependent process. A second issue is the influence of the statistical properties of the asset

time-dependent process on those of the affected feature. The asset time-dependent process may e.g. be very complex. However, the rate of the process might be very low and the amount of uncertainty contributed to the initial variation of the affected feature might be negligible. A third issue is the influence of the asset time-dependent process on the flood defence reliability, risk and life cycle cost in the context of the overarching maintenance optimisation model. This influence can be measured with importance measures as developed in chapter 4. More influential asset time-dependent processes require a more detailed statistical model. It can be decided to choose for state-dependent maintenance in figure 3.5 until the statistical model provides satisfactory time-dependent predictions.

3.f. The qualitative decomposition of the asset time-dependent process into excitation, ancillary and affected features supports practical maintenance purposes. Two examples are given. *Example 1:* An asset time-dependent process statistical model which is not properly calibrated and corroborated might not be qualified as 'Good description of course of strength' in figure 3.5. However, if it concerns an asset time-dependency that is mainly driven by recurrent events (e.g. storms or trafficking events), then the process can be organised under 'Load dependent maintenance'. Depending on the type of process it might suffice to roughly estimate the amount of damage given a recurrent event and carry out maintenance once a certain number of events have occurred. A process driven by a continuous excitation would in the same circumstances be categorised under 'State dependent maintenance' or 'Time-dependent maintenance', depending on the cost of the inspection. *Example 2:* The qualitative decomposition of the asset time-dependent process guides to which flood defence features should be paid attention to during monitoring, in addition to the overall time-dependent quantity $X_i(t)$.

8.2.4. Objective 4: demonstration time-dependent (system) reliability

The following conclusions are made with respect to the demonstration of the time-dependent reliability methods for flood defences on the Dartford Creek to Swanscombe Marshes flood defence system. The conclusions are subdivided into: the information availability, the application of the importance measures, asset time-

dependent process models, time-dependent fragility / lifetime probability of failure and the system reliability model.

Conclusions with respect to the information availability are:

4.a. The information availability on the flood defence system geometry and the hydraulic boundary conditions is good. The information availability on the soil properties is patchy, but it is possible to improve that by means of other information sources.

4.b. Due to the limited information availability all the asset time-dependent processes fall in situation 4 in table 6.3: scarce data availability on asset time-dependent quantity $X_i(t)$ represented by a hierarchical process model. The opportunities for parameter estimation, calibration and model corroboration are therefore limited.

Conclusions with respect to the application of risk-based importance measures are:

4.c. High uncertainty contributors, i.e. high direction cosines, indeed indicate which flood defence properties should be targeted with monitoring activities. Direction cosines and partial derivative based concepts inform the selection of effective operational activities and influential asset time-dependent processes.

4.d. The benefits of some operational activities can only be properly captured at a system level, such as dredging.

Conclusions with respect to the application of asset time-dependent process statistical models are:

4.e. In case a process model is available, it depends on the emphasis of the inherent uncertainties in time whether a parametric process model suffices or whether a hierarchical process model is required. Two different situations are brought forward. Firstly, settlements due to compaction are e.g. driven by a load which is static in time, whilst ancillary pore pressures are subject to inherent uncertainty in time. The influence of the pore pressures is such that the statistical properties of the hierarchical model are nearly equal to those of the parametric process model. Secondly, in some cases, the attribution of variation in measurements to inherent uncertainty in time or space affects the variation in the predictions of the hierarchical process model. If the attribution is mainly to inherent spatial uncertainty, the hierarchical process model predictions are similar to those of a parametric process model.

4.f. The gamma process model provides an approximation to the hierarchical process model for most of the asset time-dependent processes. Reasons to choose for a gamma process alternative are given in conclusion 1.h. Lack of scientific understanding or the unavailability of field information are for example reasons to choose for such an approximation. It is also possible that due to financial and time constraints in some situations a detailed approach is not feasible.

4.g. The asset time-dependent processes trafficking, seepage length reduction, anchor corrosion and toe accretion are not properly represent by a parametric process model. The variation in the time series samples of sheet pile corrosion is also very large in case of a parametric process model. The approximation of the hierarchical process model predictions by a gamma process model is incomplete for the following processes: seepage length reduction, (vegetation damage due to) trafficking, anchor corrosion and toe accretion.

Conclusions with respect to time-dependent fragility / lifetime probability results are:

4.h. Time-dependent fragility and lifetime probability reflect the influence of the asset time-dependent processes and the impact of operational activities. The influence of the processes and activities is also expressed in the probabilities of individual failure mechanisms.

4.i. The flood defence sections with a higher lifetime probability relative to other sections are not necessarily the sections with a higher initial annual probability of failure. The rate and influence of the asset time-dependent processes can increase the probability of failure of some sections faster than others.

4.j. The fragility of the reinforced concrete walls is not time-dependent in this thesis. The influence of carbonation and reinforcement corrosion on the performance of the wall is negligible. The prominent failure mechanism in the reliability model is piping directly underneath the reinforced concrete wall. The toe depth of the wall is mainly a design concern. The wall is not strong once the water level reaches the reinforced concrete wall. Two failure processes are not taken into account in the time-dependent fragility of reinforced concrete walls, i.e. deterioration of joints between reinforced concrete wall units and cracking of the reinforced concrete. Joint failure between reinforced concrete wall units is not taken into account. A failure mechanism for increased flow velocity through the gaps in the joints initiating piping underneath the reinforced concrete wall is not available. Cracking of reinforced concrete due to an increased volume of corroded

reinforcement bars is not taken into account. It is expected that cracking has a significant effect on the performance of the reinforced concrete wall.

4.k. The fragility of anchored sheet pile walls balances the destabilising influence of anchor corrosion by the stabilising influence due to toe level accretion. Sheet pile holing due to corrosion leads to a high probability of failure in 50 years time. However, this probability of failure does not include the remaining strength represented by the stability of the soil behind the anchored sheet pile wall. The damage involved with failure of the anchored sheet pile is not taken into account in the flood risk assessment.

Conclusions with respect to the system reliability model and results are:

4.l. The system reliability model represents the autocorrelation structure in a detailed way (figure 7.40). However, the method is computationally intensive and the Cholesky factor in the multivariate normal distribution is not always convenient with the representation of higher autocorrelations.

4.m. The time-dependent probability of failure of jointly failing flood defence sections shows a correlation for lower time steps. The correlation becomes smaller while the influence of the asset time-dependent processes increases. This effect is explained by the fact that the autocorrelation applied in the asset time-dependent process models is such that the simulations between flood defence sections are independent.

4.n. The autocorrelation structure therefore has an influence on jointly failing flood defence sections at a distance of a flood defence length. A further subdivision in smaller slices of the flood defence sections itself will therefore have an influence on the reliability of one flood defence section. This influence has not been further explored in this thesis.

4.o. The probability of serial system failure appropriately provides a higher probability of failure than that of the weakest flood defence section. The high results are explained by the failure mechanism piping underneath the toe of the reinforced concrete wall. The condition that the storm level must persist sufficiently long and the conservative estimate of the permeability are both sources of more piping resistance than is taken into account.

8.3. Recommendations

The recommendations below are structured according to the research objectives.

Objective 1: review

The overarching quantitative maintenance optimisation model is not specified yet for flood defence management, though significant progress has been made in the definition of parts of the building blocks (table 3.4). The existing components are drawn together in this thesis in an overarching rational maintenance approach and where possible complemented with theory from other fields in the engineering industry (conclusion 1d). Some suggestions for further improvement are made below.

It is preferable if the definition of the third building block, the operational management model, contains a rational consideration of when quantitative prioritisation is necessary or when qualitative decision-making is sufficient. Qualitatively structuring maintenance issues that are related to a quantitative optimisation model has received attention in the engineering industry. Some suggestions of existing or possible new approaches are indicated in the following.

- Reliability Centred Maintenance is a qualitative decision-making approach prioritising failure mechanisms and deriving failure indicators, section 3.2.2 and 3.2.3 (Moubray, 1997, Delft Cluster, 2001 and Environment Agency, 2004a). Merging such qualitative approaches with quantitative approaches is an interesting subject of further research.
- At an asset time-dependent process level the importance of the process determines whether it is further monitored, modelled and taken into account in life cycle costing, see conclusions 2.b, 2.c and 3.e. Once considered as relevant, the ability to make calibrated / corroborated predictions with the asset time-dependent process model influences whether a time-dependent, state-dependent, load-dependent or fault-dependent maintenance approach is chosen (conclusion 3.f).
- The use of importance measures to eliminate or select relevant maintenance intervention options reduces the size of the quantitative maintenance optimisation problem.

- Some inspections, such as visual inspections, only return qualitative information about the state of the flood defence. Their benefit is therefore hard to quantify in a quantitative rational maintenance framework.
- The design of monitoring strategies is preferable both in the context of a rational qualitative approach and a quantitative maintenance optimisation model (section 3.2.3). The monitoring strategy determines the information that is retrieved about the flood defence system. Reliability Centred Maintenance approaches, importance measures to highlight relevant processes and qualitative decomposition of the process according to figure 6.2 steer which information should be acquired.

The considerations of where quantitative prioritisation is required and where a qualitative approach suffices have consequences for the optimisation model in the fourth building block.

Objective 2: importance measures

Once a life cycle costing model for flood defence management has been defined in more detail, it would benefit from other types of importance measures than developed in this thesis. Firstly, they support making the optimisation model computationally faster. Importance measures reduce the number of relevant maintenance optimisation intervention options in the optimisation model. Secondly, more refined or other types of importance measures allow the rational comparison of operational activities without or in advance of life cycle costing.

Objective 3: modelling methodology asset time-dependency

The corroboration of statistical models for asset time-dependent processes remains an issue even as future observations become available and are incorporated. Reasons to decide to carry out further corroboration are discussed in conclusion 3.e. The reasons are: the complexity of the asset time-dependent process, the influence on the statistical properties of the affected feature and the importance in the overarching maintenance optimisation model. It can be decided to choose for state-dependent maintenance in figure 3.5 until the statistical model provides satisfactory time-dependent predictions.

Further investigation is necessary into the quality requirements for the asset time-dependent processes and overarching maintenance optimisation concepts. The

following four issues would benefit from more research in this context. Firstly, whether the additional calibration and corroboration according to the five-step analysis suggested in conclusion 3.d can be translated into a quantified approach. For example a sensitivity analysis of the asset time-dependent quantity to the excitation and ancillary features. Secondly, the use of expert elicitation in the form of a Bayesian approach to calibrate the statistical model of the asset time-dependent processes. Thirdly, the transition between further calibration or corroboration and the incorporation of future observations through Bayesian posterior analysis is not clearly defined. This transition depends on the complexity and importance of the time-dependent process, on the quality requirements and the observation availability. Finally, the specification of the quality requirements for the overarching maintenance optimisation model has consequences for those of the asset time-dependent processes. As mentioned in section 6.4.2 and figure 6.1, sensitivity analysis and expert elicitation are ways to calibrate and corroborate the (time-dependent) risk and reliability concepts. However, requirements and procedures have not been explicitly defined yet for the life cycle cost optimisation problem.

Another area of interest is the further exploration of dependencies between different asset time-dependent processes and spatially autocorrelated asset time-dependent processes.

Objective 4: demonstration time-dependent (system) reliability

The following recommendations are made with respect to the demonstration of time-dependent (system) reliability:

1. The absence of process models for some failure mechanisms prevent the quantification of important asset time-dependent processes in time-dependent fragility. Joint deterioration between reinforced concrete wall units for example is not incorporated. There is no process model for the development of piping as a result of water flow through the deteriorated joint gaps. Failure mechanisms related to important sources of deterioration benefit from further investigation.
2. Other important sources of asset time-dependency and their representation in fragility that benefit from further investigation are: the effect of third party interference and of the presence of foreign objects. Third party interference covers a broad range of problems such as: vandalism, building close to and loading flood defence structures, placing superimposed loading on earth

embankment slopes, cattle trampling, animal infestation. The presence of foreign objects can lead to concentrated flow and erosion during a storm or for example rooted trees.

3. The reliability of floodgates has not been incorporated in the Dartford Creek to Swanscombe Marshes system reliability model and would benefit from a further investigation.
4. For some asset time-dependent processes it is advisable to model them in the context of the failure mechanism which they affect. For example, the vegetation damage is modelled by a linear model. However, the way in which the erosion strength of the vegetation is derived in the original failure mechanism is not considered.
5. The economic damages related to anchored sheet pile walls and revetments protecting high grounds are not fully represented in this thesis. The incorporation of all relevant economic damages is a condition to make a rational comparison with other flood defence types in an operational framework.
6. The correlation structure increases the probability of jointly failing flood defence sections and hence the flood risk. Some issues of interest are as follows. The influence of the length of the flood defence sections on the flood risk assessment. The sensitivity of the flood defence reliability model to the correlation function and the implications for the data collection or monitoring grid. The sensitivity of the reliability model to the type of correlation structure, e.g. multivariate normal or lognormal distribution. The relationship between the breach formation process and correlated flood defence section failures.
7. The autocorrelation between asset time-dependent processes influences the time-dependent flood defence system reliability and is therefore interesting to further explore.

Appendix A

Map of flood defence sections in the Dartford Creek to Swanscombe Marshes flood defence system

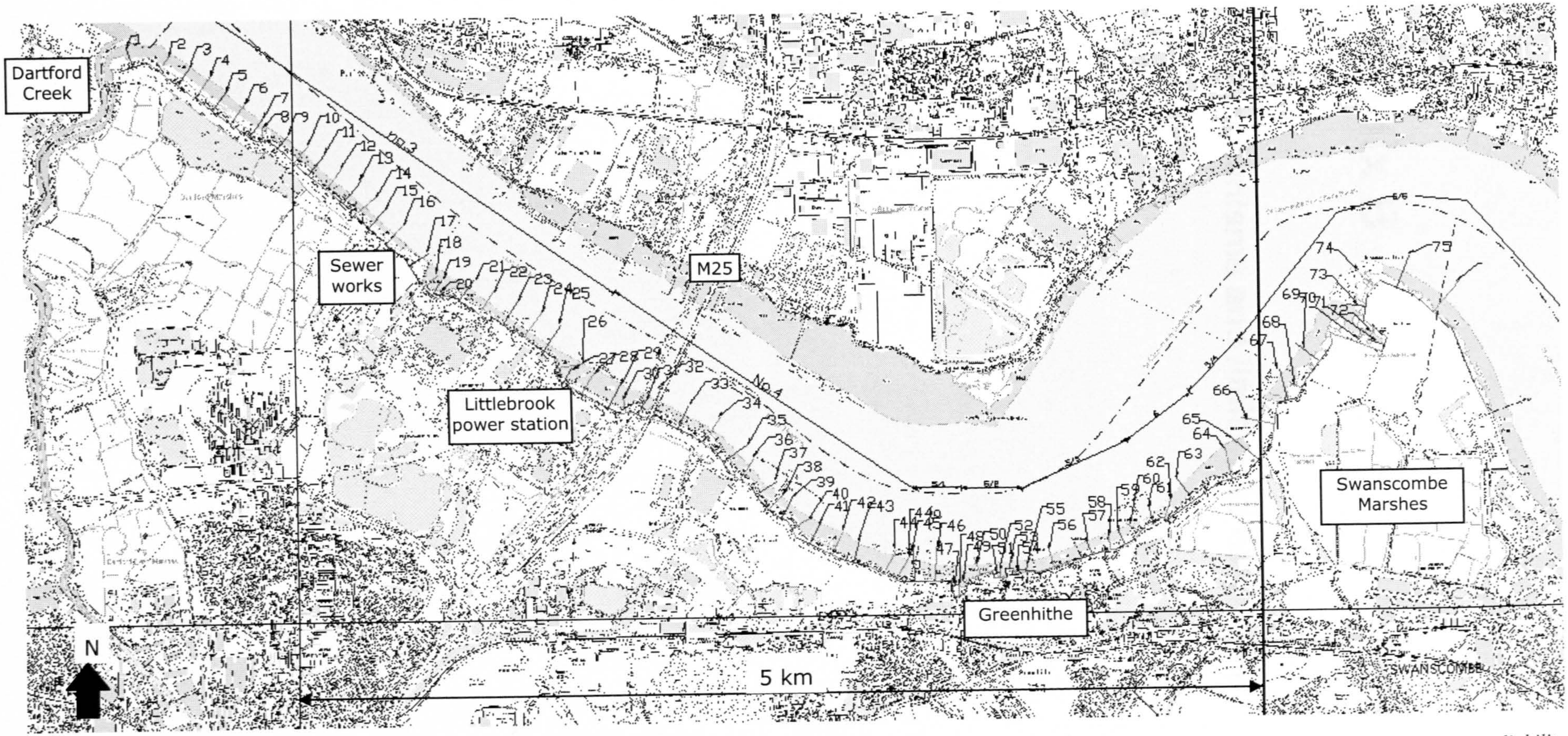

Figure A.1 Flood defence sections 1 to 75 in the Dartford Creek to Swanscombe Marshes flood defence system, sections 1 to 67 are included in the time-dependent system reliability analysis.

Appendix B

Failure mechanisms and limit state functions

B.1 Earth embankments

B.1.1 Erosion of cover of inner slope by wave overtopping or overflow

Sketch of failure mechanism:

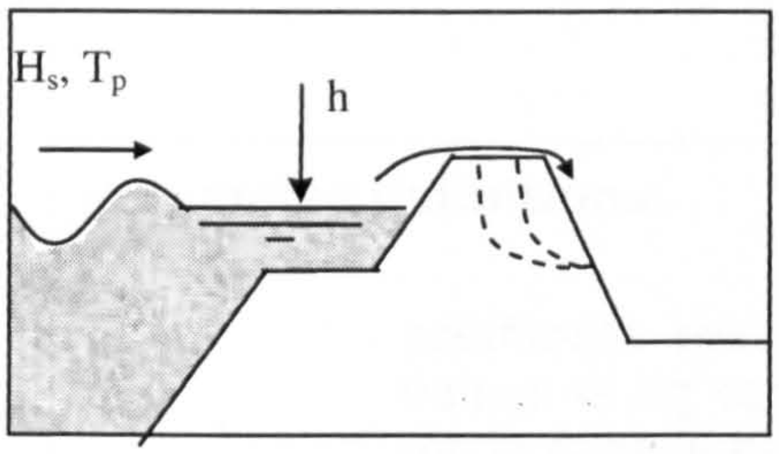

Limit state function:

Water discharges due to overtopping or overflow respectively hit or scour the inside slope of the embankment. Due to this loading of the inside slope the grass gets damaged. After the grass has been damaged, the embankment body is exposed to the overtopping/overflow water. In the end, if this erosion process continues long enough, the embankment breaches. The duration of this erosion process depends on the duration of the storm.

Limit state equation for wave overtopping:

$$Z = m_c q_c - m_a q_a$$

Wherein q_c is the critical overtopping discharge [m^2/s], m_c is the model uncertainty of the critical discharge model [-], q_a is the calculated discharge [m^2/s] and m_a is the model uncertainty associated with the actual discharge.

Limit state equation for overflow:

$$Z = h_{crest} + \Delta h_c - h$$

In which h_{crest} [mOD] is the crest level of the embankment, Δh_c [m] expresses the critical height for which almost damage of the grass occurs and h is the actual occurring water level [mOD].

Loading equations:	**Strength equations:**
The q_a is calculated with Owen's wave overtopping model. A separate sheet is incorporated for that after this template.	The critical discharge in the wave overtopping limit state equation, q_c, is calculated with the following equation:

The loading in case of overflow is caused by the difference in water level and crest level.

$$q_c = \left[\frac{3.8 \cdot c_g^{2/3}}{(6 \cdot 10^5)^{2/3} \cdot \left[1 + 0.8 \cdot \log_{10}\left(P_t \cdot t_s \cdot \frac{c_g \cdot d_w}{c_g \cdot d_w + 0.4 \cdot c_{RK} \cdot L_{K,inside}} \right) \right]} \right]^{5/2} \cdot \frac{r_i^{1/4}}{125 \cdot (\tan \alpha_i)^{3/4}}$$

Δh_c [m] in the overflow limit state equation expresses the critical height for which almost damage of the grass occurs and is calculated with the following equation:

$$\Delta h_c = \sqrt[3]{\frac{2.78 \cdot q_c^2}{g}}$$

In which g is the gravitational constant and q_c the critical discharge as calculated above.

Parameter definitions:

c_g = coefficient that represents the erosion endurance of the grass. The values of cg can range from 10^6 ms in case of good quality to $3.3 \cdot 10^5$ ms in case of bad quality. [m·s]

P_t = percentage of the time that overtopping/flowing over occurs. In case of flowing over Pt is 1 and in case of overtopping P_t takes the pulsatory character of overtopping in account [-]

t_s = duration of the storm [hours]

d_w = the depth of the grass roots. Values of d_w range between 0.05m and 0.07m, factors influencing the magnitude of this factor are: maintenance, location (sea or river embankments) and the type of vegetation. [m]

c_{RK} = coefficient with regard to the erosion endurance of the clay cover layer. The values for c_{RK} range from $7 \cdot 10^3$ m·s (bad quality clay) to $54 \cdot 10^3$ m·s (good quality clay). In case of sand $c_{RK} = 0$. [m·s]

$L_{k,inside}$ = width of the inside clay cover layer, that can be considered as the total width of the embankment. [m]

r_i = roughness factor according to Strickler of the inside slope. [s^6/m^2]

α_i = angle of the inside slope. [degrees]

Sources of failure mechanism equations / methods:

Vrouwenvelder et al. (2001a)

Sources of uncertainties in failure equations / input parameters:

Vrouwenvelder et al. (2001a)

Smooth, Impermeable, Simply sloped / Composite Seawall (Owen, 1980)

Simply sloped Seawall

Normal wave attack

Determine the mean overtopping discharge rate per metre run of seawall, Q (m^3/sec/m)

$$Q = Q_* \, T_m \, g \, H_s$$

where

Q_* - dimensionless discharge

$$Q_* = A \exp(- B R_*)$$

A, B - empirical coefficients dependent upon the cross-section of the seawall [6]

R_* - dimensionless freeboard (height of the crest of the wall above still water level)

$$R_* = R_c / \left(T_m (g H_s)^{0.5}\right),$$
$$0.05 < R_* < 0.30$$

R_c - freeboard (height of the crest of the wall above still water level) (m)

H_s - significant wave height at the toe of the structure (m)

g - acceleration due to gravity (m/sec^2)

T_m - mean wave period at the toe of the structure (sec)

Angled wave attack

$$Q_{angled\ wave\ attack} = Q_r \, Q$$

where

Q_r - ratio of discharge under angled wave attack to that under normal attack

$$Q_r = 1 - 0.000152 \beta^2,$$
$$0^0 < \beta \le 60^0$$

If $\beta > 60^0$ results for $\beta = 60^0$ should be applied

Q - mean overtopping discharge rate per metre run of seawall under normal wave attack (m^3/sec/m)

Composite Seawall

In shallow water, $h < 0.55 H_s$, an imaginary simple slope is constructed between the toe and crest of the structure.

Smooth, Impermeable, Bermed Seawall or Composite Seawall

Normal wave attack

Similar to "Smooth, Impermeable, Simply sloped Sea Wall"

Angled wave attack

$$Q_{angled\ wave\ attack} = Q_r \, Q$$

where

Q_r - ratio of discharge under angled wave attack to that under normal attack

$$Q_r = 1.99 - 1.93 \left\{1 - \left[(\beta - 60) / 69.8\right]^2\right\}^0$$
$$0^0 < \beta \le 60^0$$

If $\beta > 60^0$ results for $\beta = 60^0$ should be applied

Q - mean overtopping discharge rate per metre run of seawall under normal wave attack (m^3/sec/m)

Composite Seawall

In shallow water, $h < 0.55 H_s$, an imaginary simple slope is constructed between the toe and crest of the structure.

Rough and Armoured Seawall

Normal wave attack

Determine the mean overtopping discharge rate per metre run of seawall, Q (m^3/sec/m)

$$Q = Q_* \, T_m \, g \, H_s$$

where

Q_* - dimensionless discharge

$$Q_* = A \exp(- B R_* / r)$$

A, B - empirical coefficients dependent upon the cross-section of the sea wall (HR Wallingford, 1998)

R_* - dimensionless freeboard (height of the crest of the wall above still water level)

$$R_* = R_c / \left(T_m (g H_s)^{0.5}\right),$$
$$0.05 < R_* < 0.30$$

R_c - freeboard (height of the crest of the wall above still water level) (m)

r - roughness coefficient (HR Wallingford, 1998)

If the structure includes berm on smooth, impermeable slope, method applied to "Smooth, Impermeable, Bermed Sea Wall" will be used.

If the structure includes a permeable crest berm, a reduction factor, C_r, will be taken into account.

$$Q_{perm\ berm} = Q \times C_r$$

$$C_r = 3.06 \exp\left(-1.5 \, C_w / H_s\right)$$

where

C_w - crest berm width (m)

$C_r = 1$ when $C_w / H_s < 0.75$

Angled wave attack

Same methods as for "Smooth, Impermeable, Simply sloped Sea Wall" and "Smooth, Impermeable, Bermed Sea Wall".

B.1.2 Uplifting of impermeable layers behind earth embankment

Sketch of failure mechanism:

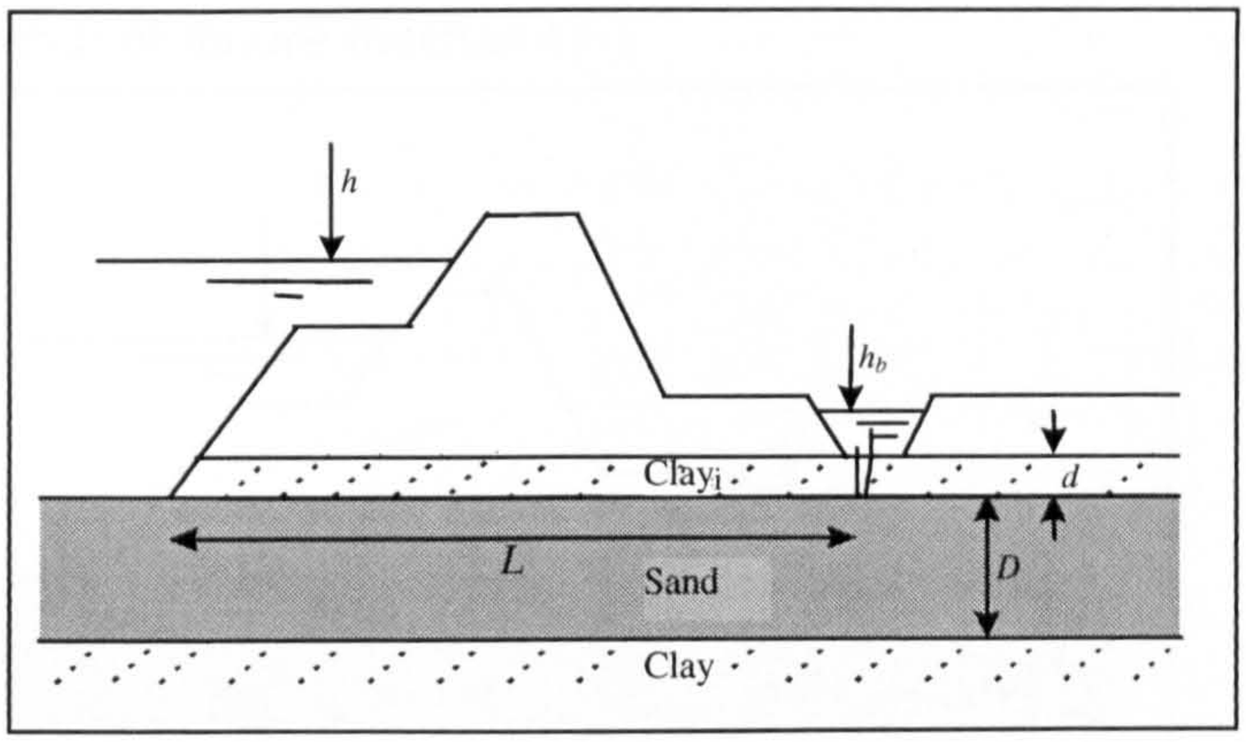

Limit state function:

Uplifting occurs if the difference between the local water level h, and the water level "inside", h_b is larger than the critical water level h_c. This is expressed in the Limit state function as:

$$Z = m_u h_c - m_h(h - h_b)$$

In which m_u [-] takes the model uncertainty of the model which determines h_c [m] in account and m_h the level of damping [-]. The critical water level expresses the limit water level for which almost uplifting occurs. This water level is based on the properties of the impervious layer.

Loading equations:

The loading is represented by the difference in water level on the river, h [mOD] and the water level in the floodplain h_b [mOD].

Strength equations:

$$h_c = \frac{\gamma_{wet} - \gamma_w}{\gamma_w} d$$

In which γ_{wet} [kN/m^3] is the saturated volumetric weight of the impermeable soil layers, γ_w [kN/m^3] is the volumetric weight of the water and d [m] is the thickness of the impermeable layers.

Parameter definitions:

Are given above

Sources of failure mechanism equations / methods:

Vrouwenvelder et al. (2001)

Sources of uncertainties in failure equations / input parameters:

Vrouwenvelder et al. (2001)

B.1.3 Piping in water conductive layer underneath the earth embankment

Sketch of failure mechanism:

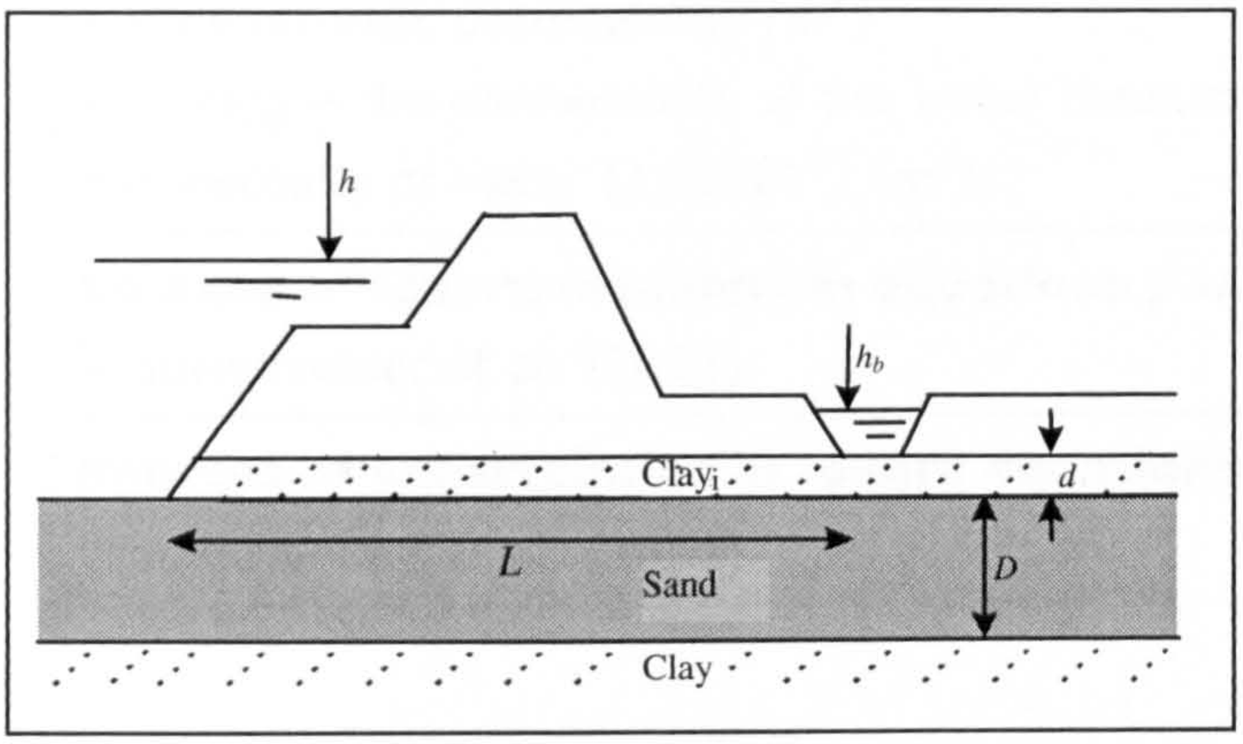

Limit state function:

The embankment fails as a consequence of piping if the difference between the local water level h and the inside water level h_b, exceeds the critical water level h_p.

$$Z = m_p h_p - (h - h_b)$$

In which m_p is the model uncertainty of the model with which hp is described. The critical water level h_p is described by Sellmeijer's model of piping

Loading equations:

The loading is represented by the difference in water level on the river, h [mOD] and the water level in the floodplain h_b [mOD].

Strength equations:

$$h_p = \alpha c L \left(\frac{\gamma_{sand}}{\gamma_w} - 1 \right) (0.68 - 0.1 \ln c) \tan\theta$$

Parameter definitions:

L - seepage length [m]

γ_{sand} -volumetric weight of the water conductive sand [kN/m^3]

γ_w -volumetric weight of the water [kN/m^3]

θ -friction angle of the sand with regard to movement [°]

a -factor reflecting the effect of a finite thickness of the water conducting layer, for expression see below

c -describes the characteristics of the sand in the erosion enduring water conducting sand layer, for expression see below

$$\alpha = \left(\frac{D}{L}\right)^{\frac{0.28}{((D/L)^{2.8}-1)}}$$

D - thickness water conductive sand layer [m]

η - the drag force factor (constant of White) [-]

d_{70} - representative of the large fraction of grains in the sand of the water conducting layer [m]

κ - the intrinsic permeability [m^2]

$k_s = \kappa\nu/g$ – the permeability of the water conductive sand [m/s]

ν = viscosity of water ($1.33 \cdot 10^{-6}$) [m^2/s]

Sources of failure mechanism equations / methods:

Vrouwenvelder et al. (2001)

Sources of uncertainties in failure equations / input parameters:

Vrouwenvelder et al. (2001)

B.2 Reinforced concrete walls

B.2.1 Sliding failure of reinforced concrete wall

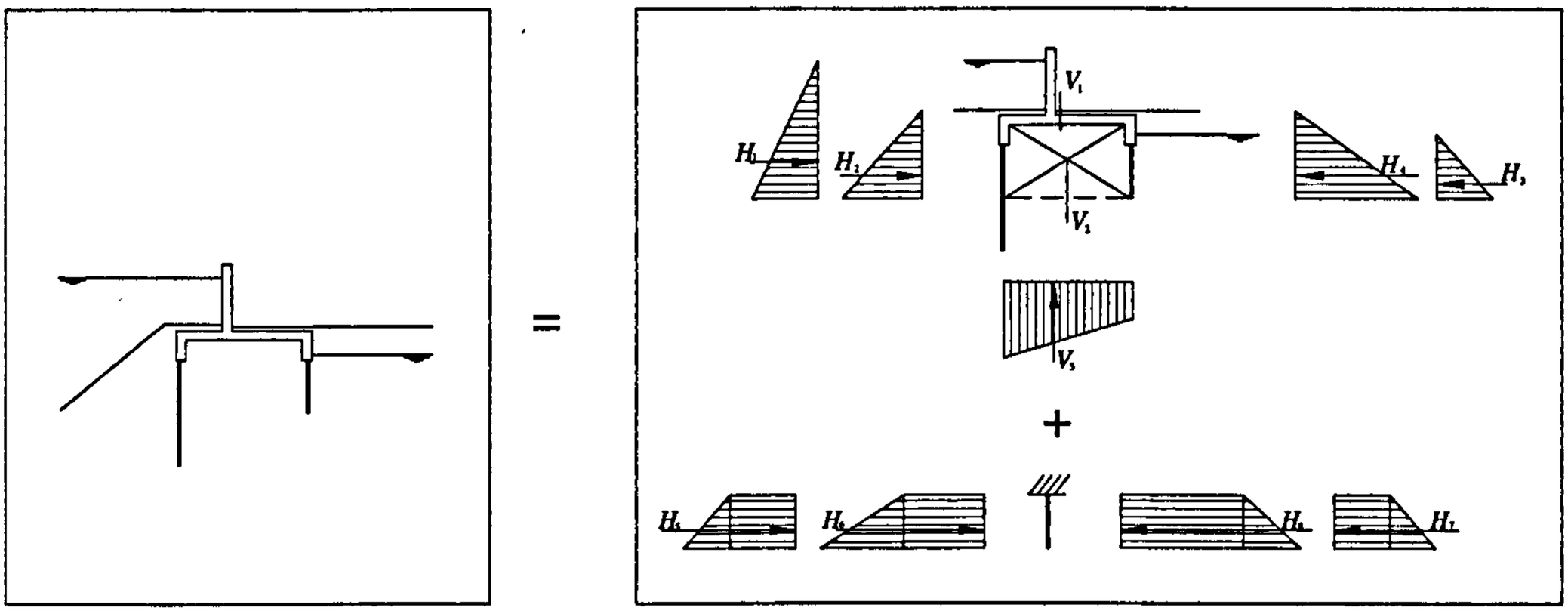

Limit state function:

Failure occurs when horizontal (and uplift) forces exceed sliding resistance. The simplest representation of this is to balance the hydrostatic loads by a friction resistance driven in turn by the (net) weight force of the crown wall. In practice, this mechanism may be unrealistic as this simple representation of friction can only be applied when the material under the wall behaves as a granular material. That would in turn probably allow seepage / piping flows to act before this failure mechanism.

The limit state function is expressed by:

$$Z = m_{c,s,R} \cdot \tan\delta \sum V - m_{c,s,S} \cdot \sum H$$

where:

ΣV	=	total resulting vertical force [kN/m]
ΣH	=	total resulting horizontal loading force [kN/m]
$m_{c;s;R}$	=	model factor for the strength model [-]
$m_{c;s;S}$	=	model factor for the loading model [-]

Loading equations:

$$H_{total} = (H_1 + H_2 + H_5 + H_6 + H_9) - (H_3 + H_4 + H_7 + H_8)$$

where:

main structure (concrete wall & mobilised soil):

$$H_1 = 0.5 \cdot \gamma_w (h - L_3)^2$$

$$H_2 = 0.5.K_a .(\gamma_s - \gamma_w)(h_1 - L_3)^2$$

$$H_3 = 0.5 .\gamma_w (g_w - L_3)^2$$

$$H_4 = 0.5.K_p .(\gamma_s - \gamma_w)(h_3 - L_3)^2$$

Sheet pile cut-off:

$$H_5 = \gamma_w (h - L_3)(L_3 - L_1) + 0.5 .\gamma_w (L_3 - L_1)^2$$

$$H_6 = K_p .(\gamma_s - \gamma_w)(h_1 - L_3)(L_3 - L_1) + 0.5.K_p .(\gamma_s - \gamma_w)(L_3 - L_1)^2$$

$$H_7 = \gamma_w (g_w - L_3)\ (L_3 - L_1) + 0.5 .\gamma_w (L_3 - L_1)^2$$

$$H_8 = K_a .(\gamma_s - \gamma_w)(h_3 - L_3)(L_3 - L_1) + 0.5.K_a .(\gamma_s - \gamma_w)(L_3 - L_1)^2$$

Wave impact:

H_9 according to B.2.6

Strength equations:

$$V_{total} = \tan\delta (V_1 + V_2 - V_3)$$

where:

V_1 is the weight of the concrete structure - depends on the geometry of the wall.

V_2 is the vertical weight of the mobilised soil:

$$V_2 = \gamma_s h_s B$$

V_3 is the upward hydraulic force

$$V_3 = \gamma_w (g_w - L_3) \cdot B + 0.5 \gamma_w (L_3 - L_1) \cdot B$$

Parameter definitions:

h	=	river water level [mOD]
g_w	=	ground water level [mOD]
d	=	friction coefficient [-]
γ_s	=	the volumetric weight of the saturated soil [kN / m^3]
γ_w	=	the volumetric weight of water [kN / m^3]
L_1	=	the level of the longest sheet pile cut-off [mOD]
L_3	=	the level of the shortest sheet pile cut-off [mOD]
h_1	=	the level of the crest in front of the concrete wall on the river side [mOD]
h_3	=	the level of the crest in front of the concrete wall on the land side [mOD]
K_a	=	the coefficient for active horizontal grain force [-]
K_p	=	the coefficient for passive horizontal grain force [-]
B	=	the width of the concrete structure between extensions [m]

h_s	=	the height of the mobilised soil [m]
Sources of failure mechanism equations / methods: See also Floodsite (2007)		
Sources of uncertainties in failure equations / input parameters: Baecher & Christian (2003); CUR (1997); Vrouwenvelder et al. (2001)		

B.2.2 Overturning failure of reinforced concrete wall

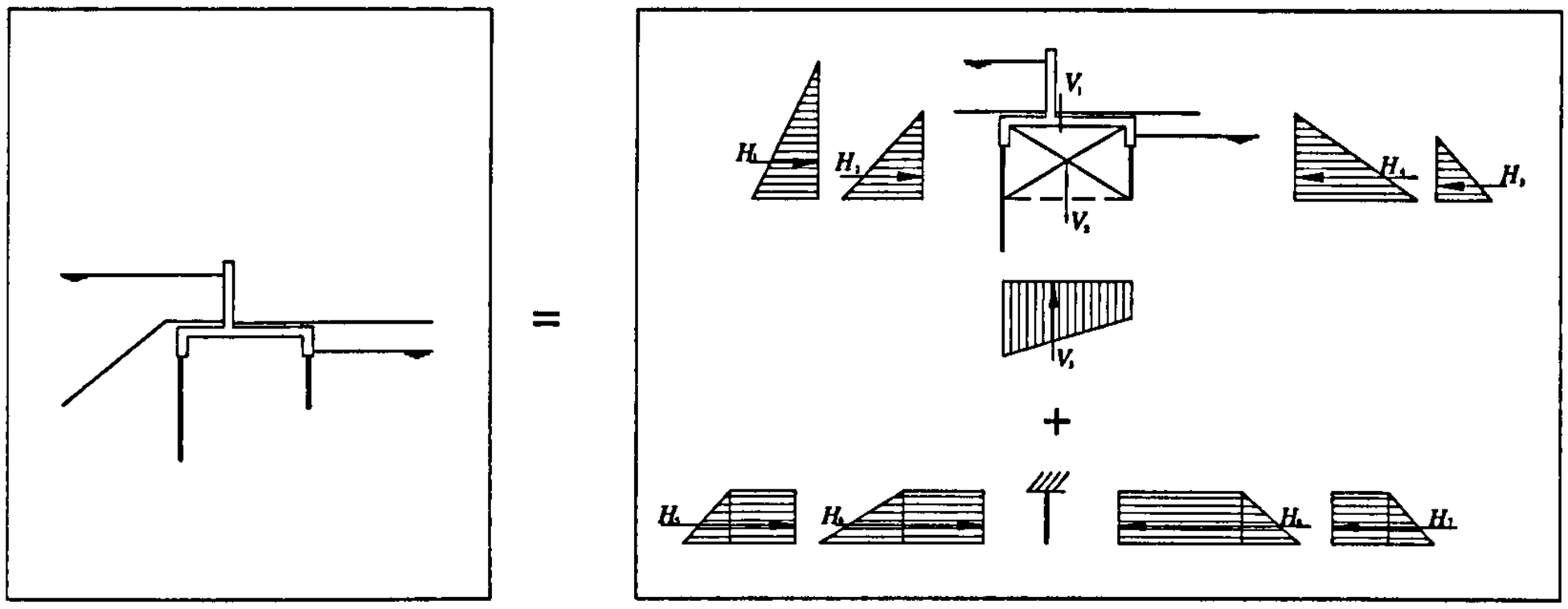

Limit state function:

When the water level reaches the concrete wall, a horizontal hydraulic force is exerted against the wall. This force can overturn the concrete structure. Resisting forces are the weight of the structure and the pressures of the ground keeping the structure into place. Overturning is assumed to occur when tensile stress occurs in the foundational plane. This assumption leads to the following limit state function:

$$Z = m_{c,o,R} \cdot \tfrac{1}{6} B_c - m_{c,o,S} \cdot \frac{\sum M}{\sum V}$$

where:

B_c	=	width of the base of the concrete structure
ΣM	=	the resulting moment [kNm /m]
ΣV	=	resulting vertical force acting on the concrete wall structure [kN / m]
$m_{c,o,;R}$	=	model factor for the strength model [-]
$m_{c,o;S}$	=	model factor for the loading model [-]

Loading equations:

The resulting moment is taken around the centre of the base of the mobilised soil and is built up as follows:

Main structure (concrete wall & mobilised soil):

Strength equations:

V_1 is the weight of the concrete structure in kN per stretching meter - depends on the geometry of the wall.

$$M_1 = 0.5 \cdot \gamma_w (h - L_3)^2 \cdot 1/3(h - L_3)$$

$$M_2 = 0.5 \cdot K_a \cdot (\gamma_s - \gamma_w)(h_1 - L_3)^2 \cdot 1/3(h_1 - L_3)$$

$$M_3 = 0.5 \cdot \gamma_w (g_w - L_3)^2 \cdot 1/3(g_w - L_3)$$

$$M_4 = 0.5 \cdot K_p \cdot (\gamma_s - \gamma_w)(h_3 - L_3)^2 \cdot 1/3(h_3 - L_3)$$

Sheet pile cut-off:

$$M_5 = \gamma_w (h - L_3)(L_3 - L_1) \cdot 1/2(L_3 - L_1) + 0.5 \cdot \gamma_w (L_3 - L_1)^2 \cdot 2/3(L_3 - L_1)$$

$$M_6 = K_p \cdot (\gamma_s - \gamma_w)(h_1 - L_3)(L_3 - L_1) \cdot 1/2(L_3 - L_1) + 0.5 \cdot K_p \cdot (\gamma_s - \gamma_w)(L_3 - L_1)^2 \cdot 2/3(L_3 - L_1)$$

$$M_7 = \gamma_w (g_w - L_3)(L_3 - L_1) \cdot 1/2(L_3 - L_1) + 0.5 \cdot \gamma_w (L_3 - L_1)^2 \cdot 2/3(L_3 - L_1)$$

$$M_8 = K_a \cdot (\gamma_s - \gamma_w)(h_3 - L_3)(L_3 - L_1) \cdot 1/2(L_3 - L_1) + 0.5 \cdot K_a \cdot (\gamma_s - \gamma_w)(L_3 - L_1)^2 \cdot 2/3(L_3 - L_1)$$

Wave impact:

$$M_9 = H_9 \cdot 0.5 \cdot (h_c - h_1)$$

H_9 according to B.2.6

Moments due to vertical forces:

$$M_{v1} = b_{gr} \cdot V_1$$

$$M_{v2} = 0$$

$$M_{v3} = 0.5 \cdot \gamma_w \cdot (L_3 - L_1) \cdot B \cdot (1/2B - 1/3B)$$

Resulting moment

$$\Sigma M = M_1 + M_2 - M_3 - M_4 - M_5 - M_6 + M_8 + M_9$$

$$- M_{v1} + M_{v3}$$

V_2 is the vertical weight of the mobilised soil in kN per stretching meter:

$$V_2 = \gamma_s h_s \cdot B$$

V_3 is the upward hydraulic force:

$$V_3 = \gamma_w \cdot (g_w - L_3) \cdot B + 0.5 \cdot \gamma_w \cdot (L_3 - L_1) \cdot B$$

Parameter definitions:

h	=	river water level [mOD]
g_w	=	ground water level [mOD]
γ_s	=	volumetric weight of the saturated soil [kN / m^3]
γ_w	=	volumetric weight of water [kN / m^3]

L_1	=	level of the longest sheet pile cut-off [mOD]
L_3	=	level of the shortest sheet pile cut-off [mOD]
h_1	=	level of the crest in front of the concrete wall on the river side [mOD]
h_3	=	level of the crest in front of the concrete wall on the land side [mOD]
K_a	=	coefficient for active horizontal grain force [-]
K_p	=	coefficient for passive horizontal grain force [-]
B	=	width of the concrete structure between extensions [m]
b_g	=	distance between the centre of gravity of the concrete structure and the centre of the mobilised soil [m]
h_s	=	height of mobilised soil [m]

Sources of failure mechanism equations / methods:

See also Floodsite (2007)

Sources of uncertainties in failure equations / input parameters:

Baecher & Christian (2003); CUR (1997); Vrouwenvelder et al. (2001)

B.2.3 Failure of vertical slab of concrete wall due to bending moments

Sketch of failure mechanism:

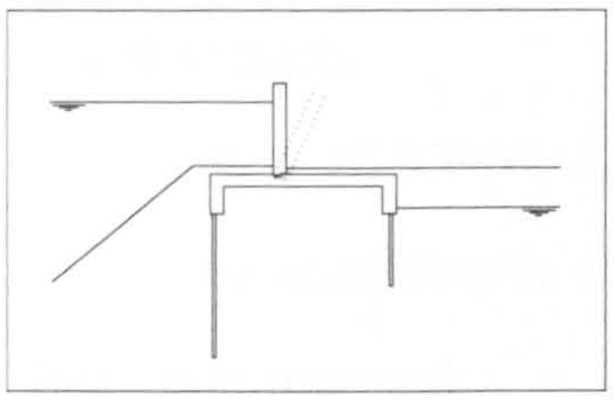

Limit state function:

The horizontal hydraulic force exerted by the river water level and the ground resting against the riverside of the concrete wall cause bending moments in the vertical slab of the wall. Failure of the vertical slab occurs when there is insufficient reinforcement to take on the tensile stress due to the bending moment:

$$Z = m_{c;b;R} \cdot M_u - m_{c;b;S} \cdot M_d$$

where:

M_u and M_d are respectively the maximum moment the cross section can take on, based on the maximum tensile stress in the reinforcement, and the actually occurring moment exerted by the hydraulic and geotechnical loading [kNm]

$m_{c;b;R}$ and $m_{c;b;S}$ are model factors for the strength and loading models [-]

The forces in the concrete cross section are modelled as illustrated below.

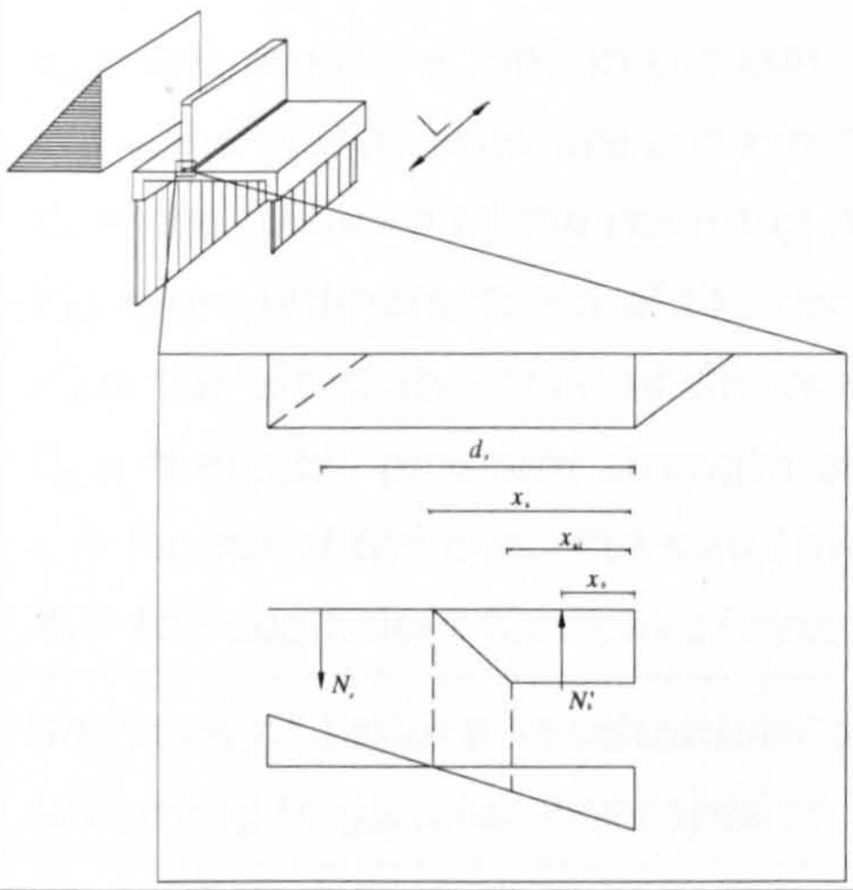

Loading equations:	**Strength equations:**
The moments are taken around the	

base of the vertical concrete slab:

$M_1 = 0.5 \cdot \gamma_w (h - (hc\text{-}d4))^2 \cdot 1/3(h - (h_c\text{-}d4))$

$M_2 = 0.5 \cdot K_a \cdot (\gamma_s - \gamma_w)(h_1 - (h_c\text{-}d4))^2 \cdot 1/3(h_1 - (h_c\text{-}d4))$

$M_3 = 0.5 \cdot K_p \cdot (\gamma_s - \gamma_w)(h_3 - (h_c\text{-}d4))^2 \cdot 1/3(h_3 - (h_c\text{-}d4))$

Wave impact:

$$M_4 = H_4 \cdot 0.5 \cdot (h_c - h_1)$$

H_4 according to B.2.6

Resulting moment

$\Sigma M = M_1 + M_2 + M_4 - M_3$

$$N_s = A_s f_s$$

$$x_u = \frac{N_s}{\frac{1}{2}\left(1 + \frac{\varepsilon'_b - \varepsilon'_{pl}}{\varepsilon'_b}\right) L \cdot f'_b}$$

$$x_{u1} = \frac{\varepsilon'_b - \varepsilon'_{pl}}{\varepsilon'_b} x_u$$

$$x_b = \frac{\frac{1}{2} x_{u1}^2 \cdot f'_b + \frac{1}{2}(x_u - x_{u1})\left(\frac{1}{3}(x_u - x_{u1}) + x_{u1}\right) f'_b}{x_{u1} f'_b + \frac{1}{2}(x_u - x_{u1}) f'_b}$$

$$M_u = N_s \cdot (d_s - x_b)$$

Parameter definitions:

h = the river water level [mOD]

h_c = the crest level of the concrete wall [mOD]

h_1 = the ground level on the riverside of the concrete wall [mOD]

h_3 = the ground level on the landside of the concrete wall [mOD]

$d4$ = the height of the vertical slab of the concrete wall [m]

γ_w = the volumetric weight of water [kN / m^3]

γ_s = the volumetric weight of saturated soil [kN / m^3]

N_s = the total tensile force in the steel reinforcement [kN]

A_s = the total area of steel reinforcement in the concrete cross section [m^2]

f_s = yield strength of reinforcement steel [kN/m^2]

x_u = the pressure zone in the concrete [m]

x_{u1} = the plastic pressure zone in the concrete [m]

x_b = the distance of the resulting pressure in the concrete from the edge [m]

ε'_{bu} = the ultimate strain of the concrete [-]

ε'_{pl} = the plasticity strain of the concrete [-]

f'_b = the cubic pressure strength of the concrete [kN/m^2]

L = length of the concrete slab [m]

K_a= the coefficient for active horizontal grain force [-]

Sources of failure mechanism equations / methods:

According to general standards on concrete design (British and Dutch)

Sources of uncertainties in failure equations / input parameters:

Baecher & Christian (2003);CUR 190 (1997);Vrouwenvelder et al. (2001);

B.2.4 Failure of vertical slab of concrete wall due to shear stress

Sketch of failure mechanism:

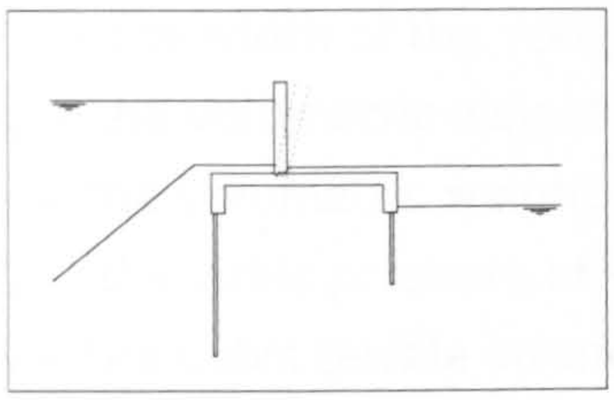

Limit state function:

The horizontal hydraulic force exerted by the river water level and the ground resting against the riverside of the concrete wall cause shear stress at the base section of the vertical slab. Failure of the vertical slab occurs if the concrete cross section has insufficient width or shear strength to take on the horizontal force. The approach below applies to concrete slabs without reinforcement for shear stress.

$$z = m_{c;sh;R} \cdot \tau_u - m_{c;sh;S} \cdot \tau_d$$

where:

τ_u and τ_d are respectively the maximum shear stress the cross section can withstand and the actually occurring shear stress exerted by the hydraulic and geotechnical loading [N/mm^2]

$m_{c;sh;R}$ and $m_{c;sh;S}$ are model factors for the strength and loading models [-]

The forces in the concrete cross section are modelled as illustrated below.

Loading equations:

The shear forces are determined in the base of the vertical concrete slab:

$H_1 = 0.5 \cdot \gamma_w (h - (h_c - d4))^2$

$H_2 = 0.5 . K_a \cdot (\gamma_s - \gamma_w)(h_1 - (h_c - d4))^2$

$H_3 = 0.5 . K_p \cdot (\gamma_s - \gamma_w)(h_3 - (h_c - d4))^2$

Wave impact:

H_4 according to B.2.6

Resulting shear force

$\Sigma H = H_1 + H_2 + H_4 - H_3$

Strength equations:

$\tau_u = \tau_1 \quad \leq \tau_2$

$\tau_1 = 0.4 f_b k_\lambda k_h \sqrt[3]{\omega_0}$

$k_\lambda = 1.0$

$k_h = 1.6 - d2 \quad \geq 1.0$

$\omega_0 = \dfrac{100 A_s}{L d2} \quad \leq 2.0$

$\tau_2 = 0.2 f_b' k_n k_\theta$

$k_n = 1.0$

$k_\theta = 1.0$

Parameter definitions:

h = the river water level [mOD]

h_c = the crest level of the concrete wall [mOD]

h_1 = the ground level on the riverside of the concrete wall [mOD]

h_3 = the ground level on the landside of the concrete wall [mOD]

$d4$ = the height of the vertical slab of the concrete wall [m]

$d2$ = the width of the vertical slab [m]

γ_w = the volumetric weight of water [kN / m^3]

γ_s = the volumetric weight of saturated soil [kN / m^3]

f'_b = the cubic pressure strength of the concrete [kN/m^2]

f_b = the cubic tensile strength of the concrete [kN/m^2]

ω_0 = reinforcement percentage [-]

τ_1 = the maximum shear stress the cross section can take on, if no shear stress reinforcement is present [kN/m^2]

k_λ, k_h, k_n, k_θ = coefficients

L = length of the concrete slab [m]

K_a= the coefficient for active horizontal grain force [-]

Sources of failure mechanism equations / methods:

According to general standards on concrete design (British and Dutch)

Sources of uncertainties in failure equations / input parameters:

Baecher & Christian (2003);

CUR 190 (1997);

Vrouwenvelder et al. (2001);

B.2.5 Piping directly underneath sheet pile cut-off

Sketch of failure mechanism:

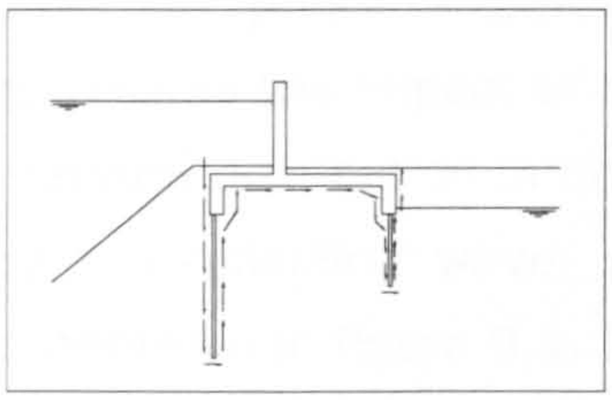

Limit state function:

Failure due to piping directly underneath the sheet pile cut-off is taken into account if the water level exceeds the ground water level in the earth bank behind the wall. This ensures a positive water head over the concrete structure, which drives the piping process. One of the requirements is that the water level persists long enough for the piping process to initiate.

$$z = m_{c;p;R} \cdot \Delta h_c - \Delta h_a$$

where:

Δh_c and Δh_a are respectively the critical head difference associated with piping underneath the sheet pile cut-off and the actual head difference occurring over the concrete structure [m]

$m_{c;p;R}$ is a model factor for the strength model [-]

Loading equations:

The head over the concrete structure:

$$\Delta h_a = h - g_w$$

Strength equations:

The critical head associated with the piping process:

$$\Delta h_c = (L_v + 1/3\ L_h)/c_t$$

Parameter definitions:

h = the river water level [mOD]

g_w = the groundwater level behind the concrete structure [mOD]

L_v = the vertical seepage length [m]

L_h = the horizontal seepage length [m]

c_t = the creep ratio [-]

Sources of failure mechanism equations / methods:

Terzaghi & Peck (1967)

Sources of uncertainties in failure equations / input parameters:

Baecher & Christian (2003); CUR 190 (1997); Vrouwenvelder et al. (2001);

B.2.6 Wave impact forces

Figure B.1 shows the wave impact model applied to calculate the wave impact pressures on the reinforced concrete wall due to broken waves. Experiments point out that two pressure peaks characterise the wave impact model. The first peak represents the impact of the wave, see p_{so} and the accompanying rectangular shaped pressure distribution in figure B.1. The second peak represents the pressures exerted by the reflecting wave, see p_p and the accompanying triangular shaped pressure distribution in figure B.1. If the waves are in the process of breaking when they reach the wave return wall the first peak is always dominant. If the incoming waves have been broken on the embankment slope before they reach the wave return wall each one of the two peaks can be dominant. The wave impact pressures in the reliability analysis of the Dartford Creek to Swanscombe Marshes flood defence system are estimated by the impact pressures. Over the unprotected region of the crown wall (above A_c) the pressure is, see figure B.1 and figure B.2:

$p_i(z) = p_{so} = C_{w1}\, \rho_w\, g\, S_o$ with $A_c + S_o > z > A_c$

$C_{w1} = 2.9\, [(R_u/H_c) \cos \alpha]^2$

$S_o = H_c\, (1 - A_c/R_u)$

In which z is the vertical coordinate, referred to a design SWL, positive upward; R_u is the run-up height of the calculation wave (H_c, T_p) on a straight infinite slope; H_c is recommended to be taken as $H_{99.8\%}$, but $1.8H_s$ is also acceptable. The latter is applied in this project. A_c is the level of armour crest above design SWL; ρ_w is the water

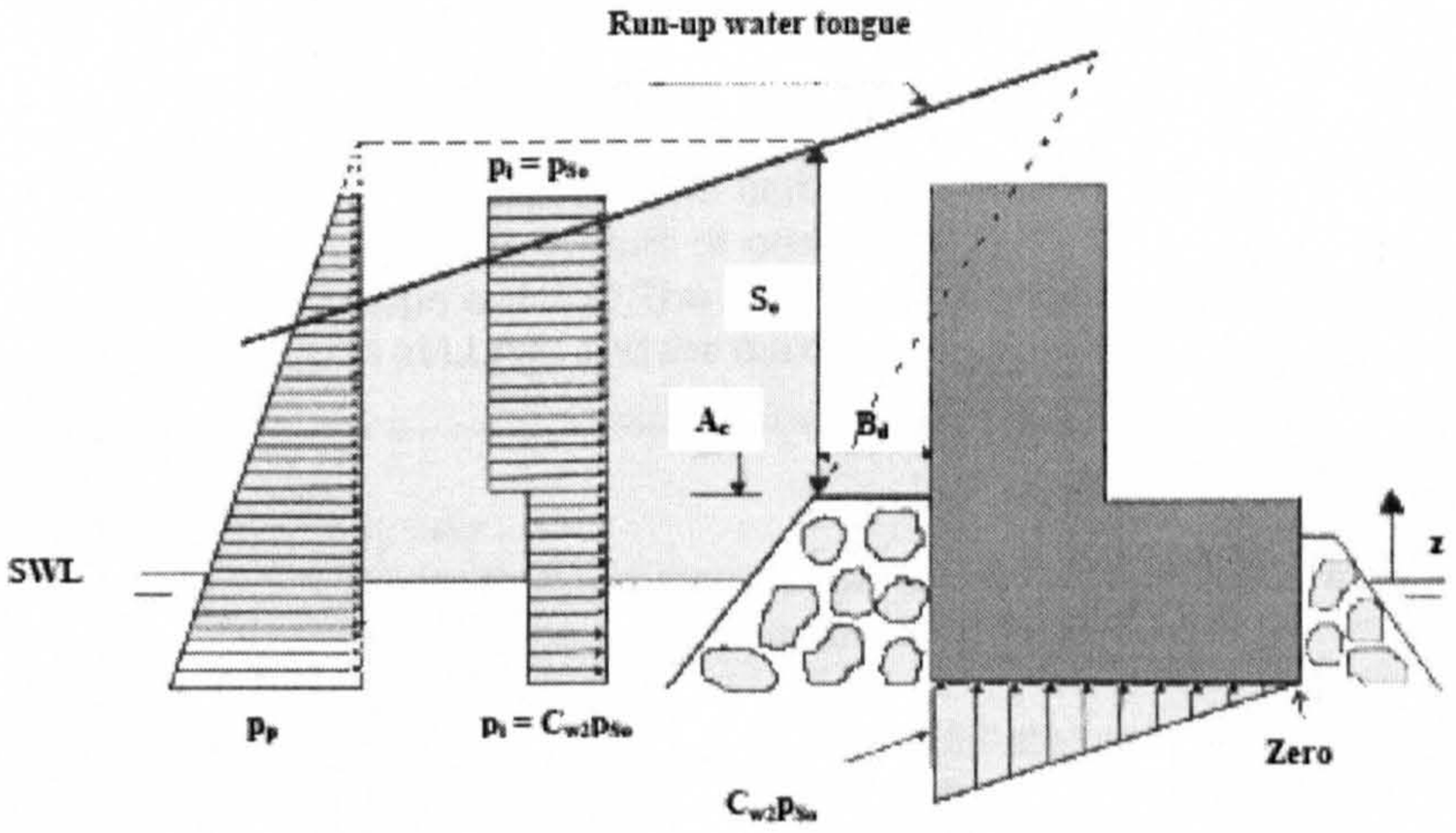

Figure B.1 *Impact pressures, p_{so}, or reflective pressures, p_p, due to a broken wave (from Martín, 1999).*

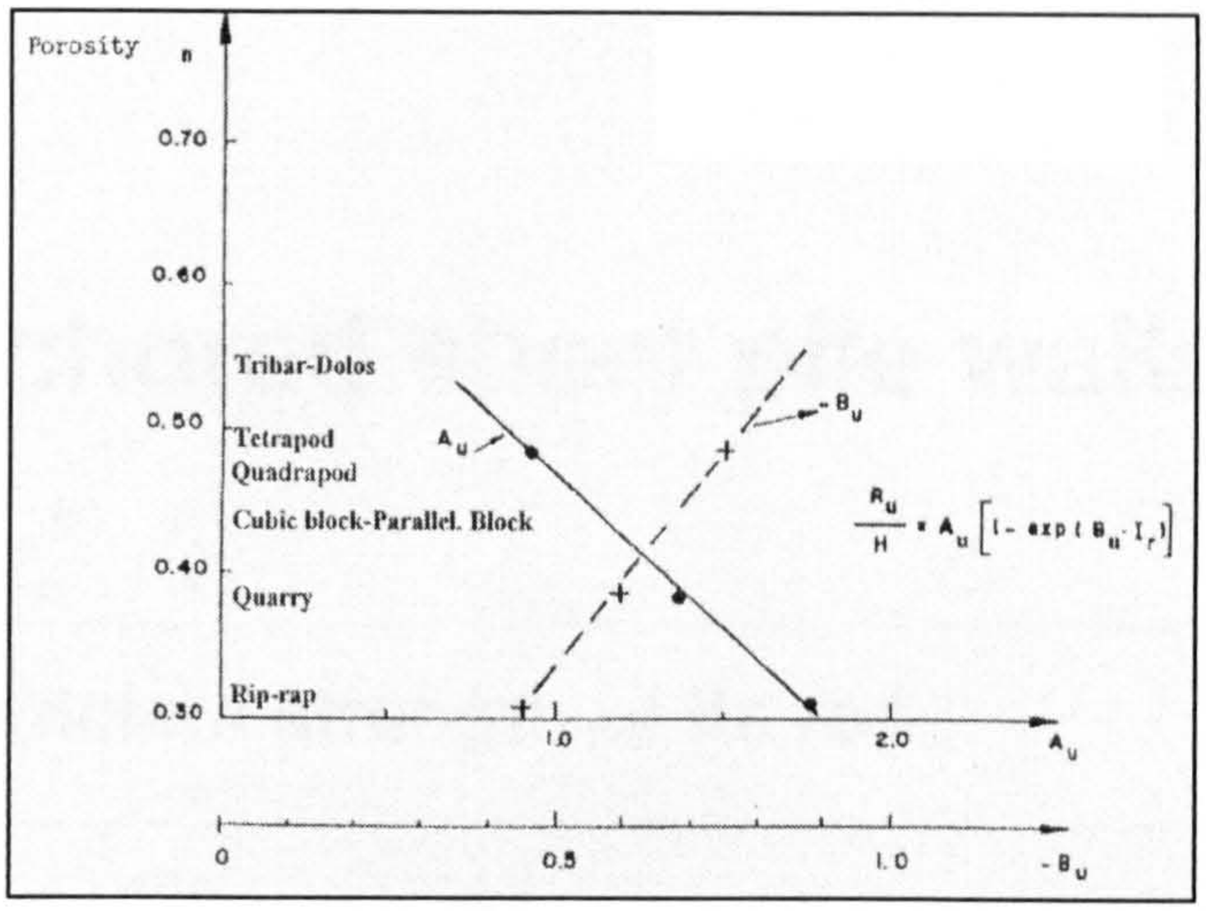

Figure B.2 A_u and B_u as a function of the layer porosity (from Martin, 1999).

density; and g is the gravitational acceleration. To calculate R_u the following equation is proposed:

$R_u/H_c = A_u\,[1 - \exp(-B_u\,Ir)]$

in which A_u and B_u are experimental coefficients, which depend on the type of armour unit, see figure B.2. In this reliability analysis the revetment of the slopes is modelled by riprap, hence A_u= 1.75 and B_u = -0.45. The water defences consist of cohesive soil with a small permeability. Therefore, the uplift pressures exerted by the waves underneath the foundation of the reinforced concrete wall are assumed negligible.

Once the water level has reached the toe of the reinforced concrete wall, the wave impact pressures are approximated by $8\rho_w g H_s$.

B.3 Anchored sheet pile walls

B.3.1 Insufficient strength of tie rod

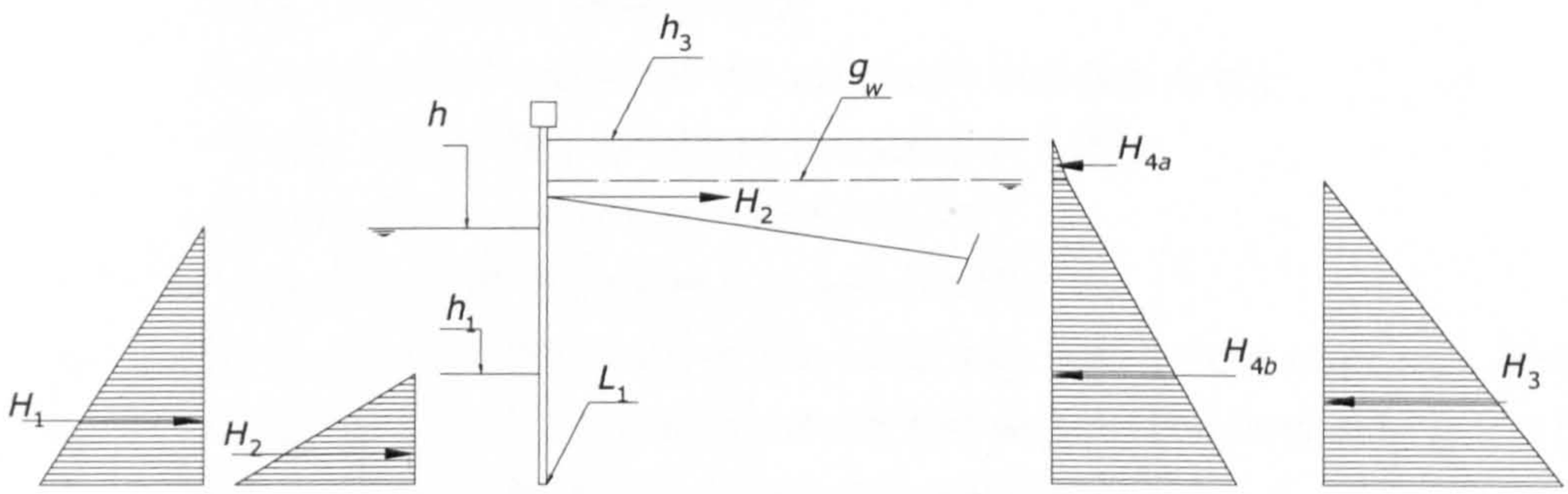

Limit state function:

The tie rod supports the sheet pile wall in taking on the forces. Failure of the tie rod occurs if the stress occurring in the tie rod exceeds the tensile strength of the steel.

$Z = m_1 F_u - m_2 \cdot F_{tot}$

where:

F_u = tensile force capacity of the tie rod [kN]

F_{tot} = total occurring force in the tie rod [kN]

m_1, m_2 = factors taking the model uncertainty into account [-]

Loading equations:

Total occurring force on the sheet pile wall F_{tot}:

$$F_{tot} = H_5 \cdot \frac{x_a}{\cos \alpha}$$

where:

$$H_5 = (H_4 + H_3 - (H_1 + H_2))$$

with:

Strength equations:

Maximum bearable force F_u:

$F_u = A_s \cdot f_s$

$$H_1 = 0.5 \cdot \gamma_w (h - L_1)^2$$

$$H_2 = 0.5 \cdot K_p (\gamma_s - \gamma_w) \cdot (h_1 - L_1)^2$$

$$H_3 = 0.5 \cdot \gamma_w (g_w - L_1)^2$$

$$H_{4a} = 0.5 \cdot K_a \cdot \gamma_d (h_3 - g_w)^2$$

$$H_{4b} = K_a \cdot \gamma_d ((h_3 - g_w) + (g_w - L_1)) + 0.5 \cdot K_a \cdot (\gamma_s - \gamma_w)(g_w - L_1)^2$$

Parameter definitions:

h	=	the river water level [mOD]
g_w	=	the ground water level [mOD]
γ_s	=	the volumetric weight of the saturated soil [kN / m^3]
γ_d	=	the dry volumetric weight of the soil [kN / m^3]
γ_w	=	the volumetric weight of water [kN /m^3]
L_1	=	the toe level of the sheet pile wall [mOD]
h_1	=	the ground level in front of the sheet pile wall on the river side [mOD]
h_3	=	the ground level next to the sheet pile wall on the land side [mOD]
K_a	=	the coefficient for active horizontal grain force [-]
K_p	=	the coefficient for passive horizontal grain force [-]
x_a	=	the distance between two tie rods [m]
A_s	=	the total area of the tie rod [m^2]
f_s	=	the yield stress of the steel, net of any factoring [kN/m^2]
α	=	the angle of inclination of the tie rod [°]

Sources of failure mechanism equations / methods:

See also Floodsite (2007)

Sources of uncertainties in failure equations / input parameters:

Baecher & Christian (2003); CUR (1997); Vrouwenvelder et al. (2001)

B.3.2 Insufficient strength of soil at anchor

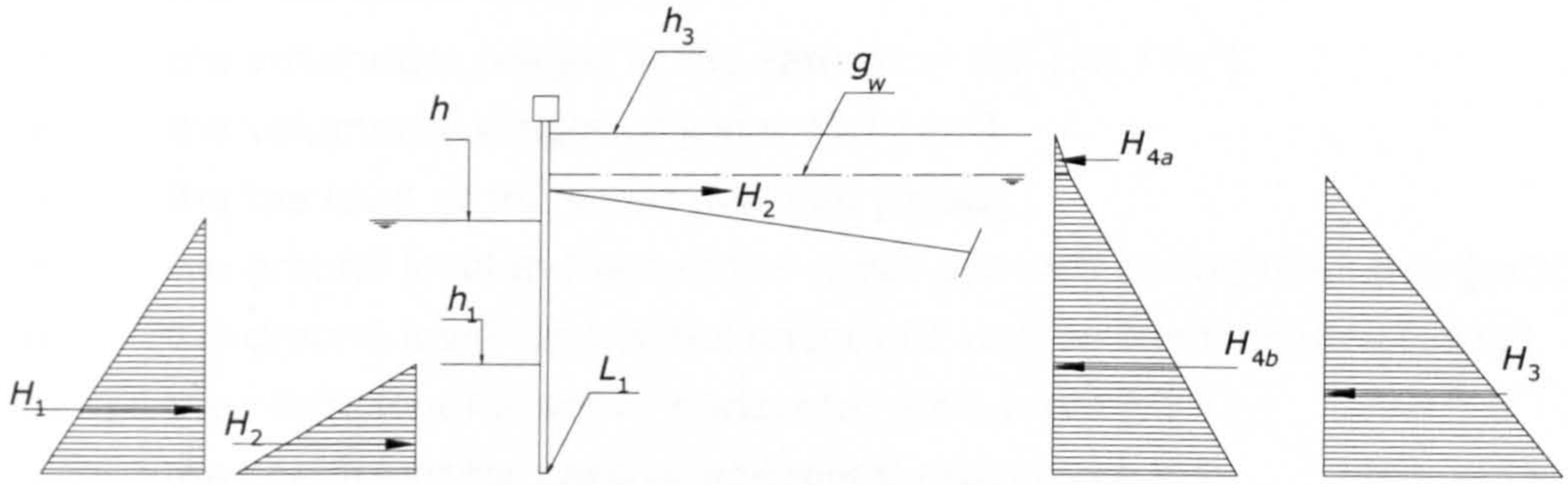

Limit state function:

The anchor head transfers the force from the tie rod to the soil. Failure occurs if the stress exerted by the anchor head exceeds the shear strength of the soil.

The limit state function reads as follows:

$$Z = m_1 \cdot F_r - m_2 \cdot F_{tot}$$

where:

F_r = force capacity of the soil around the anchor head [kN]

H_5 = total occurring force in the anchor [kN]

m_1, m_2= factors taking the model uncertainty in the strength model and the loading model into account [-]

Loading equations:

The horizontal force on the sheet pile wall F_{tot}:

$$F_{tot} = H_5$$

where:

$$H_5 = (H_4 + H_3 - (H_1 + H_2)) \cdot x_a$$

with:

$$H_1 = 0.5 \cdot \gamma_w (h - L_1)^2$$

$$H_2 = 0.5 \cdot K_p (\gamma_s - \gamma_w) \cdot (h_1 - L_1)^2$$

$$H_3 = 0.5 \cdot \gamma_w (g_w - L_1)^2$$

$$H_{4a} = 0.5 \cdot K_a \cdot \gamma_d (h_3 - g_w)^2$$

Strength equations:

The maximum force the tie rod can withstand based on the strength of the soil is defined as follows:

$$F_r = 0.5(\alpha + \beta - 1) h_a d_a^2 \gamma_d \left(\frac{1 + \sin\varphi}{1 - \sin\varphi} - \frac{1 - \sin\varphi}{1 + \sin\varphi} \right)$$

$$- q h_a d_a (\alpha + \beta - 1) \frac{1 - \sin\varphi}{1 + \sin\varphi}$$

where:

$$\alpha = b_a / h_a$$

$H_{4b} = K_a \cdot \gamma_d (h_3 - g_w)(g_w - L_1) + 0.5 \cdot K_a (\gamma_s - \gamma_w)(g_w - L_1)^2$	

Parameter definitions:

h	=	the river water level [mOD]
g_w	=	the river water level [mOD]
γ_s	=	the volumetric weight of the saturated soil [kN / m^3]
γ_w	=	the volumetric weight of water [kN / m^3]
L_1	=	the toe level of the sheet pile wall [mOD]
h_1	=	the ground level in front of the sheet pile wall on the river side [mOD]
h_3	=	the ground level next to the sheet pile wall on the land side [mOD]
K_a	=	the coefficient for active horizontal grain force [-]
K_p	=	the coefficient for passive horizontal grain force [-]
x_a	=	the distance between two tie rods [m]
h_a	=	the height of the anchor head [m]
b_a	=	the width of the anchor head [m]
d_a	=	the depth of the bottom of the anchor head [m]
γ_d	=	the dry volumetric weight of the soil [kN / m^3]
a	=	ba/ha [-]
β	=	factor according to Buchholz [-]
q	=	surcharge load behind the anchored sheet pile wall [kN / m^2]
φ	=	the angle of internal friction of the soil [°]

Sources of failure mechanism equations / methods:

See also Floodsite (2007)

Sources of uncertainties in failure equations / input parameters:

Baecher & Christian (2003); CUR (1997); Vrouwenvelder et al. (2001)

B.3.3 Failure of sheet pile wall element in bending

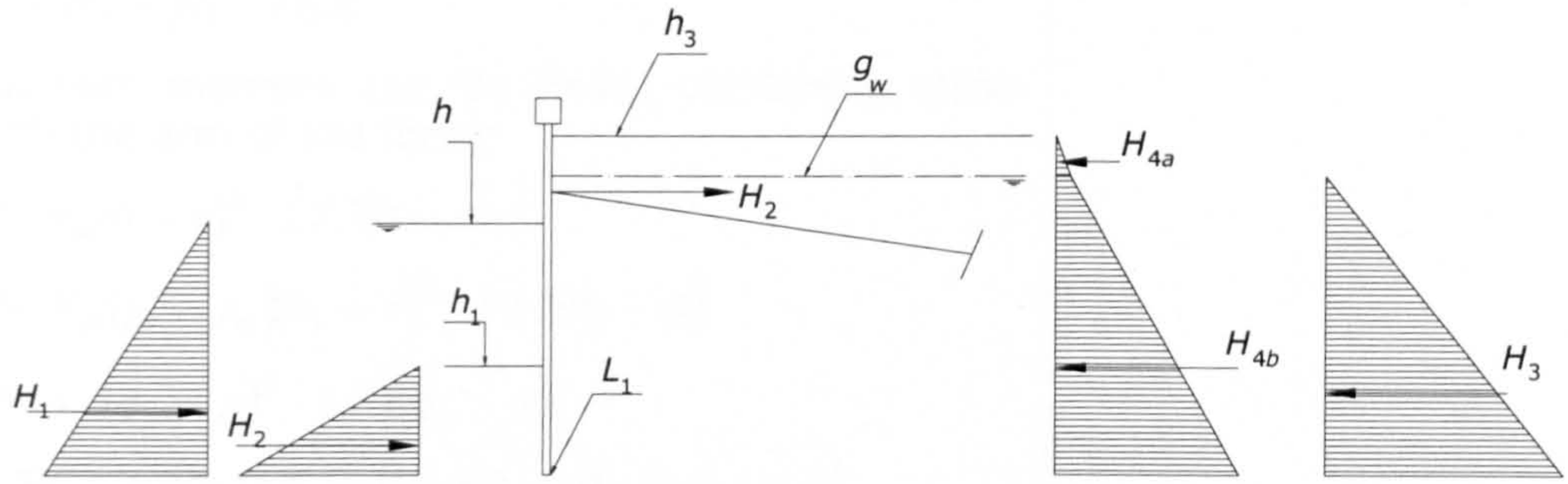

Limit state function:

Failure occurs if the capacity of the sheet pile cross section is exceeded by the actual bending moments. From the maximum bending moment in the sheet pile, a maximum tensile stress in the sheet pile wall can be derived, using the moment of inertia and the height of the section. That tensile stress is compared against the yield stress of the sheet pile steel

The limit state function reads as follows:

$$Z = m_1 \cdot f_s - m_2 \cdot \sigma_b$$

where:

f_s = yield stress of the steel cross section [kN/m^2]

σ_b = maximum tensile stress in the sheet pile [kN/m^2]

m_1, m_2 = factors taking the model uncertainty into account [-]

Loading equations:

The maximum tensile stress in the sheet pile cross section is:

$$\sigma_b = M_{\max} \cdot \frac{z}{I_z}$$

The maximum and minimum moments along the length of the sheet pile walls are found where the shear force in the cross section is 0. M_{max} is the highest of those maxima and minima. The shear force in the cross section at a level x can be found with the following equations:

$$H_1 = 0.5 \cdot \gamma_w \cdot (h - x)^2$$

$$H_2 = 0.5 \cdot K_p \cdot (\gamma_s - \gamma_w)(h_1 - x)^2$$

Strength equations:

The yield stress f_s of the steel sheet pile cross section (net of any factoring) determines the limit of the tensile stress.

f_s = 435 N/mm^2

$$H_3 = 0.5 \cdot \gamma_w (g_w - x)^2$$

$$H_{4a} = 0.5 \cdot K_a \cdot \gamma_d (h_3 - g_w)^2$$

$$H_{4b} = K_a \cdot \gamma_d (h_3 - g_w)(g_w - x) + 0.5 \cdot K_a \cdot (\gamma_s - g_w)(g_w - x)^2$$

$$H_5 = (H_4 + H_3 - (H_1 + H_2))$$

The maximum moment can be found combining shear forces with the arm of the force:

$$M_1 = 0.5 \cdot \gamma_w (h - x)^2 \cdot 1/3(h - x)$$

$$M_2 = 0.5 \cdot K_p (\gamma_s - \gamma_w)(h_1 - x)^2 \cdot 1/3(h_1 - x)$$

$$M_3 = 0.5 \cdot \gamma_w (g_w - x)^2 \cdot 1/3(g_w - x)$$

$$M_{4a} = 0.5 K_a \cdot \gamma_d (h_3 - g_w) \cdot (1/3(h_3 - g_w) + g_w - x)$$

$$M_{4b} = 0.5 \cdot K_a \cdot \gamma_d (h_3 - g_w)(g_w - x) + 0.5 \cdot K_a (\gamma_s - \gamma_w)(g_w - x)^2 1/3(g_w - x)$$

Parameter definitions:

h	=	the river water level [mOD]
g_w	=	groundwater level [mOD]
γ_d	=	the volumetric weight of the dry soil [kN / m3]
γ_s	=	the volumetric weight of the saturated soil [kN / m3]
γ_w	=	the volumetric weight of water [kN / m3]
L_1	=	the toe level of the sheet pile wall [mOD]
h_1	=	the ground level in front of the sheet pile wall on the river side [mOD]
h_3	=	the ground level next to the sheet pile wall on the land side [mOD]
K_a	=	the coefficient for active horizontal grain force [-]
K_p	=	the coefficient for passive horizontal grain force [-]
z	=	the distance between the centre of gravity and the outer edge of the sheet pile profile [m]
I_z	=	the moment of inertia of the sheet pile cross section [m^4/m]
M_{max}	=	the maximum bending moment in the sheet pile wall [kNm/m]

Sources of failure mechanism equations / methods:

See also Floodsite (2007)

Sources of uncertainties in failure equations / input parameters:

Baecher & Christian (2003); CUR (1997); Vrouwenvelder et al. (2001)

B.3.4 Rotation failure of sheet pile wall after loss of tie rod

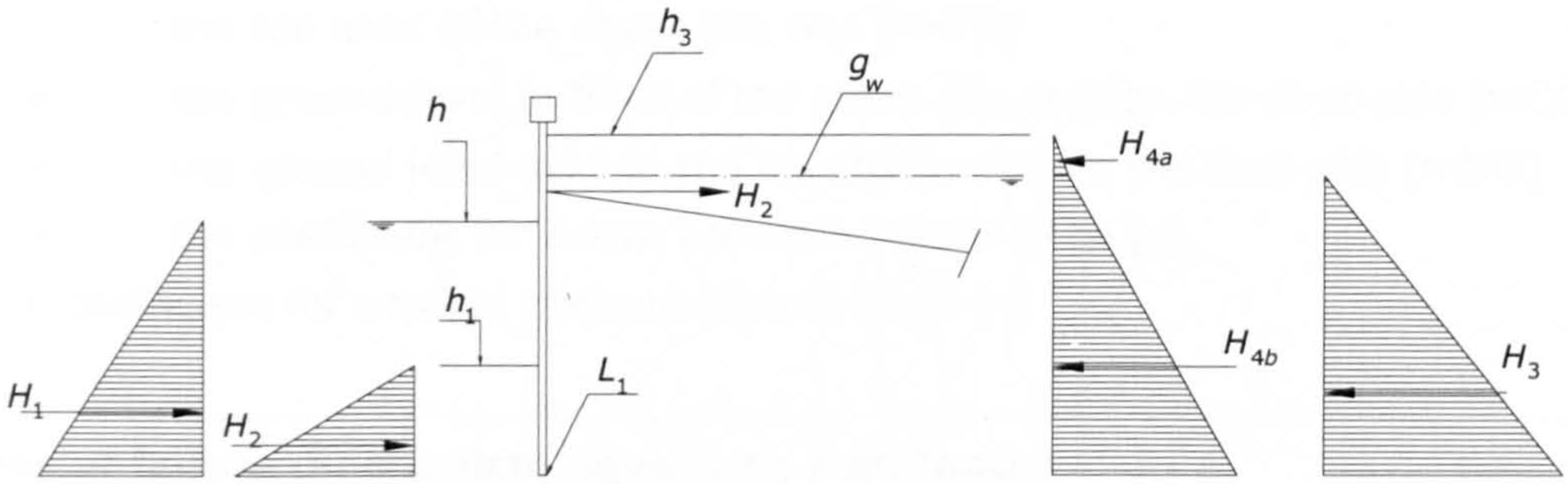

Limit state function:

Collapse of the sheet pile wall after failure of the tie rod depends on moment equilibrium around the toe of the

sheet pile.

The limit state function reads as follows:

$Z = m_{spa;m;R}\, M_r - m_{spa;m;S} \cdot M_l$

where:

M_r = resulting resisting moment [kNm/m]

M_l = resulting loading moment [kNm/m]

$m_{spa;m;R}$ = model factor for the strength model [-]

$m_{spa;m;S}$ = model factor for loading model [-]

Loading equations:

The resulting loading moment is taken around the toe of the sheet pile wall and is built up as follows:

$M_1 = M_3 + M_{4a} + M_{4b}$

where:

$M_3 = 0.5 \cdot \gamma_w (g_w - L_1)^2 \cdot 1/3(g_w - L_1)$

$M_{4a} = 0.5 \cdot K_a \cdot \gamma_d (h_3 - g_w)(1/3(h_3 - g_w) + g_w - L_1)$

$M_{4b} = 0.5 \cdot K_a \cdot \gamma_d (h_3 - g_w)(g_w - L_1)$

$+ 0.5 \cdot K_a (\gamma_s - \gamma_w)(g_w - L_1)^2 \cdot 1/3(g_w - L_1)$

Strength equations:

The resulting resisting moment is taken around the toe of the sheet pile wall and is built up as follows:

$M_r = M_1 + M_2$

where:

$M_1 = 0.5 \cdot \gamma_w (h - L_1)^2 \cdot 1/3(h - L_1)$

$M_2 = 0.5 \cdot K_p \cdot (\gamma_s - \gamma_w)(h_1 - L_1)^2 \cdot 1/3(h_1 - L_1)$

Parameter definitions:

h = the river water level [mOD]

g_w = groundwater level [mOD]

γ_s = the volumetric weight of the saturated soil [kN / m^3]

γ_w = the volumetric weight of water [kN / m^3]

L_1 = the toe level of the sheet pile wall [mOD]

h_1 = the ground level in front of the sheet pile wall on the river side [mOD]

h_3 = the ground level next to the sheet pile wall on the land side [mOD]

K_a = the coefficient for active horizontal grain force [-]

K_p = the coefficient for passive horizontal grain force [-]

Sources of failure mechanism equations / methods:

See also Floodsite (2007)

Sources of uncertainties in failure equations / input parameters:

Baecher & Christian (2003); CUR (1997); Vrouwenvelder et al. (2001)

Appendix C

Statistical distribution functions of random variables for flood defence sections 4, 16, 26, 48 and 53

C.1 Definition of the random variables of earth embankment section 4

		Flood defence section 4				
			Crest 1		Crest 2	
		Stat. dist. function	Mean value	Stdv	Mean value	Stdv
h =	water level (mOD)	JoinSea	-	-	-	-
H_s =	significant wave height (m)	Bretschneider	-	-	-	-
T_p =	Peak wave period (s)	Bretschneider	-	-	-	-
h_c =	crest level (mOD)	N	6.21	0.1	6.94	0.1
c_w =	crest width (m)	LN	3.1	0.2	3.8	0.2
tan_o =	tan outside slope (-)	N	0.375	0.01875	0.28	1.43E-02
tan_i =	tan inside slope (-)	N	0.39	1.9-02	0.32	1.58E-02
c_g =	erosion strength grass (ms)	LN	300000	30000	1000000	100000
c_{RK} =	erosion strength core (ms)	LN	340000	34000	340000	34000
d_w =	depth grass roots (m)	LN	0.1	0.02	0.1	0.02
P_t =	pulsating percentage (-)	Det	0.5	0	0.5	0
r_i =	roughness inside slope (-)	LN	0.015	0.00375	0.015	0.00375
t_s =	storm duration (h)	LN	5	1.25	5	1.25
m_{qe}=	model uncertainty erosion model (-)	LN	1	0.5	1	0.5
d =	thickness impermeable layer (m)	LN	8.1	2.43	8.1	2.43
γ_s =	Volumetric weight saturated soil (kN/m^3)	N	10.9898	0.54949	10.9898	0.54949
γ_w =	Volumetric weight water (kN/m^3)	N	10	0.1	10	0.1
h_b =	ground water level (mOD)	N	1	0.1	1	0.1
m_u =	model uncertainty uplifting (-)	LN	1.2	0.12	1.2	0.12
L =	seepage length (m)	LN	58.5	5.85	58.5	5.85
η =	constant of White (-)	LN	0.3	0.045	0.3	0.045
d_{70} =	d70 of sand (m)	LN	0.00964	0.001446	0.00964	0.001446
k_s =	permeability of sand (m/s)	LN	0.0023846 15	0.000477	0.002384615	0.000477
m_p =	model uncertainty piping (-)	LN	0.7	0.07	0.7	0.07
θ =	angle piping model (°)	LN	53	3	53	3
D =	Thickness water conductive sand layer(m)	LN	6.5	1.95	6.5	1.95
γ_{sand} =	Volumetric weight sand in water conductive layer (kN/m^3)	N	18.5	0.925	18.5	0.925
l_l1 =	layer levels (mOD)	N	1.6	0.2	1.6	0.2
l_l2 =		N	0.6	0.2	0.6	0.2
l_l3 =		N	-1.1	0.2	-1.1	0.2
l_l4 =		N	-1.9	0.2	-1.9	0.2
l_l5 =		N	-2.1	0.2	-2.1	0.2
l_l6 =		N	-2.4	0.2	-2.4	0.2
l_l7 =		N	-3.7	0.2	-3.7	0.2
l_l8 =		N	-6.2	0.2	-6.2	0.2
l_l9 =		N	-6.5	0.2	-6.5	0.2
l_l10 =		N	-6.7	0.2	-6.7	0.2
l_l11 =		N	-8.2	0.2	-8.2	0.2

γ_{s1} =	Saturated volumetric weight soil layers l_l1-l_l11 (kN/m^3)	N	15	0.75	15	0.75
γ_{s2} =		N	15	0.75	15	0.75
γ_{s3} =		N	15	0.75	15	0.75
γ_{s4} =		N	11	0.55	11	0.55
γ_{s5} =		N	15	0.75	15	0.75
γ_{s6} =		N	11	0.55	11	0.55
γ_{s7} =		N	11	0.55	11	0.55
γ_{s8} =		N	15	0.75	15	0.75
γ_{s9} =		N	11	0.55	11	0.55
γ_{s10} =		N	19.08	0.954	19.08	0.954
γ_{s11} =		N	20.81	1.0405	20.81	1.0405
γ_{d1} =	Dry volumetric weight soil layers l_l1-l_l11 (kN/m^3)	N	9	0.45	9	0.45
γ_{d2} =		N	9	0.45	9	0.45
γ_{d3} =		N	9	0.45	9	0.45
γ_{d4} =		N	3	0.15	3	0.15
γ_{d5} =		N	9	0.45	9	0.45
γ_{d6} =		N	3	0.15	3	0.15
γ_{d7} =		N	3	0.15	3	0.15
γ_{d8} =		N	9	0.45	9	0.45
γ_{d9} =		N	3	0.15	3	0.15
γ_{d10} =		N	15.22	0.761	15.22	0.761
γ_{d11} =		N	18.65	0.9325	18.65	0.9325

C.2 Definition of the random variables of reinforced concrete wall sections 16, 26 and 48

		Stat. dist. function	Section 16		Section 26		Section 48	
			Mean value	Stdv	Mean value	Stdv	Mean value	Stdv
h	= Water level (mOD)	Joinsea	-	-	-	-	-	-
H_s	= Significant wave height (m)	Bretschneider	-	-	-	-	-	-
T_p	= Peak wave period (s)	Bretschneider	-	-	-	-	-	-
h_c	= Crest level (mOD)	LN	7.1	0.1	6.88	0.1	6.98	0.1
γ_w	= Volumetric weight water (kN/m3)	LN	10	0.1	10	0.1	10	0.1
tan_o	= tan outside slope (-)	LN	0.44	2.2E-02	0.53	0.026	0.031	0.0016
β	= obliqueness waves (°)	LN	43	5	82	5	-5	5
D	= thickness impermeable layers (m)	LN	10.66	3.198	8.70	2.61	-	-
γ_s	= saturated volumetric weight of the soil (kN/m^3)	LN	13.4	0.66	15	0.75	-	-
h_b	= ground water level (mOD)	LN	1	0.1	1	0.1	-	-
m_u	= model uncertainty uplifting (-)	LN	1.2	0.12	1.2	0.12	-	-
L	= seepage length (m)	LN	100	10	100	10	-	-
η	= constant of White (-)	LN	0.3	0.045	0.3	0.045	-	-
d_{70}	= d70 of sand (m)	LN	0.009	0.001	0.009	0.001	-	-
k_s	= permeability of sand (m/s)	LN	0.0001	0.00001	0.000045	0.000009	-	-
m_p	= model uncertainty piping (-)	LN	0.7	0.07	0.7	0.07	-	-
θ	= angle piping model (°)	LN	53	3	53	3	-	-
D	= Thickness water conductive sand layer(m)	LN	6.5	1.95	6.5	1.95	-	-
γ_{sand}	= Volumetric weight sand in water conductive layer (kN/m^3)	LN	18.5	0.925	18.5	0.925	-	-
K_a	= Active horizontal grain stress coeff. (-)	LN	0.33	3.3E-02	0.33	3.3E-02	0.33	3.3E-02
K_p	= Passive horizontal grain stress coeff. (-)	LN	3	0.3	3	0.3	3	0.3
m_R	= Model uncertainty strength model (-)	LN	1	0.5	1	0.5	1	0.5
m_S	= Model uncertainty loading model (-)	LN	1	0.5	1	0.5	1	0.5
γ_c	= Volumetric weight of concrete (kN/m^3)	LN	25	0.25	25	0.25	25	0.25
δ	= Friction angle (°)	LN	40	5	40	5	40	5
$d1$	= Dimension concrete wall (m)	LN	-	-	3	0.03	2	0.02
$d2$	= Dimension concrete wall (m)	LN	0.3	0.003	0.3	0.003	0.4	0.004
$d3$	= Dimension concrete wall (m)	LN	3	0.03	-	-	2	0.02
$d4$	= Dimension concrete wall (m)	LN	1.95	0.0195	1.7	0.017	3.08	0.0308
$d5$	= Dimension concrete wall (m)	LN	0.3	0.003	0.3	0.003	0.4	0.004
$d6$	= Dimension concrete wall (m)	LN	0.6	0.006	0.7	0.007	2.4	0.024
$d7$	= Dimension concrete wall (m)	LN	0.5	0.005	0.3	0.003	0.4	0.004
$d8$	= Dimension concrete wall (m)	LN	0.5	0.005	0.3	0.003	-	-
$d9$	= Dimension concrete wall (m)	LN	0.6	0.006	0.7	0.007	-	-
$L1$	= Riverward toe level (mOD)	LN	-1	0.2	4.18	0.2	-1	0.2
$L3$	= Landward toe level (mOD)	LN	0	0.2	0	0.2	0	0.2
Lc	= Length of concrete wall unit (m)	LN	5	0.2	5	0.2	5	0.2
g_w	= Ground water level in floodplain (mOD)	LN	4.2	0.2	4.4	0.2	2.8	0.2
h_1	= Ground level floodplain side	LN	5.4	0.2	5.39	0.2	4.1	0.2
h_2	= Top of horizontal concrete slab floodplain side (mOD)	LN	5.15	0.2	5.18	0.2	3.9	0.2
h_3	= Ground level riverward side (mOD)	LN	5.2	0.2	5.4	0.2	3.8	0.2
A_s	= Area reinforcement (mm^2)	LN	2504	25.04	2504	25.04	2504	25.04
f_s	= Yield stress reinforcement steel (N/mm^2)	LN	435	4.35	435	4.35	435	4.35
f_b'	= Cubic pressure strength concrete (N/mm^2)	LN	18	0.9	18	0.9	18	0.9
f_b	= Tensile strength concrete (N/mm^2)	LN	1.275	0.06375	1.275	0.06375	1.275	0.06375
d_s	= Distance top of pressure zone concrete cross section to heart reinforcement (m)	LN	0.25	0.0025	0.25	0.0025	0.35	0.0035
ε_{bu}	= Limit strain concrete for breaking (-)	LN	3.75	0.0375	3.75	0.0375	3.75	0.0375
ε_b	= Plasticity strain concrete (-)	LN	1.75	0.0175	1.75	0.0175	1.75	0.0175
E_c	= Elasticity modulus (N/mm^2)	LN	29750	1487.5	29750	1487.5	29750	1487.5
c_T	= Terzaghi creep coefficient piping (-)	LN	6	0.1	6	0.1	6	0.1
m_t	= Model uncertainty piping toe model	LN	1	0.1	1	0.1	1	0.1
l_l1	= Transition between top layer and 2nd strata	N	5.5	0.2	3.56	0.2	3.71	0.2
l_l2	= Transition between 2nd strata and 3rd strata	N	2.01	0.2	-4.81	0.2	1.81	0.2
l_l3	=	N	1.25	0.2	-	0.2	-2.19	0.2

l_l4	=	N	0.49	0.2	-	0.2	-4.49	0.2
l_l5	=	N	-0.27	0.2	-	0.2	-16.29	0.2
l_l6	=	N	-7.43	0.2	-	0.2	-	0.2
l_l7	=	N	-7.89	0.2	-	0.2	-	0.2
l_l8	=	N	-8.8	0.2	-	0.2	-	0.2
l_l9	=	N	-10.17	0.2	-	0.2	-	0.2
l_l10	=	N	-12.15	0.2	-	0.2	-	0.2
ys1	= saturated volumetric weight of the top strata	N	15	0.75	15	0.75	19.1	0.95
ys2	= saturated volumetric weight of the 2nd strata	N	20.8	1.0	15	0.75	19.1	0.95
ys3	=	N	20.8	1.0	20.8	1.0	15	0.75
ys4	=	N	15	0.75	-	-	15	0.75
ys5	=	N	11	0.55	-	-	20.81	1.04
ys6	=	N	15	0.75	-	-	-	-
ys7	=	N	11	0.55	-	-	-	-
ys8	=	N	15	0.75	-	-	-	-
ys9	=	N	20.81	1.04	-	-	-	-
ys10	=	N	20.81	1.04	-	-	-	-
yd1	= dry volumetric weight of the top strata	N	9	0.45	9	0.45	15.22	0.76
yd2	= dry volumetric weight of the 2nd strata	N	18.7	0.9	9.0	0.5	15.2	0.8
yd3	=	N	18.7	0.9	18.7	0.9	9.0	0.5
yd4	=	N	9	0.45	-	-	9	0.45
yd5	=	N	3	0.15	-	-	18.65	0.93
yd6	=	N	9	0.45	-	-	-	-
yd7	=	N	3	0.15	-	-	-	-
yd8	=	N	9	0.45	-	-	-	-
yd9	=	N	18.65	0.93	-	-	-	-
yd10	=	N	18.65	0.93	-	-	-	-

C.3 Definition of the random variables of anchored sheet pile wall section 53

			Stat. dist. function	Section 53	
				Mean value	Stdv
h	=	Water level (mOD)	JoinSea	-	-
h_c	=	Crest level (mOD)	N	6.98	0.1
γ_w	=	Volumetric weight of the water (kN/m^3)	N	10	0.1
K_a	=	Active horizontal grain stress coeff. (-)	LN	0.33	3.3E-02
K_p	=	Passive horizontal grain stress coeff. (-)	LN	3	0.3
d_a	=	Depth anchor head underneath ground level (m)	N	18.7	0.2
α_{an}	=	Angle anchor with horizontal (°)	N	30	1.5
m_R	=	Model uncertainty strength model (-)	LN	1	0.5
m_S	=	Model uncertainty loading model (-)	LN	1	0.5
q	=	Superimposed loading behind sheet pile wall (kN/m^2)	N	50	2.5
L_1	=	Level of the sheet pile toe (mOD)	N	-7.5	0.2
L_2	=	River bed level (mOD)	N	-0.07	0.2
L_3	=	Connection anchor with sheet pile (mOD)	N	4	0.2
g_w	=	Ground water level (mOD)	N	3.91	0.2
A_s	=	Area sheet pile cross section (mm^2)	N	24200	242
h_a	=	Height anchor head (m)	N	0.5	0.2
b_a	=	Width anchor head (m)	N	0.5	0.2
h_3	=	Ground level behind the sheet pile wall (mOD)	N	1.51	0.2
A_a	=	Area of the anchor cross section (mm^2)	N	1450	14.5
x_a	=	Distance between centres of the anchors (m)	N	1.5	0.015
f_s	=	Yield stress steel (N/mm^2)	N	410	4.1
z	=	Section modulus (mm^3/m)	LN	387370000	3873700
l_l_1	=	Transition between top level and 2nd strata (mOD)	N	4.95	0.2
l_l_2	=	Transition between 2nd and 3rd strata (mOD)	N	-0.97	0.2
l_l_3	=	Transition between 3rd and 4th strata (mOD)	N	-2.97	0.2
l_l_4	=	Transition between 4th and 5th strata (mOD)	N	-6.17	0.2
l_l_5	=	Transition between 5th and 6th strata (mOD)	N	-8.97	0.2
γ_{s1}	=	Saturated volumetric weight of top strata (kN/m^3)	N	19.08	0.954
γ_{s2}	=	Saturated volumetric weight of 2nd strata (kN/m^3)	N	19.08	0.954
γ_{s3}	=	Saturated volumetric weight of 3rd strata (kN/m^3)	N	15	0.75
γ_{s4}	=	Saturated volumetric weight of 4th strata (kN/m^3)	N	20.81	1.0405
γ_{s5}	=	Saturated volumetric weight of 5th strata (kN/m^3)	N	20.81	1.0405
γ_{d1}	=	Dry volumetric weight of top strata (kN/m^3)	N	15.22	0.761
γ_{d2}	=	Dry volumetric weight of 2nd strata (kN/m^3)	N	15.22	0.761
γ_{d3}	=	Dry volumetric weight of 3rd strata (kN/m^3)	N	9	0.45
γ_{d4}	=	Dry volumetric weight of 4th strata (kN/m^3)	N	18.65	0.9325
γ_{d5}	=	Dry volumetric weight of 5th strata (kN/m^3)	N	18.65	0.9325

Appendix D

Autocorrelations and correlation distances in system reliability model

Variable	Description	Unit	Correlation distance d_x (m) (equation 2.29)	Auto-correlation ρ_x (equation 2.29)
h	water level	mOD	0	1
H_s	significant wave height	m	0	1
T_p	peak wave period	s	0	1
h_c	crest level	mOD	300	0
c_w	crest width	m	300	0
tan_o	tan outside slope	-	150	0
tan_i	tan inside slope	-	150	0
c_g	erosion strength grass	m·s	0	0
c_{RK}	erosion strength core	m·s	0	0
d_w	depth grass roots	m	150	0
P_t	pulsating percentage	-	0	0
R_i	roughness inside slope	-	300	0.5
t_s	storm duration	h	0	1
m_{qe}	model uncertainty erosion model	-	1500	0.4
r_o	roughness outside slope	-	300	0.5
β	obliqueness waves	°	0	0
A	coefficient Owen's model	-	0	0
B	idem	-	0	0
num	type of overtopping model	-	0	0
m_{qo}	model uncertainty owen's model	-	Section length	0.7
D	thickness impermeable layers	m	300	0
γ_{wet}	saturated density of the soil	kN/m^3	300	0
γ_w	density of the water	kN/m^3	300	0
g_w	ground water level in floodplain	mOD	Section length	1
m_u	model uncertainty uplifting	-	0	0
L	seepage length	m	3000	0
η	constant of White	-	0	0
d_{70}	d70 of sand in conductive layer	m	180	0
k_s	permeability of conductive sand	m/s	180	0
m_p	model uncertainty piping	-	0	0
θ	angle piping model	°	750	0
$b3$	thickness sand layer	m	0	0
$f4$	density sand	kg/m^3	0	0
l_l_1 - l_l_{14}	layer levels	mOD	300	0
phi_1-phi_{15}	effective angle of internal friction for the layers	°	50	0
c_1-c_{15}	effective cohesion of the layers	kPa	50	0
γ_{s1}-γ_{s15}	saturated density of the layers	kN/m^3	300	0

γ_{d1}-γ_{d15}	dry density of the layers	kN/m^3	300	0
K_a	coefficient horizontal grain stress; active	-	300	0
K_p	coefficient horizontal grain stress; passive	-	300	0
d_a	depth anchors	m	Section length	0
angle	angle of inclination anchors	°	Section length	0
f_y	yield stress sheet pile profile	N/m^2	Section length	0
no_anch	average number of anchors per stretching meter	-	N/A	N/A
rad	radius of anchors	m	Section length	0
moment	Section modulus	m^3/m	Section length	0
γ_c	volumetric weight concrete	kN/m^3	Section length	0
q	superimposed force behind gravity based wall	kN/m^2	0	0
δ	friction angle	°	0	0
d_1-d_9	dimension concrete wall	m	Section length	0
L_1-L_4	level concrete wall / sheet pile wall	mOD	Section length	0
L_c	Distance between two joints of concrete structure	m	Section length	0
g_{w2}	ground water level in retaining structure	mOD	0	1
A_s	Area of reinforcement in concrete	mm^2	Section length	0
f_s	yield stress of reinforcement bars	N/m^2	Section length	0
f'_b	pressure strength of concrete	N/mm^2	Section length	0
f_b	tensile strength of concrete	N/mm^2	Section length	0
ds	distance of reinforcement from outer concrete fibre	m	Section length	0
ε_{bu}	Limit strain related to breaking concrete	-	Section length	0
ε_b	Plasticity strain concrete	-	Section length	0
E_c	Elasticity modulus	N/mm^2	Section length	0
A_{sh}	Area sheet pile profile	mm^2	Section length	0
h_a	height anchor	m	N/A	0
b_a	width anchor	m	N/A	0
h_1	elevation riverside in front of concrete wall	mOD	300	0
h_2	level of top of foundational concrete slab	mOD	Section length	0
h_3	elevation ground behind concrete wall landward	mOD	300	0
A_a	Anchor area	mm^2	N/A	0
hoh_a	distance between two anchors	m	N/A	0
t_red_1-t_red_6	corrosion rates sheet pile - atmosferic, splash, tidal, intertidal, continuously immersed, mud embedded zones	mm/year	20	0
$zone_1$-$zone_6$	zone levels -atmosferic, splash, tidal, intertidal, continuously immersed, mud embedded	mOD	300	0
t_sheet	thickness steel sheet pile wall	mm	Section length	0
Cc_1-Cc_{15}	compression index	-	50	0
e_{01}-e_{015}	void ratio	-	50	0

C_{a1}-C_{a15}	secondary compression index	-	50	0
c_{v1} - c_{v15}	vertical consolidation coefficient	m^2/s	50	0
s_{11}	overall constant model uncertainty associated with settlement model	-	Section length	0
s_{12}	wave renewal seasonality both overall and associated with freatic surface	-	Section length	0
s_{21}	constant value for freatic surface	-	Section length	0
s_3	wave renewal seasonality in crest level damage due to trafficking	-	Section length	0
h_{pore}	freatic surface in the embankment	mOD	150	0
$d\sigma$	weight of the permanent loading on the embankment	kN/m^2	300	0
c_{traff}	coefficient involved with the compaction of the surface due to trafficking	-	Section length	0
Nt_{traff}	number of trafficking events in time interval of consideration	-	0	0
c_{filt}	coefficient for deterioration water conductive layer	-	300	0
h_{drain}	height of the drainpipe	mOD	0	0
Nt_{storms}	counting process of the arrival of storms	-	0	0
m_{e1}	constant model uncertainty on the sheet pile corrosion rates	-	20	0
m_{e2}	seasonality model uncertainty on the sheet pile corrosion rates	-	20	0
m_{e3}	model uncertainty capturing the smaller environmental fluctuations	-	0	0
φ_{a0}	original radius of anchor	m	0	0
rate	general corrosion rate of the anchor	mm/year	150	0
m_{w1}	constant model uncertainty general corrosion anchor	-	150	0
m_{w2}	wave renewal model uncertainty general corrosion anchor	-	150	0
m_{w3}	Brownian motion for general corrosion rate	-	0	0
$rate_{tb}$	corrosion rate at turnbuckles	mm/year	150	0
m_{tb1}	constant model uncertainty corrosion rate at turnbuckles	-	150	0
m_{tb2}	Brownian motion for corrosion rate at turnbuckles	-	0	0
m_p	model uncertainty pit corrosion	-	150	0
m_{p1}	brownian motion pit corrosion	-	0	0
$rate_{pit}$	pitting corrosion rate	mm/year	150	0
A_{a0}	original anchor area	mm^2	0	0
Nt_{pit}	number of corrosion pit arrivals	-	0	0
$dtoe_a$	accretion change in toe in front of the sheet pile wall	m	20	0
$dtoe_w$	change in toe due to wave climate	m	20	0

Appendix E

Numerical implementation of asset time-dependent processes, fragility and lifetime probability

Appendix E: Flowcharts of simulations for asset time-dependent processes, fragility and lifetime probability

E.1 Time-dependent reliability and stochastic processes

The distribution function of the lifetime L of the flood defence structure, $F_L(T)$, is of relevance for flood defence management decision-making. The lifetime distribution $F_L(T)$ corresponds with the probability of failure during a specified time period of interest [0, T]. The planning of monitoring, repair or improvement activities is triggered by reaching a particular probability of failure threshold in such a period of interest. The section below is an overview of time-dependent reliability analysis as described by equations (2.14) to (2.23) in chapter 2 and stochastic processes in section 5.1 (in specific figure 5.1).

Let failure be defined by $Z(X(t),t) \leq 0$, where $X(t)$ is a vector of processes: $X_1(t)$,..., $X_n(t)$. The lifetime probability distribution $F_L(T)$ is therefore:

$$F_L(T) = P(L \leq T) = 1 - P[Z(X(t), t) > 0] \qquad \forall t \in [0, T] \tag{E.1}$$

A variety of time-dependent processes, mainly directed at modelling loading conditions, have been discussed in the literature .Melchers (1999). Here, following Vrouwenvelder (2005) we consider three levels of representation of time-dependent processes (figure 5.1):

1. *Stochastic process:* the time-dependent variable of interest $X_i(t)$ is modelled by a stochastic process.
2. *Hierarchical process:* consisting of random variables and has one or more stochastic processes embedded in it, so for example $X_i(t) = f(D_1, .., D_i(t), .., D_n)$, where $X_i(t)$ is a function of random variables D_1 to D_n, among which $D_i(t)$ is a stochastic process.
3. *Parametric process:* $X_i(t) = f(D_1, .., D_n, t)$ so $X_i(t)$ is a deterministic function of random variables D_1,..., D_n and time t.

Strictly according to the definition of a stochastic process, e.g. Ross (2003), all three processes mentioned above are stochastic processes. The definitions are however relevant to distinguish between different types of time series representations. The distinction in practice between the parametric and stochastic process (including the hierarchical process) is illustrated in Figure E.1, which shows realisations from a typical parametric process (centre panel) and a typical stochastic or hierarchical process (right hand panel).

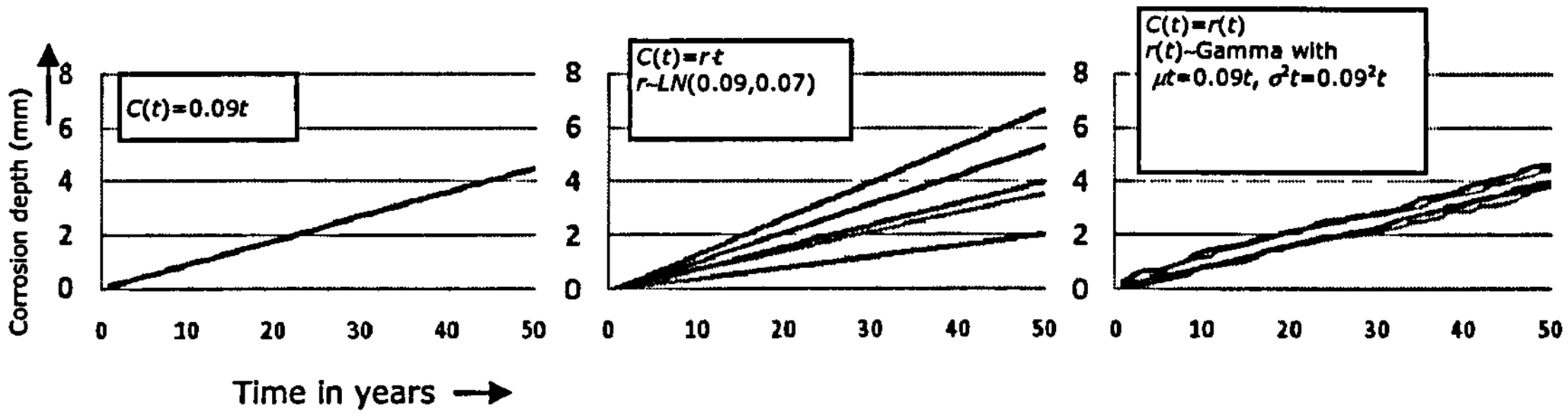

Figure E.1 Examples of corrosion depth time series samples for a deterministic model (left), a parametric process (middle) and a stochastic process (right)

Equation (E.1) can generally not be solved analytically, Engelund et al. (1995). $F_L(T)$ in equation (E.1), or the probability of failure in specified time interval [0,T] of interest can be approximated with the outcrossing approach. The probability that the lifetime L is smaller than a duration T is

$$F_L(t) = P(L \le t) \tag{E.2}$$

The outcrossing approach then approximates the lifetime probability $F_L(T)$ with a Poisson distribution based on the assumption of independent outcrossings, Engelund et al. (1995):

$$F_L(T) \approx 1 - \exp\left\{- E\left[N^+(T)\right]\right\} \tag{E.3}$$

in which $E[N^+(T)]$ is the mean number of crossings of $X(t)$ into the failure domain during [0,T]. In the stationary case $E[N^+(T)] = \nu^+T$, where ν^+ is the outcrossing intensity. In this paper the lifetime period of interest [0,T] is subdivided into N time intervals Δt. The mean number of crossings in a time interval is approximated by $P_f(\Delta t_i)$, the time-dependent probability of failure during a period Δt_i. The numerical implementation to calculate $P_f(\Delta t_i)$ is described in the following section.

Generic aspects of the numerical implementation of time-dependent processes in a flood defence reliability model are discussed here. Chapter 7 illustrates the site specific implications for the numerical implementation of time-dependent processes. The approach is based upon Monte Carlo simulation methods because, as is illustrated in chapter 7, many of the time-dependent processes are rather complex and do not succumb to algebraic solutions. Section E.2 describes the numerical implementation of stochastic processes. Section E.3 shows how these processes are incorporated in a reliability-based approach.

E.2. Numerical implementation of stochastic processes

Generic aspects about the numerical implementation of parametric, stochastic and hierarchical processes are discussed in this section.

Parametric processes

As defined in section E.1, a parametric processes is a function $X_i(t) = f(D_1, .., D_n, t)$ of random variables that are constant in time and a deterministic time. Therefore only the first simulation in the time series, for example for time t =1, requires sampling of $D_1, .., D_n$. This sampled set of $D_1, .., D_n$ remains equal throughout the rest of the time series, since they are constant in time, also illustrated in the middle panel in figure E.1. The variables $D_1, .., D_n$ can be any type of flood defence property such as soil properties, revetment weight or geometry.

Stochastic processes

If a stochastic process represents one variable $X_i(t)$ as defined in section E.2, the first simulation in the time series, for example for time $t = 1$, requires sampling of the increment of $X_i(t)$ between $t = 0$ and $t = 1$. For each subsequent time step the increment of $X_i(t)$ is sampled and accumulated. The result of such type of time series samples is illustrated in the right panel in figure E.1.

Hierarchical processes

A hierarchical process is defined in section E.2 as a function $X_i(t) = f(D_1, .., D_i(t), .., D_n)$ in which $D_1, ..., D_{i-1}, D_{i+1}, ..., D_n$ are constant variables in time and $D_i(t)$ is a stochastic process. The first simulation in the time series sample requires sampling of $D_1, ..., D_{i-1}, D_{i+1}, ..., D_n$ and a sample of the increment of $D_i(t)$ in the interval $t = 0$ and $t = 1$. In subsequent time steps the sample of $D_1, ..., D_{i-1}, D_{i+1}, ..., D_n$ remains equal to the first and constant throughout the time series. The increment of $D_i(t)$ is sampled and accumulated for each subsequent time interval. Based on $D_1, ..., D_{i-1}, D_{i+1}, ..., D_n$ and the accumulated $D_i(t)$ the overall quantity $X_i(t)$ is calculated for each time step. The appearance of time series samples is similar to those illustrated for the stochastic process in figure E.1 (right panel).

E.3 Numerical implementation of stochastic processes in time-dependent reliability

The flood defence system is subdivided into a number of flood defence sections. Each of these sections is characterised by one cross section, i.e. geometry, revetment, soil properties. Each cross section can fail in multiple ways, the failure mechanisms. A limit state equation is used to define a failure mechanism. The logical relations between the failure mechanisms are organised according to a fault tree. The flood defence properties in the limit state equations form a vector of random variables $X_1,..,X_{i-1}$, $X_i(t)$, $X_{i+1},..., X_n$. One or more of these variables is a time-dependent process, $X_i(t)$, according to the definitions in section E.1. Figure E.2 provides an overview of the description of the numerical implementation below.

The first simulation in the time series, for example for time $t = 1$, requires sampling of all random variables $X_1,..,X_{i-1}$, $X_i(t)$, $X_{i+1},..., X_n$. If $X_i(t)$ is a time-dependent function $X_i(t) = f(D_1, .., D_i(t), .., D_n)$, the vector $D_1, .., D_i(t), .., D_n$ is also sampled. Based on the sample of the random variables the limit state equations corresponding with the different failure mechanisms are computed and evaluated whether $Z(X(t) \leq 0)$. According to the logical relations between the failure mechanisms an evaluation is made of whether the cross section fails or not. For the subsequent time steps only the time-dependent quantities $X_i(t)$ are sampled and accumulated as explained in section E.2, the time independent flood defence properties remain equal to the first sample. For the subsequent time steps and the newly sampled values of $X_i(t)$ the limit state equations are evaluated. After completing the evaluation of the limit state equations for one time series all the time-dependent and time independent variables are sampled in a second time series simulation. The sample of the time independent variables remains equal throughout the time series, while the time-dependent quantities $X_i(t)$ are sampled and accumulated as explained in section E.2. This simulation procedure is repeated a large number of times to calculate the overall probability of failure of the cross section as a function of time, $P_f(t)$, see also figure E.2 for an overview:

$$P_f(t) = \frac{N_{top \leq 0}}{N_{tot}} \tag{E.4}$$

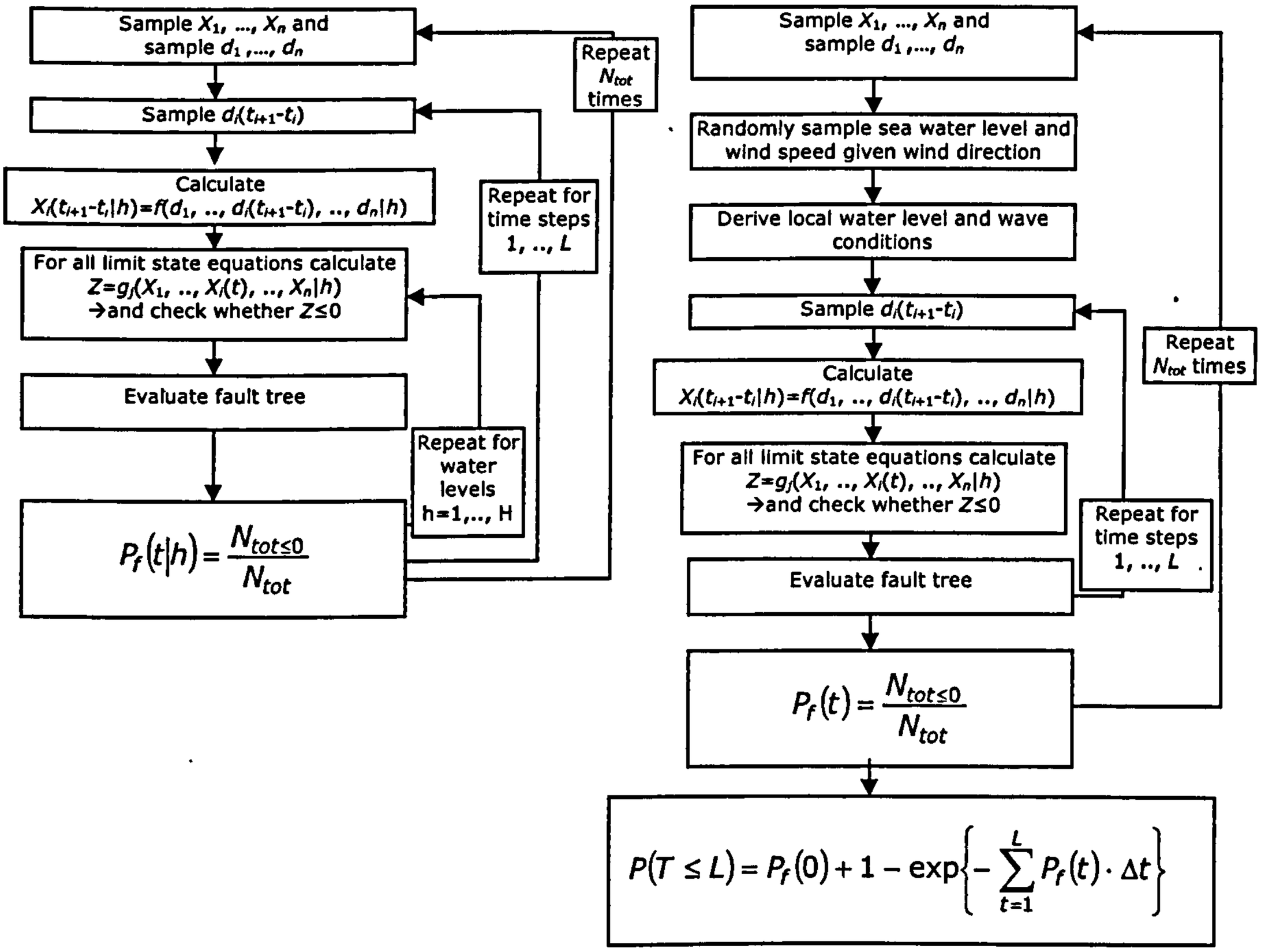

Figure E.2 Flow chart for the calculation of the probability of failure in a time interval of interest (right) and the calculation of time-dependent fragility (left).

in which $N_{top\leq 0}$ is the number of simulations for which the evaluation of the limit state equations entails failure of the cross section and N_{tot} is the total number of simulations. During the simulations the time period [0,T] is discretised into a number of time intervals Δt_i for which the time-dependent processes are sampled and the probability of failure is calculated. The probability of failure $P_f(\Delta t_i)$ is representative for the time interval Δt_i and is implemented in equation (E.4) and (E.3).

As mentioned before, a further result of interest is time-dependent fragility, or the probability of failure conditional upon different deterministic water levels. The procedure is similar to that described above except that the water level is not considered as a random variable. The water level is instead subdivided into a number of intervals. The time interval [0,T] is discretised into time intervals Δt_i and for each moment in time the probability of failure given a water level h is calculated as $P_f(t|h)$

$$P_f\left(t|h\right)=\frac{N_{top\leq 0}}{N_{tot}} \tag{E.5}$$

in which $N_{top\leq 0}$ is the number of simulations for which the evaluation of the limit state equations entails failure of the cross section given a water level h and N_{tot} is the total number of simulations given a water level h.

References

Abdel-Hameed, M., (1975), *A gamma wear process*, IEEE transactions on Reliability, 24 (2): pp. 152-153

Armstrong, M.J., (1995), Joint Reliability-Importance of Components, *IEEE Transactions on Reliability*, Vol. 44, no. 3

Baecher, G.B., Christian, J.T., (2003), *Reliability and statistics in Geotechnical Engineering*, Wiley and sons

Bakker, J.D., Van Noortwijk, J.M., (2004), Inspection validation model for life-cycle analysis, *Proc. 2nd int. conf. on Bridge Maintenance, Safety and Management (IABMAS)* (eds. E. Watanabe, D.M. Frangopol, T. Utsonomiya), Kyoto, Japan, 18-22 October 2004, London, Taylor and Francis Group

Barlow, R.E., Proschan, F., (1975), Importance of system components and fault tree events, *Stochastic Processes and their applications*, 3, pp. 153-173

Beck, M.B., Jining Chen, (2000), Assuring the quality of models designed for predictive tasks, in: *Sensitivity Analysis*, eds. Saltelli et al.

Benjamin, J.R., Cornell, C.A., (1970), *Probability, statistics and decision for civil engineers*, McGraw-Hill, NY

Bernardo, J.M., (1976), Algorithm AS 103: Psi (digamma) function. *Applied Statistics 25,* pp. 315-317

Bernardo, J.M., Smith, A.F.M., (2003), *Bayesian Theory,* John Wiley and sons

Borgonovo, E., Apostolakis, G.E., (2001), A new importance measure for risk-informed decision making, *Reliability Engineering & System Safety*, 72, pp. 193-212

Borst, van der, M., Schoonakker, H., (2001), An overview of PSA importance measures, *Reliability Engineering and System Safety*, 72, pp. 241-245

BRE Centre for Concrete Construction / DETR, (2000), *Corrosion of steel in concrete, investigation and assessment,* Digest 444, part 2, February 2000

BRE Centre for Concrete Construction, (2001), *Modelling degradation processes affecting concrete,* CRC ltd. London, 2001

Breitung, K. 1984. Asymptotic approximations for multinormal integrals. *Journal of Engineering Mechanics*, ASCE, Engineering Mechanics Division, vol. 110, pp. 357-366.

British Standard 1537:2000, *Execution of special geotechnical work – ground anchors*, ISBN 0580345009

British Standard, BS 8081:1989, *British Standard Code of Practice for Ground Anchorages*

British Steel (1997), *Piling Handbook, Seventh edition,* British Steel 1997

Buijs, F. A., van Gelder, P.H.A.J.M., Vrijling, J.K., Vrouwenvelder, A.C.W.M, Hall, J.W., Sayers, P.B., Wehrung, M.J., (2003), Application of Dutch reliability-based flood defence design in the UK, *proc. Conf. ESREL 2003 (1)*: 311-319, Maastricht, The Netherlands, June 15-18 2003

Buijs, F.A., Hall, J.W., Sayers, P.B., Van Noortwijk, J.M., (2005a), Time-dependent reliability analysis of flood defences using gamma processes, *proc. ICOSSAR*, Rome, Italy, June 2005

Buijs, F.A., Hall, J.W., Sayers, P.B., (2005b) Exploring sensitivity of flood defence reliability to time-dependent processes, *Proc. Int. Conf. ISSH*, Nijmegen, the Netherlands, May 2005

Buijs, F., Sayers, S., Gouldby, B., (2006), *Preliminary reliability analysis on the Thames Estuary: Dartford Creek to Gravesend, Floodsite task 7*, HR Wallingford, UK

Buijs, F.A., Hall, J.W., Sayers, P.B., (2007) Importance measures supporting the risk-based management of flood defences (in press), *Proc. ICASP 10*, Tokyo, Japan

Calle, E.O.F., Heijnen, W.J., (1983), *Probabilistic stability analysis, report 'Model and philosophy'*, (in Dutch, Probabilistische stabiliteitsanalyse, rapport 'Model en filosofie'), CO-251433/6, Laboratorium voor grondmechanica delft

Casciati, F. and Faravelli, L. (1991) *Fragility Analysis of Complex Structural Systems.* Research Studies Press, Taunton

Casella, G., Berger, R.L., (2002), Statistical inference, 2nd edition, Duxbury, US

Castanier, B., Bérenguer, C., Grall, A. (2003), A sequential condition-based repair/replacement policy with non-periodic inspections for a system subject to continuous wear, *Appl. Stochastic Models Bus. Ind.*, 19:327–347

Cherubini, U, Luciano, E., Vecchiato, W., (2004), *Copula methods in finance,* John Wiley & Sons Inc

Cho, Nam Zin, Jung, Woo Sik, (1989), A new method for evaluating system-level importance measures based on singular value decomposition, *Reliability Engineering & System Safety*, 25, pp. 197-205

Chun-Ching Li, Der Kiuregian, A. (1993) Optimal discretization of random fields, *Journal of engineering mechanics*, Vol. 119, no.6, June 1993

CIRIA, (1991), *Manual on the use of rock in coastal and shoreline engineering, CIRIA 83 / CUR 154,* London

CIRIA, (1996), *Beach Management manual,* Report 153, CIRIA

CIRIA, (2005), *Management of accelerated low water corrosion in steel maritime structures*, C634, CIRIA, London

CIRIA, (2007), *The Rock Manual. The use of rock in hydraulic engineering (2nd edition), C683,* CIRIA / CUR / CETMEF, London

Concrete Society, Arya, C., Wood, L.A., *The relevance of cracking in concrete to corrosion of reinforcement,* Technical report no. 44 of the Concrete Society, 1995

Concrete Society, *Diagnosis of deterioration in concrete structures,* Technical report no. 54 of the Concrete Society, 2000

Cooke, R.M., (1991), *Experts in uncertainty*, Oxford University Press

Cooke, R.M., Van Noortwijk, J.M., (1999), Local probabilistic sensitivity measures for comparing FORM and Monte Carlo calculations illustrated with dike ring reliability calculations, special issue on sensitivity analysis*, Computer Physics Communications,* 117, pp. 86-98

Cooke, R.M., Goossens, L.H.J., (2004), Expert judgement elicitation for risk assessments of critical infrastructures, *Journal of Risk Research*, 7 (6), pp. 643-656

Cox, D.R., (1962), *Renewal Theory,* Methuen's monographs, London

CUR 141 (1990), *Probabilistic design of flood defences,* Gouda, the Netherlands

CUR 162, Tol, van A.F., Oostveen, J.P., (1999) *Constructing with ground. Structures made of ground on and in soil with little bearing capacity and strong compressible subsoil (in Dutch)*, Delft 1999

CUR 190 (1997), *Chances in Civil Engineering, Part 1: Probabilistic design in theory (in Dutch: Kansen in de civiele techniek, deel1: Probabilistisch ontwerpen in theorie)*, Gouda, the Netherlands

Dawson, R. J. and Hall, J. W. (2002) Probabilistic condition characterisation of coastal structures using imprecise information. In: J. McKee Smith (ed) *Coastal Engineering 2002, Proceedings of the 28th International Conference, Cardiff UK, July 8-12, 2002.* New Jersey: World Scientific, vol.2: 2348-2359.

Dawson, R.J., Hall, J.W., (2002), Improved condition characterization of coastal defense infrastructure, *Coastlines, Structures, Breakwaters 2001, (NWH Allsop (ed),* Thomas Telford, pp. 123-134

Dawson, R.J., Hall, J.W., Sayers, P.B., Bates, P., Rosu, C., (2005), Sampling-based flood risk analysis for fluvial dike systems, *Stoch. Environ. Res. Risk. Assess*, 19: pp. 388-402

Dawson, R.J., (2006), Adaptive importance sampling for risk analysis of complex infrastructure systems, *Proc. R. Soc. A*, 462, pp. 3343-3362

Defra, (2004), *National Assessment of Defence Needs and Costs for flood and coastal erosion management (NADNAC),* summary report, Defra – Flood Defence Management Division

Defra / Environment Agency (2002), *Risk, Performance and Uncertainty in Flood and Coastal Defence – A Review, SR587,* Environment Agency

Defra / Environment Agency (2003), *Flood and Coastal Defence Project Appraisal Guidance, FCDPAG 6, Performance Evaluation,* Environment Agency

Defra / Environment Agency (2004a), *PAMS – Phase 1 Scoping Study, Task 2 interim report: Review of existing methodologies,* Environment Agency

Defra / Environment Agency (2004b), *PAMS – Phase 1 Scoping Study, Task 1 interim report: Logical framework for O&M activity,* Environment Agency

Defra / Environment Agency (2004c), *PAMS – Phase 1 Scoping Study, Task 3 interim report: options for performance based asset management systems,* Environment Agency

Defra / Environment Agency (2005), *PAMS Phase II, WP2: Defence prioritisation (Draft)*, Environment Agency

Dekker, R. (1995) Integrating optimisation, priority setting, planning and combining of maintenance activities, *European Journal of Operational Research,* 82, pp. 225-240

Dekker, R., (1996) Applications of maintenance optimization models: a review and analysis, *Reliability and System Safety,* 51, pp. 229-240

Dekker, R., Scarf, P.A. (1998) On the impact of optimisation models in maintenance decision-making: the state of the art, *Rel.Eng. and Sys. Safety*, 60, pp. 111-119

Delft Cluster (2001), Monitoring philosophy HerMes: Why, What, Where, When and to Which degree measure and incorporate (in Dutch: Monitoringsfilosofie HerMes: Waarom, Wat, Waar, Wanneer en in welke mate meten en verwerken), Report no. CO-710107/53, Delft

Delft Cluster (2003), Monitoring philosophy HerMes, Case: Rational monitoring of indirect indicators instead of direct condition indicators (in Dutch), Delft Cluster publication 01.01.07-11, Delft

Delta Commission, (1960), *Rapport Deltacommissie* (Report of Delta Commission, in Dutch). Staatsuitgeverij

Devroye, L., (1986), *Non-uniform random variate generation,* chapter 11, Springer-Verlag

Diermanse, F., Lammers, I., Thonus, B., Den Heijer, F., (2001), *Flood Risks and Safety in the Netherlands, phase 1: hydraulic loading models and information collection, report Q3028, (in Dutch: Veiligheid van Nederland in kaart, fase 1: belastingmodellen en gegevensverzameling)*, DWW Rijkswaterstaat

Diermanse, F.L.M., Van der Klis, H., (2005), Modelling statistical dependence using copulas, *Proc. ISSH,* Nijmegen, the Netherlands, May 2005

Ditlevsen, O., Madsen, H.O., (1996), *Structural Reliability Methods,* John Wiley and sons

DWW, Rijkswaterstaat (Directorate for Public Works), (2006), *Flood Risks and Safety in the Netherlands, DWW-2006-014,* Delft, 29 August 2006

Duthie, J.C., Robertson, M.I., Clayton, A.M., Lidbury, D.P.G. (1998) Risk-based approaches to ageing and maintenance management, *Nuclear Engineering and Design 184* (1998) 27–38

Edvardsen, C., Mohr, L., (1999) 'Duracrete – a guideline for durability-based design of concrete structures', Procs. FIB Symposium 'Structural Concrete – the Bridge between People', Prague

Eisenberg, N.A., Sagar, B., (2000), Importance measures for nuclear waste repositories, *Reliability Engineering & System Safety*, 70, pp. 217-239

Engelund, S., Sorensen, J.D., Krenk, S., (1995) *Estimation of the time to initiation of corrosion in uncracked concrete structures,* ICASP7

Engelund, S., Rackwitz, R., Lange, C., (1995b), Approximations of first-passage times for differentiable processes based on higher-order threshold crossings, *Probabilistic Engineering Mechanics*, 10, pp. 53-60

Environment Agency (1996), *Flood Defence Management Manual (FDMM),* Bristol, 1996

Environment Agency (2002) *National Flood Risk Assessment,* HR Wallingford Report EX 4722.

Environment Agency (2004a), Reducing the risk of embankment failure under extreme conditions: Report 1 – Good practice review. Defra / EA project FD2411

Environment Agency (2004b), Performance and Reliability of Flood and Coastal Defences – Phase I: A Review of Flood and Coastal Defence Failures and Failure processes. Defra / EA joint research programme project report

Environment Agency (2004c), Performance and Reliability of Flood and Coastal Defences – Phase I: Literature review. Defra / EA joint research programme project report

Environment Agency (2006), *Project appraisal report, Dartford Creek to Gravesend 30 year asset study,* Environment Agency, Southern Region

ERDC, Engineer Research and Development Center (1996a), *REMR Management Systems for Civil Works Structures,* US Army Corps of Engineers, Washington DC

ERDC, Engineer Research and Development Center (1996b), *The REMR Condition Index: Condition Assessment for Maintenance Management pf Civil Works Facilities,* US Army Corps of Engineers, Washington DC

ERDC, Engineer Research and Development Center (2000), *REMR Program Overview and Guide,* US Army Corps of Engineers, Washington DC

ERDC, Engineer Research and Development Center (2001), *Understanding condition indexes, Current Status and Future Opportunities,* US Army Corps of Engineers, Washington DC

Faber, M.H., Berge, H.E., Tiller, I., Hall, M.E., (1999) *Reliability based assessment of offshore concrete structures subject to chloride ingress,* OMAE-99, paper no. 99-6043

Faber, M.H. (2000), Risk Based Inspection – the Framework, Proc. ESRA workshop on Risk Based Inspection Planning, Zürich, December 2000

Faber, M.H., Sorensen, J.D. (2000), Indicators for assessment and inspection planning, Proc. ESRA workshop on Risk Based Inspection Planning, Zürich, December 2000

Floodsite, (2007), *Failure mechanisms for flood defence structures, Floodsite Task 4,* edited by: HR Wallingford, Wallingford, UK

Frangopol, D.M., Kallen, M.J., Van Noortwijk, (2004), J.M., Probabilistic Models for Life-Cycle Performance of Deteriorating Structures: Review and future directions, *Progress in Structural Engineering and Materials*, 6(4): 197-212

Gilbert, S., Horner, R., (1984), *The Thames Barrier*, Thomas Telford Ltd.

Grimmet, G. R., Stirzaker, D. R., (2001), *Probability and Random Processes,* Oxford University Press

Hartford, D.N.D., Baecher, G.B., (2004), Risk and Uncertainty in Dam Safety, Thomas Telford ltd. London

Harvey, A.C., (1989), *Forecasting, structural time series models and the Kalman filter,* Cambridge University Press

Hall, J.W., Dawson, R.J., Sayers, P.B., Sayers, P.B., Rosu, C., Chatterton, J.B., Deakin, R., (2003), A methodology for national-scale flood risk assessment, *Proc. ICE Water and Maritime Engineering*, v156, n3, pp.235-247

Halcrow (2006), *Environment Agency Dartford to Gravesend 30 Year Asset Study Technical Note – Greenhithe sheet piling, Snodland*, Kent, UK

Hasofer, A.M.; Lind, N.C. 1974. An exact and invariant first order reliability format. *Journal of the Engineering Mechanics Division*, ASCE, vol. 100, pp. 111-121.

Hawkes, P.J., (1999), Mean overtopping rate in swell and bimodal seas, *Proc. ICE Water, Maritime and Energy*, v136, n4, pp. 235-238

Hawkes, P.J., Gouldby, B.P., Tawn, J.A., Owen, M.W., (2002), The joint probability of waves and water levels in coastal engineering design, *Journal of Hydraulic Research*, v40, n3, pp. 241-251

Hohenbichler, M., Rackwitz, R. (1983) First order concepts in system reliability. *Structural Safety*, 1, 1983, pp. 177-188

Hohenbichler, M., Rackwitz, R., (1986), Sensitivity and importance measures in structural reliability, Civ. Engng Syst. Vol.3, pp. 203-209

Holický, M., (2000), Probabilistic modelling of carbonation effects, Procs. ESRA Risk-based Inspection plannign workshop Zurich, December 14-15 2000

Homma, T., Saltelli, A., (1996), Importance measures in global sensitivity analysis of nonlinear models, *Reliability Engineering & System Safety*, 52, pp. 1-17

Hong, Jung Sik, Lie, Chang Hoon, (1993), Joint Reliability-Importance of Two Edges in an undirected Network, *IEEE Transactions on Reliability*, vol. 42, n.1

Hontelez, J.A.M., Burger, H.H., Wijnmalen, D.J.D., (1996), Optimum condition-based maintenance policies for deteriorating systems with partial information, *Reliability Engineering and System Safety,* 51, pp. 267-274

HR Wallingford, (1998a), *The Joint probability of waves and water levels: JOIN-SEA, a rigorous but practical new approach*, SR537, Wallingford, UK

HRWallingford, (1998b), *Wave overtopping of seawalls, Design and assessment manual*, R&D Progress report W5/006/2, Environment Agency

HR Wallingford (1999), *Assessment of the wind and waves for the Thames Tidal Walls (West) Strategy Study Area,* Wallingford

HR Wallingford (2004a), *Risk Assessment for Flood and Coastal Defence for Strategic Planning, a summary*. Report W5B-030/TR, Wallingford

HR Wallingford (2004b), *Performance and Reliability of Flood and Coastal Defences – Phase I, Literature review, R&D interim technical report,* HR Wallingford

HR Wallingford (2004c), *Performance and Reliability of Flood and Coastal Defences – Phase I, A review of Flood and Coastal Defence failures and failure processes, R&D interim technical report,* HR Wallingford

HR Wallingford (2004d*), Joint probability issues within estuaries – a numerical case study for the tidal Thames*, HR Wallingford report TR 143

HR Wallingford (2005), *Performance and Reliability of Flood and Coastal Defences, FD2318/TR1,* Wallingford

Janssen, P.H.M., Slob, W., Rotmans, J., (1990), *Sensitivity Analysis and Uncertainty Analysis: A Review of Ideas, Methods and Techniques (in Dutch: Gevoeligheidsanalyse en Onzekerheidsanalyse: een Inventarisatie van Ideeën, Methoden en Technieken),* RIVM, Bilthoven

Jarzemba, M.S., Sagar, B., (2000), A parameter tree approach to estimating system sensitivities to parameter sets, *Reliability Engineering & System Safety*, 67, pp. 89-102

Kallen, M.J., Van Noortwijk, J.M., (2006), Optimal periodic inspection of a deterioration process with sequential condition states, International Journal of Pressure Vessels and Piping, 83, pp. 249-255

Karadeniz, H., Vrouwenvelder, A.C.W.M., (2003), *Saferelnet, task 5.1, Overview reliability methods,* TU Delft

Konikow, L.F., Bredehoeft, J.D., (1992), Ground-water models cannot be validated, *Advances in Water Resources,* 15, pp. 75-83

Kortenhaus, A., Oumeraci, H, (2002), ProDeich: *Probabilistische Bemessungsmethoden für Seedeiche (Probabilistic design methods for sea dikes (in German))*, Leichtweiss Institut für Wasserbau

Kotz, S., Balakrishnan, N., Johnson, N.L. , (2000), *Continuous Multivariate Distributions, Volume 1, Models and Applications*, John Wiley & Sons Ltd.

Lannoy, A., (2004), Lifetime Management of Structures, ESReDA working group, Det Norske Veritas, Norway

Lassing, B.L., Vrouwenvelder, A.C.W.M., Waarts, P.H., 2003. Reliability analysis of flood defense systems in the Netherlands, *proc. Conf. ESREL 2003* (2): 1005-1013, Maastricht, The Netherlands, June 15-18

MAFF, Ministry of Agriculture, Fishery and Food (now Defra), (2001), *Flood and Coastal Defence Project Appraisal Guidance, FCDPAG 1, Overview (including general guidance)*

Mani Raj Dahal, Bela Petry, Van Gelder, P.H.A.J.M., Gupta, S., Vrijling, J.K., (2005), Reliability analysis of Large Hydraulic Models using Importance Sampling and Response Database, *Proc. ISSH – Stochastic Hydraulics*, Nijmegen, the Netherlands

Marian Scot, E., Saltelli, A., Sørensen, T., (2000), Practical experience in applying sensitivity and uncertainty analysis, in: *Sensitivity Analysis*, eds. Saltelli et al.

Marsland, A., Randolph, F., (1978), Variation and effects of water pressures in pervious strata underlying Crayford Marshes, *Geotechnique* 28, no. 4, pp. 435-464

Martín, F.L., (1999), *Experimental study of wave forces on rubble mound break water crown walls,* pages 5-17 PIANC bulletin, no. 102

Melchers, R., (1999), *Structural reliability analysis and prediction*, University of Newcastle, Australia

Ministerie van Verkeer en Waterstaat (2004), *De veiligheid van de primaire keringen in Nederland, Voorschrift Toetsen op Veiligheid voor de tweede toetsronde 2001-2006 (VTV) (The safety of the primary flood defences in the Netherlands, Guideline for Safety Assessment for the second testing round 2001-2006, in Dutch),* Ministerie van Verkeer en Waterstaat, the Netherlands.

Moubray, J. (1997), *Reliability Centred Maintenance*, Butterworth-Heinemann, Oxford

Newnan, D.G., Lavelle, J.P., Eschenbach, T.G., (2000), *Engineering economic analysis*, Engineering Press, Austin

Noortwijk, van, J.M., Cooke, (1995), R.M., Kok, M., *A Bayesian failure model based on isotropic deterioration,* European Journal of Operational Research 82, pp.270-282

Noortwijk, Van, J.M., Gelder, Van, P.H.A.J.M., (1996) *Optimal maintenance decisions for berm breakwaters,* Structural Safety Vol.18, No.4, pp. 293-309

Noortwijk, Van, J.M., Kok, M., Cooke, R., (1997) *Optimal maintenance decisions for the sea-bed protection of the Eastern-Scheldt Barrier,* In Engineering Probabilistic

Design and Maintenance for Flood Protection (R. Cooke et al. eds) pp. 25-56, Kluwer Academic Publishers, 1997

Noortwijk, Van, J.M., Klatter, H.E., (1999), *Optimal inspection decisions for the block mats of the Eastern-Scheldt barrier,* Reliability Engineering and System Safety 65: pp. 203-211

Noortwijk, Van, J.M., Pandey, M.D., (2004), A deterioration process for time-dependent reliability analysis, Proc. of the 11th IFIP WG 7.5 Working Conf. on Reliability and Optimization of Structural Systems, 2-5 November 2003, Banff Canada, pp. 259-265

Oakley, J., (2004), Decision-theoretic Sensitivity Analysis using Value of Information, *Proc. 4th Int. Conf. SAMO* (eds. K.M. Hanson & F.M. Hemez), pp. 90-95

Oreskes, N., Shrader-Frechette, K., Belitz, K., (1994), Verification, validation and confirmation of numerical models in the earth sciences, *Science*, 263, pp. 641-646

Pandey, M.D., Van Noortwijk, J.M., (2004), Gamma process model for time-dependent structural reliability analysis, *Proc. of the 2nd Int. Conf. on Bridge Maintenance, Safety and Management (IABMAS),* (eds. E. Watanabe, D.M. Frangopol, and T. Utsonomiya) Kyoto, Japan, 18-22 October 2004. London: Taylor & Francis Group.

Paté-Cornell, M.E., (1996), Uncertainties in risk analysis: Six levels of treatment, *Reliability Engineering and System Safety,* 54, pp. 95-111

Percival, D.B., and Walden, A.T., (1993), *Spectral analysis for physical applications*: Cambridge University Press.

Petterson, L., Simola, K., (2006), *Ageing of Components and Systems,* ESReDA Working Group Report

PIANC, (2007), Life *Cycle Management of Port Structures Recommended Practice for Implementation,* Report of WG 42-MarCom, 7th draft

PIANC, (1998), *Life Cycle Management of port structures, General principles,* Report WG 31-PTCII, Supplement to Bulletin no. 99

Pierskalla, W.P., Voelker, J.A., (1976), A survey of maintenance models: the control and surveillance of deterioration systems. *Naval Res. Logistics Quart.* 23, pp.353-388

Pratt, J.W., Raiffa, H., Schlaifer, R., (1995), *Introduction to Statistical Decision Theory,* MIT Press

Press, W.H., Vetterling, W.T., Teukolsky, S.A., Flannery, B.P., (1992) Numerical Recipes in Fortran, the art of scientific computing, 2nd edition, Cambridge University Press

Popper, K., (1959), *The logic of scientific discovery*, Harper and Row, New York

Quillin, K., Modelling degradation processes affecting concrete, BRE Centre for Concrete construction, 2001

Raiffa, H., Schlaifer, R., (1961), *Applied statistical decision theory*, Harvard University Press, Cambridge, Mass.

Rice, S.O., (1944), Mathematical analysis of random noise, *Bell System Tech. J.*, 23, pp.282-332 (1945), 24, pp. 46-156. Reprinted in Wax, N. (1954) *Selected papers on Noise and Stochastic Processes*, Dover Publications

Ross, S.M., (2003), *Introduction to probability models,* Academic Press, an Imprint of Elsevier Science

Saltelli, A., Scot, M., (1997), Guest editorial: The role of sensitivity analysis in the corroboration of models and its link to model structural and parametric uncertainty, *J. of Rel. Eng. & Syst. Safety, special issue on sensitivity analysis,* 57, pp. 1-4

Saltelli, A., Chan, K., Marian Scot, E., (1999), Preface, special issue on sensitivity analysis, *Computer Physics Communications*, 117, pp. ix-xiv

Saltelli, A., Chan, K., Marian Scot, E., (2000), *Sensitivity analysis*, John Wiley & Sons Inc

Sayers, P.B., Hall, J.W., Meadowcroft, I.C., (2002), Towards risk-based flood hazard management in the UK, *Proc. ICE Civil Engineering*, v150, n1, special issue: Floods – a new approach, pp. 36-42

Sellmijer, J.B., (1988), *On the mechanism of piping under impervious structures,* PhD thesis, Delft University of Technology

Simm, J., Wallis, M., Sayers,P., Gouldby, B., Buijs, F., Flikweert, J., Hamer, B. (2006), Developing a Performance-based Management System Tool for Flood and Coastal Defence Assets, *Proc. 41st Defra Flood and Coastal Management Conf.*, 4 July – 6 July 2006, York

Slijkhuis, K., Frijters, M., Cooke, R.M., Vrouwenvelder, A.C.W.M., (1998), Probability of flooding: an uncertainty analysis, in: *Safety and Reliability*, eds. K. Lydersen, Hansen & Sandtorv, Balkema, Rotterdam, the Netherlands

Smith, A.M. (1993), *Reliability Centred Maintenance*, McGraw-Hill, New York

Soil Mechanics (2006), *Dartford Creek to Gravesend 30 year asset study, factual report on ground investigation, part A & B,* Halcrow / Environment Agency

Sørensen, J.D., Faber, M.H., (2001), Simplified, Generic Inspection Planning for Steel Structures, in: *Life Cycle Cost Analysis and Design of Civil Infrastructure Systems* (eds. D.M. Frangopol and H. Fututa, ASCE Special Issue), pp. 271-288

Southern Water, (1989), *Thames Tidal Flood Defences, Length 5/2 Land 4E*, Sir Bruce White, Wolfe Barry & Partners, London

Speijker, L.J.P., Van Noortwijk, J.M., Kok, M., Cooke, R.M., (2000) *Optimal maintenance decisions for dikes,* Probability in the Engineering and Informational Sciences, 14, pp.101-121

Spon Press (ed. Davis Langdon), (2005), *Spon's civil engineering and highway works price book*, 19th edition, Spon Press, Taylor & Francis group, London

TAW (1985), *Leidraad voor het ontwerpen van rivierdijken; deel 1 – bovenrivierengebied (Guideline for the design or riverdikes; part 1 – upper fluvial area, in Dutch).* Staatsuitgeverij, 's-Gravenhage

TAW (1989), *Leidraad voor het ontwerpen van rivierdijken; deel 2 – benedenrivierengebied (Guideline for the design or riverdikes; part 1 – lower fluvial area, in Dutch).* Staatsuitgeverij, 's-Gravenhage

TAW (1995), *Leidraad zandige kust. Basisrapport zandige kust (Guideline sandy coast. Main report sandy coast, in Dutch).* Staatsuitgeverij, 's-Gravenhage

TAW (1997), *Leidraad waterkerende kunstwerken en bijzondere constructies (Guideline water retaining structures and special stuctures, in Dutch).* Rijkswaterstaat, DWW, division public works.

TAW (1999), *Leidraad Zee- en meerdijken (Guideline Sea and lakedikes, in Dutch).* Rijkswaterstaat, DWW, division of public works.

Technical Advisory Committee for flood defences, TAW, (2000), *From probability of exceedance to probability of inundation, main report (in Dutch),* Gouda

Terzaghi, K, and Peck, R.B. (1967) *Soil Mechanics in Engineering Practice.* John Wiley & Sons, New York.

The Concrete Society, (2000), Diagnosis of deterioration in concrete structures, identification of defects, evaluation and development, technical report 54, The Concrete Society

Thoft-Christensen, P., Baker, M.J., (1982), *Structural reliability theory and its applications,* Springer-Verlag

Tung, Y.K., Mays, L.W., (1980), Risk analysis for hydraulic design, *ASCE J. Hydraulic Div.*, v106, n5, pp. 893-913

Van Baars, S., Kuijper, H.K.T., Bezuyen, K.G., Vrijling, J.K., (2003), *Manual for Structural Hydraulic Engineering,* Lecture notes, TUDelft

Van der Borst, M., Schoonakker, H., (2001), An overview of PSA importance measures, *Reliability Engineering and System Safety*, 72, pp. 241-245

Van Dantzig, D., (1956). Economic decision problems for flood prevention. *Econometrica* 24, pp. 276-287

Van de Graaff, J., (1986), Probabilistic design of dunes; an example from the Netherlands, *Coastal Engineering*, v.9, n.5, pp.479-500

Van Gelder, P.H.A.J.M., (1999), *Statistical methods for the risk-based design of civil structures*, PhD thesis, Delft University of Technology, Delft, the Netherlands

Vanmarcke, E., (1983), *Random Fields: Analysis and Synthesis,* MIT Press

Veseley, W.M., (1999), Principles of resource-effectiveness and regulatory-effectiveness for risk-informed applications: Reducing burdens by improving effectiveness, *Reliability Engineering & System Safety*, 63, pp. 283-292

Voortman, H., (2003), *Design- and Optimisation Methods for Flood Protection*, PhD thesis, Delft University of Technology

Vrijling, J.K., Bruinsma, J., (1980), Hydraulic Boundary Conditions, *Proc. Symposium on Hydraulic aspects of coastal structures*, Rotterdam

Vrijling, J.K., Van Gelder, P.H.A.J.M., (1998), The effect of inherent uncertainty in time and space on the reliability of flood protection, *Safety and Reliability* (Lydersen, Hansen & Sanotorv (eds)), pp. 451-456, Balkema, Rotterdam

Vrijling, J.K., Van Gelder, P.H.A.J.M., (2000), *Probabilistic design, lecture notes IHE Delft*, TUDelft

Vrijling, J.K., 2001. Probabilistic design of water defense systems in The Netherlands, *Reliab. Eng. Syst. Safe.* 74(3): pp. 337-344

Vrijling, J.K. (2003), Probabilistic design and maintenance of water defence systems *Proceedings Risk-based Maintenance of Civil Structures (eds. Van Gelder & Vrouwenvelder)*, Serie Workshop Proceedings no.8, TUDelft, January 21st 2003

Vrijling, J.K., Van Gelder, P.H.A.J.M., (2005), Implications of uncertainties on flood defence policy, *Proc. Int. Conf. ISSH*, Nijmegen, the Netherlands, 23-24 May 2005

Vrouwenvelder, A.C.W.M., Struik, P., (1991) Safety philosophy for dike design in the Netherlands, *Proc. of the Coastal Eng. Conf.*, v2, pp. 1254-1267

Vrouwenvelder, A.C.W.M., (1999) Theoretical manual of PC-Ring, Part C: Calculation methods (in Dutch), 98-CON-R1204, Delft

Vrouwenvelder, A.C.W.M. , Steenbergen, H.M.G.M., Slijkhuis, K.A.H., (2001a), *Theoretical manual of PC-Ring, Part A: descriptions of failure modes (in Dutch)*, Nr. 98-CON-R1430, Delft 2001

Vrouwenvelder, A.C.W.M. , Steenbergen, H.M.G.M., Slijkhuis, K.A.H., (2001b), *Theoretical manual of PC-Ring, Part B: Statistical models (in Dutch)*, Nr. 98-CON-R1431, Delft 2001

Vrouwenvelder, A.C.W.M., (2005), *PhD Course Reliability; Theory and Applications Time variant problems,* TUDelft

Wicki, R., Malioka, V., Faber,M.H., Condition indicators for inspection and maintenance planning, *Proceedings Risk-based Maintenance of Civil Structures (eds. Van Gelder & Vrouwenvelder)*, Serie Workshop Proceedings no.8, TUDelft, January 21st 2003

Worm, J.M., Van Harten, A. (1996) Model based decision support for planning of road maintenance, *Rel. Eng. and Sys. Safety*, 51, pp. 305-316

Yen, B.C., Tung, Y.K. (eds.), (1993), *Reliability and uncertainty analysis in hydraulic design*, ASCE, 287 p.